VOLTAGE DISTRIBUTION IN ELECTRICAL MACHINE STATOR COILS DUE TO FAST FRONTED SWITCHING SURGES.

by

KEITH McLEAY B.Sc. (Hons.)

Submitted for the

DEGREE OF DOCTOR OF PHILOSOPHY

at

HERIOT - WATT UNIVERSITY,

DEPARTMENT OF ELECTRICAL AND ELECTRONIC ENGINEERING.

MAY, 1982.

TEXT BOUND CLOSE TO THE SPINE IN THE ORIGINAL THESIS

CONTENTS.

CONTENTS.

CONTENTS.

CONTENTS.

ACKNOWLEDGEMENTS.

The author wishes to acknowleage botn the Science and Engineering Research Council and Parsons Peebles Motors and Generators for their financial support of this study. In addition thanks go to Dr. M. T. Wright of Parsons Peebles Motors and Generators for initiating the study and for many helpful discussions and guidance. The support and guidance of Dr. S.J. Yang of Heriot - Watt University are also acknowledged.

The advice on the experimental work from Mr. H. R. Johnston and the facilities provided by Mr. W. A. Sharpley, both of Parsons Peebles Research Division, were greatly appreciated.

Finally, heartfelt thanks are expressed for the unstinting support and encouragement of the authors wife, Isobel.

ABSTRACT.

The objective of the work which is described in this thesis was the provision of a method of accurately predicting voltage distribution in large machine stator coils when subjected to fast fronted switching surges and to use such a model to investigate the effects of various winding and surge parameters on the voltage distribution. An original method of analysis, using lossless multiconductor transmission line and scatter matrix theories is developed and is shown to be capable of predicting transient voltages on a two turn coil with a degree of accuracy which has not been previously possible. Extending the analysis to multi-turn coils and multi-coil windings is shown to be successful. A junction scatter matrix which includes discrete loss elements is developed and used in the analysis. The lossy model predicts both turn to ground voltages and interturn voltages with satisfactory accuracy. The analysis is then used to investigate the effect of various parameters on the distribution of voltages within the line end coil of the winding. The concept of a winding surge impedance is shown to be of limited value. The results of the investigation into distribution variation due to parameter changes are compared to the commonly used standards on coil insulation. A description of the computer programming methods used is given. The analysis has achieved much greater accuracy than previous methods and can be used in machine design and in the setting of test levels.

LIST OF SYMBOLS.

A	Average area normal to interturn electric field
A'	Average area normal to turn to ground electric field.
(C)	Capacitance matrix.
C_p	Interturn capacitance per metre.
$C_{g_{1,2..}}$	Turn to ground capacitance per metre.
c	Speed of E.M. radiation in free space.
d	Depth of penetration of E.M. radiation into copper.
f	Frequency.
(G)	Junction conductance matrix.
G_p	Interturn conductance per metre.
G_g	Turn to ground conductance per metre.
$G_{23,34..}$	Interturn conductance.
$G_{1,2..}$	Turn to ground conductance.
(I)	Junction current column matrix.
$(I)^{in}, (I)^{r}$	Incident and reflected junction current column matrices.
$i_{1,2..}$	Conductor current.
k_p	Proximity factor.
(L)	Inductance matrix.
L	Conductor self inductance per metre.
M	Interturn mutual inductance per metre.

m	Turn number.
n	Number of turns.
(R)	Junction resistance matrix.
$R_{1,2..}$	Conductor resistance.
(S)	Lossless junction voltage scatter matrix.
(S_L)	Lossy junction voltage scatter matrix.
T	Interturn insulation thickness.
T'	Turn to ground insulation thickness.
t	Time.
u	Speed of E.M. radiation in coil.
(V)	Junction voltage column matrix.
$(V)^{in}$, $(V)^{re}$	Incident and reflected junction voltage column matrices.
$v_{1,2...}$	Conductor voltage to ground.
x	Displacement.
(Y)	Addmittance matrix.
(Z)	Impedance matrix.
$z_{23,34..}$	Interturn characteristic impedance.
$z_{1,2,3..}$	Turn to ground characteristic impedance.
ε	Permittivity of insulation.
ε_r	Relative permittivity of insulation.
λ	Wavelength.
μ_c	Permeability of copper.
μ_i	Permeability of iron.
μ_o	Permeability of insulation.

μ_r	Relative permeability of insulation.
ρ_c	Resistivity of copper.
σ	Conductivity of insulation.
σ_i	Conductivity of iron.
ω	Angular frequency.

CHAPTER ONE.

INTRODUCTION.

The most common mode of failure of large induction motors is bearing failure. The next most common mode of failure is stator coil interturn insulation failure, which may or may not lead to turn to ground insulation failure. Interturn insulation failure can be due to either of two causes.

The first of these is due to flaws introduced during manufacture, which lead to weak points in the interturn insulation. These flaws can be irregularities on the conductor surface which cause high localised stressing of the insulation, or flaws in the insulation itself. Breakdown can occur immediately voltage stress is applied or, alternatively, as a result of long term degradation of the insulation at the weak point.

Failure may also occur because the working interturn voltage is greater than that which the interturn insulation was designed to withstand. As before breakdown may occur immediately or after long term degradation due to continual overstressing.

It is in order to alleviate this second cause of interturn insulation failure that this investigation has been carried out.

The problem of interturn insulation failure is more prevalent now than in the past. There are a number of reasons for this:

(i) It is well known that high interturn stresses can be produced by large steep fronted voltage surges impinging on the stator coils, therefore any increase in the severity or number of these surges will increase the likelyhood of interturn insulation failure. This, coupled with the recent trend towards using very low loss power cables for the connection of large motors to their associated switchgear, has meant that transients, produced by the switchgear, are transmitted almost unaltered to the motor (1). In the past, lossy cables had the effect of increasing the rise time of the surge and so reducing the interturn stresses on the motor coils.

(ii) The undoubted advantages of using vacuum switching devices in conjunction with large motors i.e. low fire risk, good reliability, low maintenance costs and small overall dimensions, have led to their increased use, particularly in the petrochemical industry. Unfortunately these devices are capable of repetitively producing very steep fronted transients (2,3) and therefore can lead to an increase in the severity of the conditions which interturn insulation has to withstand.

(iii) The continuing increase in the power output to size ratio of modern motors has put pressure on the coil designer to minimise the size of the coils. Thus the insulation on modern coils leaves less margin for error, although the better quality of modern insulation materials has offset this to some extent.

(iv) An associated factor which has caused the problem of interturn insulation failure to become more serious is the increasing cost of unscheduled stoppages in industrial processes. Consequently there has been an increased emphasis on reliability. This is of particular

importance in the production of offshore oil and gas.

This thesis deals specifically with the effect of steep fronted voltage surges impinging on motor coils. The purpose of the study is to enhance the understanding of the propagation of steep fronted surges through motor windings by providing an accurate analysis of the phenomenon. This should enable coils to be confidently designed against a background of realistic estimates of interturn stress. The work should also provide the system designer with a knowledge of the severity of transient surges that the machine winding can withstand so that the machine protection system can be appropriately specified.

Following a study of pertinent work on voltage distribution in motor windings due to steep fronted transients it was decided that further development of these theories would be ineffective and that a completely new analysis was required. The analysis had to be able to predict the voltages on any part of a coil, if it was to be useful as a design aid.

The analysis is developed, in the lossless form for a simple two turn coil and the results obtained from this model are compared with those from experimental work carried on a two turn coil subjected to a fast rising, low voltage pulse. The model was then developed for a general coil and the results from this model, analysing a twelve turn coil, were compared to experimental results obtained from an actual twelve turn coil.

The comparison of experimental and theoretical results was encouraging and at this point it was decided to include losses into the

analysis in an attempt to improve correlation between theoretical and experimental results.

Following the success of the method (including losses) at predicting the voltage distribution in the coil with good accuracy, it was used to investigate how voltage distribution varied with the parameters of the coils. The model is used to predict voltages on coils with various insulation dimensions and also coils with differing shapes. These results give a clear indication of the effects of the coil parameters on the coil withstand level for a range of surge front times.

A description of the computing methods used in the analysis is also given.

Whilst the analysis presented in this thesis was developed principally for large induction motor stator windings, the similarity of the stator coils in all large machines ensures that the coil model is general for all form wound coils.

CHAPTER TWO.

REVIEW OF PAST INVESTIGATIONS.

The simplest approach to analysing voltages due to surges in machine windings is to treat the winding as a simple transmission line; the well known transmission line equations are then used to calculate the voltages at any point on the winding. The parameters of the transmission line are found by approximating the coils as the elemental sections of the line, each represented by a series inductance and a shunt capacitance. This approach is used, for example, by Knable (4) but has the inherant disadvantage of being unable to predict voltages inside the coil. It is further erroneous in that it takes no account of the behaviour of the winding as a low pass filter. Any flattening of the surge front must, according to this theory, be due to losses. It will be shown later that coils act as low pass filters even when losses are not included in the analysis. (See chapter 4.)

A comparison of the work done on transient voltage distribution in motor coils with that done on transformer coils, shows that the latter has received most attention. The result of this has been that previously derived theories for transformer coils have been applied to motor coils, in preference to a fundamental analysis of the subject. This approach has met with only partial success because the theories for transformer coils have been able only to calculate coil voltages (voltages at the coil terminals) and not turn voltages.

The transformer coil analysis developed by Rudenburg (5) which took into account mutual inductance and capacitance between adjacent turns or

sections, was applied by him to the analysis of motor coils. In this work the elemental unit used to develop the winding model was a single coil. Consequently it is to be expected that, at best, the distribution of coil voltages throughout the winding can be calculated by this method. However the accuracy is doubtful because it is implicitly assumed that there is a sufficiently large number of coils in the phase to enable the problem to be classified as a distributed parameter system.

It has been suggested by Jackson (6) that the motor winding should be treated as a series of transformer coils, thus enabling the coil voltages to be calculated and also indicating the manner in which the surge propagates through each coil. However, if a distributed parameter model, such as Rudenburg's (which was developed for coils with very large numbers of turns) was used for each coil, significant errors would be introduced because form wound motor coils often consist of only a few turns. In addition Rudenburg accounted only for mutual inductance between adjacent turns or sections.

Lewis (7) used a ladder network to represent a machine winding and took a whole coil as a section of the network. This ladder network approach was more suitable for machine windings, which are constructed as a series of individual sections. However, no attempt was made to analyse voltage propagation within individual coils. If Lewis's analysis was to be adapted to represent a single coil, using a turn as a section of the network, some calculations concerning turn voltages could be carried out. This would not however lead to correct results, because the ladder network method used does not take into account inter-sectional

mutual inductances which, in motor coils, are not negligible.

In both Rudenburg's and Lewis's analyses of machine windings, whether applied to the whole winding or to a single coil, no account was taken of the two distinct regions of a motor coil, i.e. the portion embedded in the core iron and the portion which constitutes the end winding. Either the coil or the turn was treated as a distinct element, with no further subdivisions.

Heller and Veverka (8) performed a detailed analysis of a wave propagating along a single conductor embedded in an iron core and found that at high frequencies the iron acted as a flux barrier and so confined the surge to the conductor insulation. In their analysis this result was then promptly ignored and a ladder network, using each coil as a section, was approximated by differential equations. It was assumed that due to the large capacitance between turns, the voltage distribution within the coil was fairly uniform. The voltage distribution in the remaining coils was said to be less severe since each coil behaved as a low pass filter and so `flattened out' the wave front. Heller and Veverka advised machine designers to design line end coils with increased turn insulation. A method of calculating the surge impedance was developed and was said to conform well with experimental measurements, although no mention was made of the variation of the surge impedance with the rise time of the surge.

The ladder network analysis developed by Lewis was superceded by Rozsa and Lovass - Nagy (9) who proposed, and solved, an alternating ladder network model of a machine winding. This method was superior to Lewis's in that mutual inductance between adjacent sections could be

accounted for. However no account was taken of mutual inductance between sections which were not adjacent, and so this method cannot be correctly applied to a single coil.

In a review of publications (to 1964) on surge distribution in motor coils, Clowes (10) stated that;

> "The simpler theories give only the general features of the phenomena, whilst detailed comparison with experimental results is lacking for the more complicated equivalent networks".

Parrot (11) carried out an experimental investigation into surge distribution within the coils of two motors. It was found that for surges with short wave - front times (less than 600 ns) the interturn voltage distribution showed `a departure from uniformity', and that the largest interturn voltages occurred towards the end of the line connected coil.

Parrot compared the results of several investigations on peak coil voltages and concluded that a simple transmission line approach by Kagonov (12) (which stated that each coil had a constant travel time and that comparison of this with the rise time of the surge would provide an indication of the likely interturn voltages) was alone in consistently overestimating measured results and, so, should be used to ensure safe design. This conclusion shows the general lack of accurate analyses of the problem at that time. It should be noted however that Parrot's results led him to state that the travelling wave in the coil

"appears to be superimposed upon another voltage determined by the direct coupling between the turns".

This conclusion has never been incorporated into any concise theory.

Another experimental investigation, by Christiansen and Pederson, (13) found that again non - uniform distribution within the line end coil occurred when the winding was subjected to fast rising surges, (the highest voltages being towards the end of the coil) and that a simple transmission line model was inadequate. It was stated that the winding as a whole, acted as a series of low pass filters and could consequently be treated as a ladder network.

It can be seen from the results published by Parrot and Pederson that part of the surge is transmitted to each turn simultaneously. This fact is confirmed by the results of Jonnston (14).

Petrov and Abramov (15) carried out an experimental investigation in which they clearly demonstrated that part of the applied surge is transmitted turn by turn along the coil and a reflection takes place each time this surge reaches the either end of the coil. It was also stated in the study that the number of turns in the coil had little effect on the interturn voltages produced by the surges. In addition it was shown that the voltages on the first few coils are not affected by whether the surge arrives on one phase only or on all three phases.

Cornick and Adjaye (16) analysed the distribution of coil voltages with the use of cascaded two port networks which included losses. It was assumed that turn voltages are uniformly distributed throughout the coil. This assumption was said to lead to only slight errors in

predicting interturn voltages. Once again any attempt to modify this model in order to represent a single coil would be of limited value since mutual inductances are not accounted for. Cornick and Adjaye's investigation is extensive in that a complete system including source, cable and switchgear as well as the motor winding itself is modelled. While reasonable comparisons with experimental results were claimed for the coil voltages, no attempt was made to analyse voltage distribution in the coil.

Recent publications by Cornick and Thompson (1,17) give the results of extensive but mainly experimental work done on the topic of switching transients and their effect on motor coils. The conclusion of the work on the mechanisms which cause steep fronted surges to be produced, states that it is feasible for very steep fronted surges (less than 200 ns) to be produced with magnitudes of 4 - 5 p.u.. It was demonstrated that modern low loss cables cause little distortion to the wave front and so cannot be thought of as protection against fast fronted waves.

The section of Cornick and Thompson's work which deals with voltage distribution within the coils of a motor winding due to surges, utilises a very simple transmission line model of the winding and so no useful sub-coil voltage predictions are possible. It is shown, experimentally, that there is a negative reflection of the surge at the inner end of the line end coil. This is used to explain the result that the maximum interturn voltage occurs at that point. This result is in contradiction to the simple winding model used in the study. The negative reflection at the neutral end of the coil was said to be the result of flux starting to penetrate the core thus increasing the surge impedance of the

second coil in the phase. (In section 9.2 of this thesis this explanation is shown to be incorrect.) It was also shown that applying the surge to a single coil with its neutral end grounded did not accurately simulate conditions in the line end coil of a phase winding. Additionally, it was shown that a surge applied to an unconnected coil in a stator had, initially, no effect on other coils in the stator. Thus demonstrating that during the high frequency part of the surge there is no mutual coupling between coils. This is due to the iron core acting as a flux barrier.

It is clear that none of the investigations reviewed above have developed a model for a coil which is able to predict any interturn voltage for any shape of surge. In addition the analyses are erroneous since mutual coupling in the coil models is limited to coupling between adjacent turns to make the models tractable. Therefore no modification of these analyses will result in an accurate coil model.

Heller and Veverka's result concerning the role of core iron as a flux barrier to wave propagation in conductors embedded in iron is of importance in the following analysis.

CHAPTER THREE.

DEVELOPMENT OF LOSSLESS COIL MODEL.

The factors which contribute to the need for an improved analysis of transient voltage distribution have been explained in chapter 1. It was pointed out in chapter 2 that previous theories or any further development of them would be ineffective in meeting the need. It was therefore decided that a new approach to the problem was justified. The method of analysis which was developed is detailed in this chapter.

3.1. CONSTITUENTS OF A STATOR WINDING.

Before a detailed analysis of a coil can begin it is necessary to examine the properties of the constituent materials of the winding to determine how they behave when the coil is subjected to steep fronted voltage surges. This study is concerned only with the transient voltage distribution in the coils of high voltage machines and, therefore, only with form wound coils of the single or multi-stack type. The constituent materials of the coil are copper and the insulation material which is usually epoxy based resin and mica. The iron core also has properties which must be accounted for in the analysis.

3.1.1. Copper Conductor.

The resistance of the copper in such a complex configuration as a motor coil when subjected to high, multi-frequency excitation can not be readily calculated nor can it be easily measured. An approximate value of conductor resistance was obtained at a single frequency, since this enables the development of the analysis to proceed.

It has been found (6,10,11,13,14,18) that it is only very steep fronted surges which cause high interturn stressing i.e. surges with rise times below 1000 nanoseconds (ns), therefore the frequency used to find the approximate conductor resistance was 4 MHz. At this frequency the depth of penetration of electromagnetic waves into the copper, d, is given from one dimensional theory by:-

$$d = \sqrt{\frac{2\rho_c}{\mu_c \omega}}$$

$$= 3.2 \times 10^{-5} \quad m$$

(Although application of the classical skin depth of copper may not be strictly valid, it is considered adequate in view of the relative magnitude of the skin depth when compared to that of typical conductor dimensions.)

A typical cross section of a single conductor is 6.3mm x 2.0mm. Thus if we assume that all current flows in an outer skin of depth d = 0.032mm the resistance per unit length is R = 0.032 ohm/m. This value of R was considered (even if the value was increased by the proximity effect, see section 7.3) to be sufficiently low as to have only a secondary effect on voltage distribution in coils, and so, in the initial development of the coil model, the effect of the copper losses was ignored. In chapter 7 however resistive losses are re - introduced into the analysis.

3.1.2. Insulation Material.

It is assumed that the insulation material is homogeneous and that its properties were frequency independent. The value of the lossy component of the insulation was computed from a knowledge of the loss tangent requirements of the commonly used Electrical Supply Industry Standard on machine insulation systems (19). The E.S.I. standard states that the maximum value for the loss tangent of the insulation at line voltage is 0.048. (This is pessimistic, most modern insulation materials have a Tanδ value well below the maximum permissible value. However the pessimism is justified since Tanδ values are measured only up to V_L, the rated line voltage. Overvoltages of several times V_L can occur and thus Tanδ will increase significantly.)

Thus $\quad \text{Tan}\,\delta = \frac{\sigma}{\omega\varepsilon} \Rightarrow \sigma = 6.7 \times 10^{-10}$ S/m

Therefore $\quad G_p = \frac{\sigma A}{T} = 6.7 \times 10^{-9}$ S/m

$\quad G_g = \frac{\sigma A'}{T'} = 2.0 \times 10^{-8}$ S/m

for a typical coil

These values are extremely low and will be assumed, for now, to have only a secondary effect on voltage distribution in the coil.

As in the case of conductor losses, it was decided to defer the inclusion of dielectric losses until the lossless model had been developed. Thus enabling the basic processes involved in the distribution of surges to be built into the model without the added complica-

tions of secondary factors such as losses. Losses are reconsidered in chapter 7.

3.1.3. Core Iron.

Under the effects of high frequency excitation, machine core iron behaves in a completely different manner to that when it is excited at power frequencies. The skin effect at high frequency can cause the iron to act, not as a low reluctance flux path, as it does at power frequencies, but as a flux barrier. This is because the depth if penetration at these high frequencies (approximately 4 MHz. as in section 3.1.1) is very small even when compared to the lamination thickness. It follows that the core iron behaves simply as an impenetrable earthed sheath and may, for the purposes of experimentation be replaced by any other more convenient earthed sheath, provided that this is also impenetrable to the same high frequency electromagnetic waves. (This is experimentally verified later, see section 6.2.) A detailed analysis of this phenomenon can be found in reference 12, pp. 364-386. The result of this analysis of steep fronted waves travelling on a single conductor embedded in iron is that the response U(x,t) to a step function is given by;-

$$U(x,t) = 1 - \Phi\left[\frac{k_u x}{(t - \sqrt{LC}\, x)^{1/2}}\right]$$

where $$k_u = \frac{\left(\frac{C\mu_i}{L\sigma_i}\right)^{1/2}}{8\pi}$$

and $$\Phi(y) = \frac{2}{\sqrt{\pi}} \int_0^y e^{-u^2} du$$

If approximate figures relating to the dimensions of a high voltage motor coil are inserted into the above expression, k_u is given by;

$$k_u = 2 \times 10^{-7}$$

If an idealised step voltage is applied at x = 0, then by the time it has travelled 36m (about the total copper length of a typical 12 turn coil) the wave front time will have increased from zero to approximately 3×10^{-3} ns. Therefore the distortion of a travelling wave in a coil due to the effects of the iron can be reasonably neglected.

The part of the above expression, $(t - \sqrt{LC}\, x)$, shows that if copper losses are neglected then the speed of travel of the waves, u, will be given by;-

$$u = \frac{1}{\sqrt{LC}}$$

The impenetrable nature of the iron when excited by surges containing high frequencies enables the analysis of a machine winding to be considerably simplified. Inductive and capacitive coupling does not exist between slot portions of adjacent coils due to the barrier effect of the iron.

The result of this barrier effect at high frequencies is that the only significant element of mutual coupling which exists between adjacent coils in a stator winding is the coupling in the end winding

region. This, wnen compared to the coupling within a single coil, is extremely weak and will be neglected here.

Coupling between coils in the same slot will also be weak compared to the interturn coupling due to the two layers of coil insulation and the earthed corona shield around each coil. Any coupling which does exist can be ignored since any coil side which is in the same slot as the lead coil will be electrically remote from the line end of the phase and so has negligible effect on the lead coil voltage distribution. Thus coils can be treated separately.

3.2. GENERAL BASIS FOR ANALYSIS.

As explained in section 3.1 the iron core acts as a flux barrier during coil excitation by fast transients. It is therefore erroneous to treat the coil as a classical inductor because the only regions where flux is enclosed by the coil are the two end regions and these are separated from each other by the core iron. It consequently follows that two distinct regions can be categorised for a stator coil: the slot region and the end winding region. The sections of the coil which occupy these regions are separate from each other, i.e. the two sections of coil which occupy the slot region are connected to each other only through the end windings and the end windings are only connected to each other through the slot regions. Further, one of the end winding sections is interrupted at, or about, the mid - point by the coil terminals. The coil can then be thought of as comprising five sections which are interconnected at five junctions. (See figure 3.1). The five interconnections constitute five discontinuities, four of which are discontinuities due to the iron - air interface and the fifth due to the interruption of a

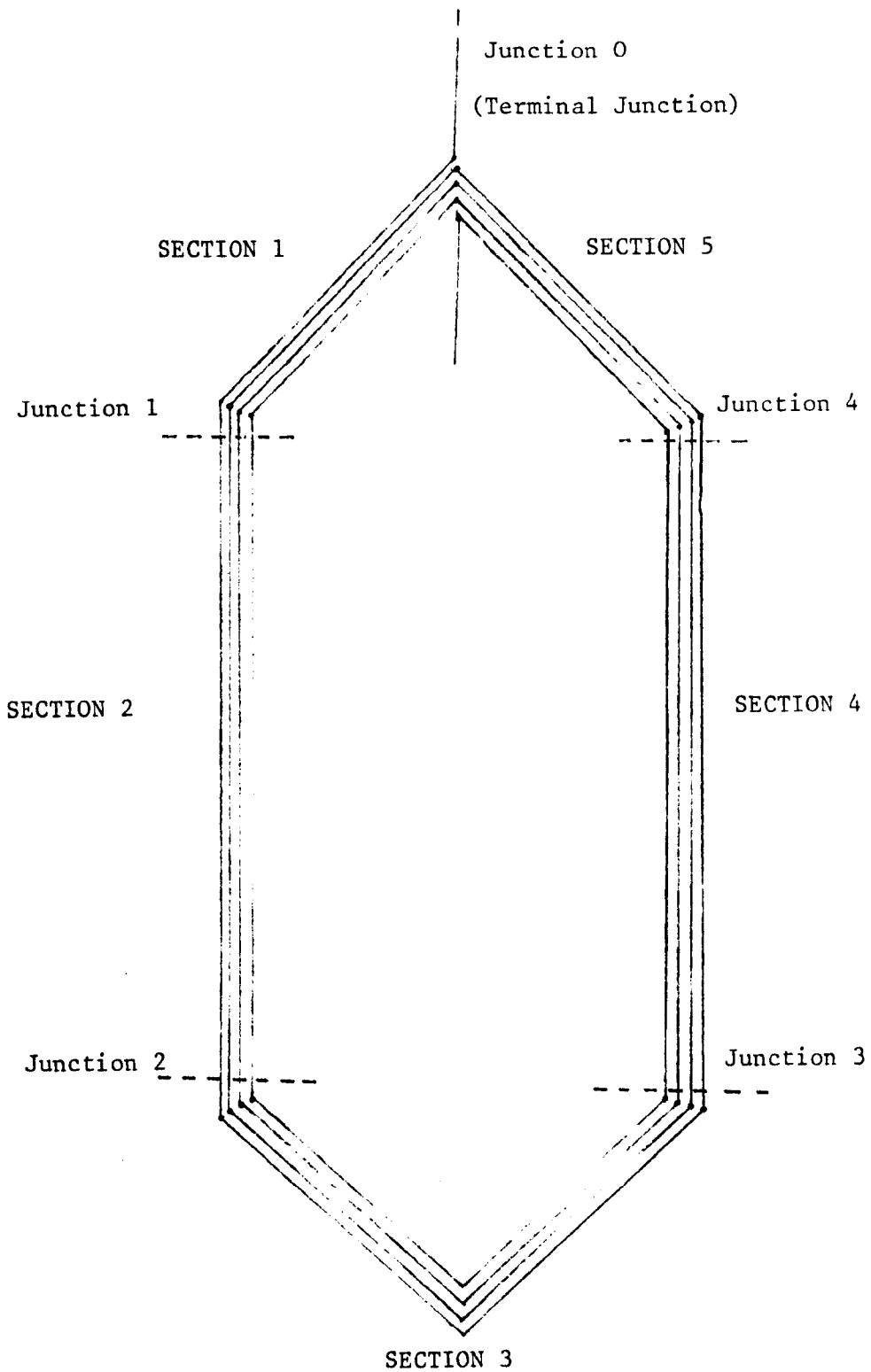

FIGURE 3.1 Sectionalised 4 turn coil

section by the coil terminals.

It is the division of the coil into the five sections, as described above, which forms the basis of the analysis. This approach is original, as far as is known.

The problem now resolves into two parts: firstly, that of analysing the electromagnetic waves as they propagate along each section of coil; secondly, analysing how the electromagnetic excitation is introduced into the coil from the supply cable and how the discontinuities affect propagation of the waves.

3.3. PROPAGATION OF ELECTROMAGNETIC WAVES IN COIL SECTIONS.

3.3.1. Slot Portion.

A detailed electromagnetic analysis of the slot portion of the coil at high frequency would have been extremely time consuming and well beyond the scope of the present study. However since the minimum rise time of the switching surges which are likely to impinge on a motor coil are approximately known, then the upper limit of the frequency spectrum is known. Thus some reasonable approximations can be made.

The minimum rise time of an impinging wave is unlikely to be less than 10 ns and so the maximum frequency involved is of the order of 100 MHz. At this frequency the minimum possible wavelength in a dielectric with a typical relative permittivity of 5, is given by;-

$$\lambda = \frac{c}{\sqrt{\varepsilon_r} f} = \frac{3 \times 10^8}{\sqrt{5} \times 10^8} \doteq 1.3 \text{ m}$$

The dimensions of an average coil are such that the maximum distance between any turn and ground in a slot is approximately 4mm i.e. the thickness of the slot insulation. Any transverse electric (TE) or transverse magnetic (TM) wave would be highly unstable in such a small space at such frequencies and so these modes are unlikely to exist. Thus since all the complementary waves can be ruled out, only the principle mode of propagation need be considered i.e. the TEM mode, and so the problem resolves into one of analysing a multiconductor transmission line.

Multiconductor transmission line theory is well known and is developed in a similar manner to single conductor transmission line theory. A mathematical treatment of the theory is included, in Appendix I, for completeness. In the lossless case multiconductor transmission line theory predicts that travelling waves simply propagate along the line in an unattenuated and distortionless manner at a speed given by u, where;-

$$u = \frac{c}{\sqrt{\mu_r \varepsilon_r}} \qquad (3.1)$$

From the above it can be deduced that any section of multiconductor transmission line, if it is assumed to be lossless, can be treated simply as a delay line. It therefore follows that the slot portion of a coil can be similarly treated as such.

3.3.2. The End Winding Region.

In the end winding region there are two types of insulation, the

applied coil insulation and the air spaces between the coil and the surrounding earthed conducting surface (i.e. core, rotor shaft, machine frame, etc.). A rigorous analysis of wave propagation in the end winding region taking these aspects into account would be prohibitive. It is therefore assumed that the mode of wave propagation is similar to that of an ideal multiconductor transmission line i.e. that all voltage propagation takes place at the same speed. It is also assumed that the coil insulation is sufficiently thick to have the dominant effect on the propagation speed, therefore the speed is equal to that in the slot and is again given by equation 3.1.

The propagation voltages on each turn in the end region can, under this assumption, be predicted using multiconductor transmission line theory. If the end region is assumed to be a lossless multiconductor transmission line like the slot region then it also can be treated as a simple delay line.

3.4. VOLTAGE SCATTERING AT COIL SECTION JUNCTIONS.

3.4.1. Types of Junction.

A junction, in multiconductor transmission line theory, is defined as a point at which two or more multiconductor transmission lines meet. There are two forms of multiconductor transmission line (or coil section) junctions in a form wound motor coil.

Firstly there is the slot/end winding junction: at this point there is a discontinuity of multiconductor transmission line parameters and therefore a junction exists. (It should be noted that most high voltage coils have a voltage grading coating applied at this point. This

coating, usually a very thin layer of semiconducting paint, is applied in order to avoid high electric field strengths at the point of entry into the core. Since the coating is applied to only a short length of the coil it is reasonable to neglect its effect on wave propagation).

The slot/end winding junction is a junction of two n conductor lines and there are four such junctions per coil. (See figure 3.1).

The second form of junction is the terminal junction: at this point two similar n conductor lines and two single conductor lines meet as shown in figure 3.2. It can be seen from examination of a high voltage motor coil that the coil terminals join the coil either side of the apex of the end winding evolute. However since the distance between these coil terminals is small it is neglected here (although it should be noted that it could be accounted for by modelling the terminal junction as two separate junctions each comprising an n conductor line, an n-1 conductor line and a single conductor line as shown in figure 3.3).

3.4.2. Scatter Matrices

The method of calculating the effect of travelling waves impinging on these junctions will be described for the case of the terminal junction, since this is the more complex of the two junction types and so all the details will be illustrated. For simplicity the development of the method will be illustrated using a two turn coil in order to avoid large matrices in the mathematics. (The treatment is however perfectly general.)

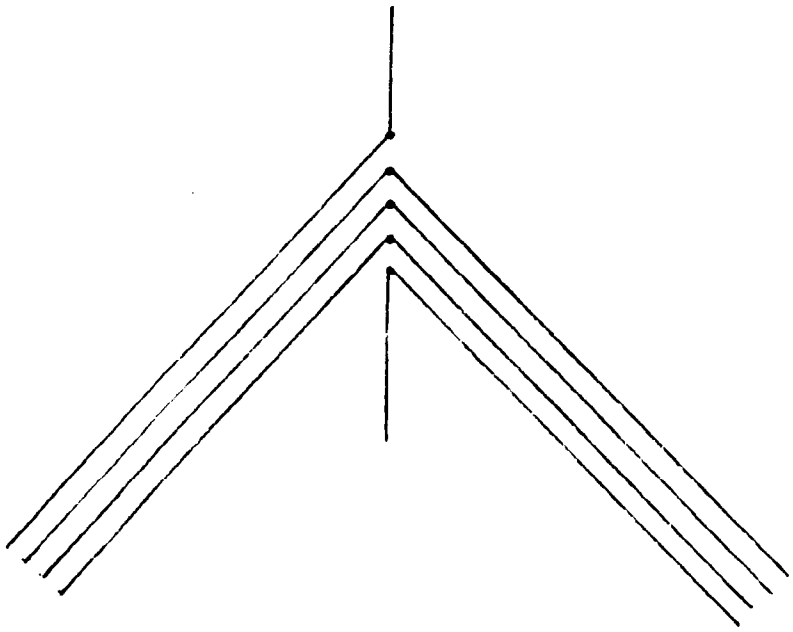

FIGURE 3.2 Terminal junction of a 4 turn coil.

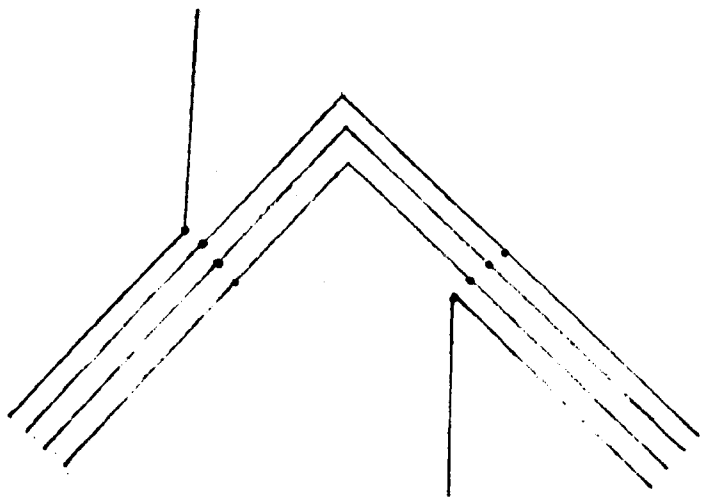

FIGURE 3.3 Two part terminal junction of a 4 turn coil.

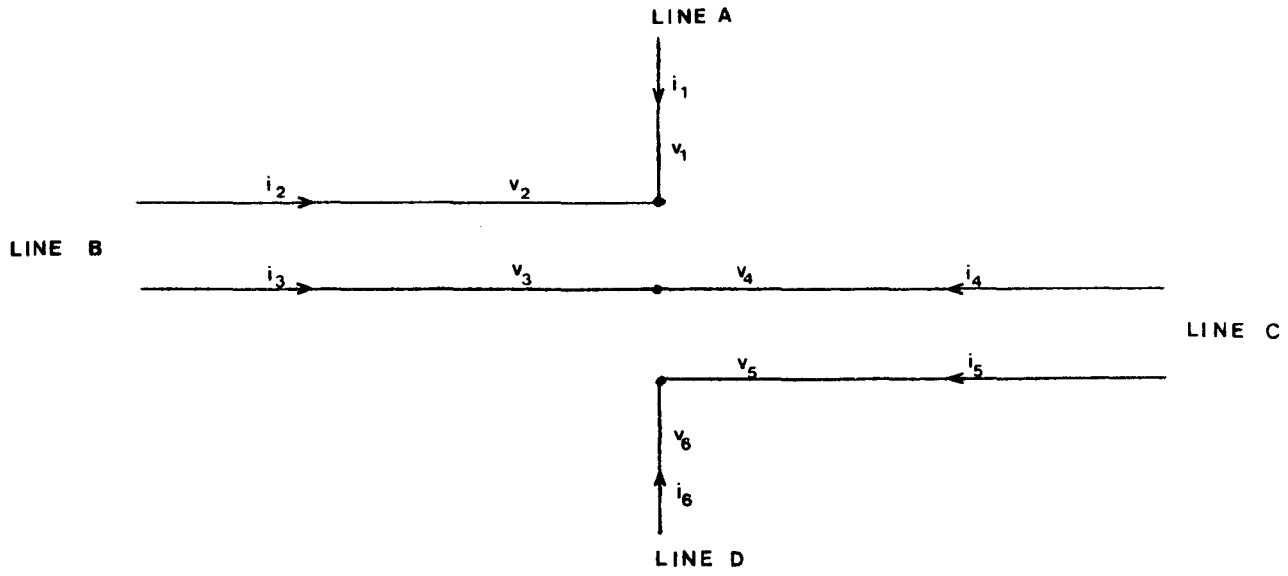

FIGURE 3.4 TERMINAL JUNCTION OF A TWO TURN COIL.

Figure 3.4, above, shows the terminal junction of a two turn coil. It can be seen that the voltages on each conductor, at the junction are related by;-

$$\begin{aligned} V_1 - V_2 &= 0 \\ V_3 - V_4 &= 0 \\ V_5 - V_6 &= 0 \end{aligned}$$

or, more concisely

$$(C_V)(V) = 0 \qquad (3.2)$$

where $(C_V) = \begin{bmatrix} 1 & -1 & 0 & 0 & 0 & 0 \\ 0 & 0 & 1 & -1 & 0 & 0 \\ 0 & 0 & 0 & 0 & 1 & -1 \end{bmatrix}$

and $(V) = \begin{bmatrix} V_1 \\ V_2 \\ V_3 \\ V_4 \\ V_5 \\ V_6 \end{bmatrix}$

(C_V) is called the Voltage Connection Matrix as the elements are deter-

mined by the connections of the conductors at the junction.

Similarly the currents at the junction are related by;-

$$\begin{aligned} i_1 + i_2 &= 0 \\ i_3 + i_4 &= 0 \\ i_5 + i_6 &= 0 \end{aligned}$$

or, more concisely

$$(C_i)(I) = 0 \qquad (3.3)$$

where $(C_i) = \begin{bmatrix} 1 & 1 & 0 & 0 & 0 & 0 \\ 0 & 0 & 1 & 1 & 0 & 0 \\ 0 & 0 & 0 & 0 & 1 & 1 \end{bmatrix}$

and $(I) = \begin{bmatrix} i_1 \\ i_2 \\ i_3 \\ i_4 \\ i_5 \\ i_6 \end{bmatrix}$

(C_i) is called the Current Connection Matrix.

The voltage entries in (V) and the current entries in (I) are the sum of all the incident and reflected travelling waves at the junction at any particular time. Therefore we have;-

$$(V) = (V)^{in} + (V)^{re} \qquad (3.4)$$

and

$$(I) = (I)^{in} + (I)^{re} \qquad (3.5)$$

Travelling wave voltages and currents are related to each other by their characteristic impedance matrices, i.e. -

$$\begin{bmatrix} V_1 \end{bmatrix}^{in} = \begin{bmatrix} Z_1 \end{bmatrix}\begin{bmatrix} i_1 \end{bmatrix}^{in} \quad \Rightarrow \quad (V_A)^{in} = (Z_A)(I_A)^{in}$$

$$\begin{bmatrix} V_2 \\ V_3 \end{bmatrix}^{in} = \begin{bmatrix} Z_2 & Z_{23} \\ Z_{23} & Z_3 \end{bmatrix}\begin{bmatrix} i_2 \\ i_3 \end{bmatrix}^{in} \quad \Rightarrow \quad (V_B)^{in} = (Z_B)(I_B)^{in}$$

$$\begin{bmatrix} V_4 \\ V_5 \end{bmatrix}^{in} = \begin{bmatrix} Z_4 & Z_{45} \\ Z_{45} & Z_5 \end{bmatrix}\begin{bmatrix} i_4 \\ i_5 \end{bmatrix}^{in} \quad \Rightarrow \quad (V_C)^{in} = (Z_C)(I_C)^{in}$$

$$\begin{bmatrix} V_6 \end{bmatrix}^{in} = \begin{bmatrix} Z_6 \end{bmatrix}\begin{bmatrix} i_6 \end{bmatrix}^{in} \quad \Rightarrow \quad (V_D)^{in} = (Z_D)(I_D)^{in}$$

or $(V)^{in} = (Z)(I)^{in}$ in concise form.

where $(Z) = \begin{bmatrix} (Z_A) & 0 & 0 & 0 \\ 0 & (Z_B) & 0 & 0 \\ 0 & 0 & (Z_C) & 0 \\ 0 & 0 & 0 & (Z_D) \end{bmatrix} = \begin{bmatrix} Z_1 & 0 & 0 & 0 & 0 & 0 \\ 0 & Z_2 & Z_{23} & 0 & 0 & 0 \\ 0 & Z_{23} & Z_3 & 0 & 0 & 0 \\ 0 & 0 & 0 & Z_4 & Z_{45} & 0 \\ 0 & 0 & 0 & Z_{45} & Z_5 & 0 \\ 0 & 0 & 0 & 0 & 0 & Z_6 \end{bmatrix}$

and similarly $(V)^{re} = -(Z)(I)^{re}$

(The positive direction is defined as towards the junction. Therefore current and voltage travelling waves which propagate away from the junction are related by a negative surge impedance.)

Alternatively the admittance matrix may be used, i.e. -

$$(I)^{in} = (Y)(V)^{in} \tag{3.6}$$

$$(I)^{re} = -(Y)(V)^{re} \tag{3.7}$$

where $(Y) = (Z)^{-1}$

This form proves to be more useful.

Multiplying equation (3.4) by (C_v) gives

$$(C_v)(V) = (C_v)(V)^{in} + (C_v)(V)^{re}$$

but $(C_v)(V) = 0$. Therefore

$$(C_v)(V)^{in} = -(C_v)(V)^{re} \tag{3.8}$$

likewise

$$(C_i)(I)^{in} = -(C_i)(I)^{re} \tag{3.9}$$

giving

$$(C_i)(Y)(V)^{in} = (C_i)(Y)(V)^{re} \tag{3.10}$$

Since neither (C_v) nor (C_i) is square, it is not possible to extract $(V)^{re}$ as a function of $(V)^{in}$ from either equation (3.8) or equation (3.10). However if we combine them we have;-

$$\begin{bmatrix} -(C_v) \\ (C_i)(Y) \end{bmatrix} (V)^{re} = \begin{bmatrix} (C_v) \\ (C_i)(Y) \end{bmatrix} (V)^{in}$$

Now we have a matrix equation in which the pre-multiplying matrices of the voltage column vectors are square, therefore;

$$(V)^{re} = \begin{bmatrix} -(C_v) \\ (C_i)(Y) \end{bmatrix}^{-1} \begin{bmatrix} (C_v) \\ (C_i)(Y) \end{bmatrix} (V)^{in} \tag{3.11}$$

or $(V)^{re} = (S)(V)^{in}$, where (S) is the **Voltage Scatter Matrix** for the junction.

Any travelling wave or waves arriving at the junction will therefore in general, cause reflections to occur on all the conductors which form the junction, the magnitudes of all these reflections may be calculated using the scatter matrix.

A scatter matrix can be developed for any junction of multiconductor transmission lines. The other type of junction of interest here is the iron - air junction shown in figure 3.5, below.

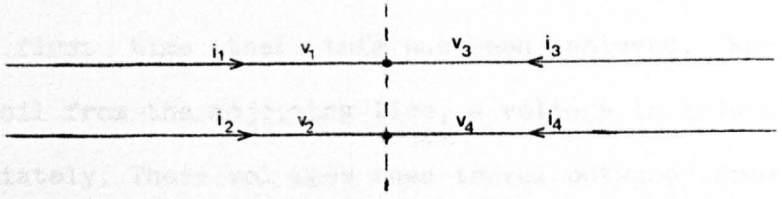

FIGURE 3.5 IRON/AIR JUNCTION OF A TWO TURN COIL.

In this case the column vectors have only four entries and the connection matrices are given by;-

$$(C_v) = \begin{bmatrix} 1 & 0 & -1 & 0 \\ 0 & 1 & 0 & -1 \end{bmatrix}$$

and

$$(C_i) = \begin{bmatrix} 1 & 0 & 1 & 0 \\ 0 & 1 & 0 & 1 \end{bmatrix}$$

This scatter matrix technique which was developed by Agrawal et al (20) applies only to lossless lines. It should be noted that for all coils the terminal junction scatter matrix is a (2n + 2) X (2n + 2) matrix while the slot/end winding matrix is of order (2n). These two scatter matrices, and the travel times for each section of coil, completely characterise the coil and so enable its ability to withstand steeply rising transient disturbances to be determined.

3.4.3. Application of Scatter Matrix and Multiconductor Transmission Line Theories to a Coil Model.

In the analysis above, by using multiconductor transmission line techniques, all the electric and magnetic interdependence between the turns in a coil is automatically taken into account. It is believed that this is first time that this has been achieved. When a surge impinges on a coil from the adjoining line, a voltage is induced in all the turns immediately. These voltages then travel outwards from the terminal junction in both directions, i.e. from junction 0 to junction 1 and from junction 0 to junction 4. (See figure 3.1). At junctions 1 and 4 the voltages are partially reflected and partially refracted. The reflected voltages journey back to junction 0 to be reflected and refracted again while the refracted waves go on to junctions 2 and 3, again to be reflected and refracted. In order to build up a picture of the total voltage on each turn (the total voltage is the algebraic sum of all the travelling wave voltages) some method of `bookkeeping' is necessary. A digital computer was used for this purpose.

A programme modelling the junctions described above and their interconnecting coil sections (or multiconductor transmission lines) can be used as a model for a single coil. Such a programme is described in chapter 12.

If it is assumed initially that the coil is excited by a single impulse with unity amplitude and a duration which tends towards zero, then the response to this will be the impulse response of the coil. Since the coil model assumes no distortion, the impulse response at any point on the coil will consist of a train of impulses. These impulses vary in terms of magnitude and time separation. This impulse response can then be transformed into the actual time response of the coil to any

particular surge by the use of time - convolution. (See chapter 12.)

3.5. CALCULATION OF PARAMETERS.

In order to carry out the analysis on a particular system, certain parameters must be calculated. Calculation of the admittance matrix for the slot section of the two turn coil necessitated the evaluation of two capacitances, the interturn capacitance and the turn to ground capacitance. See figure 3.6 below;

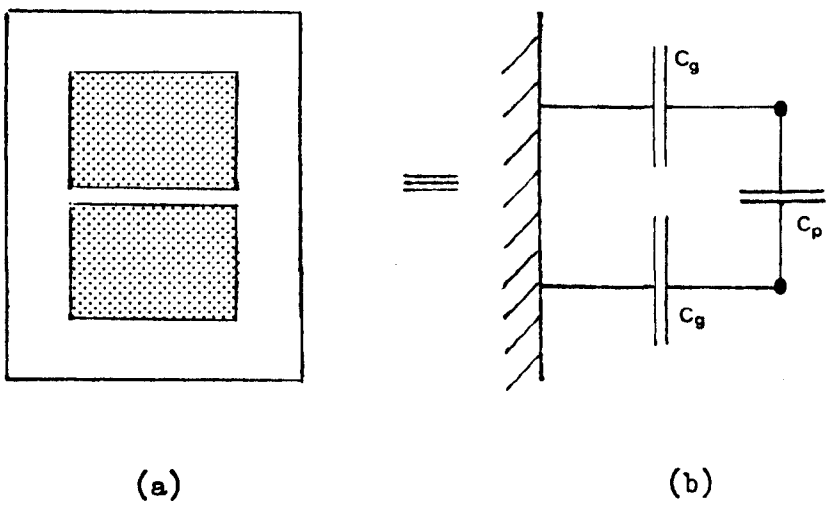

FIGURE 3.6 CAPACITANCES IN THE SLOT PORTION OF A TWO TURN COIL.

The capacitances were evaluated by approximating them to parallel plate capacitors. A true evaluation of these capacitances would involve either a detailed finite element approach to solving the electric field in the insulation region of figure 3.6(a), or a field plotting experiment. Since both these methods are too time consuming to be used in everyday design work, it was decided that a less cumbersome method was justified despite the loss of accuracy. Using Cp and Cg to construct the capacitance matrix, it can be seen from Appendix I that;

$$(C) = \begin{bmatrix} Cp + Cg & -Cp \\ -Cp & Cp + Cg \end{bmatrix}$$

It has been shown by Weeks (21) that for a lossless multiconductor transmission line in a homogeneous medium;

$$(L)(C) = \frac{1}{u^2}(1) \qquad (3.12)$$

where (1) is the identity matrix. From multiconductor transmission line theory we know that;

$$(Z) = u(L)$$

therefore

$$(Z) = \frac{1}{u}(C)^{-1}$$

and

$$(Y) = u(C) = u \begin{bmatrix} Cp + Cg & -Cp \\ -Cp & Cp + Cg \end{bmatrix}$$

Thus it can be seen that the admittance matrix can be calculated without first evaluating the inductance matrix of the coil section.

The same method can be applied to the evaluation of the admittance matrix for the end winding region of the coil, though in this case the accuracy will be diminished since the end winding electric field is less uniform than the electric field in the slot.

3.6. LIMITATIONS OF THE MODEL.

One limitation of this coil model is that it is only valid for a

short time after the transient has impinged on the coil. The assumption which was made during the development of the analysis i.e. that the surge contains very high frequency components, loses validity as time progresses. This limitation does little to detract from the practical value of the model however, since it has been verified in the past (1,11,13,14,15) that it is only during the initial period of the transient disturbance that high interturn stresses occur.

A second limitation of the model is that is computer based. An analytical method would have been preferable as the precise effects of each parameter in the system could then have been readily understood. In addition an analytical method would enable coil design to proceed directly from the initial surge specification to the dimensions of the required coil. The computer method however, necessarily uses the reverse procedure i.e. predicting the coil's performance from a given set of dimensions. Nevertheless, a computer based method can be used to build up extensive data on how differing types of coil behave under transient conditions and can be used to predict the transient performance of various windings under various surge conditions and so can indicate trends which could be used effectively in machine design. (The analysis itself will, however, remain necessary in order that the final design can be checked.)

The scatter matrix technique used here can only be used in the idealised case of lossless lines. Thus losses cannot be included directly into the analysis, however other methods, although less exact, may be employed to account for the effect of losses. These will be examined in chapter 7.

3.7. ADVANTAGES OVER OTHER COIL MODELS.

It is believed that this coil model is the first to be developed which is able to predict transient voltages on any turn in the coil. Additionally, since both the speed and magnitude of all travelling waves in the coil are known, it is possible to calculate voltages on any part of any turn in the coil. The method of analysis developed here can be used with any shape of applied surge, provided that the initial assumptions (i.e. high frequency and short time) are not invalidated.

The measurement of the coil parameters has proved, in the past, to be difficult, and therefore the results of previous studies have been prone to significant errors even before the effects of erroneous analysis have been taken into account. It is shown in section 3.5 that a few simple calculations from the coil dimensions are all that is necessary to enable this model to be used. Since no frequency analysis of the coil is necessary, no parameters of variable frequency need to be measured or calculated.

CHAPTER FOUR.

VERIFICATION OF THE TWO TURN COIL MODEL.

4.1. EXPERIMENTAL WORK ON THE TWO TURN COIL.

The theoretical model described in chapter 3 was developed for a two turn coil. In order that the validity of the model could be tested at this stage, a two turn motor coil was constructed and tests were carried out.

The coil was constructed in the normal manner by Parsons Peebles Motors and Generators, Edinburgh. The coil consisted of three uninsulated sub - conductors formed into a large two turn diamond coil with an insulation level of 6.6 kV. Details are given in Appendix II(a).

The test apparatus and the test procedure were required to simulate as far as was possible practical situations. It was also necessary that they should be simple and easy to reconstruct in a computer model so that direct comparisons could readily be made between experimental and theoretical results. The cable between the switchgear and the motor was represented by a length of single core co-axial cable. The theoretical model as described in chapter 3 was used to represent the first coil in a motor winding and a simple resistor was used to represent the remainder of the winding.

It is reasonable to represent one phase of the three phase system by a single phase system since the transient phenomena under investigation are short lived and so the time interval between pole closures or interruptions in the switching device will be much longer than the time

of interest here. Representing one phase of a three phase cable by a single phase cable is certainly valid in the case of cables in which each phase conductor has its own earthed sheath (assuming sheath voltages are negligible). In the case of cables where the conductors have a common earth sheath, voltages will be induced in the phases which are not directly energised. However, these indirectly energised phases will have only a small effect on the directly energised phase and so their influence can be neglected (15). A resistance was used to model the remaining coils in the phase winding. Although it does not truly represent the coils, at this stage it is not necessary to do so. The neutral end of the coil must have a termination of some kind, a resistance is convenient for experimental purposes and easy to simulate in the model.

The resistance used to model the remaining coils of the phase winding does not accurately represent them. However, at this stage in the investigation it is not necessary to do so. The neutral end of the coil must have some termination and a resistance is convenient for experimental purposes and easy to simulate in the model. The model for a whole phase winding will be dealt with in chapter 8.

In order that the turn voltages could be measured a strip of insulation was removed from the coil at its terminal junction. This enabled the probes from the oscilloscope to be connected to the copper of each turn. Since the insulation was removed the tests could only be carried out at low voltage. It was assumed that the system was linear with respect to voltage and therefore the results were in direct correspondence with similar high voltage tests which were not feasible. The

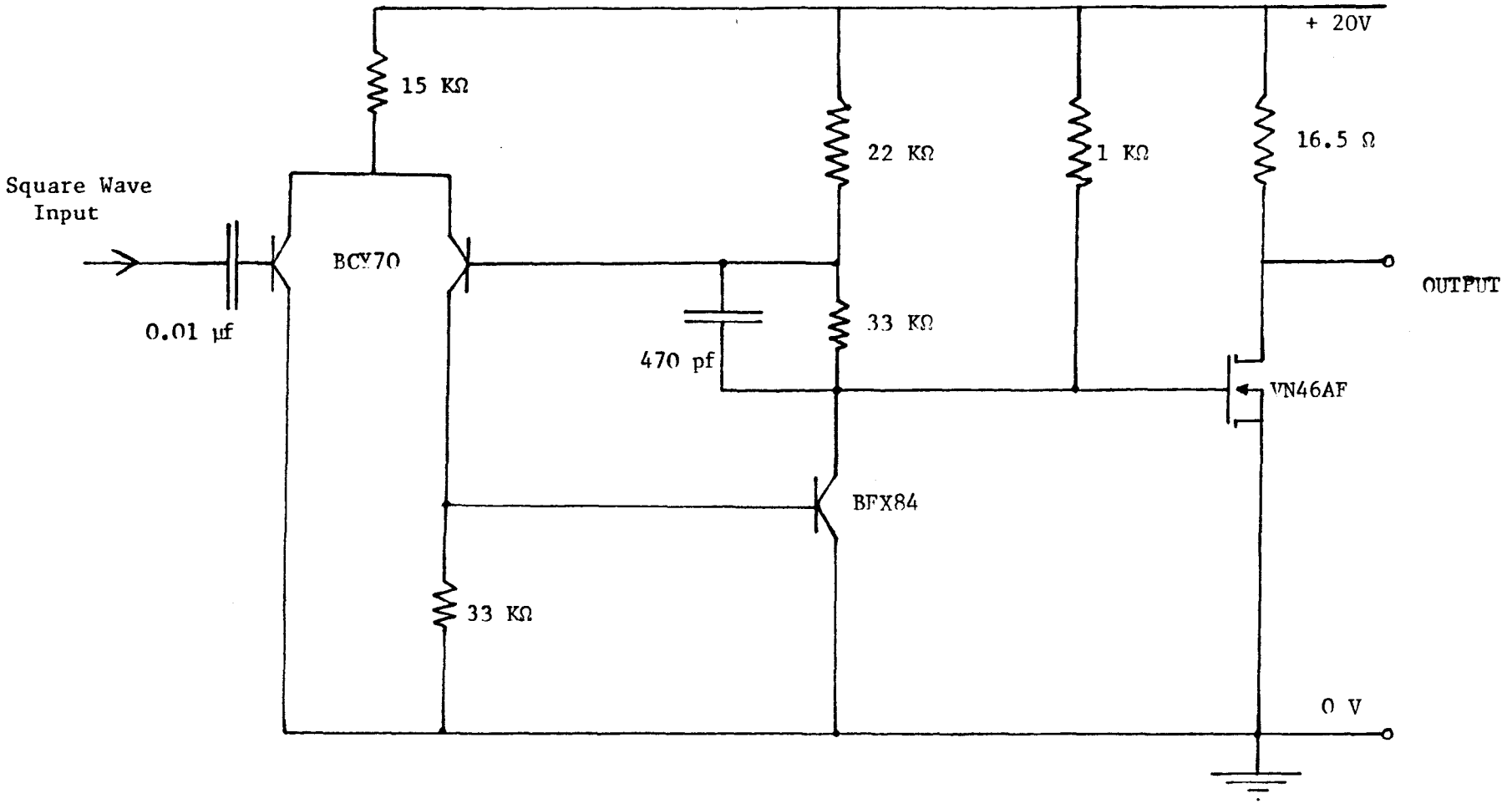

FIGURE 4.1 "Schmitt Trigger" steep fronted surge generator

surge generator used to represent the switchgear, which produced the fast rising surges, was a low voltage electronic device, triggered by a square wave from a wave form generator. A "Schmitt Trigger" arrangement (see figure 4.1) was used which, when connected to an infinitely long, or (more practically) a matched line produced a surge as shown in figure 4.2 below.

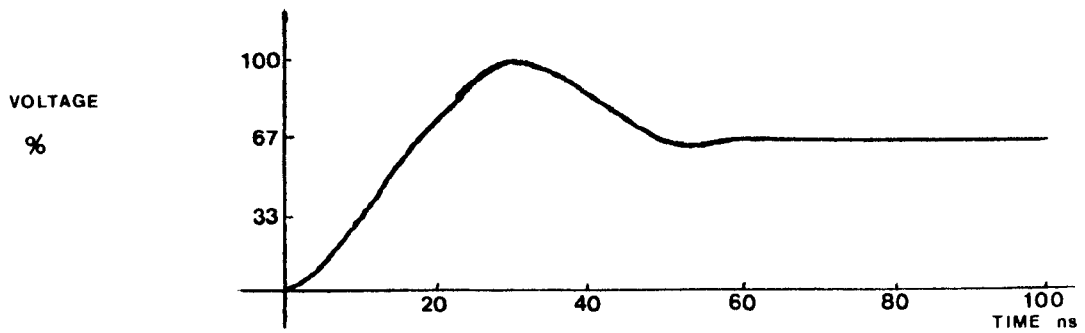

FIGURE 4.2 WAVE SHAPE PRODUCED BY SURGE GENERATOR.

This surge was considered to be sufficiently irregular in shape to provide a good test for the theoretical model. Some simple experimentation carried out with the surge generator sending pulses into a matched and an open circuited line, yielded the reflection factor at the surge generator. This knowledge is necessary if the voltage distribution in the coil is to be calculated for a period of time longer than twice the travel time of the interconnecting cable. The value of this reflection factor was found to be -0.35.

A schematic of the test system is show in figure 4.3, overleaf.

During the tests the coil was placed on a steel sheet, which acted as an earth. The slot portions of the coil were wrapped in grounded aluminium conducting tape to represent earthing conditions in the slot, as explained in section 3.1.3. It was found that removing the conducting

tape and the earthing sheet had an effect on the shape of the voltage waveforms at the coil terminals.

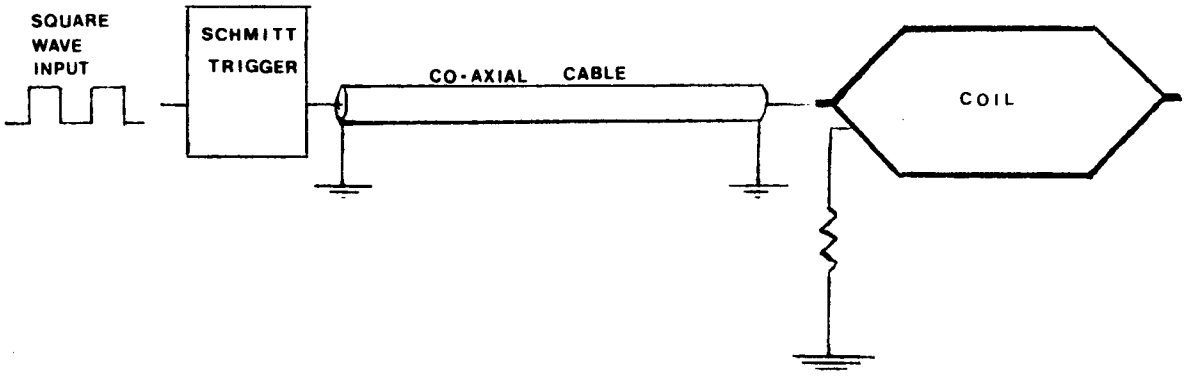

FIGURE 4.3 SCHEMATIC OF TEST ARRANGEMENT.

An oscillogram of the voltage appearing on the coil terminals due to the applied voltage surge was taken. This is shown in figure 4.4. (In order to present the results clearly, and consistently, all voltages in this thesis will be expressed as a percentage of the peak voltage of the applied surge.)

4.2. DISCUSSION OF THE RESULTS OF THE INVESTIGATION ON THE TWO TURN COIL.

A comparison of the experimental and predicted results obtained from the two turn coil (figures 4.4 and 4.5) shows that the computer model can predict reasonably well, the terminal voltages on the coil. The results also confirm the general conclusion of previous studies in showing that the coil filters out the high frequency components of the applied surge. This can be seen by comparing the voltages at the coil input and the coil output. This has previously been explained simply as

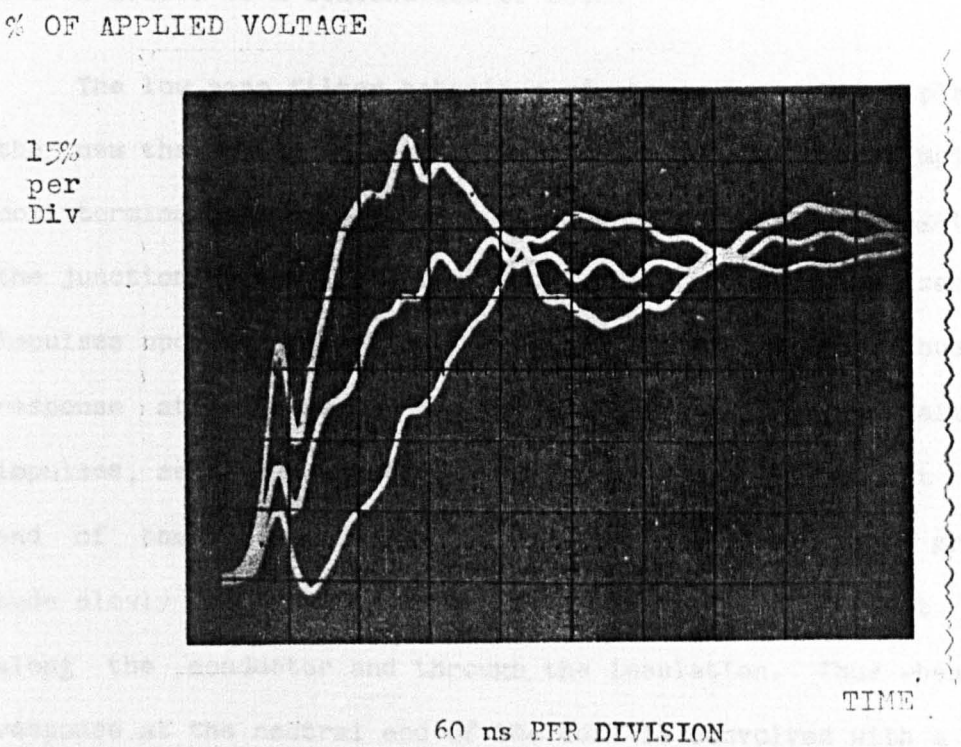

FIGURE 4.4 Measured turn to ground voltages (two turn coil)

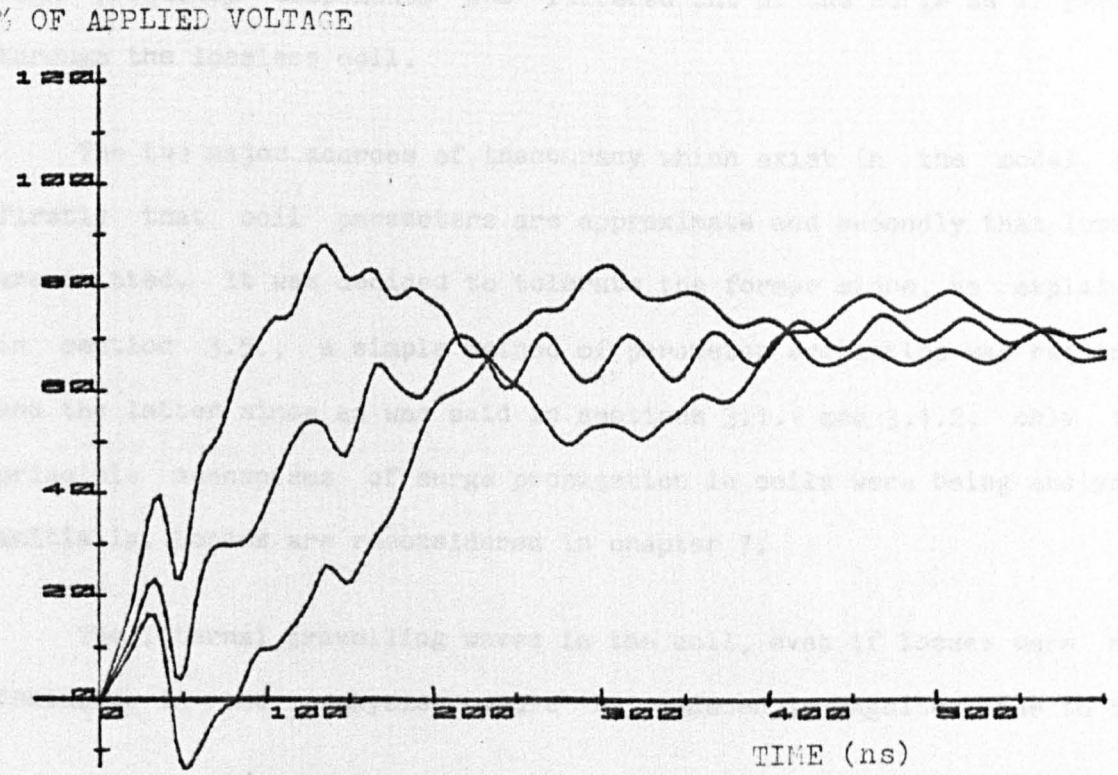

FIGURE 4.5 Computed turn to ground voltages (lossless two turn coil).

the result of series inductance and shunt capacitance or as distortion due to losses or a combination of both.

The low pass filter behaviour of the coil can be explained, using the new theory, as follows. The result of the impulse impinging on the coil terminal junction is that a number of impulses propagate out from the junction (one on each conductor). Each of these impulses causes more impulses upon subsequent reflection at other junctions. Thus the impulse response at any point on the coil is a series of relatively small impulses, see figure 4.6(i). In particular the response at the neutral end of the coil will be a series of impulses which will grow in magnitude slowly as the surge is gradually transferred to that point, both along the conductor and through the insulation. Thus when the impulse response at the neutral end of the coil is convolved with a surge which has a finite rise time (figure 4.6(ii)(a)), the resulting waveform has a significantly longer rise time (figure 4.6(ii)(b)). In other words the high frequency components are filtered out of the surge as it passes through the lossless coil.

The two major sources of inaccuracy which exist in the model are firstly that coil parameters are approximate and secondly that losses are omitted. It was decided to tolerate the former since, as explained in section 3.5., a simple method of parameter evaluation was required and the latter since as was said in sections 3.1.1 and 3.1.2, only the principle mechanisms of surge propagation in coils were being analysed initially. Losses are reconsidered in chapter 7.

The internal travelling waves in the coil, even if losses were not included in the analysis, would be reduced in magnitude due to the

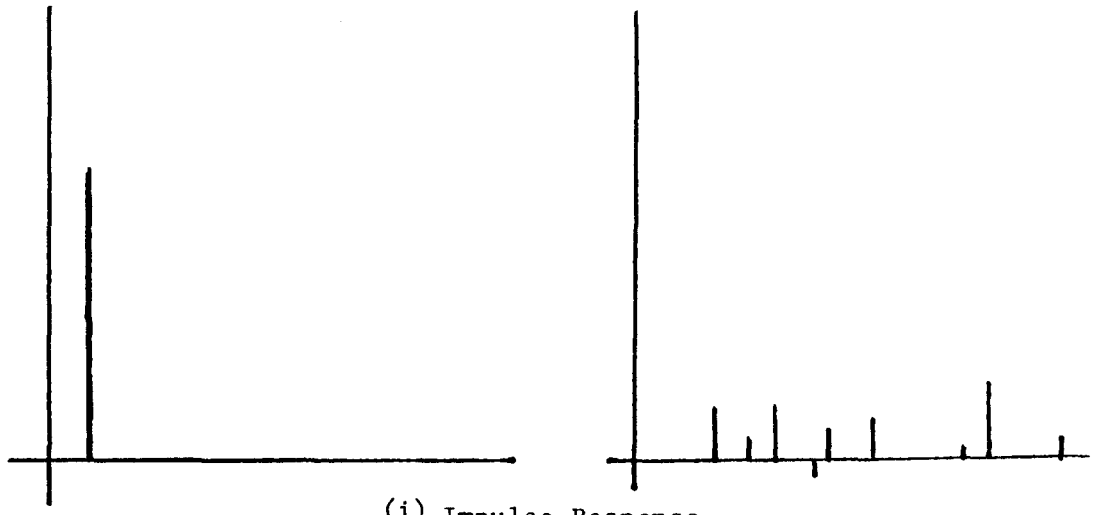

(i) Impulse Response

(a)
INPUT

(b)
OUTPUT

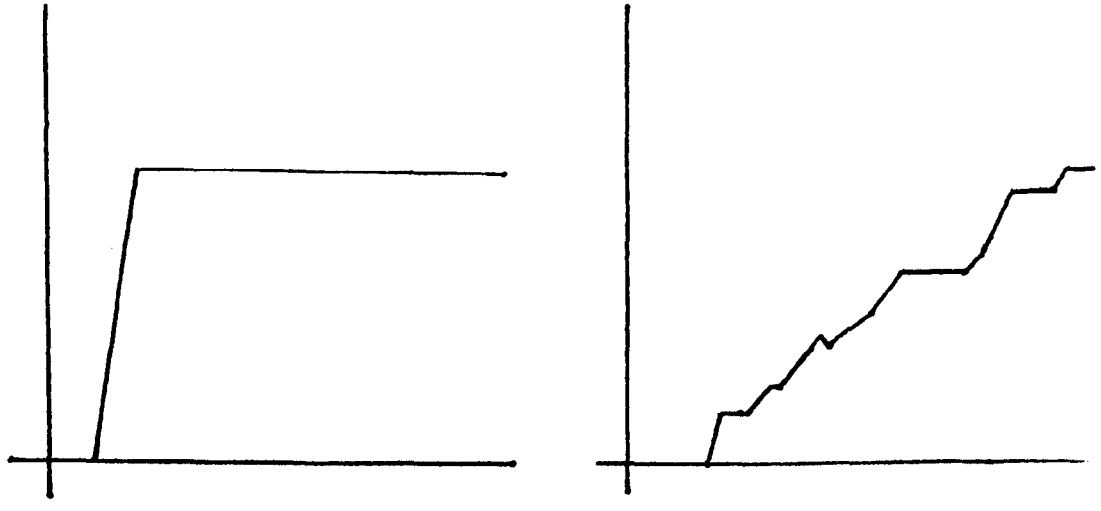

(ii) Ramp Response

(a)
INPUT

(b)
OUTPUT

FIGURE 4.6 Impulse Response Convolution

continual reflection and refraction at the coil junctions. However these travelling waves will be damped to a greater extent in a real coil. Thus it is to be expected that the minor oscillations in the response of the coil to a steep fronted surge, will be more pronounced in the idealised, lossless case than in the real coil in the experimental work. The results demonstrate that this is so.

The results show that turn voltages, and therefore interturn voltages, can be predicted with reasonable accuracy. The omission of losses in the analysis causes small errors to be introduced. The model developed here is a significant improvement on previous models and thus the study, at this stage, is successful. The next stage in the study is the expansion of the model to represent multiturn coils.

CHAPTER FIVE.

EXPANDING THE COIL MODEL TO ANALYSE VOLTAGES IN MULTI-TURN COILS.

5.1. INTRODUCTION.

It has been shown in the preceding sections that the multiconductor transmission line model of a coil is capable of analysing surge distribution in a two turn coil. In this section the model is expanded to enable the analysis of transients in multi-turn coils to take place. Multi-turn form wound coils may be divided into two categories: the single stack type and the multi stack type. Cross sections of a coil side of each of tnese types are shown in figure 5.1 below. The development of the multiturn coil model is identical for the two types of coil. However, since the mathematics is less tedious in the case of the single stack coil, because there is interturn coupling in one direction only, only this development will be given. By simply replacing the admittance matrices of the single coil sections by those for the multi-stack coil sections the model can be used to analyse multi-stack coils.

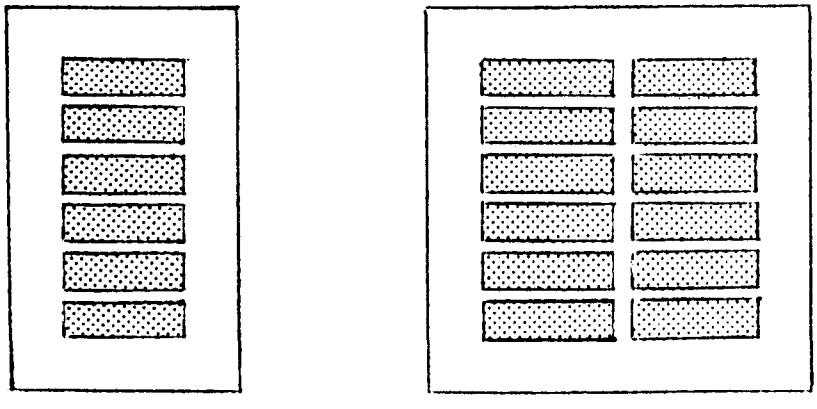

(a)
Single Stack
Coil Side

(b)
Multi Stack
Coil Side

FIGURE 5.1.

5.2. DEVELOPMENT OF THE MULTI-TURN COILS MODEL.

The assumptions made concerning the behaviour of the copper, the coil insulation and the iron core (sections 3.1.1, 3.1.2 and 3.1.3. respectively) are valid for coils with any number of turns. Therefore in this case coils will initially be treated as lossless and the core iron will again be approximated by a flux barrier.

The basis of the analysis is exactly the same as that in the two turn case i.e. the coil is divided into five sections which are connected at five discontinuities or junctions. The derivation of the scatter matrix for a multi-turn coil with a large number of turns is similar to that detailed in section 3.4.2 for the two turn coil. The matrices involved in the derivation are, of course, much larger due to the increased number of turns, however, the end result is unchanged i.e. the incident and reflected voltages are related by the scatter matrix (S) as shown below.

$$(V)^{re} = (S)\ (V)^{in} \tag{5.1}$$

where

$$(S) = \begin{bmatrix} -(C_v) \\ (C_i)(Y) \end{bmatrix}^{-1} \begin{bmatrix} (C_v) \\ (C_i)(Y) \end{bmatrix} \tag{5.2}$$

In the case of a twelve turn coil terminal junction (Y) would be given by;

$$(Y) = \begin{bmatrix} (Z_A) & 0 & 0 & 0 \\ 0 & (Z_B) & 0 & 0 \\ 0 & 0 & (Z_C) & 0 \\ 0 & 0 & 0 & (Z_D) \end{bmatrix}^{-1}$$

where (Z_A) and (Z_D) are 1 x 1 matrices and (Z_B) and (Z_C) are 12 x 12 matrices.

5.3. CALCULATION OF PARAMETERS.

In calculating the parameters for a multiturn coil model as opposed to a two turn coil model some additional considerations are necessary. In the two turn case, ground capacitance was equal for both the turns, whereas in a coil with more than two turns the first and last turns will have a greater ground capacitance than the remainder of the turns. This is because the middle turns present only their edges to ground while the first and last turns present one broad side as well as both edges to ground, (see figure 5.2 below for the slot section of a coil). This is also true for the end winding region of the coil.

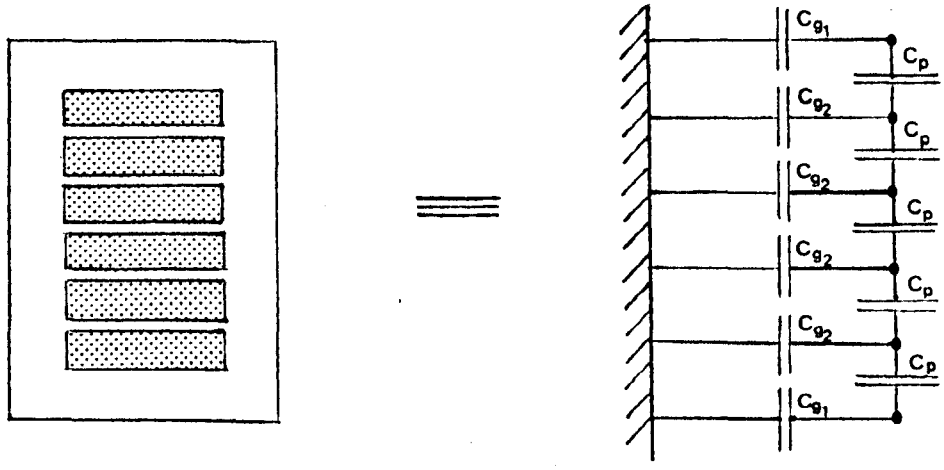

FIGURE 5.2 CAPACITANCES IN THE SLOT PORTION OF MULTICONDUCTOR COIL SIDE.

All the capacitances are again approximated by treating them as parallel plate capacitors in order to keep the calculations simple. The accuracy of this method may be increased, by allowing for fringing of the electric field. This fringing will be small in the interturn field

since there is a high width/seperation ratio, but in the turn to ground field this is not so and therefore fringing will be significant. An estimate of the degree of fringing can be obtained from a curvilinear square analysis of the region in question. Alternatively a field plotting experiment could be carried out.

CHAPTER SIX.

VERIFICATION OF THE MULTI-TURN COIL MODEL.

6.1. RESULTS FROM THE COMPUTER MODEL.

The model for the multi-turn coil developed above was used to analyse transient voltage distribution in a twelve turn coil of the single stack type. (The coil details are shown in Appendix II(b)). The predicted voltages at the terminal junction of a twelve turn, 11 kV coil are shown in figure 6.1. (There are actually thirteen turn voltages shown because at the terminal junction, voltages at both input and output lines can be measured or computed).

6.2. EXPERIMENTAL RESULTS.

The tests were carried out as for the two turn coil. A strip of insulation was removed at the terminal junction of the coil to facilitate the measurement of all the turn voltages. The voltages between each turn and ground are shown, in figure 6.2, for the 600 ns directly following the application of the surge to the coil terminals.

The coil was placed in a stator segment to represent the core iron to test the assumption that the core iron acted as a flux barrier during surges containing high frequency components. The stator core segment which was used had a slot length of approximately half the length of the slot portion of the coil. This, it was felt, was adequate to show whether or not the replacement of the earthed sheath by core iron had any significant effect on the results. The part of the slot portion which was not in the slot was again covered with the earthed sheath. The

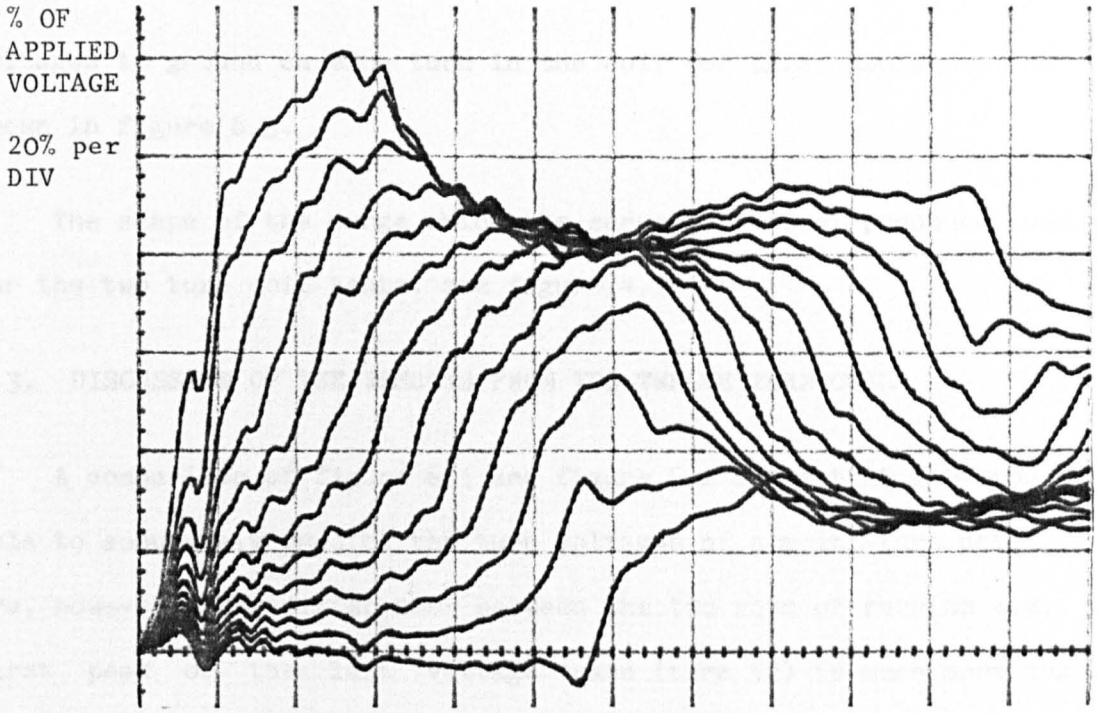

FIGURE 6.1 COMPUTED TURN TO GROUND VOLTAGES ON A SINGLE, LOSSLESS 12 TURN COIL (IN AIR WITH EARTHED SLOT PORTION)

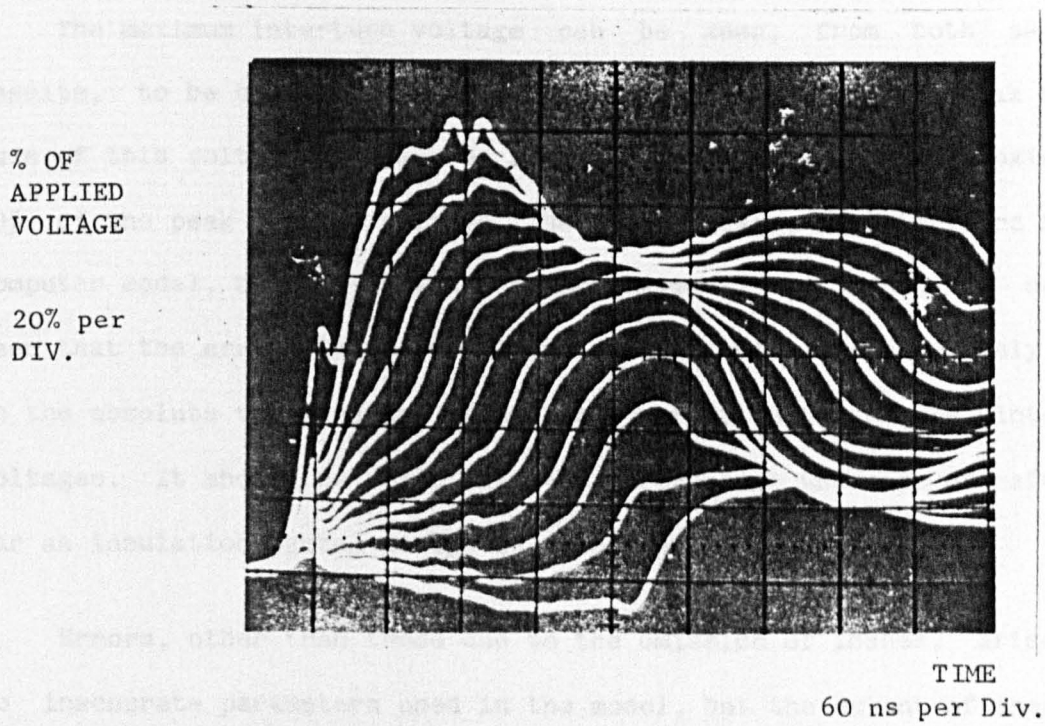

FIGURE 6.2 MEASURED TURN TO GROUND VOLTAGES ON A SINGLE 12 TURN COIL(IN AIR WITH EARTHED SLOT PORTION)

voltages to ground on each turn in the coil for this configuration are shown in figure 6.3.

The shape of the surge which the surge generator produced was as for the two turn coil tests, see figure 4.2.

6.3. DISCUSSION OF THE RESULTS FROM THE TWELVE TURN COIL.

A comparison of figure 6.1 and figure 6.2 shows that the model is able to accurately predict the turn voltages of a multi-turn coil. There are, however, some differences between the two sets of results e.g. the first peak of the last voltage trace (turn 12) is much more sharply defined for the predicted voltage than the measured voltage. In general the minor oscillations of the voltage wave forms are more significant in the predicted voltages. This can be explained, as in section 4.2, by the omission of the losses from the analysis.

The maximum interturn voltage can be seen, from both sets of results, to be between the final two turns of the coil. The peak magnitude of this voltage as measured from the oscillogram is approximately 30% of the peak applied voltage. The same voltage, as calculated by the computer model, has a peak value of approximately 40%. Thus it can be seen that the errors in the predicted results which are relatively small in the absolute voltages can cause large errors (33%) in the interturn voltages. It should be noted that the error is on the side of safety as far as insulation system design is concerned.

Errors, other than those due to the omission of losses, arise due to inaccurate parameters used in the model, but the extent of these can not be seen until a comparison with results from a lossy model has been

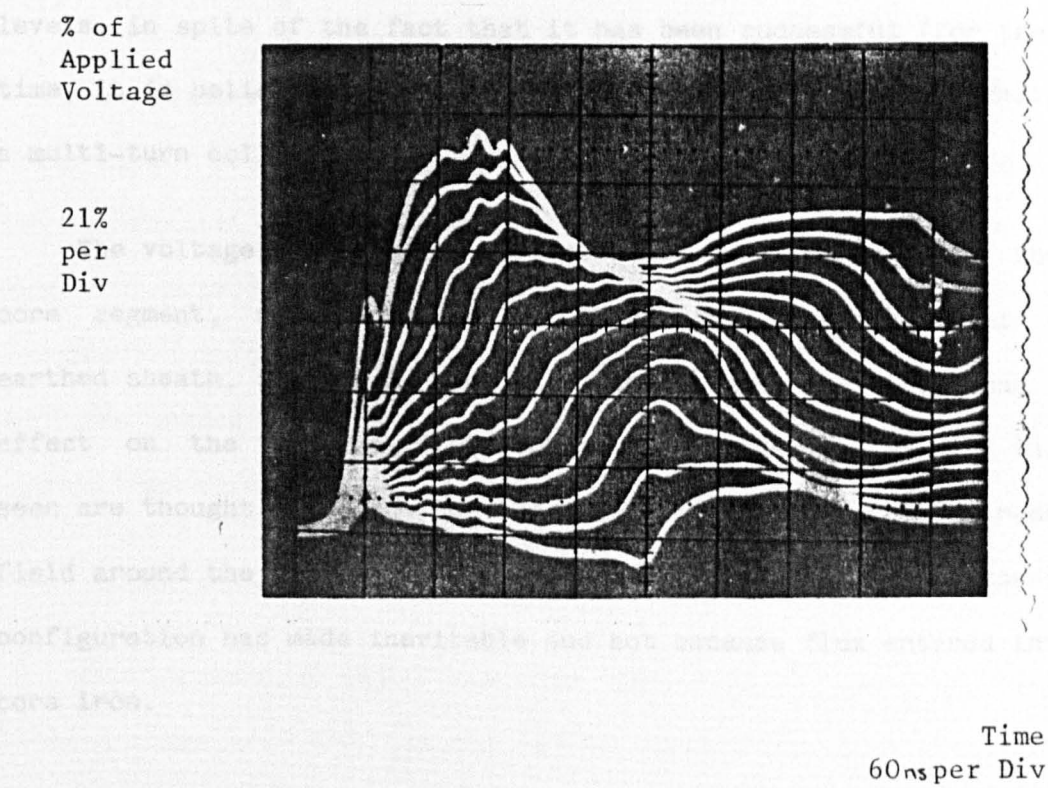

FIGURE 6.3 Measured turn to ground voltages on a single, 12 turn coil in iron

carried out. Until the discrepancies between predicted and measured interturn voltages, pointed out above, have been greatly reduced, the method is limited in its value in the design of interturn insulation levels, in spite of the fact that it has been successful (for the first time, it is believed) in predicting reasonably well the turn voltages in a multi-turn coil.

The voltage traces which were obtained from the coil in the iron core segment, when compared to those from the coil in air with an earthed sheath, (figure 6.2 and 6.3), show that the iron has little effect on the voltage distribution. The slight differences which are seen are thought to be due to the slightly different electromagnetic field around the end region of the coil which the different experimental configuration has made inevitable and not because flux entered into the core iron.

In order that the accuracy of the predicted results could be improved, it was decided to include losses into the coil model at this stage.

CHAPTER SEVEN.

METHOD OF INCLUDING LOSSES IN THE ANALYSIS.

7.1. INTRODUCTION.

The lossless model of a coil has been found to be more accurate than other methods of surge analysis. However there are significant inaccuracies in the predicted interturn voltages. It is therefore necessary to introduce losses into the analysis. While it is possible to develop the multiconductor transmission line part of the analysis to include losses, it is not possible to use scatter matrices with lossy lines. Thus an alternative method must be devised.

7.2. ASSUMPTIONS AND APPROXIMATIONS.

The frequencies which comprise the initial part of the steep fronted surge are very high. It can be assumed that they limit the depth of penetration into the copper to a very small fraction of the cross sectional dimensions of the turn, see section 3.1.1. It follows that even when losses are present it is reasonable to ignore any effect which the internal inductances have on the coil section inductance matrix.

The main effect of the losses will be to decay travelling waves as they propagate along the coil section. Since the contribution of any single travelling wave to the total voltage on any turn is small, it is not necessary to take account of the losses continuously during the transient disturbance. If the losses are lumped at discrete intervals along the coil side, then their effect is adequately taken into account. It is proposed here that losses are adequately accounted for by lumping

them at each end of a coil section. Thus each coil junction will become a junction of lossless multiconductor transmission lines tied together (and to ground, if insulation losses are included) by a network of resistances. It will be shown (see section 7.2) that these resistances can be included in the scatter matrix.

The inclusion of losses in multiconductor transmission line theory means that there will be at least two modes of propagation in the coil sections. However, since the time interval between reflections in the coil is small compared to the surge rise times (even if the rise time is as small as 25 ns) then the time difference between when each part of the surge arrives at the next junction will be very small and is neglected here.

The speed of wave propagation will be slightly diminished by the losses in the coil. However, since the losses are small their effect on the speed of the waves will be neglected here and the lossless speed will be used. Distortion of each travelling wave is also neglected since the time of interest is so short.

In addition, no account is taken of the dependence of the losses on frequency since the losses were calculated at one particular frequency. The approximation of frequency independence is reasonable in view of the fact that during the short period of the transient to be analysed the upper frequency limit will not vary greatly. In any case, Lammeraner and Stafl (22) show that for high frequencies the conductor resistance approaches a constant value due to skin and proximity effects (see following section).

7.3. CALCULATION OF LOSS PARAMETERS.

There are two types of losses to be accounted for in the coil. Firstly copper losses, which can be thought of as being in series with each conductor and secondly dielectric losses due to leakage current in the coil insulation which are represented by high resistance shunt paths both between turns and to ground.

The values of the shunt losses associated with any section of conductor can be calculated as in section 3.1.2. Calculation of copper losses is more complex. There are two effects which must be taken into account. Firstly the skin effect in the conductor due to the self induced e.m.f. caused by the current in that conductor. Secondly the skin effect due to the e.m.f. caused by the currents in all the other conductors of the coil. This second effect is known as the proximity effect.

The effect of the skin effect on the conductor resistances can be calculated simply at a single frequency by assuming that all the current flows in a thin outer layer of the conductor. The proximity effect is more complex since the influence of adjacent conductors will depend on conductor and insulation geometry. A rigorous analysis of the proximity effect in a coil side at high frequency is almost certainly impossible. In fact even an approximate analysis with good accuracy is not available in the literature and is beyond the scope of this investigation. Therefore some relatively crude approximations are justified. The following approximations are found to give good results.

Since the frequencies are high the intrinsic skin depth of the

copper (as calculated from one dimensional theory) is much smaller than the conductor cross-sectional dimensions. It has been shown by Lammeraner and Stafl (22) that, providing frequencies are even moderately high, the proximity factor for a given conductor arrangement approaches an asymptotic value which is independent of the frequency. Therefore, for the range of frequencies which comprise the surges of interest in this study, a single valued proximity factor can be used. Thus

$$R = k_p R_{a.c.}$$

where $R_{a.c.}$ is the a.c. resistance of the conductor itself with no external influence from neighbouring conductors i.e. allowing for skin effect only. (k_p is the proximity factor.)

In the case of a perfectly coupled two turn coil (i.e. all the flux from one turn links with the other turn) the asymptotic value of k_p is given as

$$k_p = 1 + \frac{2}{3}(n^2 - 1)$$
$$= 3$$

by Lammeraner and Stafl (22) pp. 124. In a multi-turn coil side with perfect coupling k_p will incease significantly with the number of turns, however since the iron acts as a flux barrier and not as the near perfect, low reluctance path assumed by Lammeraner and Stafl, then their value of k_p must be modified to take account of the imperfect coupling. To this end it is assumed that the proximity effect on any turn is determined only by the adjacent turns and that k_p due to the influence of the immediatly adjacent conductors (i.e. as for a three turn coil side) is modified by a factor which is the ratio of the copper depth to

the sum of the copper depth and the interturn insulation depth i.e. $\frac{2 \cdot 0}{2 \cdot 6}$ = 0.77 since this approximately represents the fraction of the flux from the current carrying turn which will link with the next turn. Thus the value of k_p is 0.77 x $1 + \frac{2}{3}(n^2 - 1)$ for all coils with more than three turns, i.e. k_p = 4.9, for the coil in Appendix II(b).

In calculating the depth of penetration of the surge into the conductor, the frequency used corresponded to that of treating the front time of the surge as a quarter sine wave.

7.4. GENERAL BASIS OF THE METHOD.

To introduce the series losses into the analysis the losses in each section of conductor are modelled by two resistors (one at each end of the section). Thus each junction becomes a junction of a lossless conductors interconnected by discrete resistances. In the lossless case a scatter matrix was developed by utilising relationships between travelling waves on each line. It is now shown that discrete resistances at the junction can be included in the development of the scatter matrix.

Shunt losses (i.e. losses due the imperfect dielectric) can also be represented by lumped resistances which, in this case, interconnect the parallel lossless lines and also connect them to ground. These losses are calculated from the loss tangent of the insulation and can also be included in the development of the scatter matrix.

7.5. DEVELOPMENT OF THE LOSSY SCATTER MATRIX.

By using figure 7.1, below, as a model for a multiconductor transmission line junction (in this case the terminal junction, although

the theory is valid for any junction type) in which lossy elements are present at the end of each section, a scatter matrix can be developed which when used in the complete model will take into account both copper and dielectric losses.

The development of the lossy scatter matrix is similar to the development of the lossless scatter matrix due to Agrawal and shown in section 3.4.2. The lossy scatter matrix can be developed to include either the series losses or the insulation losses. Alternatively the generalised lossy scatter matrix can be developed to include all losses, it is the latter which is developed below. In order to examine the effects of each type of loss seperately the generalised lossy scatter matrix can be used with the appropriate parameters set to zero.

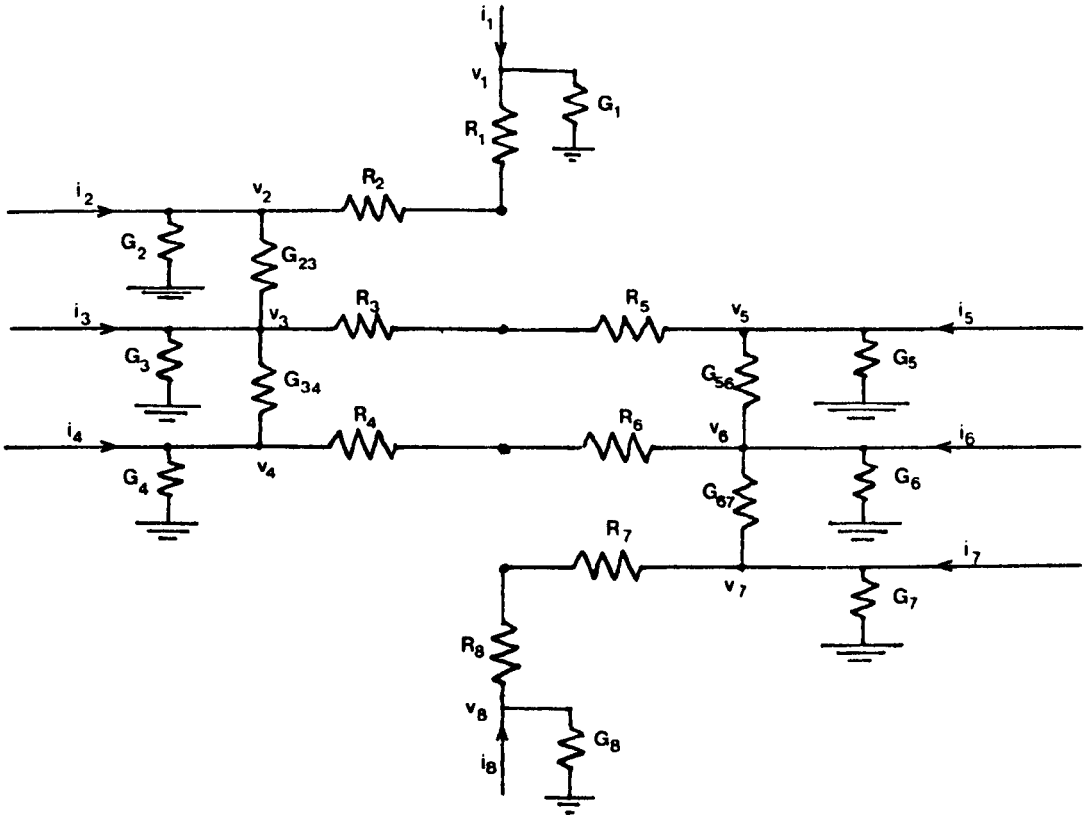

FIGURE 7.1 LOSSY TERMINAL JUNCTION OF A THREE TURN COIL.

Figure 7.1 shows the terminal junction of a three turn coil. Applying Kirchhoff's voltage law gives

$$v_1 - (i_1 - v_1G_1)R_1 - v_2 + \left[i_2 - v_2G_2 - (v_2 - v_3)G_{23}\right]R_2 = 0$$

$$v_3 - \left[i_3 - v_3G_3 - (v_3 - v_4)G_{34} - (v_3 - v_2)G_{23}\right]R_3 - v_5 + \left[i_5 - v_5G_5 - (v_5 - v_6)G_{56}\right]R_5 = 0$$

$$v_4 - \left[i_4 - v_4G_4 - (v_4 - v_3)G_{34}\right]R_4 - v_6 + \left[i_6 - v_6G_6 - (v_6 - v_5)G_{56} - (v_6 - v_7)G_{67}\right]R_6 = 0$$

$$v_7 - \left[i_7 - v_7G_7 - (v_7 - v_6)G_{67}\right]R_7 - v_8 + (i_8 - v_8G_8)R_8 = 0$$

The right hand sides of the above equations can be combined into a single matrix which is equated to zero. The terms v_1, v_2, ... etc. can be isolated into their own matrix which can be further decomposed (in the same manner as in section 3.4.2) i.e.

$$\begin{bmatrix} v_1 - v_2 \\ v_3 - v_5 \\ v_4 - v_6 \\ v_7 - v_8 \end{bmatrix} = \begin{bmatrix} 1 & -1 & 0 & 0 & 0 & 0 & 0 & 0 \\ 0 & 0 & 1 & 0 & -1 & 0 & 0 & 0 \\ 0 & 0 & 0 & 1 & 0 & -1 & 0 & 0 \\ 0 & 0 & 0 & 0 & 0 & 0 & 1 & -1 \end{bmatrix} \begin{bmatrix} v_1 \\ v_2 \\ v_3 \\ v_4 \\ v_5 \\ v_6 \\ v_7 \\ v_8 \end{bmatrix} = (C_v)(V) \qquad (7.2)$$

In addition the terms i_1R_1, i_2R_2, ... etc. can be isolated and expressed as

$$\begin{bmatrix} -i_1R_1 + i_2R_2 \\ -i_3R_3 + i_5R_5 \\ -i_4R_4 + i_6R_6 \\ -i_7R_7 + i_8R_8 \end{bmatrix} = -\begin{bmatrix} 1 & -1 & 0 & 0 & 0 & 0 & 0 & 0 \\ 0 & 0 & 1 & 0 & -1 & 0 & 0 & 0 \\ 0 & 0 & 0 & 1 & 0 & -1 & 0 & 0 \\ 0 & 0 & 0 & 0 & 0 & 0 & 1 & -1 \end{bmatrix} X$$

$$\begin{bmatrix} R_1 & 0 & 0 & 0 & 0 & 0 & 0 & 0 \\ 0 & R_2 & 0 & 0 & 0 & 0 & 0 & 0 \\ 0 & 0 & R_3 & 0 & 0 & 0 & 0 & 0 \\ 0 & 0 & 0 & R_4 & 0 & 0 & 0 & 0 \\ 0 & 0 & 0 & 0 & R_5 & 0 & 0 & 0 \\ 0 & 0 & 0 & 0 & 0 & R_6 & 0 & 0 \\ 0 & 0 & 0 & 0 & 0 & 0 & R_7 & 0 \\ 0 & 0 & 0 & 0 & 0 & 0 & 0 & R_8 \end{bmatrix} \begin{bmatrix} i_1 \\ i_2 \\ i_3 \\ i_4 \\ i_5 \\ i_6 \\ i_7 \\ i_8 \end{bmatrix} = -(C_v)(R)(I) \qquad (7.3)$$

The remaining terms can be expressed as

$$\begin{bmatrix} v_1 G_1 R_1 - v_2 G_2 R_2 - (v_2 - v_3) G_{23} R_2 \\ v_3 G_3 R_3 - (v_3 - v_2) G_{23} R_3 - (v_3 - v_4) G_{34} R_3 - v_5 G_5 R_5 - (v_5 - v_6) G_{56} R_5 \\ v_4 G_4 R_4 - (v_4 - v_3) G_{34} R_4 - v_6 G_6 R_6 - (v_6 - v_5) G_{56} R_6 - (v_6 - v_7) G_{67} R_6 \\ v_7 G_7 R_7 - (v_7 - v_6) G_{67} R_7 - v_8 G_8 R_8 \end{bmatrix}$$

$$= (C_v)(R)(G)(V) \qquad (7.4)$$

where

$$(G) = \begin{bmatrix} G_1 & 0 & 0 & 0 & 0 & 0 & 0 & 0 \\ 0 & (G_2+G_{23}) & -G_{23} & 0 & 0 & 0 & 0 & 0 \\ 0 & -G_{23} & (G_{23}+G_3+G_{34}) & -G_{34} & 0 & 0 & 0 & 0 \\ 0 & 0 & -G_{34} & (G_4+G_{34}) & 0 & 0 & 0 & 0 \\ 0 & 0 & 0 & 0 & (G_5+G_{56}) & -G_{56} & 0 & 0 \\ 0 & 0 & 0 & 0 & -G_{56} & (G_{56}+G_6+G_{67}) & -G_{67} & 0 \\ 0 & 0 & 0 & 0 & 0 & -G_{67} & (G_7+G_{67}) & 0 \\ 0 & 0 & 0 & 0 & 0 & 0 & 0 & G_8 \end{bmatrix}$$

Combining equations (7.1) to (7.4) gives a single matrix equation

$$(C_v)(V) - (C_v)(R)(I) + (C_v)(R)(G)(V) = 0 \qquad (7.5)$$

It should be noted that the construction of the conductance matrix (G) is equivalent to that of the capacitance matrix (C), thus enabling (G) to be constructed using the same programme as for (C).

By splitting the current and voltage matrices into their incident and reflected components using equations 3.4 and 3.5 and by using the equations relating incident and reflected currents to incident and reflected voltages (equations 3.6 and 3.7), equation 7.5 can be reduced to one relating reflected voltage to incident voltage, i.e.

$$\left[(C_v) - (C_v)(R)(Y) + (C_v)(G)(R)\right](V)^{in} = \left[-(C_v) - (C_v)(R)(Y) - (C_v)(G)(R)\right](V)^{re} \qquad (7.6)$$

The current equations for the junction are

$$i_1 - v_1G_1 + i_2 - v_2G_2 - (v_2 - v_3)G_{23} = 0$$

$$i_3 - v_3G_3 - (v_3 - v_2)G_{23} - (v_3 - v_4)G_{34} + i_5 - v_5G_5 - (v_5 - v_6)G_{56} = 0$$

$$i_4 - v_4G_4 - (v_4 - v_3)G_{34} + i_6 - (v_6 - v_5)G_{56} - v_6G_6 - (v_6 - v_7)G_{67} = 0$$

$$i_7 - v_7G_7 - (v_7 - v_6)G_{67} + i_8 - v_8G_8 = 0$$

These too can be rearranged to give a single matrix equation, i.e.

$$(C_i)(I) - (C_i)(G)(V) = 0 \qquad (7.7)$$

where

$$(C_i) = \begin{bmatrix} 1 & 1 & 0 & 0 & 0 & 0 & 0 & 0 \\ 0 & 0 & 1 & 0 & 1 & 0 & 0 & 0 \\ 0 & 0 & 0 & 1 & 0 & 1 & 0 & 0 \\ 0 & 0 & 0 & 0 & 0 & 0 & 1 & 1 \end{bmatrix}$$

Both (C_v) and (C_i) remain unchanged from the lossless coil.

From 7.7 also we can derive an expression connecting reflected voltage to incident voltage by using equations 3.4, 3.5, 3.6 and 3.7 again to give

$$\left[(C_i)(Y) - (C_i)(G)\right](V)^{in} = \left[(C_i)(Y) + (C_i)(G)\right](V)^{re} \qquad (7.8)$$

Equations 7.6 and 7.8 can be combined, in order to obtain invertible, square matrices, giving;-

$$(V)^{in} = (S_L)\,(V)^{re} \qquad (7.9)$$

where

$$(S_L) = \begin{bmatrix} -(C_v) - (C_v)(R)(Y) - (C_v)(G)(R) \\ (C_i)(Y) + (C_i)(G) \end{bmatrix}^{-1} \begin{bmatrix} (C_v) - (C_v)(R)(Y) + (C_v)(G)(R) \\ (C_i)(Y) - (C_i)(G) \end{bmatrix}$$

and is the lossy scatter matrix for the junction. It should be noted that this method predicts voltages v_1 , v_2 , v_3 ,... etc. which are not the actual voltages at the junction, (see figure 7.1).

7.6. USE OF THE LOSSY SCATTER MATRIX IN THE ANALYSIS.

This method of including losses into the coil model has the advantage that the programmes which were developed to calculate the impulse response from the scatter matrices for the lossless model can be used, with only minimal alteration, in the lossy model. The only alteration which has to be made is to the programme which constructs the scatter matrices.

A problem which arises when using the lossy model is that it predicts voltages which do not actually exist. This occurs because the voltages which are predicted are those appearing on the `imaginary' lossless lines which are connected to the junction through resistances and therefore differ from the junction voltages (see figure 7.2 below).

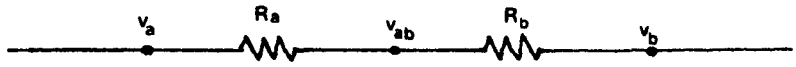

FIGURE 7.2 LOSSY JUNCTION OF TWO CONDUCTORS.

This difficulty can be overcome by noting that the power loss in each section of each turn of the model is equal to the power loss in each section of each turn of the actual coil. Thus if v_a and v_b are the voltages predicted by the lossy scatter matrix, then v_{ab} can be found from

$$v_{ab} = v_a + \left(\frac{v_b - v_a}{R_a + R_b}\right) R_a \qquad \Rightarrow$$

$$\Rightarrow \qquad v_{ab} = \frac{v_a R_b + v_b R_a}{R_a + R_b}$$

Thus the actual junction voltage v_{ab} is easily obtained.

In the lossless model it is be possible to predict the voltage at any point on the coil since the magnitude, and velocity of all waves in all sections of the coil can be calculated. In the lossy case the lossless lines do not actually exist and so predicting the mid-section voltages by calculating the summation of travelling waves at such a point is not valid. However, the voltage difference between points on the same turn (at neighbouring junctions) will be small and so a knowledge of all turn voltages at all the coil junctions, but not at mid section points, will be adequate in analysing any particular coil response. If, however, more detail is required then a model with more junctions can be used.

Greater accuracy could be obtained by splitting the losses up into smaller resistances at points along each conductor section. This will, however, increase the number of junctions in the model (as each point where there is a resistance will have to be treated as a junction) and so increase the number of calculations necessary, and so increase numerical errors built up by each successive calculation. Also, computation time will be greatly increased.

The lossy scatter matrix developed above is, it is believed, original and was developed in this study as the most straight forward method of including losses into the multiconductor transmission line model of motor coils.

An alternative method of accounting for losses in the analysis was considered. In this method every travelling wave in the coil is modified by a decay factor which would allow for the attenuation of the waves as they propagated along each conductor. The difficulty in calculating these decay factors when compared to the simplicity of the lossy scatter matrix method combined with the ability of the latter to utilise the lossless coil impulse response programme were adequate reasons to chose the lossy scatter matrix method as the method to be adopted.

CHAPTER EIGHT.

EXTENDING THE MODEL TO REPRESENT A MACHINE WINDING.

Machine windings consist of many coils of the type analysed in the preceding sections. It was stated in section 3.1.3 that coils in windings could be treated separately since the iron acted as a flux barrier between successive coils and that intercoil coupling in the end winding region can be neglected. Having constructed a model which represents a single coil, a model for a whole phase of a machine winding can be built up using a number of the single coil models in cascade.

In a machine winding, successive coils are connected by copper leads which are covered with insulation of the same quality and dimensions as the turn to ground insulation of the end winding region of the coils, therefore the capacitance per unit length, and so the characteristic admittance, of the interlinks can be calculated by the same method. If these interlinks are treated as short transmission lines it can be seen that for a multi-coil winding there will be three distinct types of terminal junction i.e. (i) where two coil sections meet the input line and an interlink, (ii) where two coil sections meet two interlinks and (iii) where two coil sections meet an interlink and the neutral termination. Therefore three different terminal junction scatter matrices must be formed. The iron to air junctions will be identical for all the coils in the winding since all the coils will be identical in every respect.

This model of a winding can predict any voltage on any turn of any coil although, as in the single coil model, voltage prediction at exist-

ing coil junctions (terminal or iron/air) is easier. However, it is unlikely that there will be any need to predict voltages on any coil except the line end coil, as previous experimental investigations on windings and also the preceding study of single coils have shown that it is the first coil in which the high interturn voltages occur.

The model can be used in either the lossless or the lossy form with little alteration to the impulse response programme, the losses being embodied in the scatter matrix.

The extended model representing two series connected coils was used to predict the response of the first of the coils to the same surge that was used for testing the single coil model. The predicted voltages on the first coil are shown with those for the single coil model in figure 8.1. It can be seen, from figure 8.1, that it is only in the latter part of the first coil that the turn voltages are affected by the addition of more coils to the model. It is also clear that these voltages are only affected after approximately 270 ns, and so there is little effect on the magnitude or position of the peak interturn voltages. The reason for this is as follows. The electromagnetic coupling between turns, although important in the analysis of the coil, is responsible for only part of the transfer of the surge from the input of the coil to the output. The remainder of the surge, the largest part, must travel through the coil, turn by turn. Thus very little of the surge appears at the coil output (turn 12 in this case) until a certain period of time (approximately n x the travel time of one turn) has elapsed. The coil in question has a turn travel time of 22.4 ns, therefore it is not until a time period of 268.8 ns (=12 x 22.4 ns) has elapsed that a significant

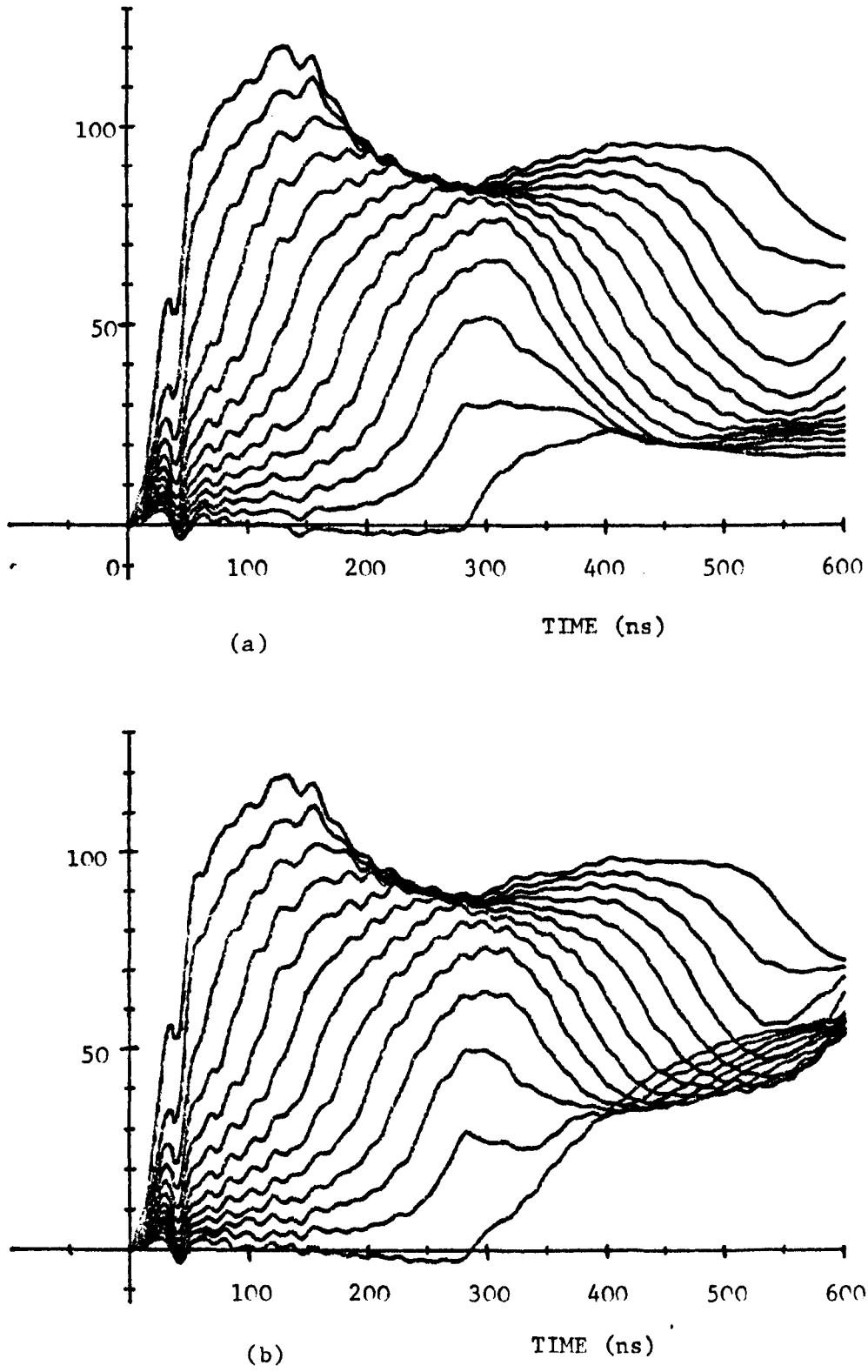

FIGURE 8.1 Turn to ground voltages on a twelve turn, 11kV coil.

(a) Single coil
(b) First coil of winding

voltage appears on the coil output. Thus, since very little of the surge emerges from the first coil until after 268.8 ns, the remaining coils in the winding can have very little effect on the voltages within the first coil until that time.

The voltages shown in figure 9.4(a) are those predicted in the second of the two coils of the model. This confirms that very little of the applied surge can reach the second coil until it has travelled, turn by turn, through the first coil. Therefore for a third coil to have an effect on the voltages in the first coil, the surge must travel through both the first and second coils and also back through the second coil, a time totaling approximately 800 ns. This time is beyond that at which very large interturn voltages may occur and so a model of two coils is sufficient to predict the voltages in the first coil of a 12 turns per coil winding during the time of interest. Consequently much computer time and storage space can be saved by using a truncated winding model. However it should be noted that the number of coils needed to give the voltage distribution in the first coil is dependent on the number of turns per coil. Decreasing the turns per coil will result in an increase in the number of coils needed in the winding model.

To use the model to predict voltages in windings where there are a number of parallel paths an additional junction can be introduced at the common line end point. Since all the paths will be identical, the reflections in all of them need not be computed. By noting that all the impulses arriving at the common point, from the parallel windings are equal a simple 2 x 2 scatter matrix can be calculated which will enable voltages in the cable and in one of the parallel windings to be computed

thus saving much computation time.

CHAPTER NINE.

VERIFICATION OF THE LOSSY MODEL FOR SINGLE AND MULTI-COIL WINDINGS.

9.1. RESULTS.

The lossy coil model, representing the two turn coil, was used to predict the voltages on each turn of that coil. The effect of increasing the losses can be seen in figure 9.1 in which the turn voltages for (a) the losses as calculated and (b) half the calculated losses are shown. It can be seen from the comparison of figure 4.4 and 4.5 with figure 9.1 that the inclusion of losses improves the accuracy of the model.

Figure 9.2 shows the voltages predicted by both the lossless and the lossy models of the single twelve turn coil. These predicted results can be compared with the measured results in figure 6.2.

The tests on the two 12 turn coils in series were carried out with the coils in the stator core segment. This was done to ensure that the separation between the coils was adequate. This is not important for the slot portions of the coil, due to the flux barrier effect of the iron, but is so for the end winding portions. The coils were placed in adjacent slots and connected in series. The neutral lead of the second coil was connected to earth through a resistance which represented the remainder of the winding. The test surge (see figure 4.2) was applied to the coils as in section 4.1. The voltage distribution recorded in the line end coil is shown in figure 9.3(a). The voltage distribution recorded in the second coil is shown in figure 9.4(b).

Oscillograms of the interturn voltages in the first of the two

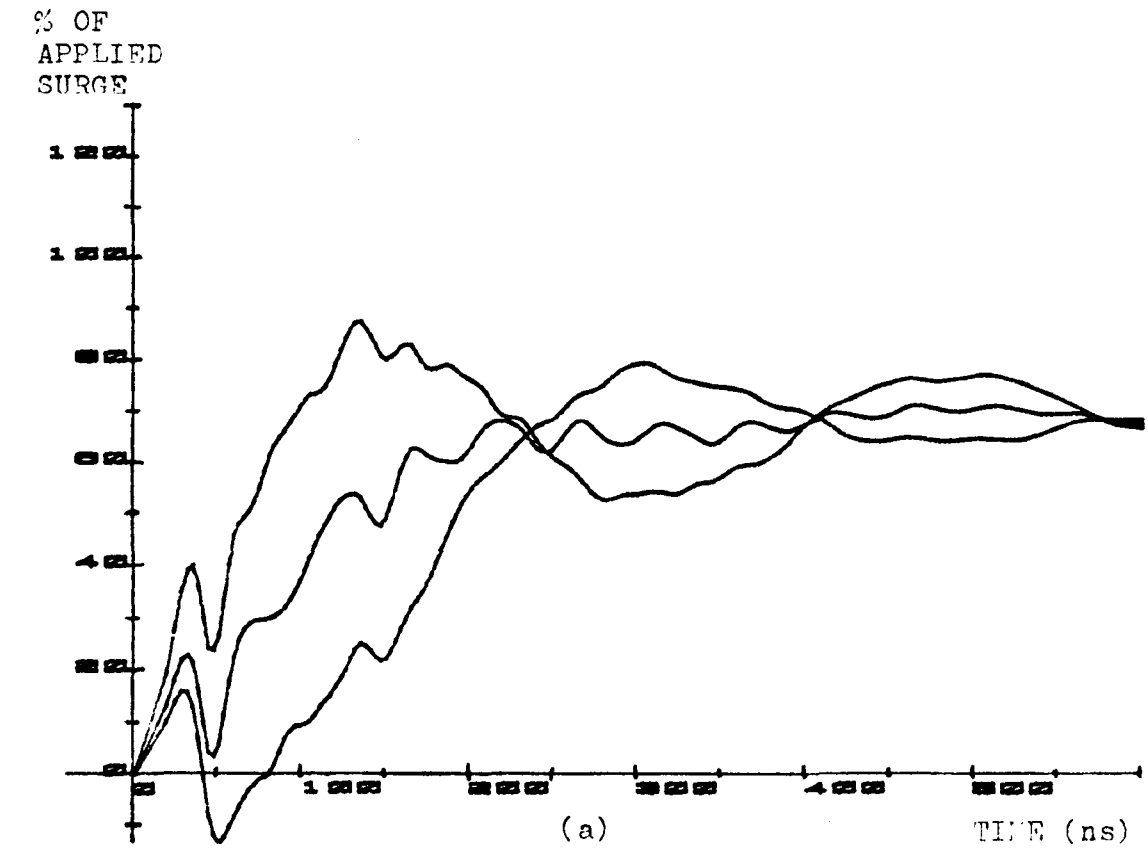

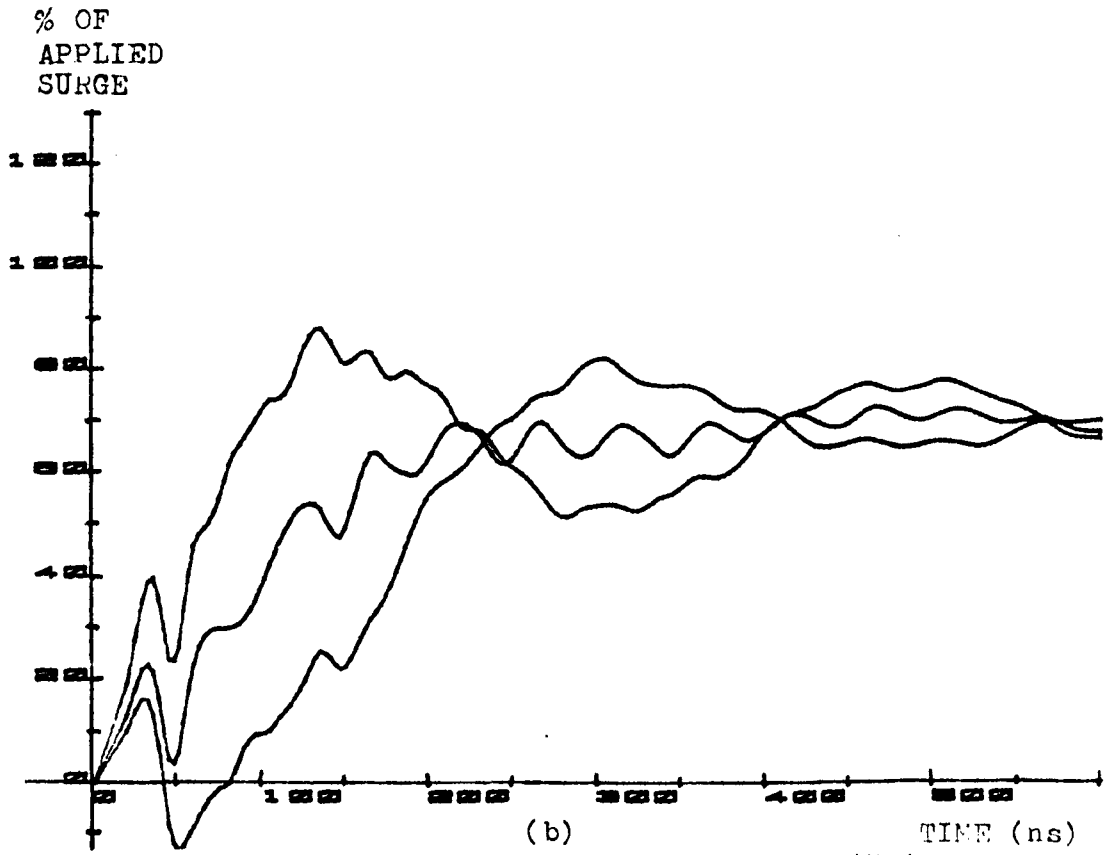

FIGURE 9.1 COMPUTED TURN TO GROUND VOLTAGES ON A TWO TURN COIL (a) Including losses as calculated (b) Including 50% of calculated losses

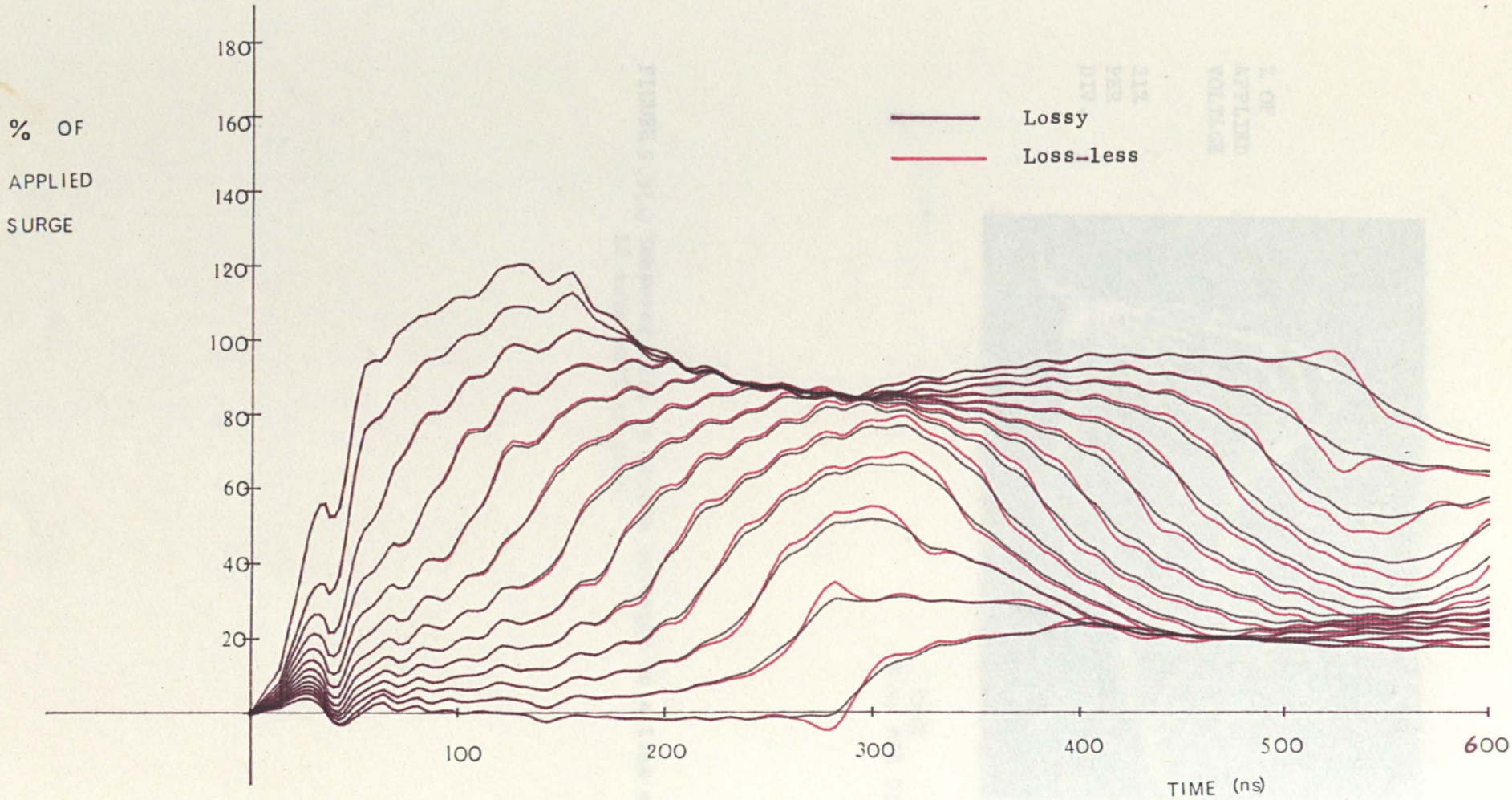

FIGURE 9.2 Loss-less and lossy turn to ground voltages on an 11kV, 12 turn, single coil - test pulse.

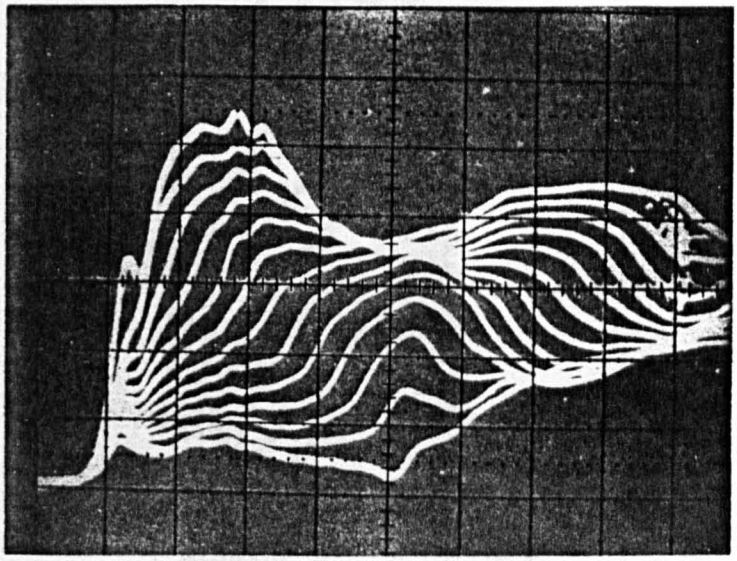

FIGURE 9.3(a) Measured turn to ground voltages on a line end, 12 turn coil in iron.

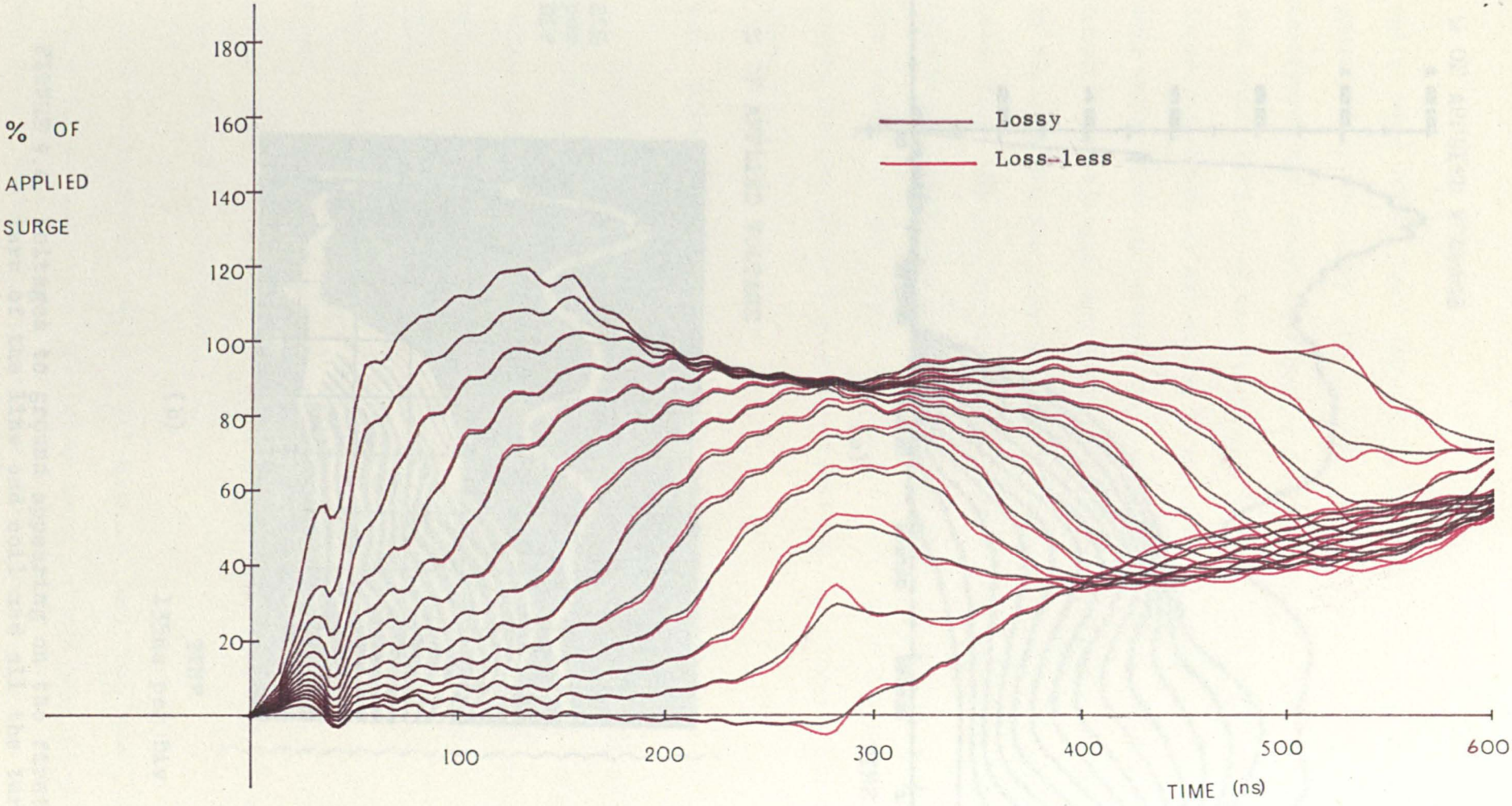

FIGURE 9.3(b) Loss less and lossy turn to ground voltages on an 11kV, 12 turn, line end coil-test pulse.

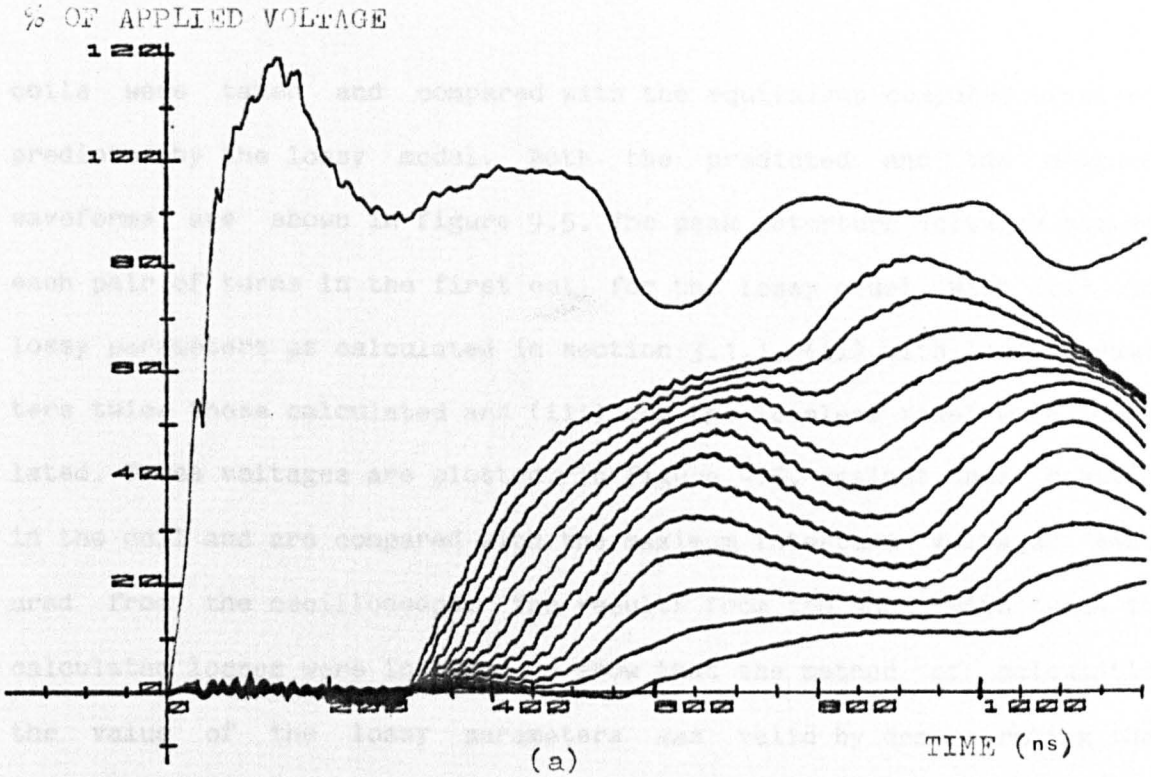

(a)

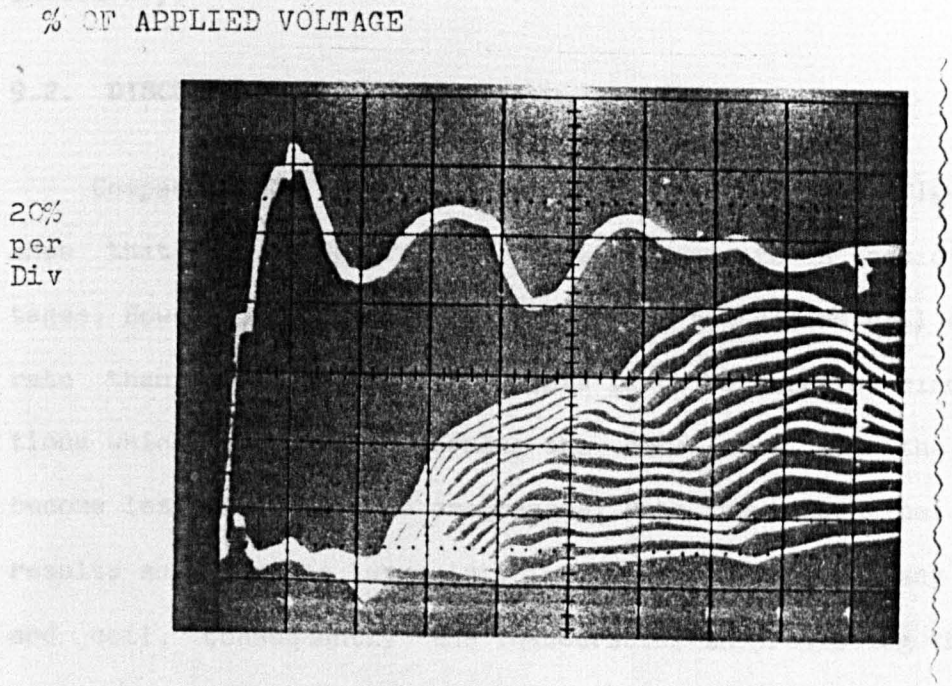

(b)

FIGURE 9.4 Voltages to ground appearing on the first turn of the line end coil and all the turns of the second coil.

(a) Computed

(b) Measured

coils were taken and compared with the equivalent computed waveforms predicted by the lossy model. Both the predicted and the measured waveforms are shown in figure 9.5. The peak interturn voltages between each pair of turns in the first coil for the lossy model with (i) the lossy parameters as calculated in section 3.1.1, (ii) with lossy parameters twice those calculated and (iii) for the lossless model were calculated. These voltages are plotted, in figure 9.6, against their position in the coil and are compared with the maximum interturn voltages measured from the oscilloscope. The results from the model with twice the calculated losses were included to show that the method of calculating the value of the lossy parameters was valid by demonstrating that overestimation, as well as underestimation, of losses could lead to inaccuracy.

9.2. DISCUSSION OF RESULTS.

Comparisons of measured and predicted results (figures 9.3-9.6) show that the model for two coils is accurate in predicting turn voltages. However, the predicted voltages in the second coil are less accurate than those for the first. This is to be expected since the assumptions which were made concerning the core iron and the losses will become less valid as time progresses. Both the theoretical and predicted results show that no large interturn voltages occur in any but the line end coil. Consequently the inaccuracies in predicting the second coil turn voltages are acceptable.

A comparison of predicted voltages obtained from the lossy model including and omitting dielectric losses showed that these losses had almost no discernible effect on the turn voltages. The largest

% OF APPLIED VOLTAGE

10% per Div

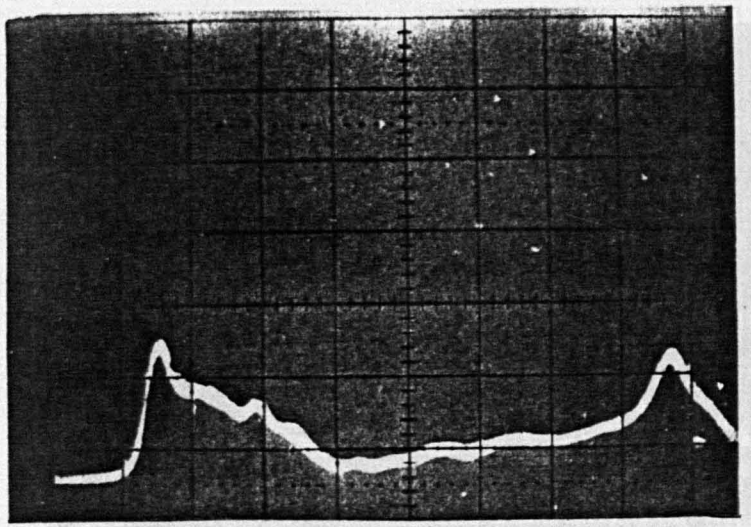

Voltage between line end and turn 1

(a)

(b)

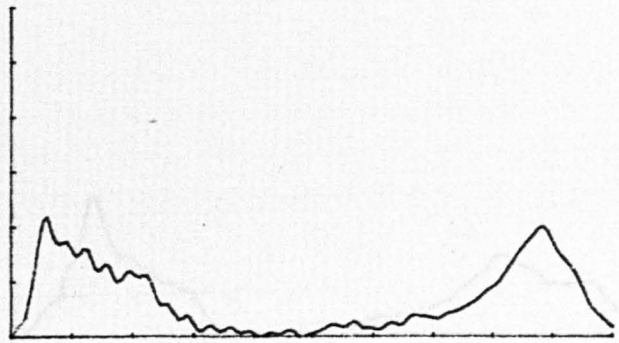

% OF APPLIED VOLTAGE

10% per Div

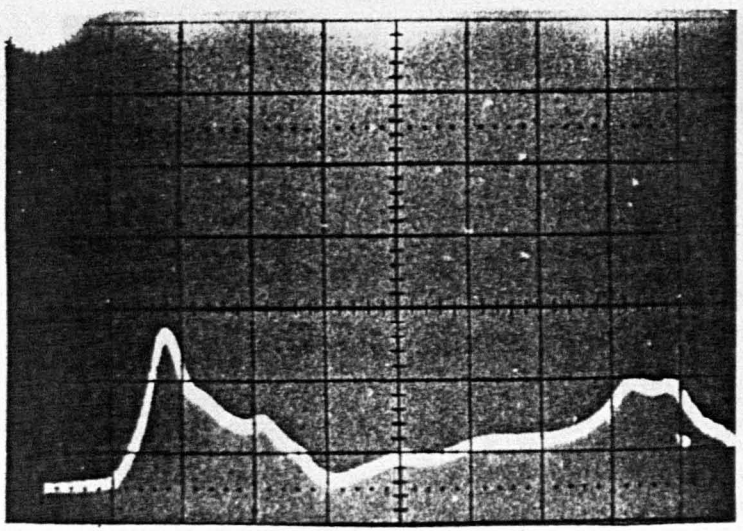

Voltage between turn 1 and 2

(a)

(b)

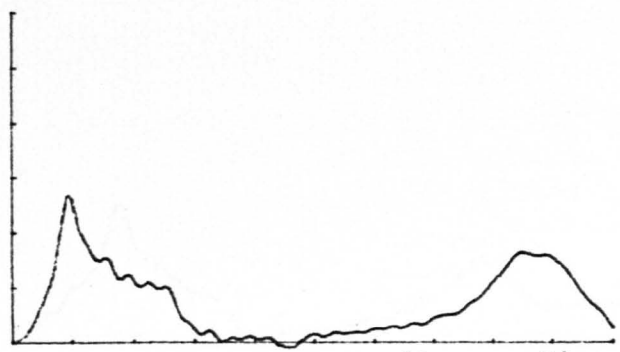

FIGURE 9.5 Measured and computed interturn voltages

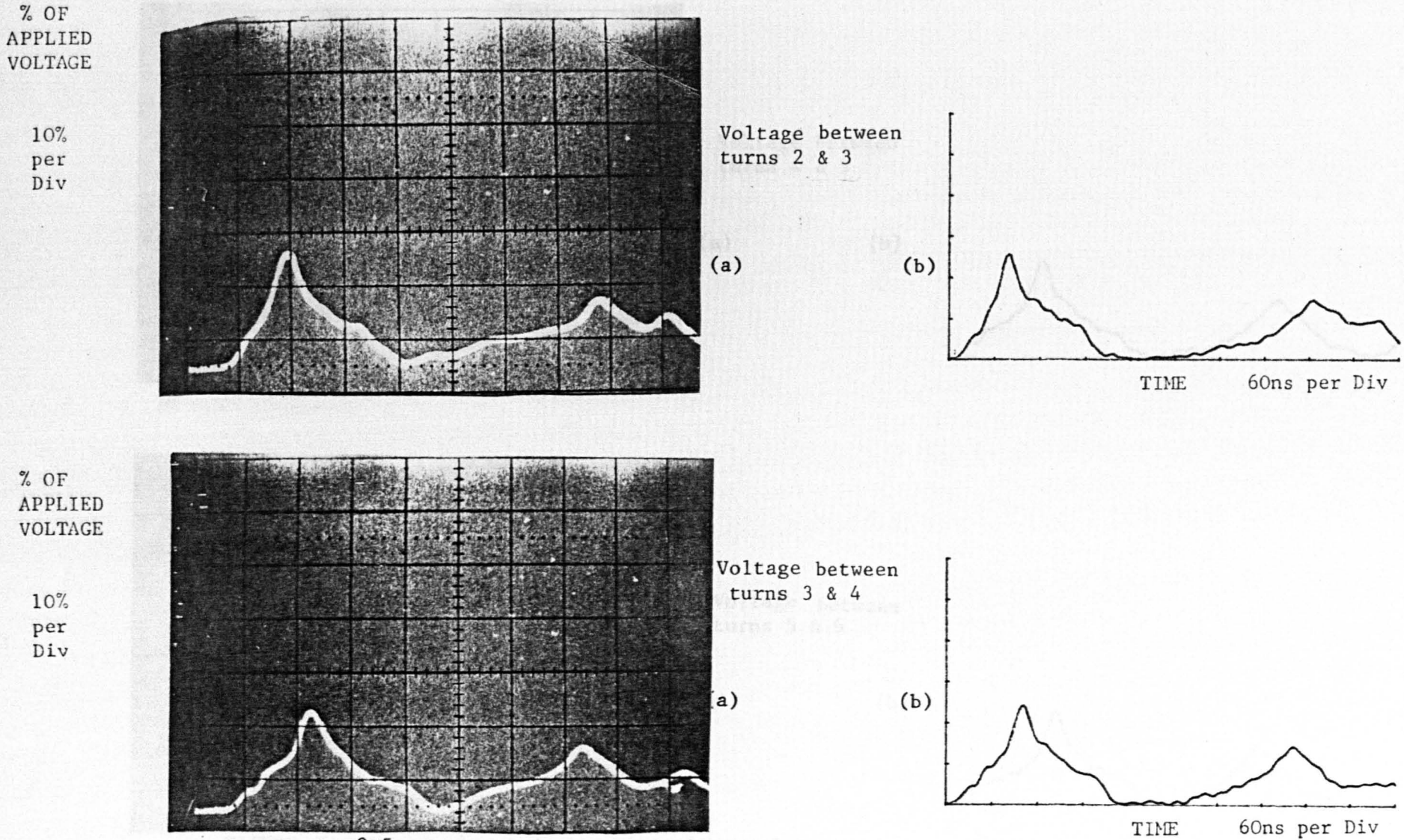

FIGURE 9.5 Measured and computed interturn voltages.

% OF APPLIED VOLTAGE

10% per Div

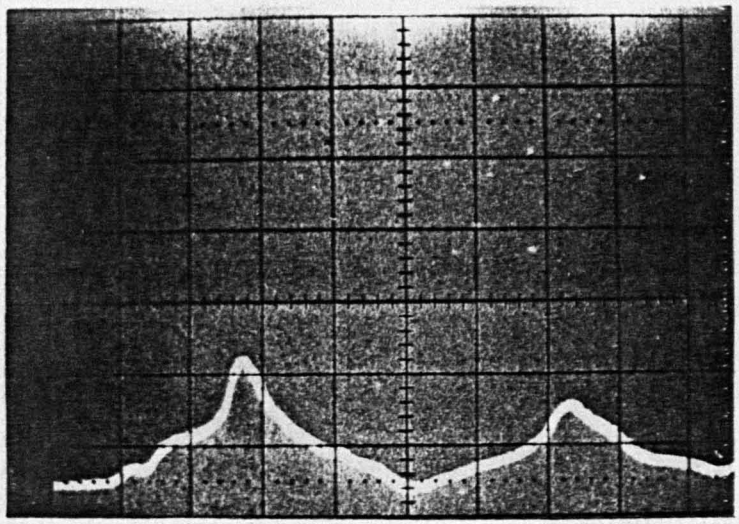

Voltage between turns 4 & 5

(a)

(b)

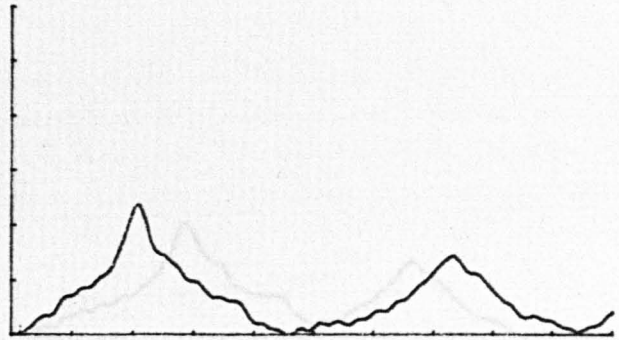

TIME 60ns per Div

% OF APPLIED VOLTAGE

10% per Div

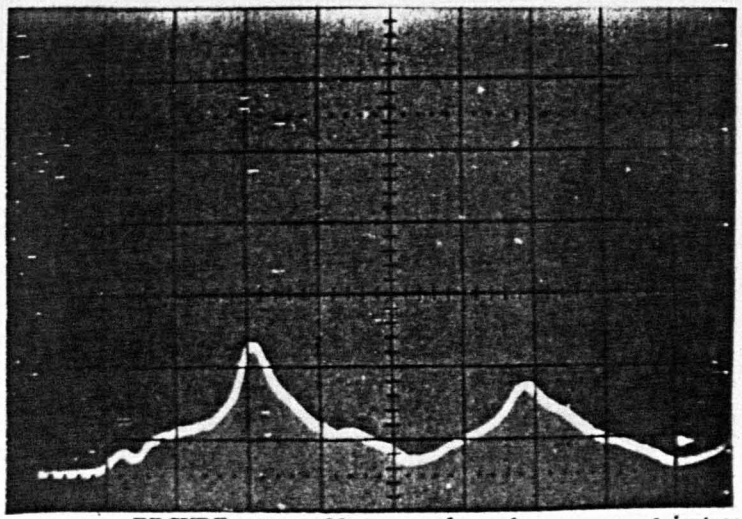

Voltage between turns 5 & 6

(a)

(b)

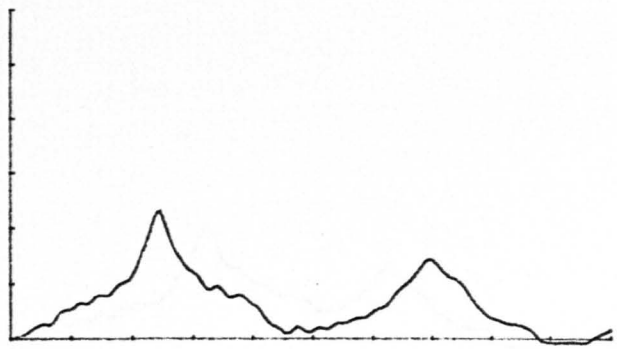

TIME 60ns per Div

FIGURE 9.5 Measured and computed interturn voltages

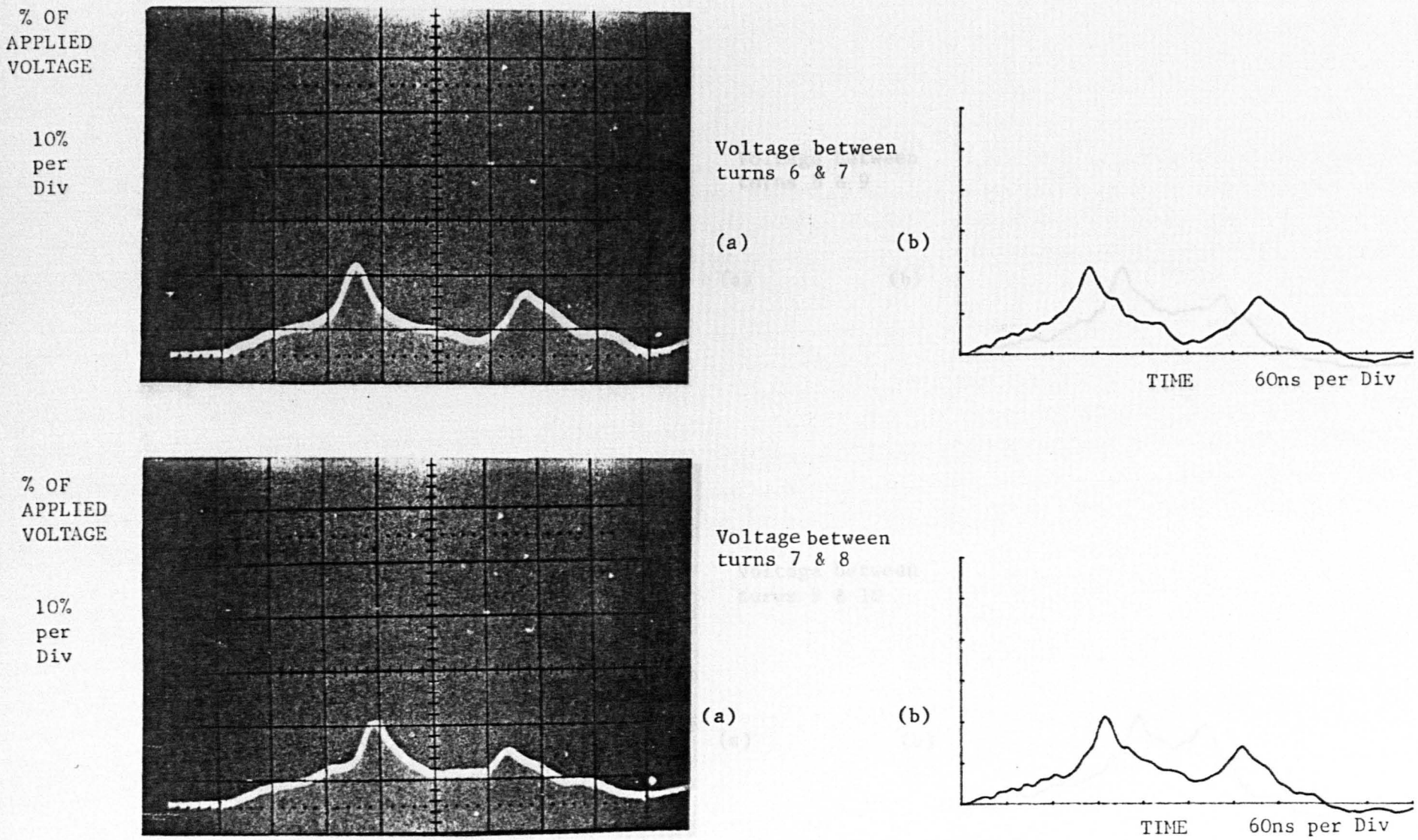

FIGURE 9.5 Measured and computed interturn voltages.

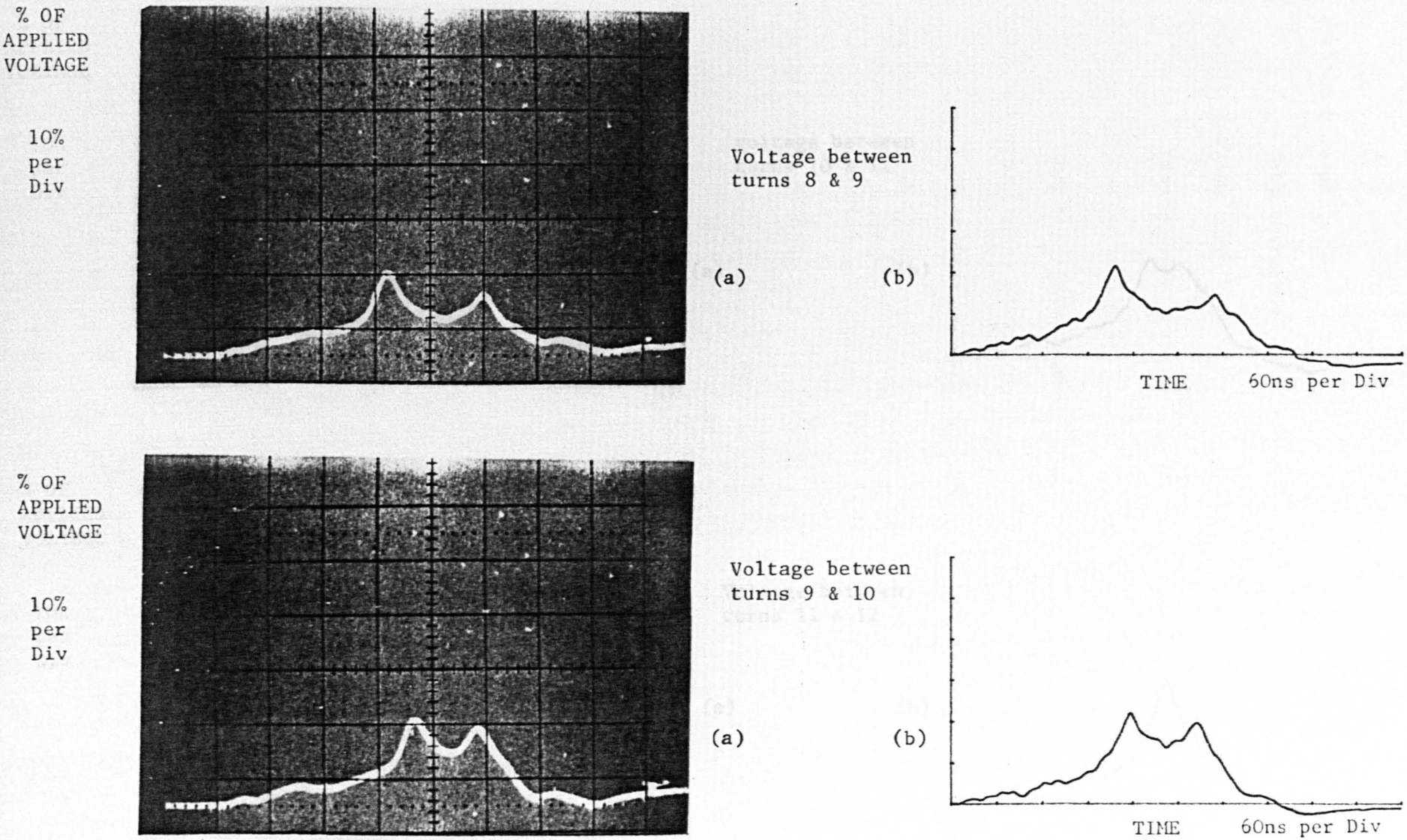

FIGURE 9.5 Measured and computed interturn voltages.

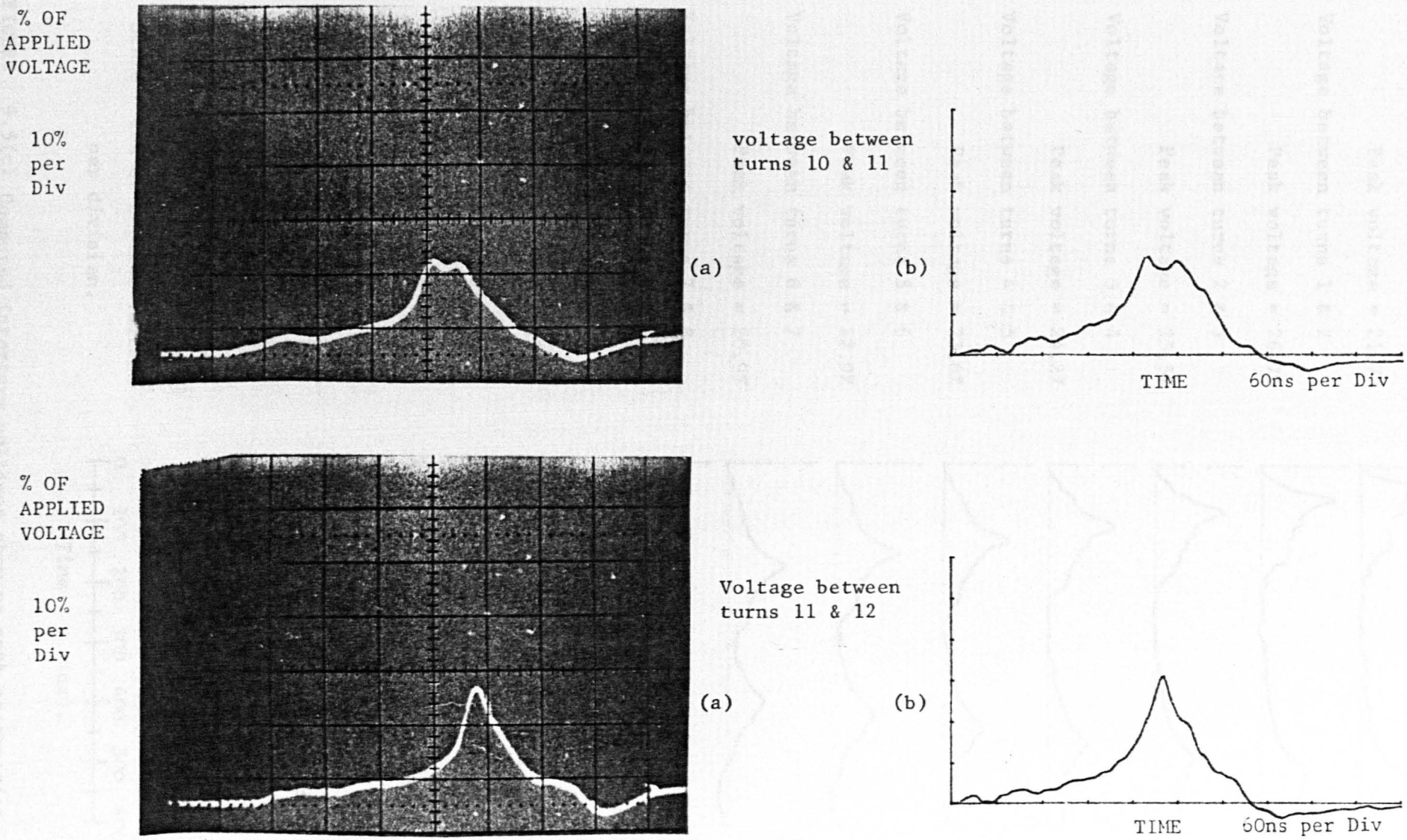

FIGURE 9.5 Measured and computed interturn voltages.

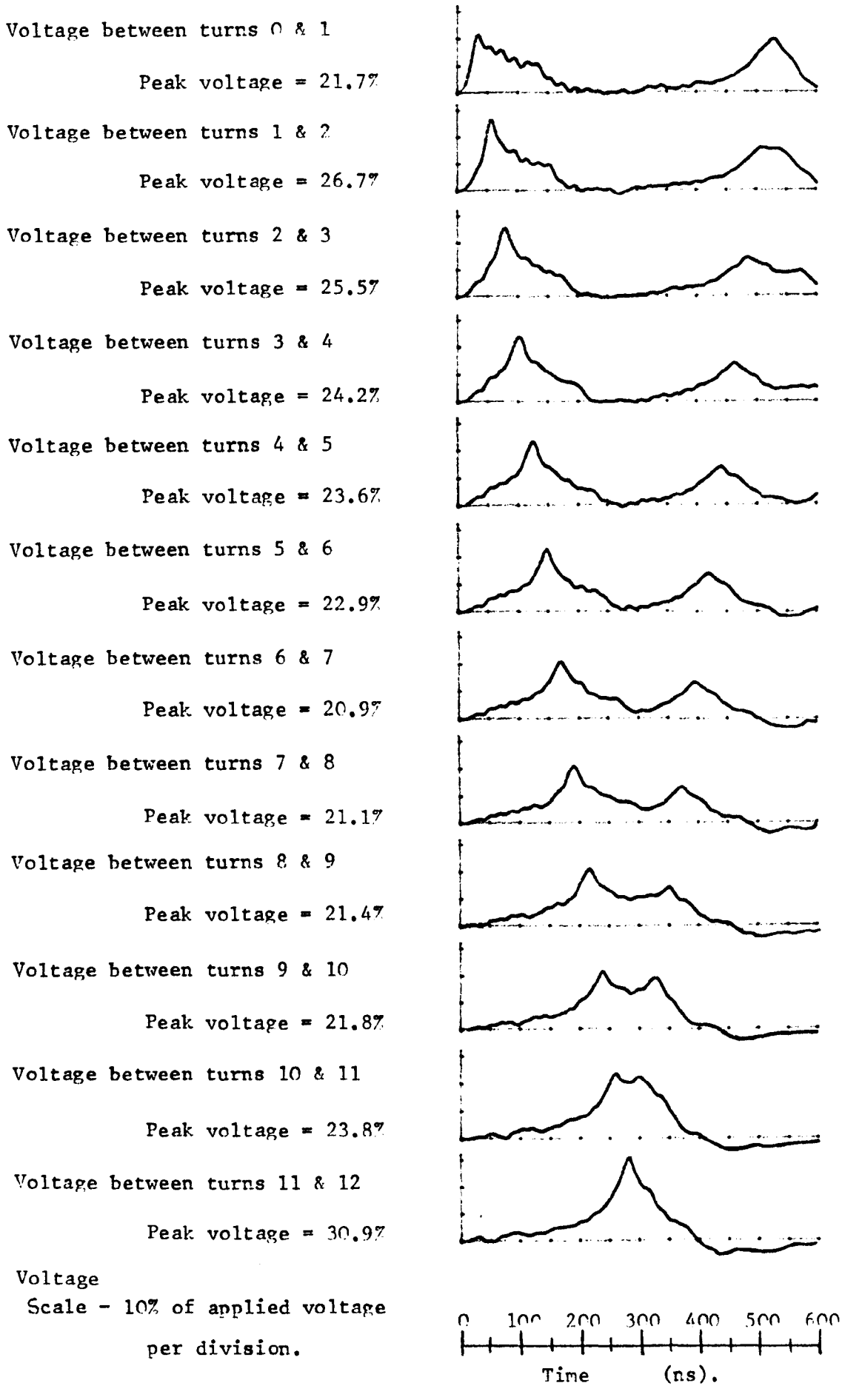

FIGURE 9.5(c) Computed interturn voltages showing peak progression.

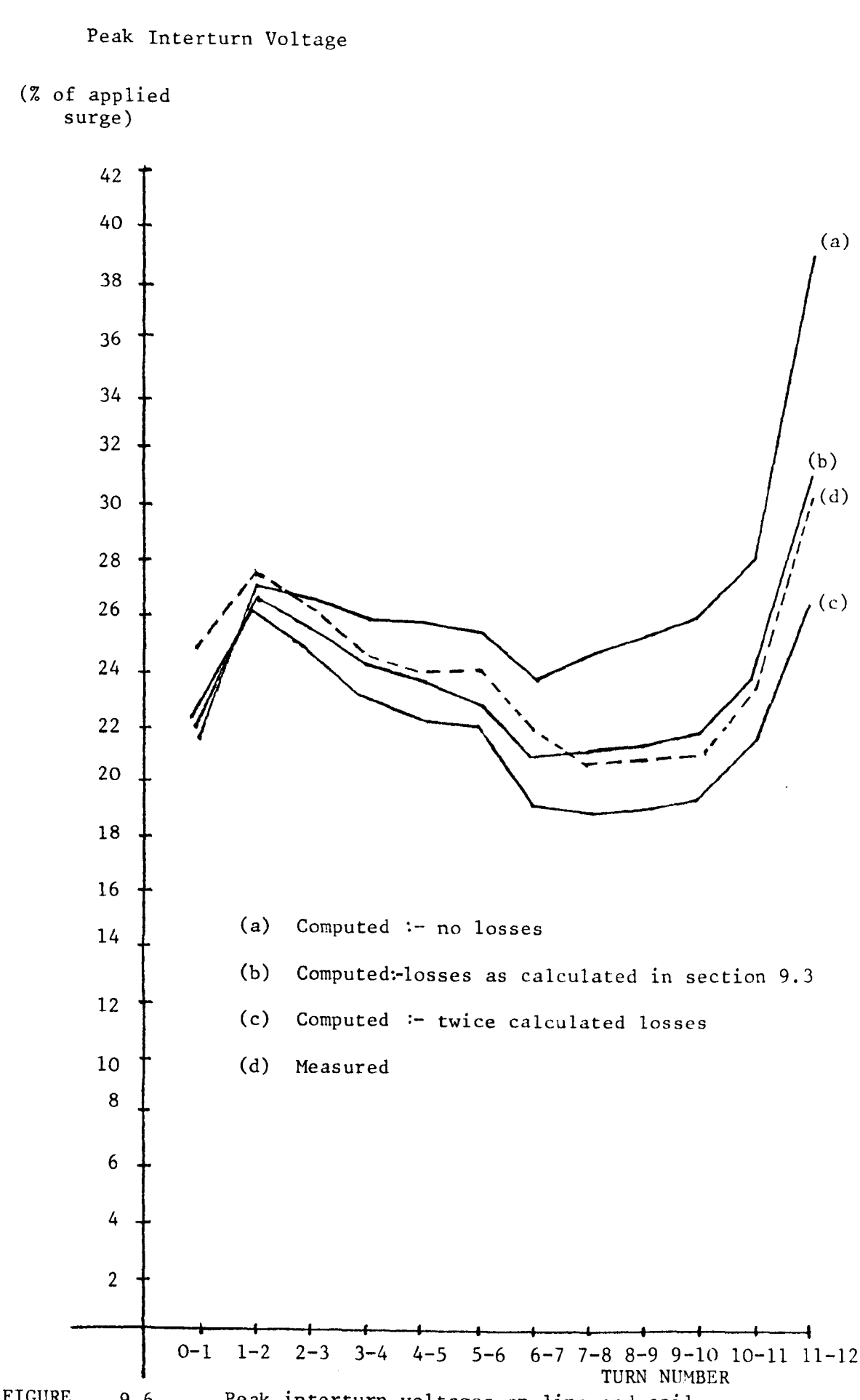

FIGURE 9.6 Peak interturn voltages on line end coil due to test surge

difference recorded between the two predictions was approximately 10^{-2} % of the applied voltage surge. Thus dielectric losses can be neglected.

The results from the single coil model, both lossy and lossless, shown in figure 9.2, together with the equivalent measured voltages, figure 6.2, indicate that including losses leads to an improvement in the accuracy of the predicted voltages to ground. The interturn voltages predicted in the first of the two coils also compare well with the equivalent measured voltages (figure 9.5). It can be seen from the comparison of the maximum interturn voltages between each of the pairs of turns, shown in figure 9.6, that it is necessary to include losses if good accuracy is desired for the interturn voltages. Neglecting the losses, leads in this case to an overestimation of the maximum peak interturn voltage of approximately 30% of the measured voltage, whereas the lossy model gives a result which is only 3% out when predicting this voltage. The voltages obtained from the lossy model with twice the calculated losses tend to significantly underestimate the actual voltages. This gives confidence in the methods adopted to calculate the lossy parameters.

Figures 9.5 (a) and (b) display the excellent correlation between the shape of the predicted and measured interturn voltages. Examination of the successive interturn voltages, figure 9.5 (c), reveals that the peak interturn voltage between each pair of turns occurs successively through the coil, indicating that a portion of the surge travels through the coil turn by turn. It can also be seen that a reflection takes place at the end of the coil causing another peak to travel back, turn by turn, to the beginning of the coil. Care must be taken when analysing

this phenomenon since the voltages shown in figure 9.5 are not absolute voltages but voltages between parts of the coil. A positive ramped step travelling wave progressing, turn by turn, from the line end to the neutral end of the coil will appear as a positive peak between turns m and m+1. However, a negative wave travelling from the neutral end to the line end will also show up as a positive peak between turns m and m+1. This is because as the negative wave propagates in the reverse direction i.e. from the nuetral end to the line end, it will cause the voltage on turn m+1 to take a negative dip before the voltage on turn m does so. Thus the voltage between turns m and m+1 will show a positive peak. Therefore it can be seen that the voltage which is reflected from the end of the coil must be negative. It can also be seen from figures 9.5(a) V_{0-1}, V_{1-2} and V_{2-3} that another reflection takes place at the line end of the coil causing another surge to travel down the coil.

The time interval between the two peaks in each waveform decreases on each successive turn. The amount by which it decreases is equivalent to two turn travel times i.e. 2 x 22.4ns, within acceptable limits, in both the measured and the computed results.

The travelling wave phenomenon which is shown in figure 9.5 and explained above is similar to some early theories of wave propagation in motor coils, see chapter 2. However the travelling wave concept by itself does not explain the result that voltages appear at points in the coil before the surge has travelled, turn by turn, to that point. Thus the travelling wave model is proved to be, qualitatively, only partially true. Quantitatively the model is wholly inadequate since it would predict that the test surge (32 ns rise time) would cause a voltage

between the first two turns of (22.4/32.0 =) 70% of the transmitted surge which, as can be seen, is not the case.

An explanation of the negative wave reflecting back from the end of the coil has been given by Cornick and Thompson (17) who said it was due to an increase in the effective inductance, and hence surge impedance, of the second coil which is caused by the flux starting to penetrate the iron. Figure 9.5 (c) shows this to be incorrect since the computer model clearly (and accurately) predicts this phenomenon, but is based on the assumption that no flux at all penetrates into the core and that there is no coupling between coils.

CHAPTER TEN.

FURTHER STUDIES CARRIED OUT USING THE MODEL.

10.1. THE EFFECT OF SURGE RISE TIME ON VOLTAGE DISTRIBUTION.

In the previous section it has been demonstrated that the lossy multiconductor transmission line model for a winding can accurately predict turn and interturn voltages within the first coil of a winding. It is therefore possible to use this model to investigate voltage distribution in line end coils when they are subjected to various types of surges.

A range of five different surges were used to analyse the effect that various rise times had on voltage distribution within the line end coils. These were surges having rise times of 25 ns, 50 ns, 100 ns, 200 ns and 400 ns, see figure 10.1. It should be remembered that the surges shown in figure 10.1 are those which would appear on the line if it were infinitely long (or matched) and because of reflections in the system do not actually appear at any point on the switch, cable, winding configuration. The voltage distributions on the line end coil of a winding of 11 kV twelve turns coils (as used previously) for the range of surge rise times are shown in figures 10.2-10.6.

It can be seen that the rise time of the surge which appears on the line end of the winding can differ greatly from the rise time of the surge which is produced at the switch. This is evident particularly for the shorter rise times, e.g. the 25 ns rise time surge appears on the coil with a rise time of over 100 ns in the case of the 11 kV insulation level (see figure 10.3). The cause of this increase in rise time must

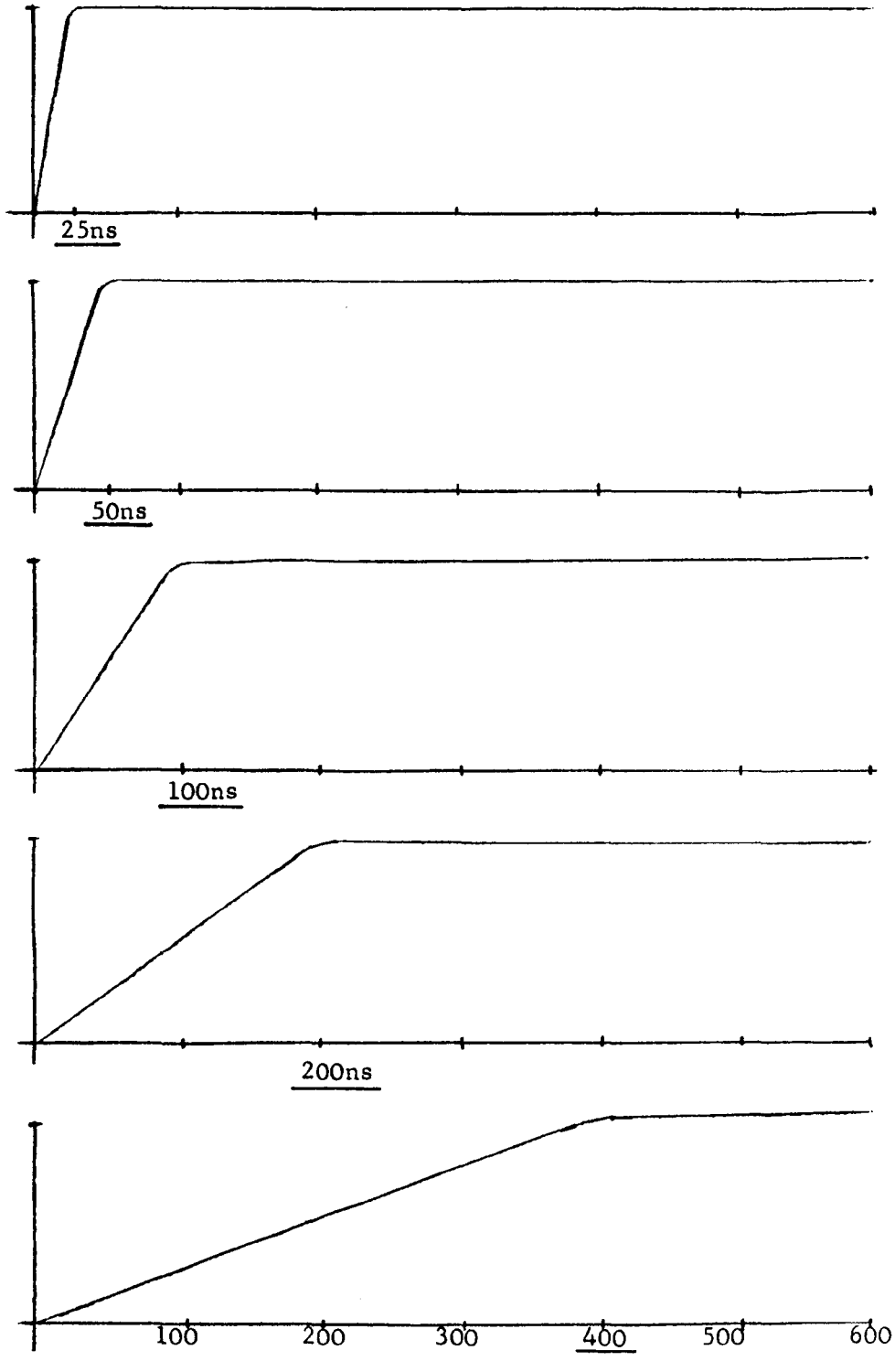

FIGURE 10.1 Range of surges used to investigate the effect of surge rise time.

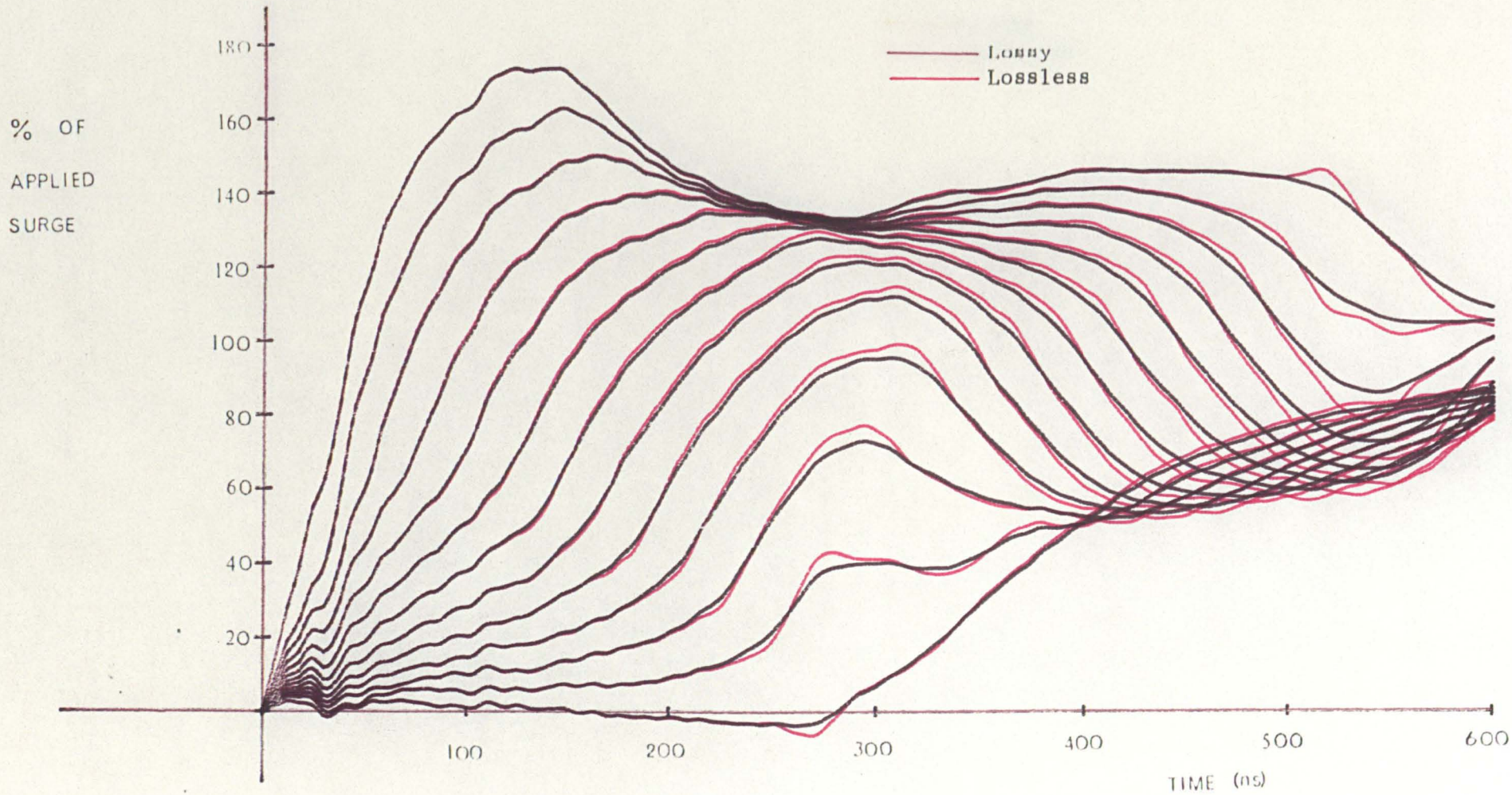

FIGURE 10.2 Lossless and lossy turn to ground voltages on an 11kV, 12 turn, line end coil - 25 ns rise time.

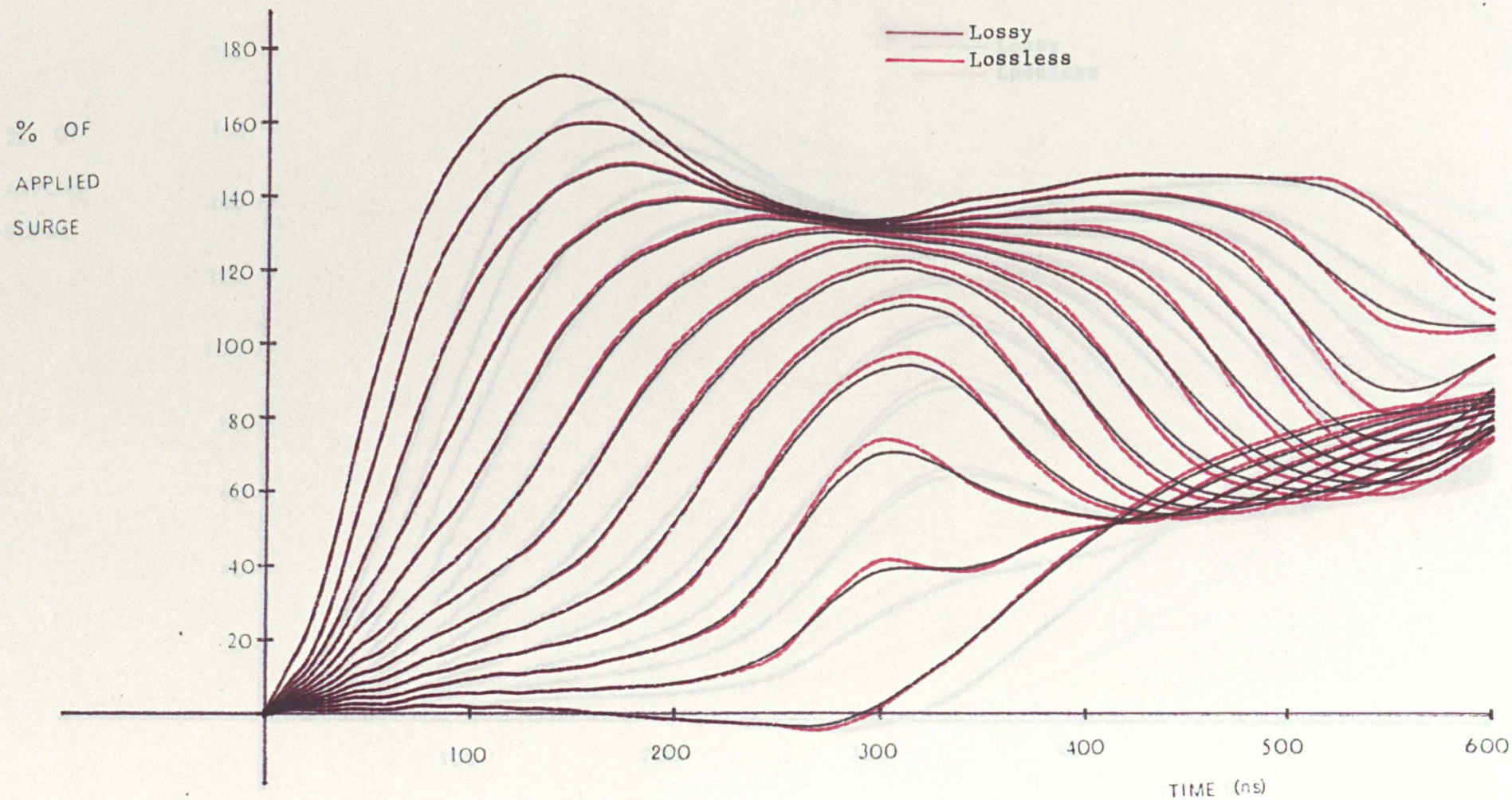

FIGURE 10.3 Lossless and lossy turn to ground voltages on an 11kV, 12 turn, line end coil - 50 ns rise time.

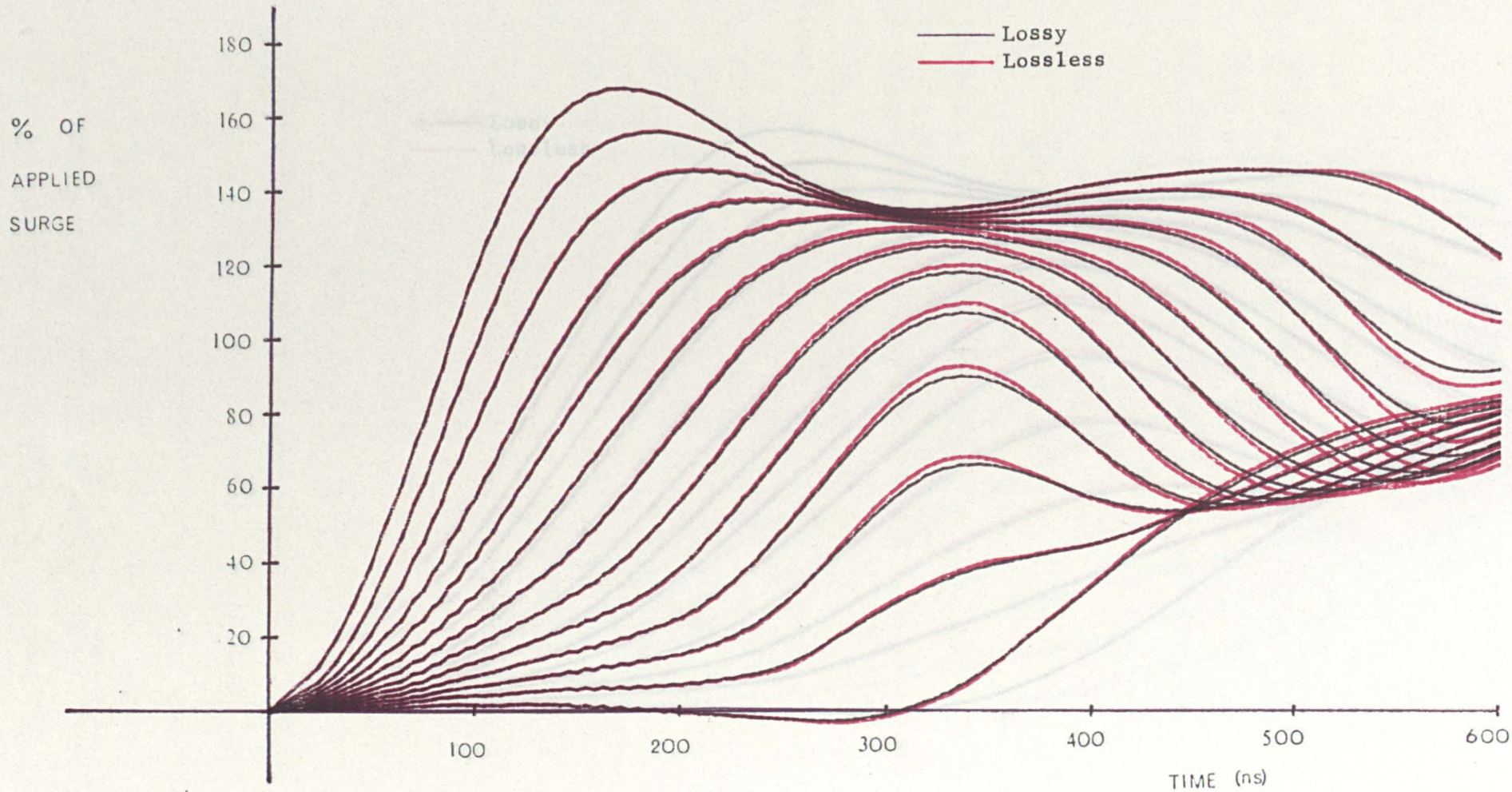

FIGURE 10.4 Lossless and lossy turn to ground voltages on an 11kV, 12 turn, line end coil - 100 ns rise time.

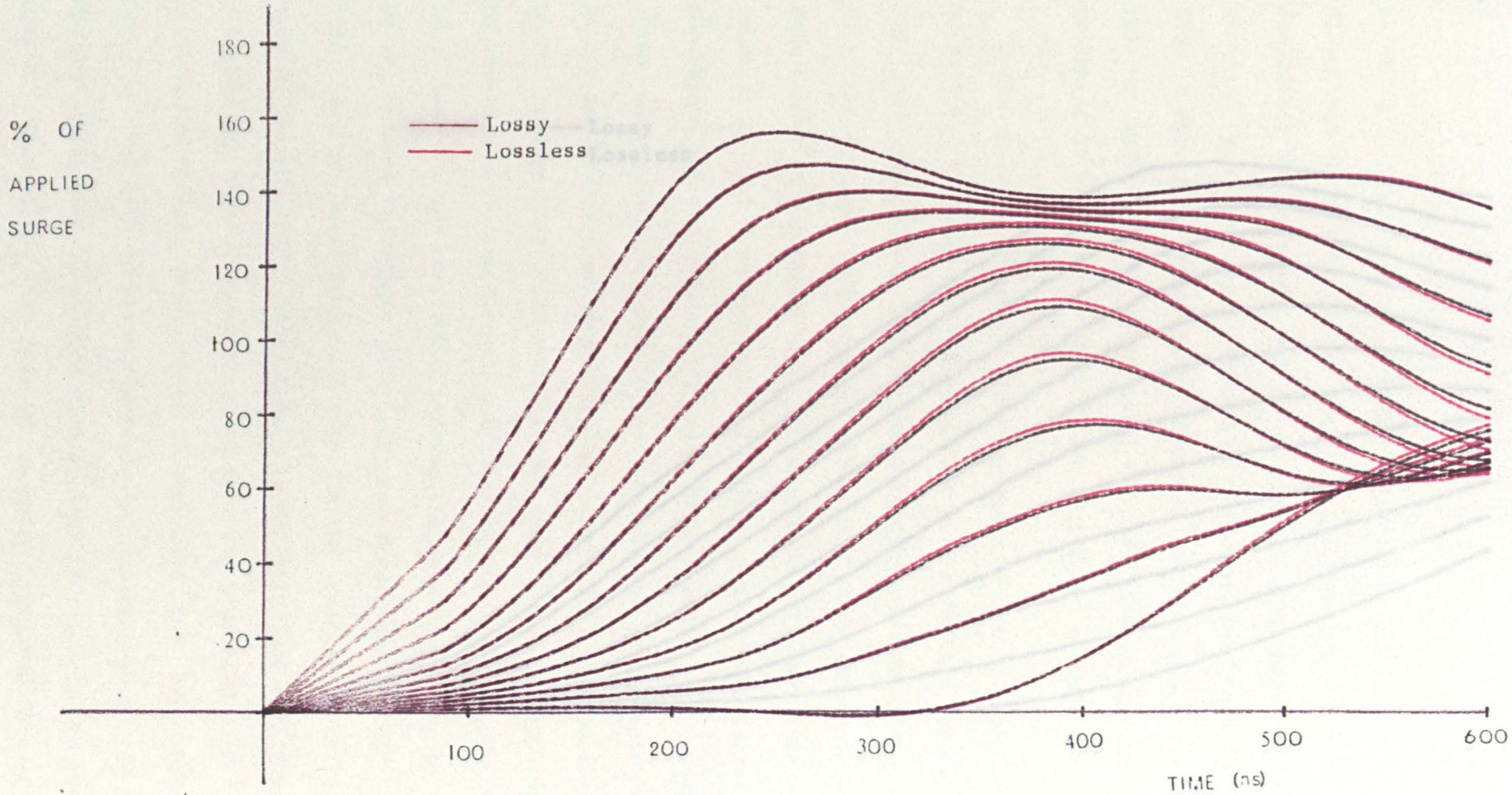

Figure 10.5 Lossless and lossy turn to ground voltages on an 11kV, 12 turn end coil 200 ns rise time.

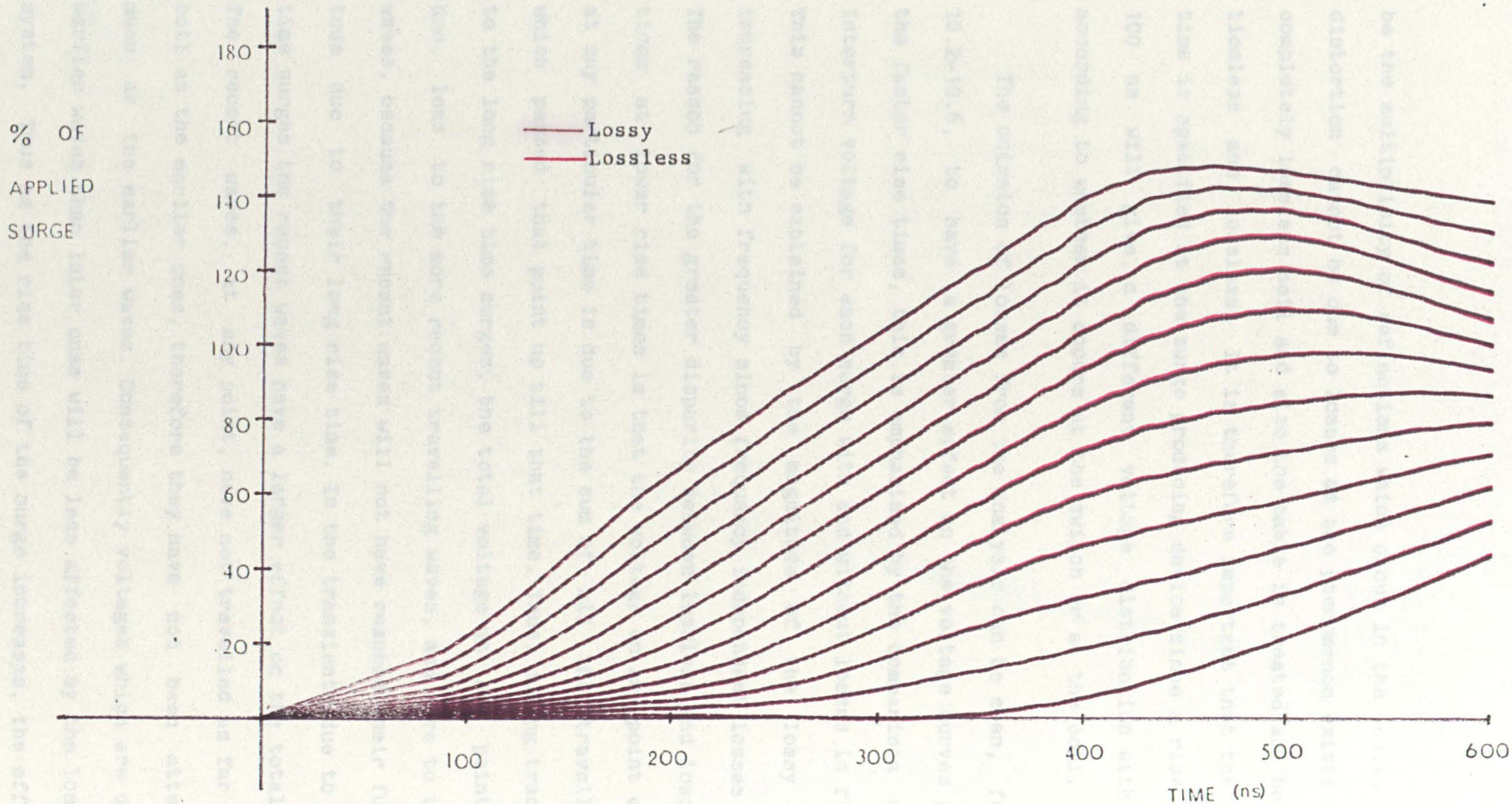

Figure 10.6 Lossless and lossy turn to ground voltages on an 11kV, 12 turn, line end coil - 400ns rise time.

be the multiplicity of reflections which occur in the coil, since the distortion cannot be due to losses as the phenomenon exists even in the completely lossless coil and also the cable is treated as both distortionless and lossless. It is therefore important that the surge rise time is specified at the surge producing device since a rise time of say 100 ns will give a different voltage distribution within the coil according to whether it occurs at the switch or at the coil.

The omission of losses from the analysis can be seen, from figure 10.2-10.6, to have a greater effect on the voltage curves produced by the faster rise times, this is emphasised by the comparison of maximum interturn voltage for each surge with and witnout losses in figure 10.7. This cannot be explained by the magnitude of the lossy parameters increasing with frequency since frequency independent losses were used. The reason for the greater disparity between lossless and lossy predictions at lower rise times is that the voltage on any point on any turn at any particular time is due to the sum of all the travelling waves which passed that point up till that time. Thus, during transients due to the long rise time surges, the total voltage at any point will be due, less to the more recent travelling waves, and more to the earlier waves, because the recent waves will not have reached their full magnitude due to their long rise time. In the transients due to short rise time surges the recent waves have a larger effect on the total voltage. The recent waves, at any point, have not travelled as far inside the coil as the earlier ones, therefore they have not been attenuated as much as the earlier waves. Consequently voltages which are due more to earlier waves than later ones will be less affected by the losses in the system. Thus as the rise time of the surge increases, the effect of the

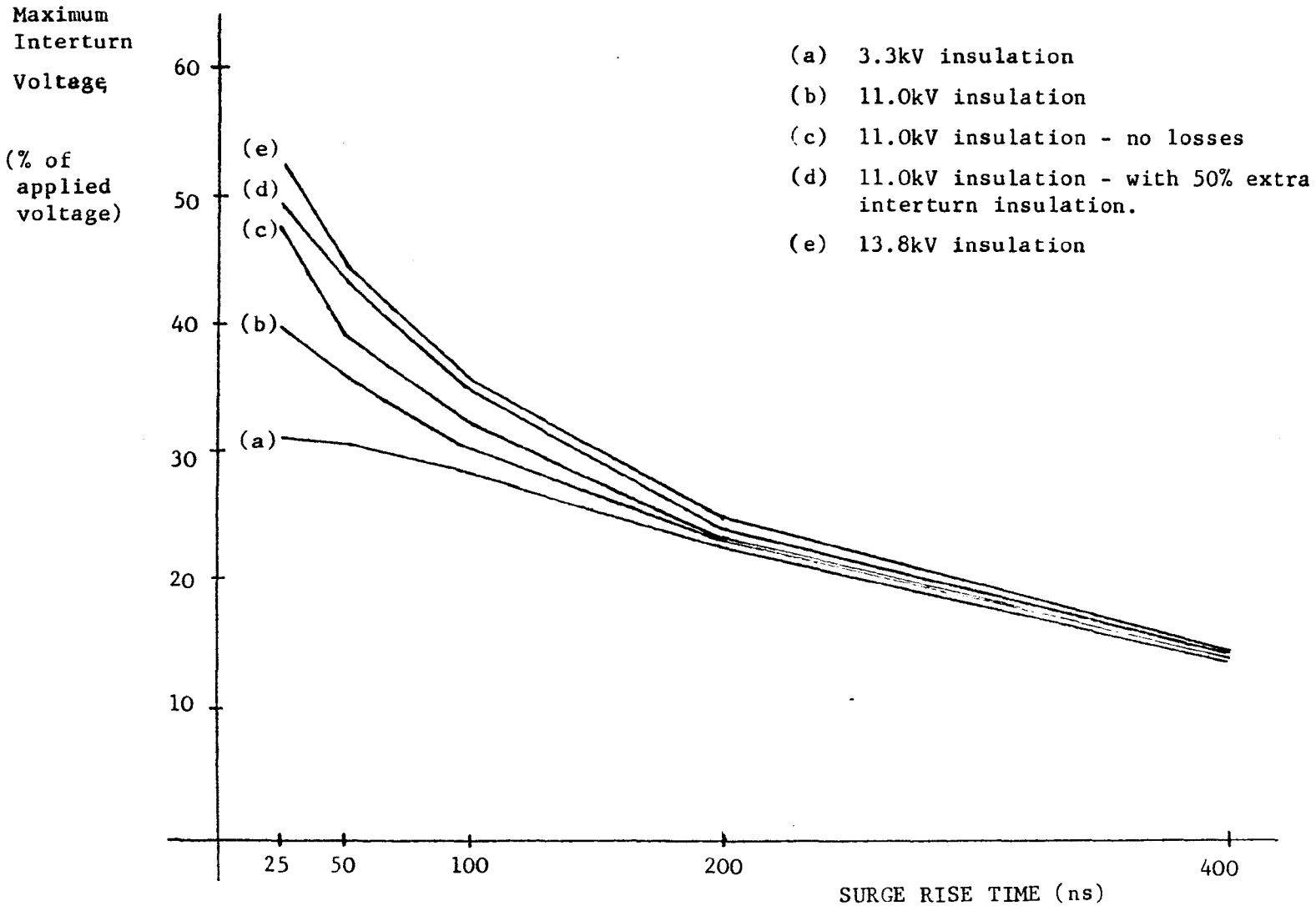

Figure 10.7 Maximum interturn voltage vs. Surge rise time for various coil insulations.

losses on the voltage decreases. This phenomenon causes the effect of the losses to be frequency dependent even though frequency independent parameters are used.

It can be seen that the effect of the increasing the rise time of the applied surge is to decrease the magnitude of the interturn voltages occurring in the line end coil. This conforms with previous experimental results on interturn voltages (11,13,14).

Figure 10.8 shows the maximum interturn voltage between each pair of turns in the line end coil for each of the five surge rise times for the lossy coil model. It is seen that the maximum interturn voltage occurs at, or near, the neutral end of the line end coil, again in accordance with previous results. It can also be seen from this that as the rise time increases the distribution of voltage over the whole coil becomes more uniform and that the maximum interturn voltage tends to occur between more than just the last pair of turns. The general shape of the curves for the 200 ns and 400 ns rise time surges correspond with the experimental results published by Parrot (11) for an eight turn coil winding using surge rise times of 160 ns and 360 ns, although the experimental arrangement was different from the system modelled here. (Parrot used very short leads between the surge generator and a winding which consisted of 3.3 kV coils with eight turns each). Similar curves were also obtained experimentally by Petrov and Abramov (15) and Cornick and Thompson (17).

It should be noted that the interturn voltages can have two distinct peaks. This was demonstrated in figure 9.5 for the irregularly shaped test pulse, but is also true for more regularly shaped pulses. It

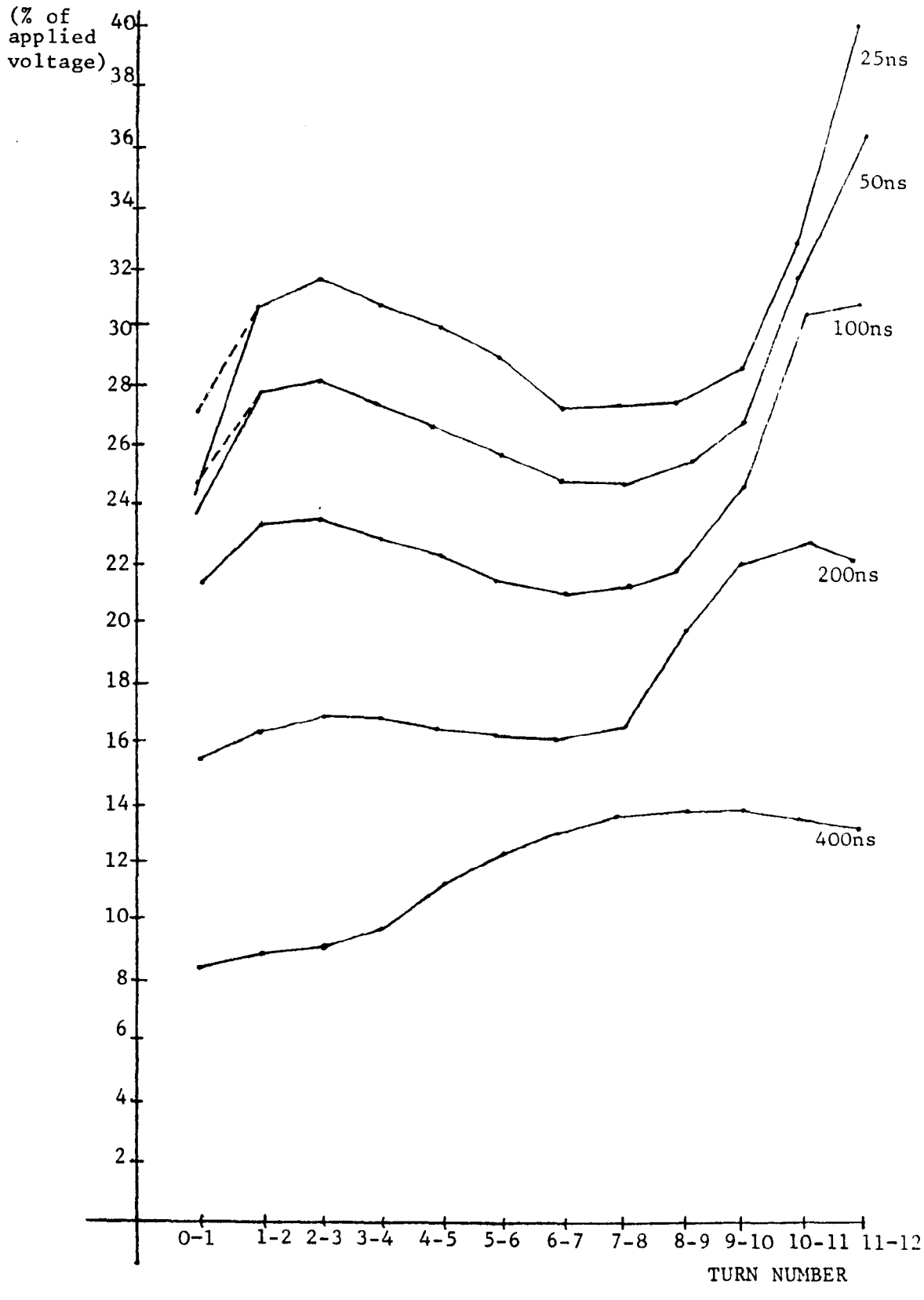

FIGURE 10.8 Peak interturn voltage vs turns for an 11kV line end coil - various rise times

was found that the second voltage peak of the interturn voltage between the first pair of turns was slightly in excess of the first peak, for the fast rising surges. The difference between the two peaks varied with the losses in the model. For the 50 ns rise time the lossless model produced a second peak which was 7% of the applied voltage above the first, while overestimating the losses by a factor of two gave the first peak larger than the second. The most accurate model, i.e. that which included the losses as calculated gave the second peak as only 1% of the applied voltage above the first in this case. The reduction in the size of the second peak as the losses increase is due to the attenuation of the series component of the surge. Thus the series part of the surge diminishes the longer it remains in the coil.

Since the second peak of this first interturn voltage is less than the first over most of the range of rise times used (it only occurred due to the 25 ns and the 50 ns surges), the first peak was plotted with the other peak interturn voltages in order that the pattern of the variation in magnitude of the peaks could be seen over the whole range of the surge rise times. The magnitude of the second peak voltage is also plotted (in dotted lines) in figure 10.8, in the cases where it exceeds that of the first peak.

The results shown in figure 10.8 show that the upper end of the range of surge rise times i.e. 400 ns was sufficiently large to establish that surges with rise times of this duration and longer can cause neither large interturn voltages nor a substantial degree of non-uniformity in the voltage distribution within the coil. Even with this long rise time, however, the simple transmission line model for the coil

would be of little use in predicting the interturn voltages since it would give an interturn voltage of (22.4/400) = 5.6% between all pairs of turns, thus underestimating the problem considerably.

At the lower end of the range of surge rise times i.e. 25 ns it is clear that very large interturn voltages and substantial non-uniformity of voltage distribution can occur. In this case the simple transmission line model would predict an interturn voltage of (22.4/25.0) = 88.2% between turns, this greatly overestimates the magnitude of the voltages. Thus it is clear from a comparison of results from the simple transmission line model and the new multiconductor transmission line model that the former is totally unacceptable for the purposes of design.

From figures 10.2-10.6 it can be seen that the maximum voltage of the applied surge, i.e. 100%, is less than the maximum voltage appearing on the coil. The increase in voltage is not due to the surge impedance presented to the cable by the line end coil terminal junction, but is due to the aggregate effect of all the voltages travelling back and forward in the coil and in the cable. Since the travel time of waves in each section of coil is much less than even the short surge rise times, the true surge impedance of the coil cannot be found from the increase in voltage at the coil terminal. The true surge impedance of the coil can be found from the first element in the terminal junction scatter matrix for the line end coil since this will give the initial reflection back into the cable. However, since this true surge impedance does not, by itself, cause the maximum voltage on the coil, it is of little interest.

An effective surge impedance can be calculated by assuming that the

voltage increase is due to the mismatch between the cable surge impedance and the coil effective surge impedance. This effective surge impedance is of use in system studies, however it should be used with care as it is frequency dependent. It is calculated using

$$\frac{\Delta V}{V^{in}} = \frac{Z_e - Z_o}{Z_e + Z_o}$$

where ΔV is the difference between the voltage at the line end terminal and the incident voltages. Z_o and Z_e are the cable surge impedance and the effective surge impedance of the winding respectively.

The effective surge impedance of the 11 kV coil is plotted in figure 10.9 against the rise time of the applied surge. There is a marked variation of this impedance with the surge rise time.

The results obtained for the test surge, figure 9.3, showed that although the rise time was short (32 ns) the maximum voltage was limited to 120% of the applied surge peak voltage. When this result is compared to those for the differently shaped 25 and 50 ns surges it becomes clear that the effective surge impedance is dependent on the shape of the applied surge as well as the front rise time of the surge. (The effective surge impedance of the winding to the test surge is included in figure 10.9 for comparison.) Therefore, as the effective surge impedance has both the surge front rise time and the surge shape as variables, it is clear that the concept of coil surge impedance can be misleading and is no substitute for a full understanding of surge propagation in coils.

The difference between the magnitude of the surge at either end of

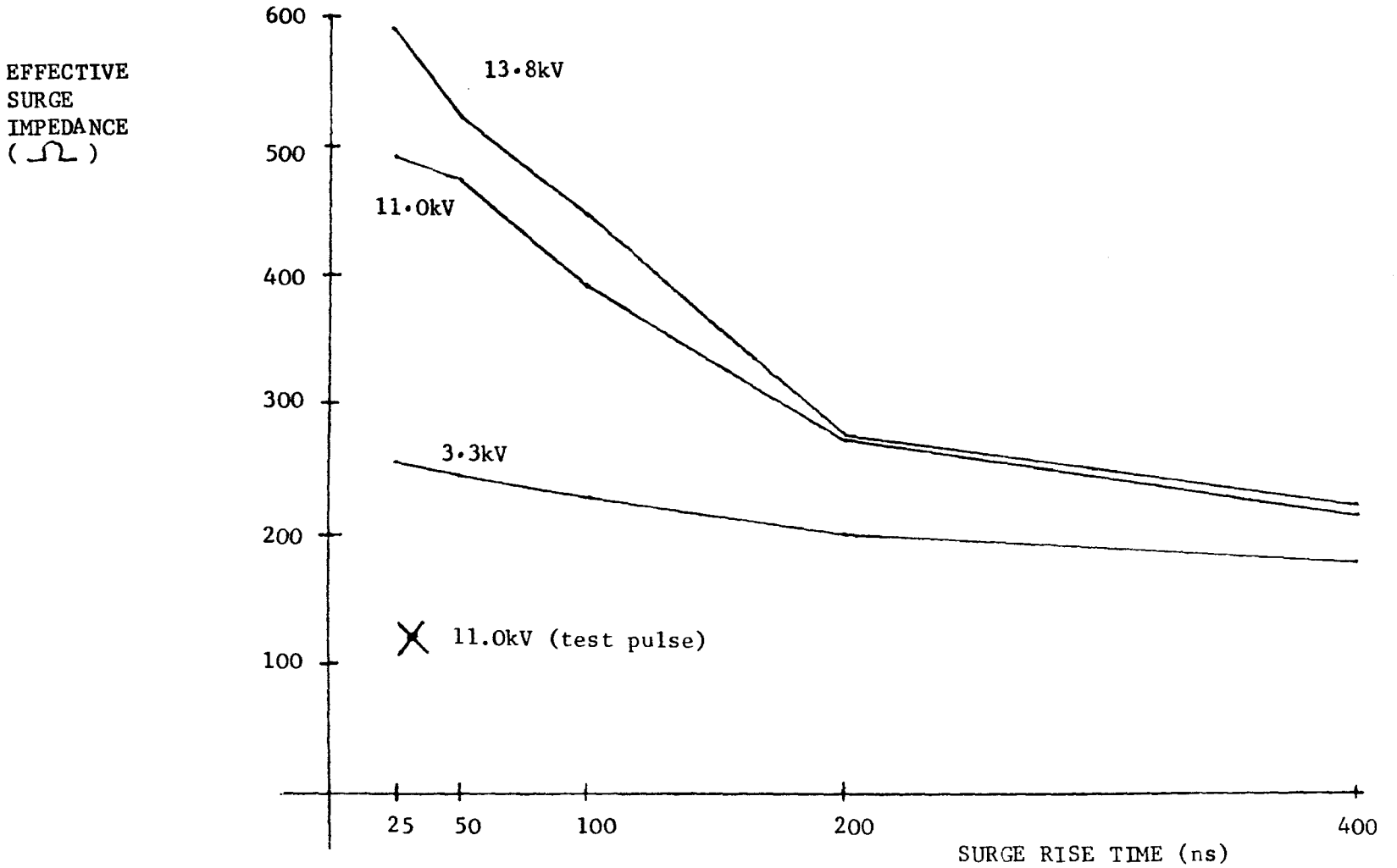

FIGURE 10.9 Effective surge impedance vs Rise time for various insulation levels.

the cable, combined with the difference between rise times at the switch and at the motor winding means that in specifying a surge, the point on the system where that surge occurs must be clearly stated. From the point of view of analysing the effects of surges in coils, the surge data should pertain to the shape and magnitude of the surge at the switching device.

10.2. THE EFFECT OF INSULATION DIMENSIONS ON VOLTAGE DISTRIBUTION.

10.2.1. Variation in the Insulation Level.

Section 10.1 explained the effects on an 11 kV winding of switching surges of various rise times. It was decided to extend this work to include winding insulation levels other than 11 kV. To this end, coil insulation levels of 13.8 kV and 3.3 kV were used, since these are the upper and lower limits of the range of what are normally regarded as high voltage motors. The cross sectional dimensions of the coils used in the computation are shown in Appendix III.

The voltage distributions shown within the line end coils of 3.3 kV and 13.8 kV windings which consisted of twelve turn coils were computed for the same range of rise times as before i.e. 25, 50, 100, 200 and 400 ns. The resulting maximum voltage between each pair of turns is plotted for each of the voltage levels and shown in figures 10.10 and 10.11. The voltages to ground on each turn of the line end coils for each rise time are shown in figures 10.12-10.16 for the 3.3 kV winding and figures 10.17-10.21 for the 13.8 kV winding.

It is clear, from these results, that as the insulation level, and hence the thickness of the insulation increase, so do the interturn

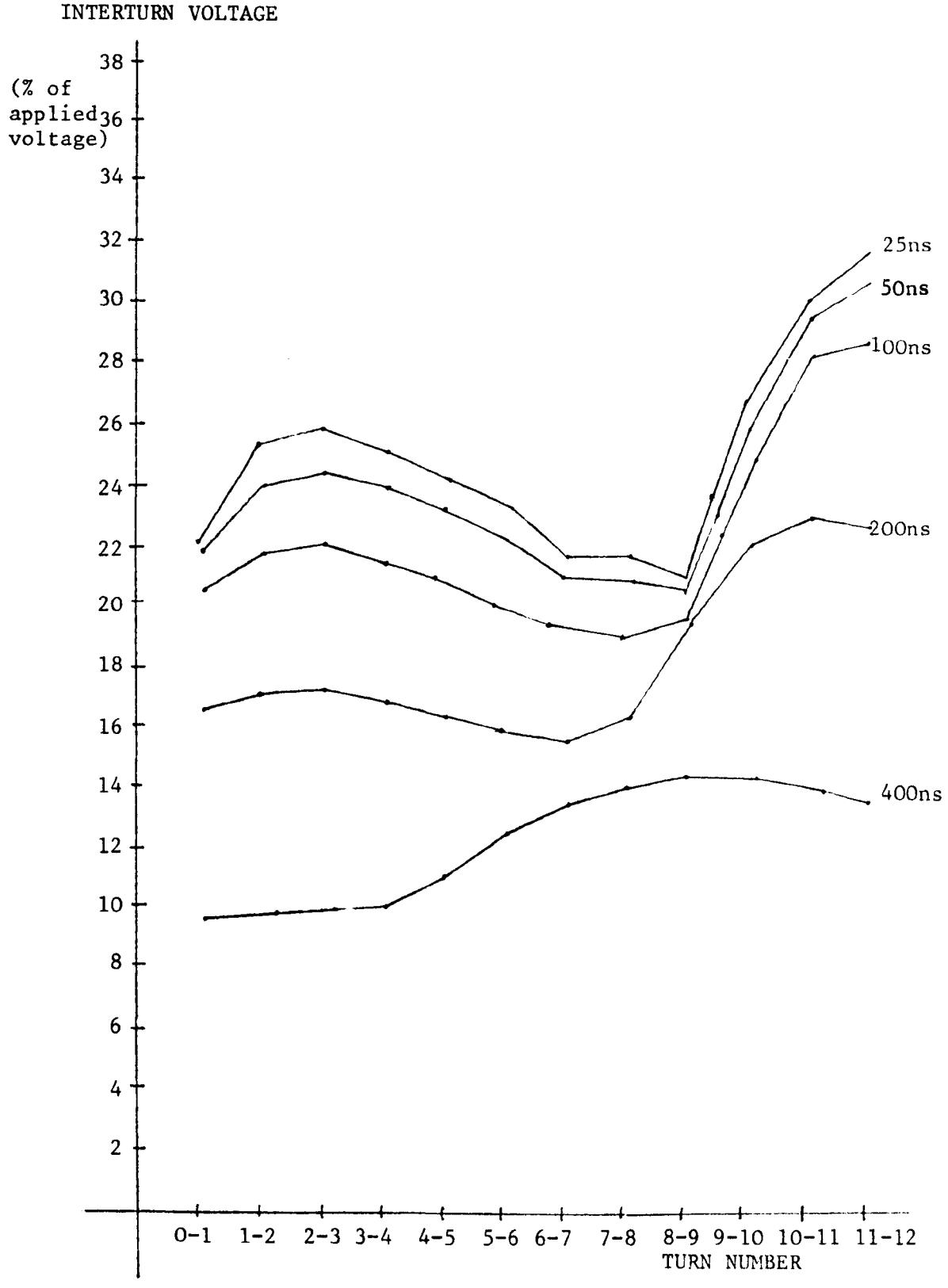

FIGURE 10.10 Peak interturn voltage vs turns for a 3.3kV line end coil - various rise times.

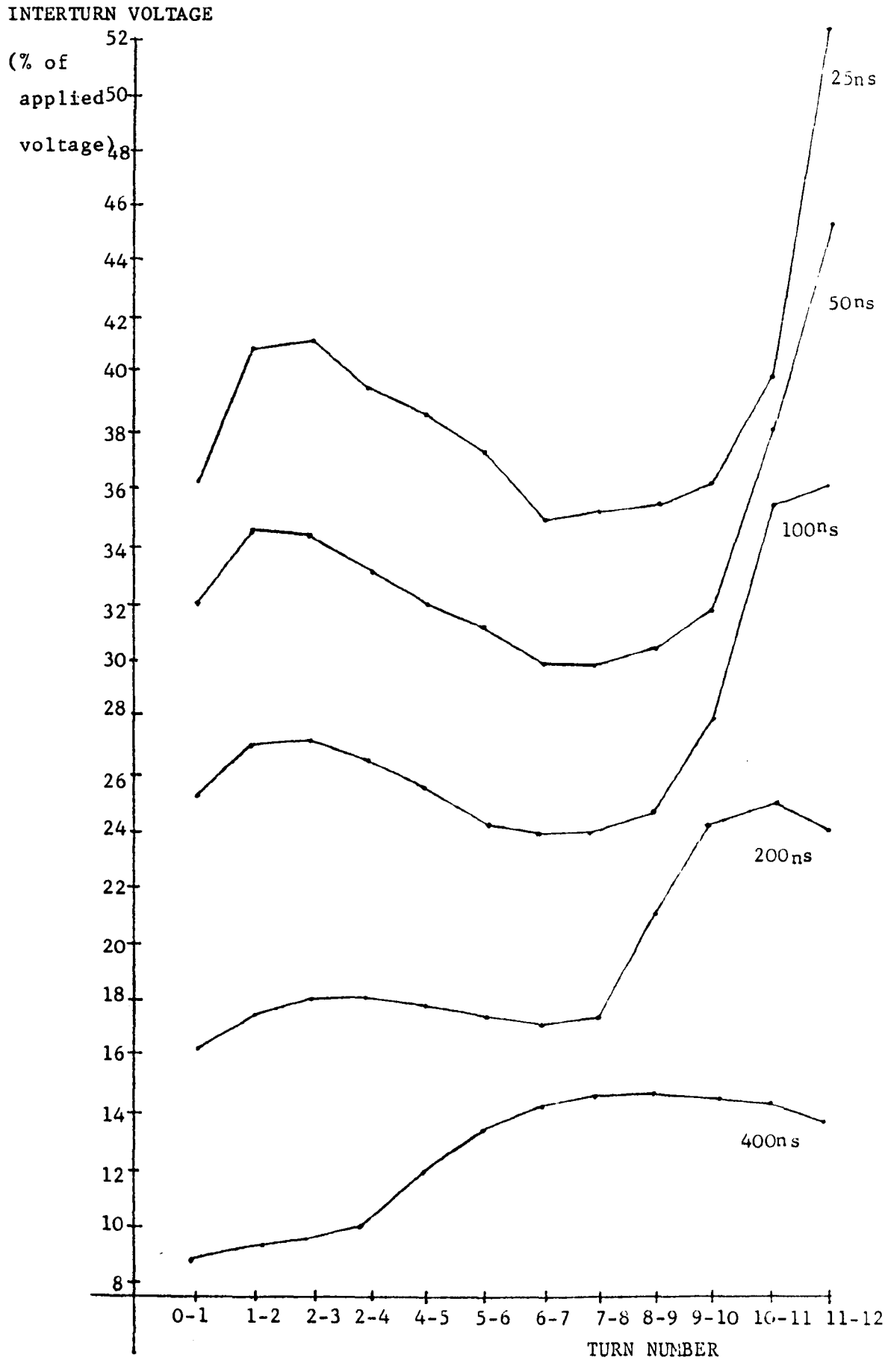

Figure 10.11 Peak interturn voltages vs. turn number on a 13.8kV line end coil - various rise times.

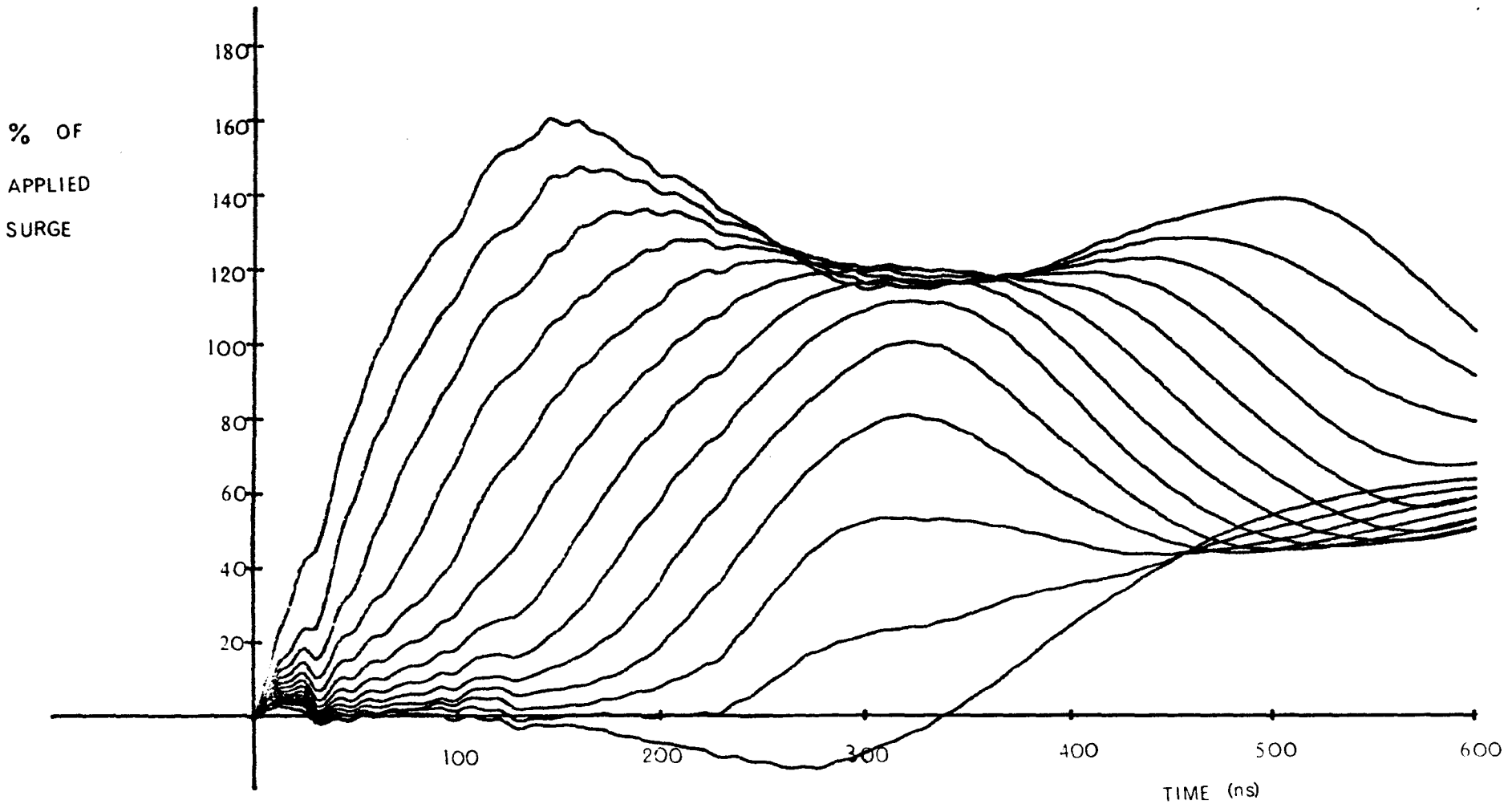

Figure 10.12 Turn to ground voltages on a 3.3kV, 12 turn line end coil - 25ns Rise Time

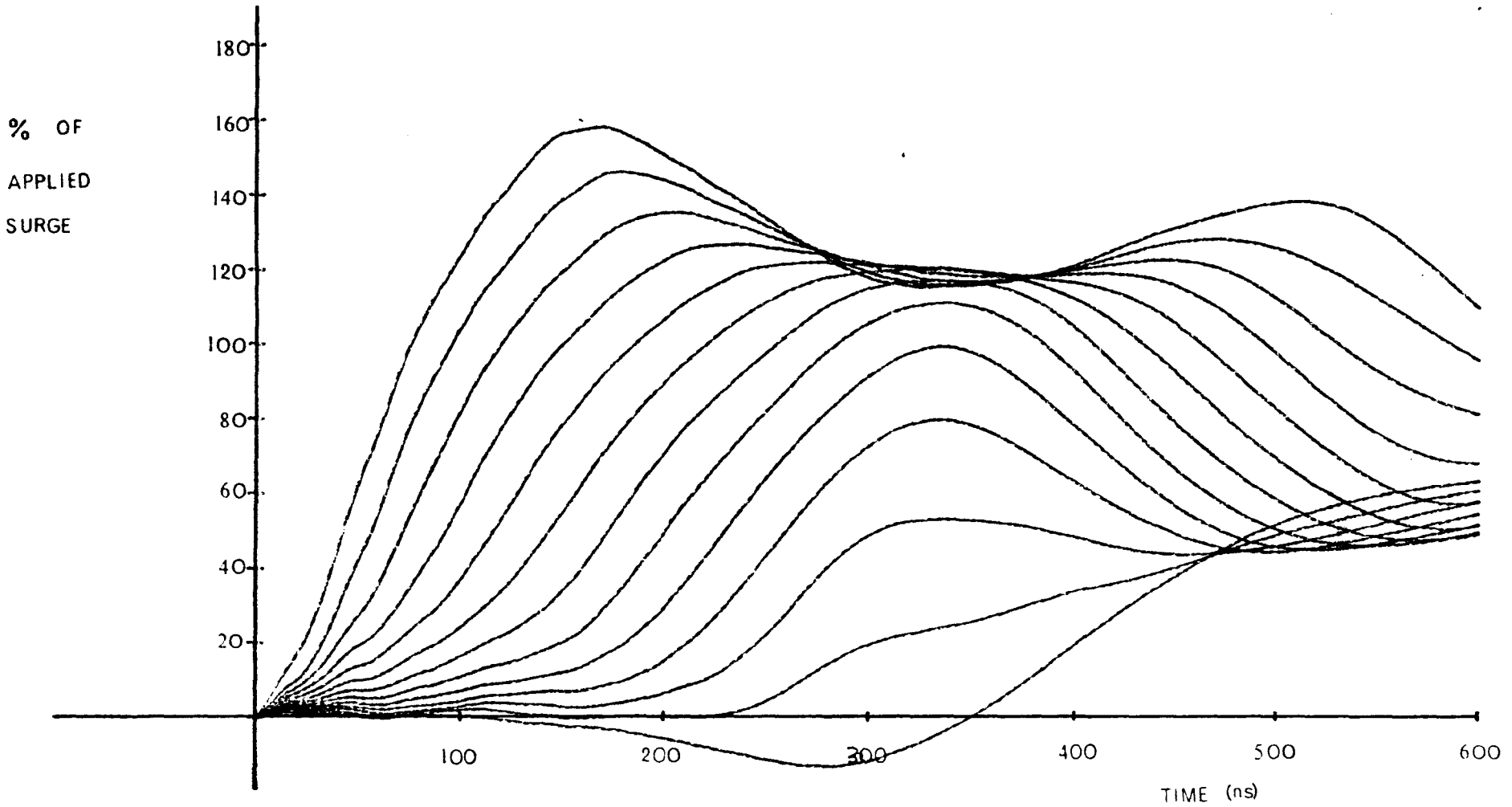

Figure 10.13 Turn to ground voltages on a 3.3kV, 12 turn, line end coil - 50 ns Rise Time

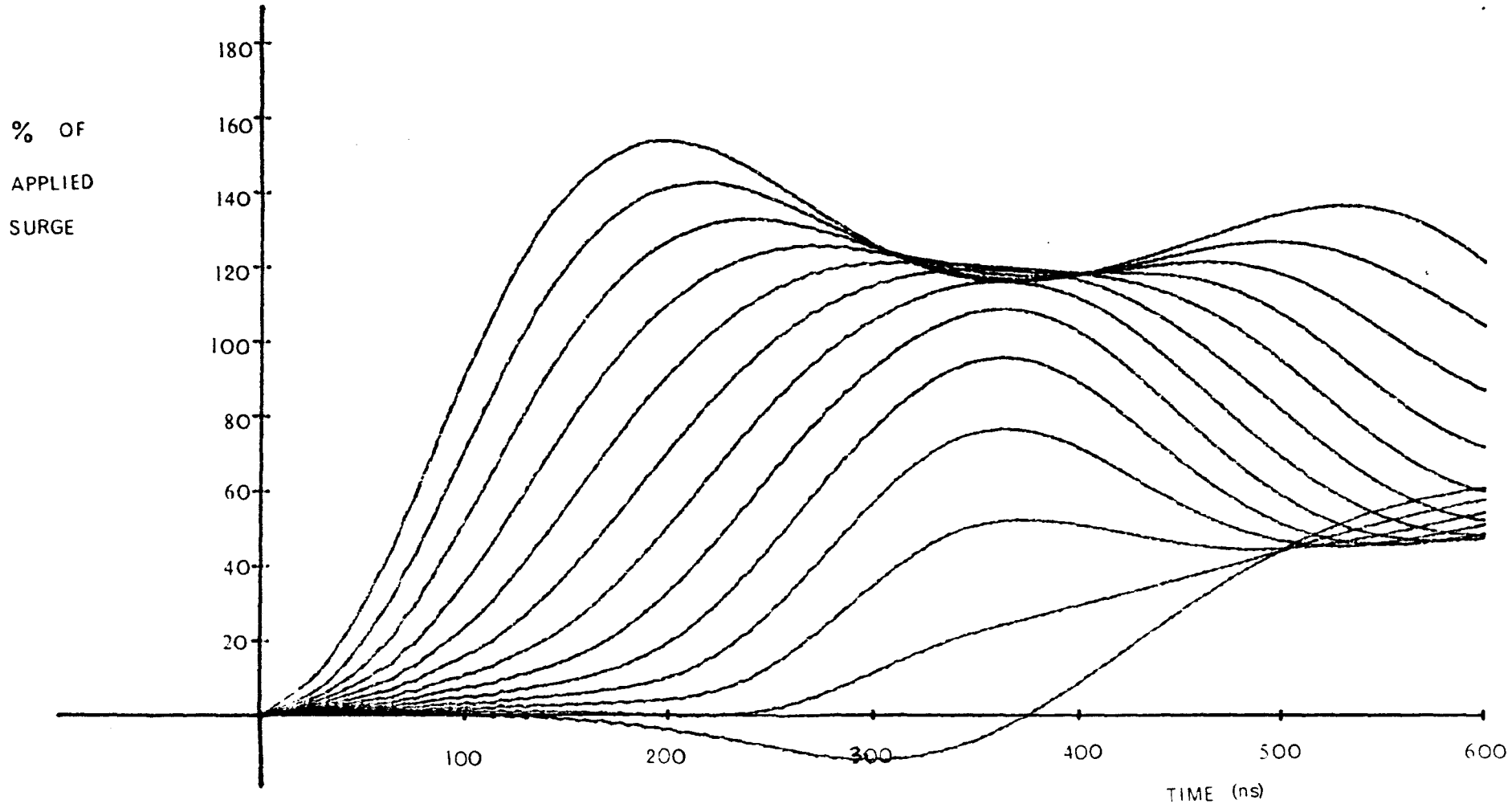

Figure 10.14 Turn to ground voltages on a 3.3kV, 12 turn line end coil - 100ns Rise Time

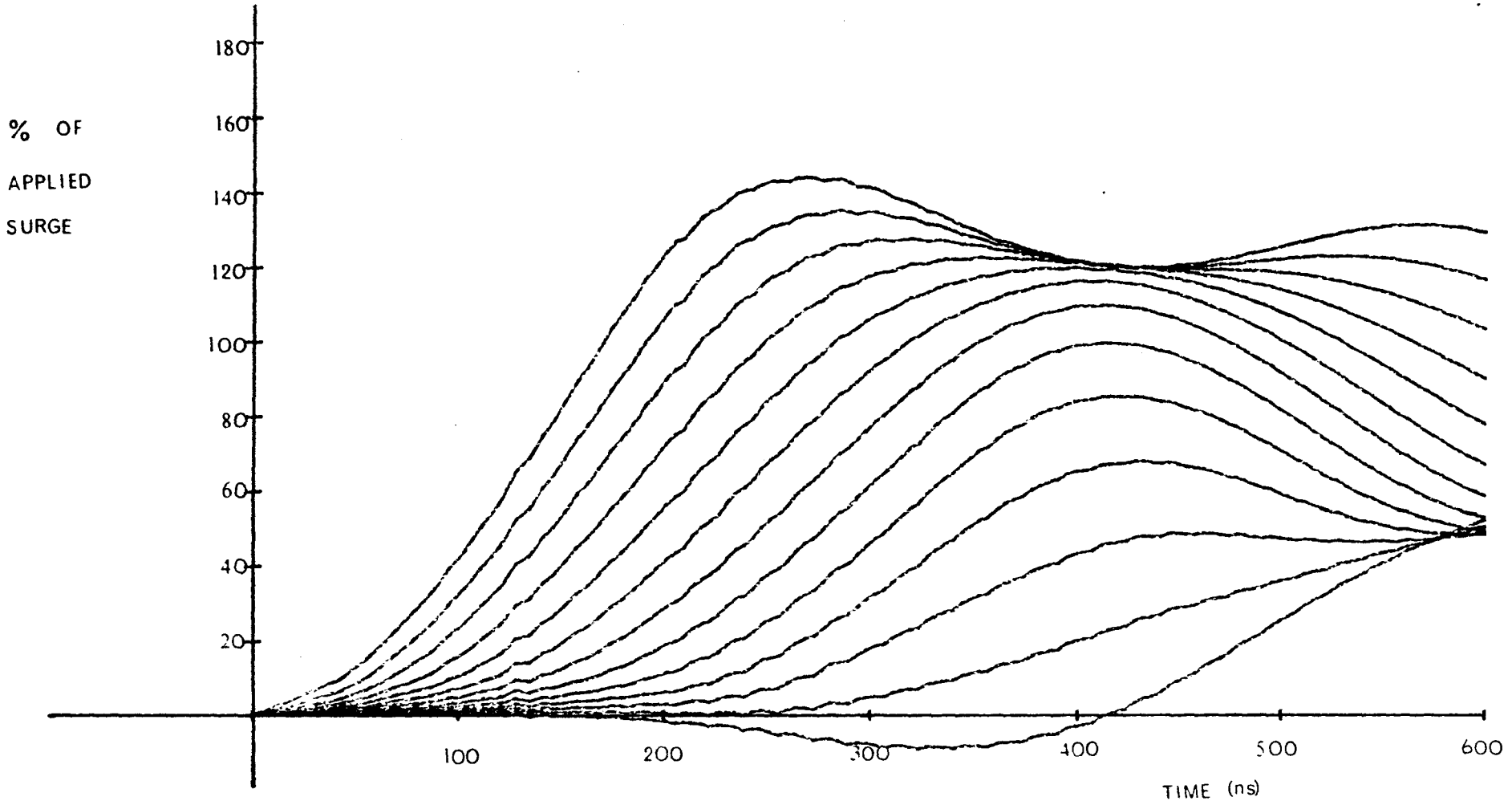

Figure 10.15 Turn to ground voltages on a 3.3kV, 12 turn, line end coil - 200ns Rise Time

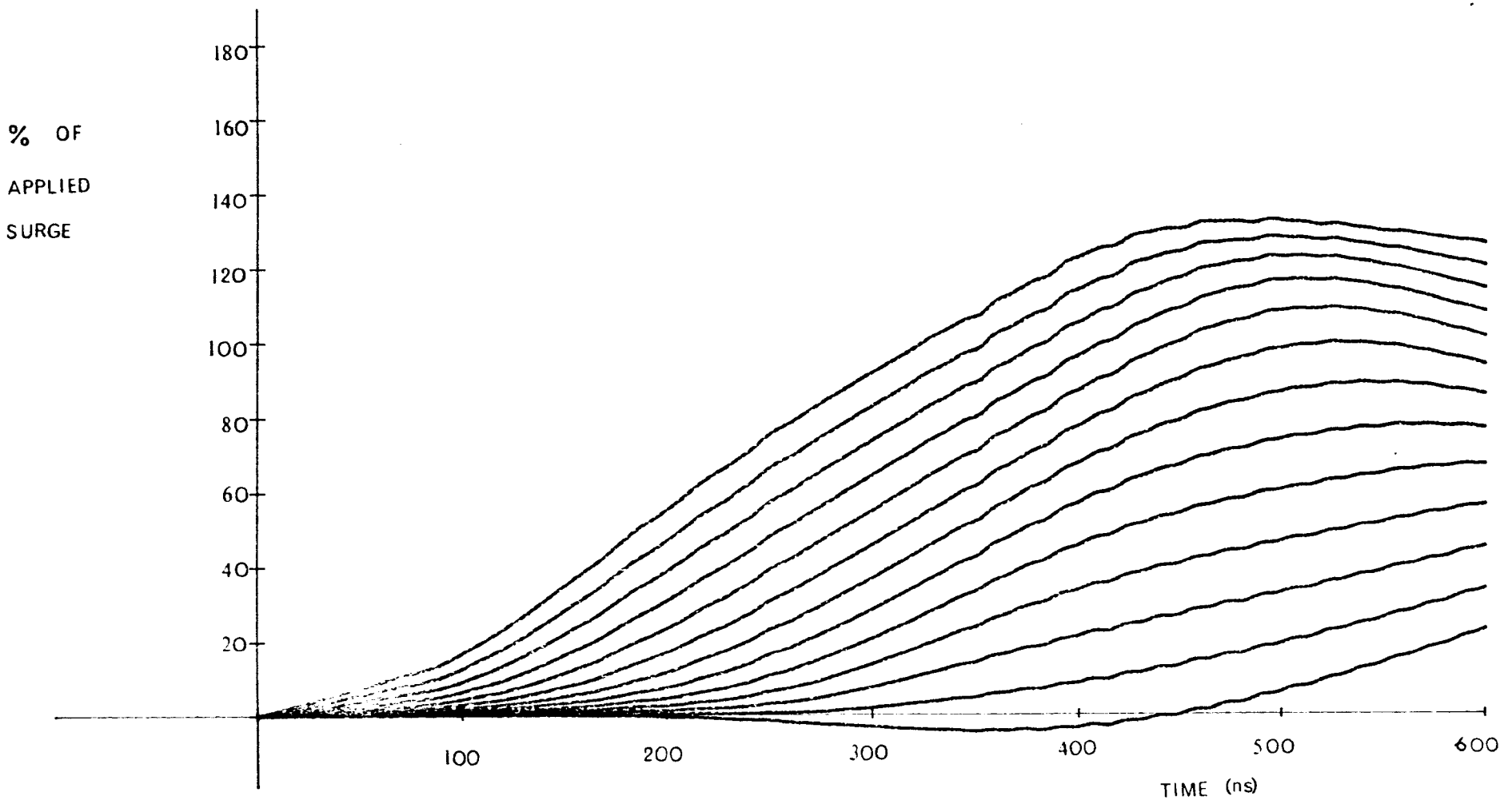

Figure 10.16 Turn to ground voltages on a 3.3kV, 12 turn, line end coil - 4oons Rise Time

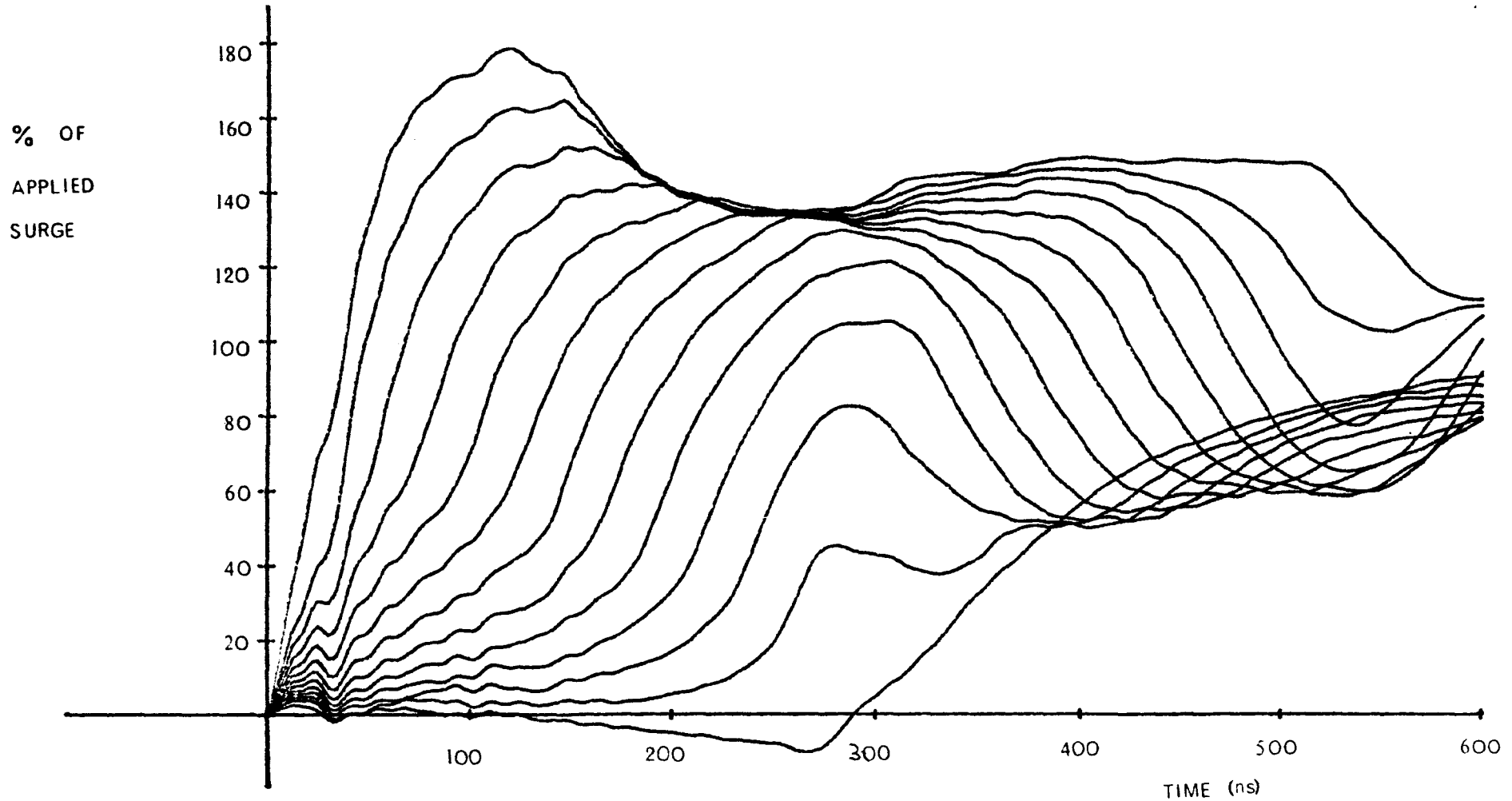

FIGURE 10.17 Turn to ground voltages on a 12 turn, 13.8kV line end coil, 25ns rise time

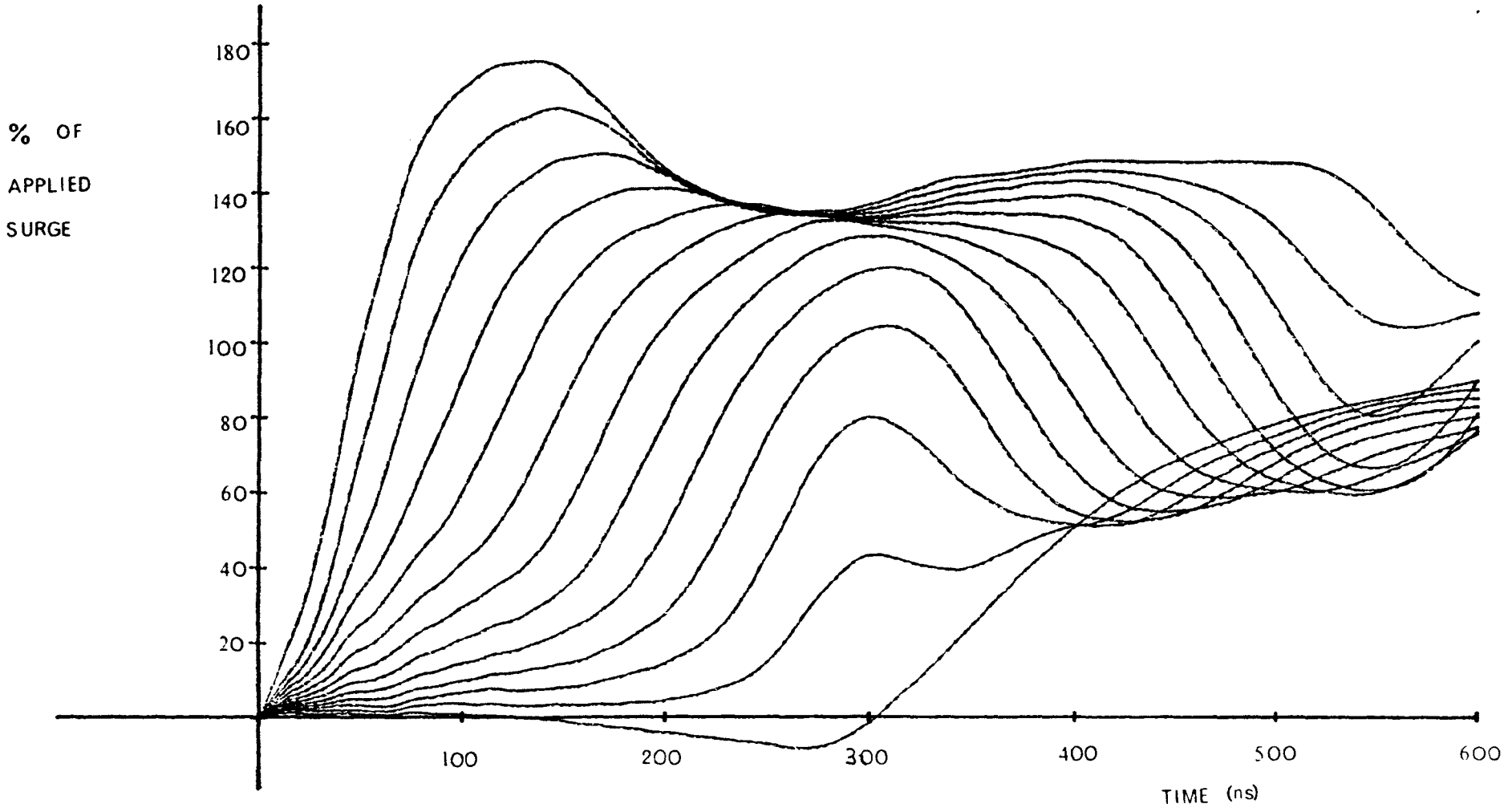

FIGURE 10.18 Turn to ground voltages on a 12 turn, 13.8kV line end coil, 50ns rise time

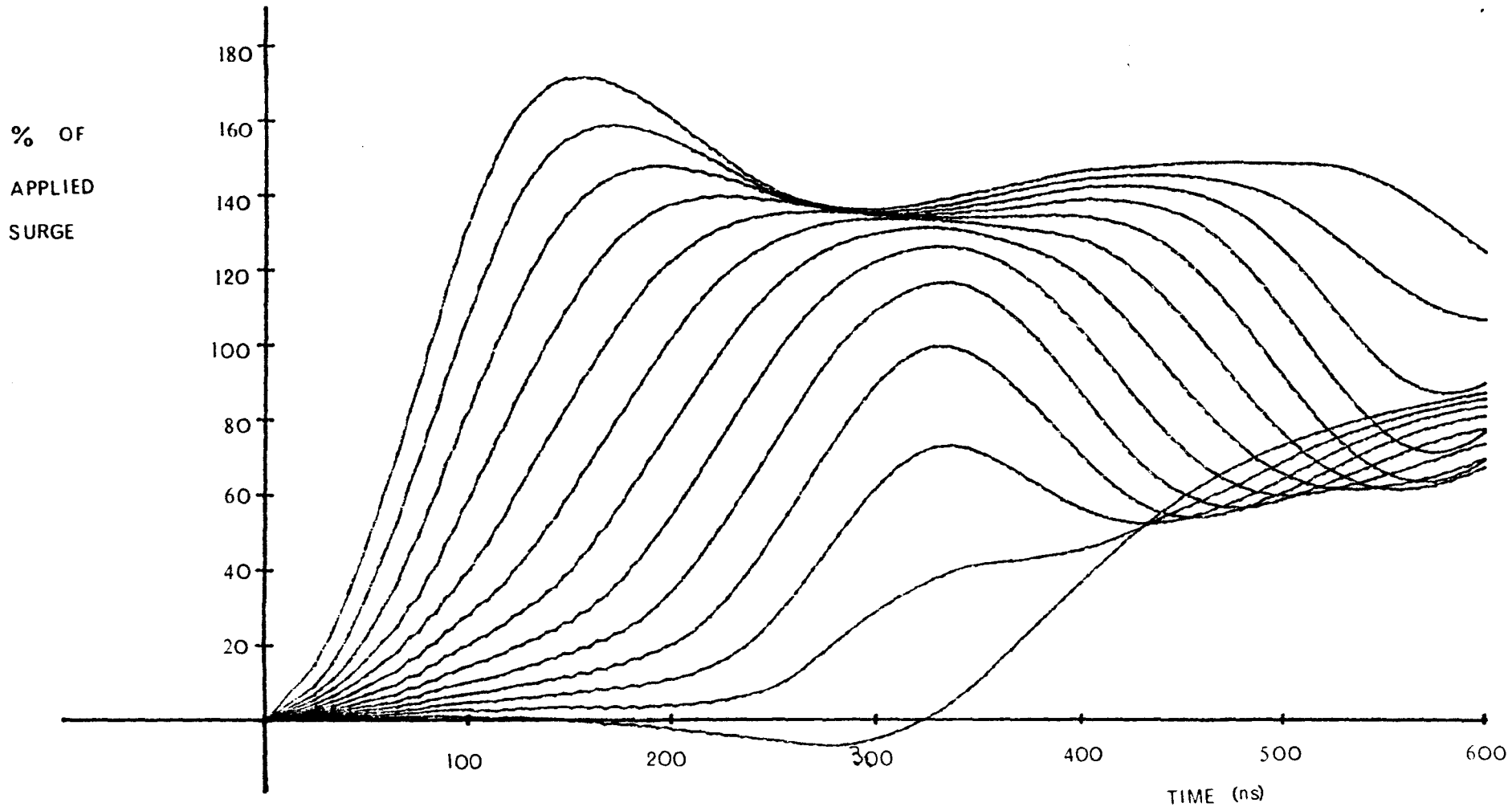

FIGURE 10.19 Turn to ground voltages on a 12 turn, 13.8kV line end coil, 100 ns rise time

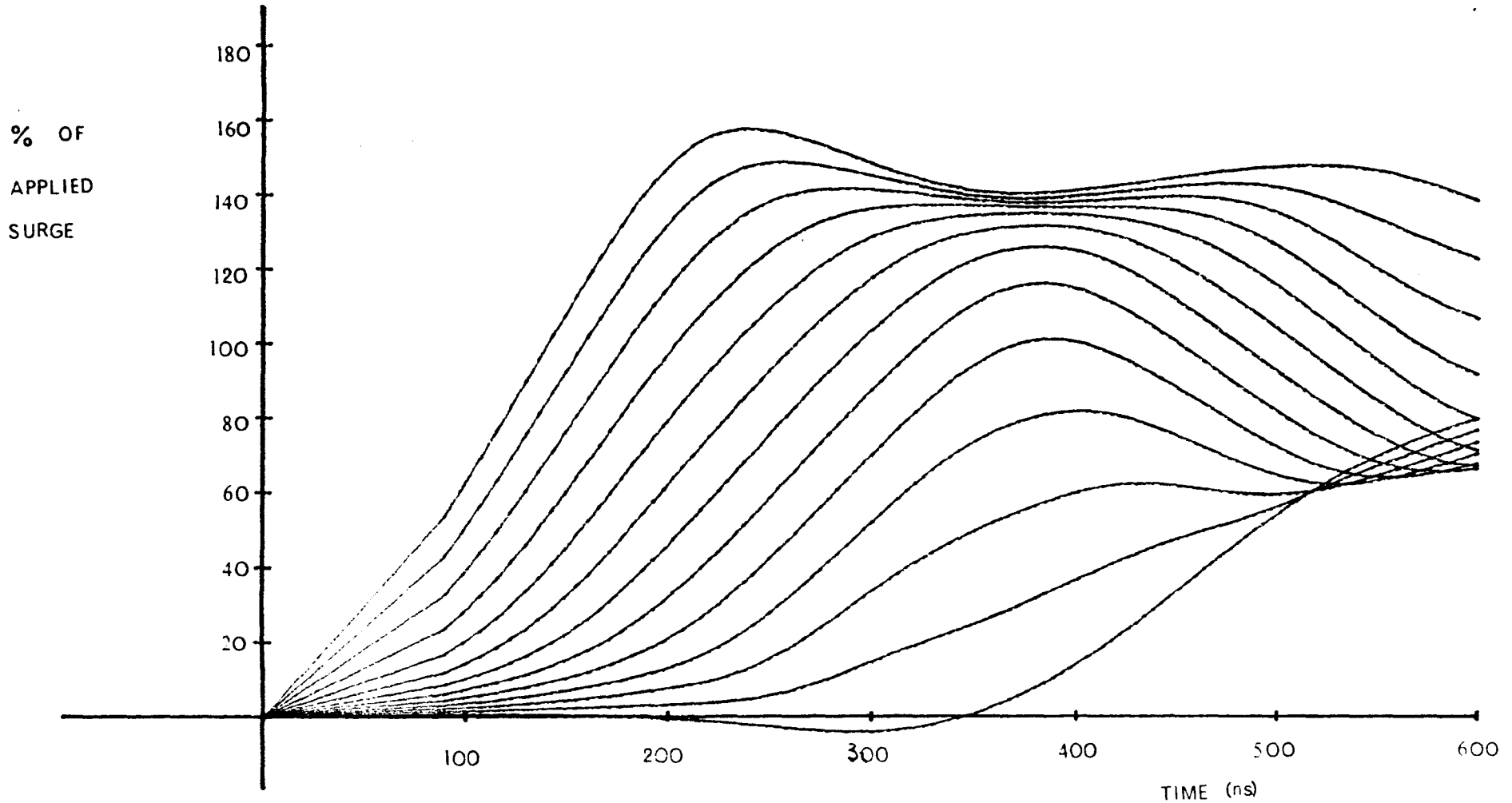

FIGURE 10.20 Turn to ground voltages on a 12 turn, 13.8kV line end coil, 200ns rise time

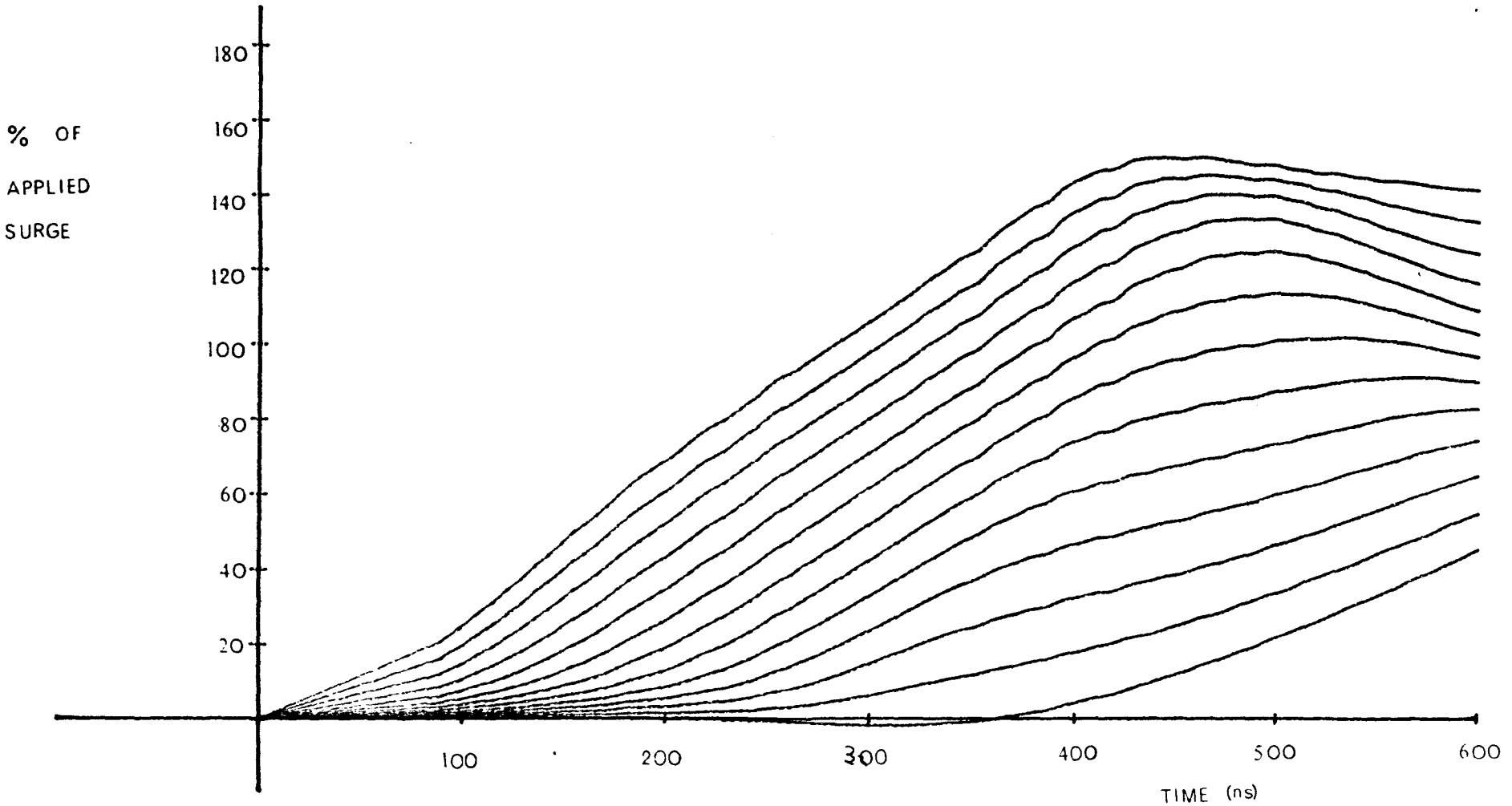

FIGURE 10.21 Turn to ground voltages on a 12 turn, 13.8kV line end coil, 400ns rise time

voltages which are produced by the surges. The maximum interturn voltage generated in the 13.8 kV coil was 53% of the applied voltage, compared with 40% for the 11 kV coil. Both these voltage peaks occurred due to the 25 ns rise time surge. (It should be remembered that these results were obtained from coils whose insulation systems are representative of only one manufacturer. Coils produced by other manufacturers will probably give different results.) While the actual interturn voltage increased by

$$\left[\frac{53\% \times 13.8\ \text{kV}}{40\% \times 11.0\ \text{kV}} - 1\right] \times 100\% = 66\%$$

the interturn insulation thickness increased by

$$\frac{(1.0 - 0.6)\ \text{mm}}{0.6\ \text{mm}} \times 100\% = 67\%$$

(see Appendix III).

Therefore in this case the safety factor is equal for the 13.8 kV and the 11 kV coils. Whether or not the safety factor is adequate depends on the quality of the insulation and on the per unit magnitude of the transient surges in the system.

In the case of the 3.3 kV coil the maximum interturn voltage was 32%, therefore the actual voltage is reduced by

$$\left[1 - \frac{32\% \times 3.3\ \text{kV}}{40\% \times 11.0\ \text{kV}}\right] \times 100\% = 76\%$$

compared with the 11 kV coil, whereas the interturn insulation thickness is reduced by

$$\frac{(0.6 - 0.5)\ \text{mm}}{0.6\ \text{mm}} \times 100\% = 17\%$$

(see appendix III).

Thus for the coils used in this study the 3.3 kV coil would seem to have a higher interturn factor of safety than the 11 kV and 13.8 kV coils. However, it should be noted that the safety factors are based on the assumptions that the per unit surge magnitudes are equal for all three voltage levels and that the quality of the insulation is equal in all three cases.

The quality of insulation is unlikely to be as good for the thinner insulation since it comprises fewer layers and therefore the effect of one defective layer is more serious than where a large number of layers insulate the conductors. This is why a larger safety factor is used in the 3.3 kV coils.

10.2.2. Variation in Interturn Insulation.

The increase in relative turn voltage with voltage level can be explained by the hypothesis stating that: as interturn insulation becomes thicker the electromagnetic coupling between turns decreases, thus turn voltages become more dependent on the portion of the surge which travels in a series manner, i.e. turn by turn, through the coil, and less dependent on the portion of the surge which is transmitted to each turn by electromagnetic coupling. In order that the validity of

this explanation could be fully tested, the voltage distributions for a coil whose insulation was as for the 11 kV coil except that the interturn insulation thickness was increased by 50% (see Appendix III), were computed for surges of 25, 50, 100 and 200 ns rise time. These voltages are shown in figures 10.22-10.25 and the peak voltage between each pair of turns are plotted in figure 10.26. Comparing these interturn voltages with those for the original 11 kV coil (figure 10.8) shows that the effect of increasing the interturn insulation by 50% is to increase the maximum interturn voltage by as much as 24.4%. This result is significant because at present E.S.I. interturn insulation standards (19) take no account of interturn voltage distribution (see chapter 11), therefore machine manufacturers may increase the insulation to pass a test level but in doing so they will also increase the possible interturn voltage magnitude. An interturn test which did allow for voltage distribution would have a higher interturn test level for coils with lower interturn coupling. For example, coils which are made with broad conductors will have a large interturn capacitance and so will have a better interturn surge capability than would otherwise have been the case. At present the E.S.I. test methods make no allowance for this.

A measure of the non-uniformity of the interturn voltage distribution can be obtained by defining a non-uniformity factor (N.U.F.) given by

$$\text{N.U.F.} = \frac{\text{maximum interturn voltage}}{\text{average interturn voltage}}$$

Non-uniformity factors for the various coils are shown in Table I. The standard deviation σ_{n-1} is also included to give an alternative measure of

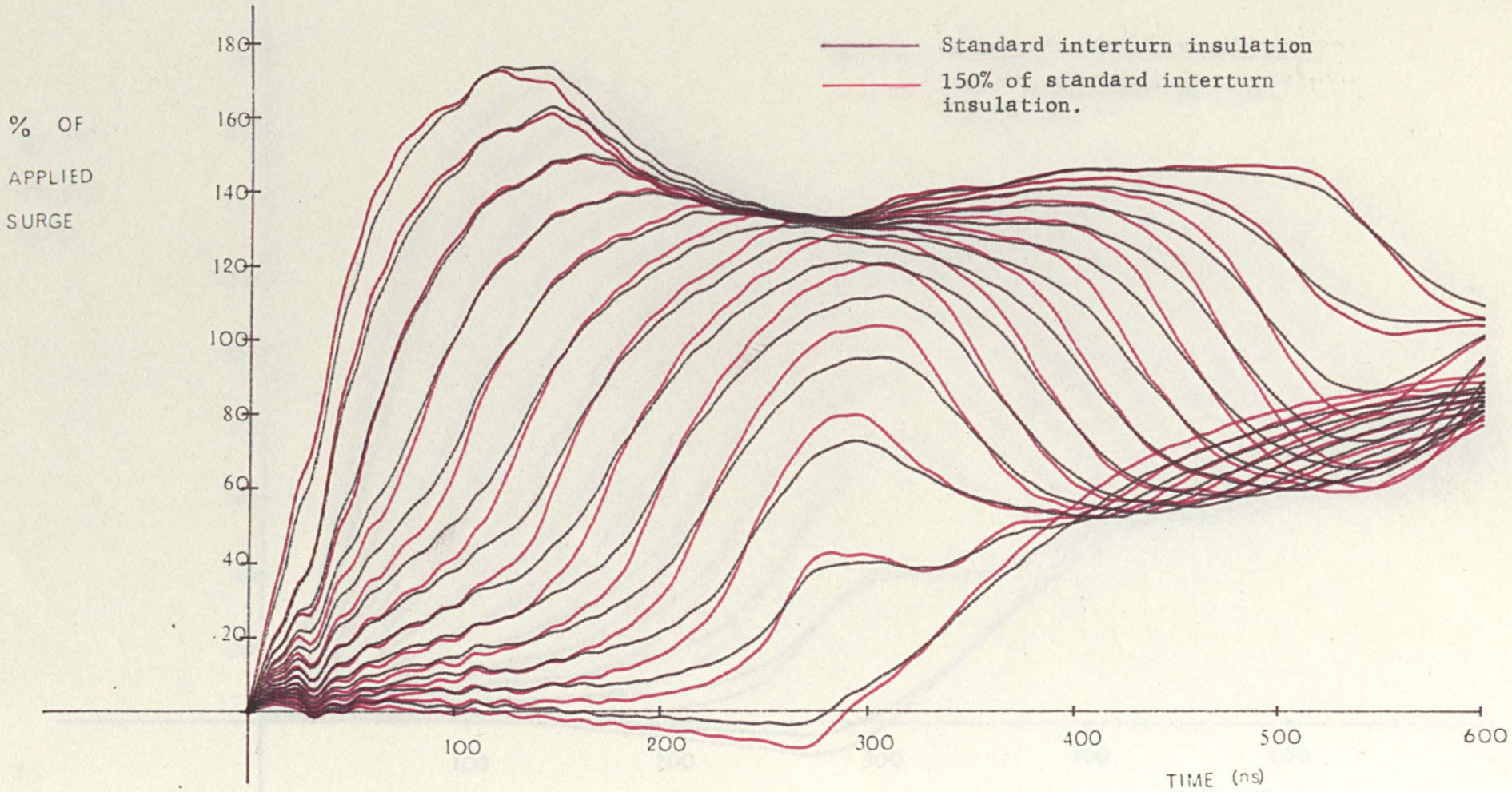

FIGURE 10.22 Turn to ground voltages on an 11kV, 12 turn, line end coil with two interturn insulation levels - 25 ns rise time.

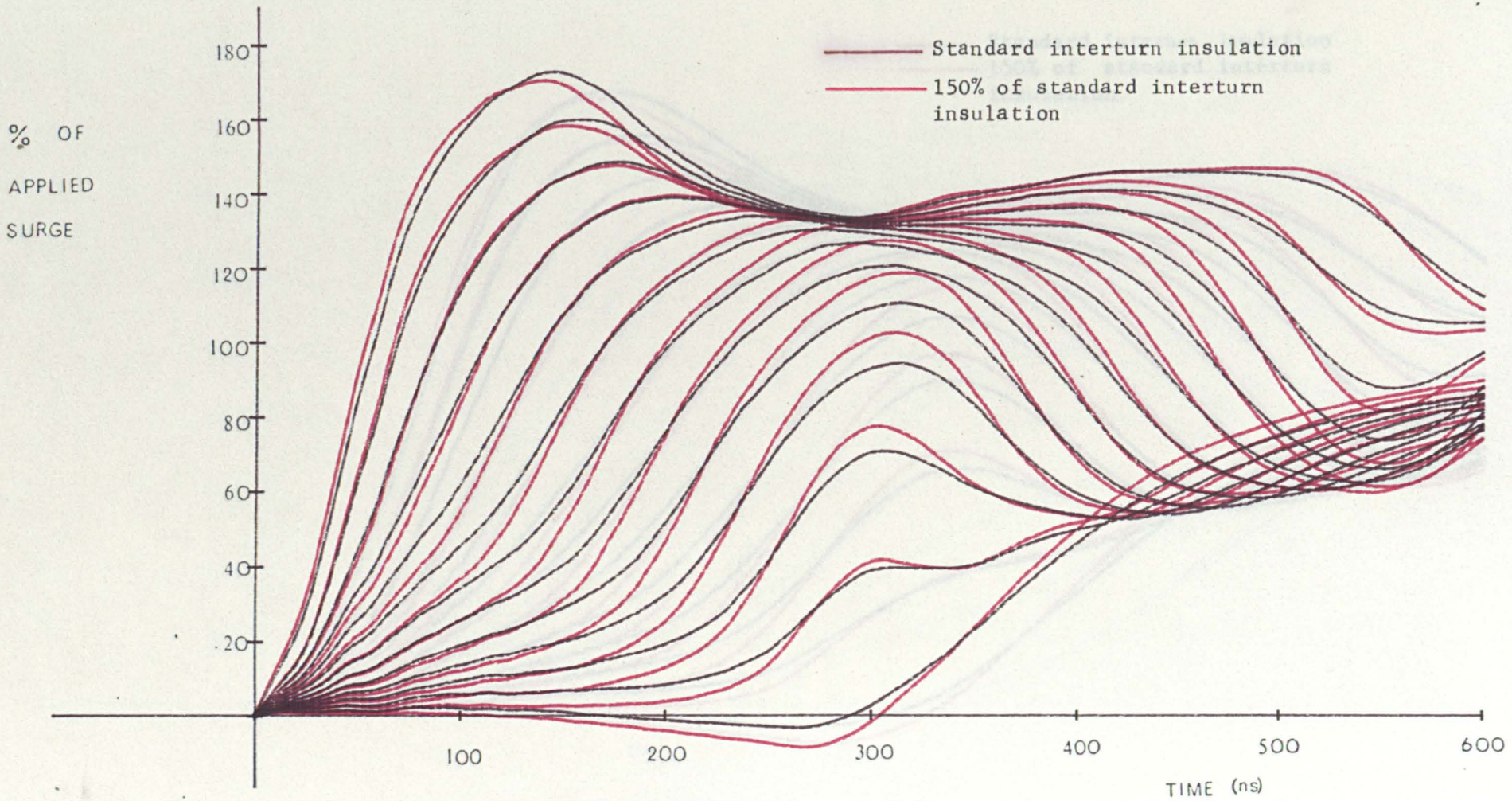

FIGURE 10.23Turn to ground voltages on an 11kV, 12 turn, line end coil with two interturn insulation levels - 50 ns rise time.

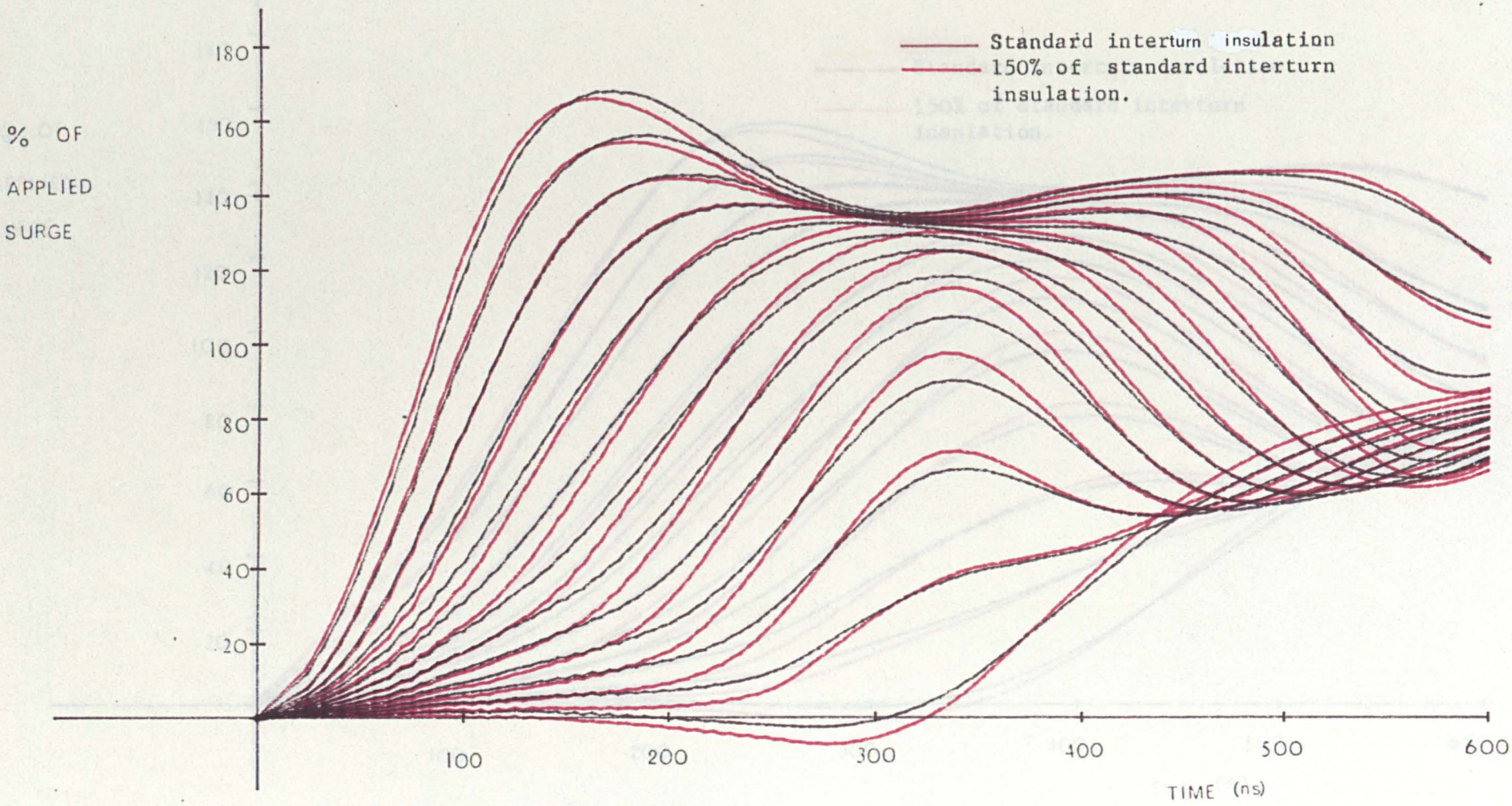

Figure 10.24 Turn to ground voltages on an 11kV, 12 turn, line end coil with two interturn insulation levels - 100ns rise time.

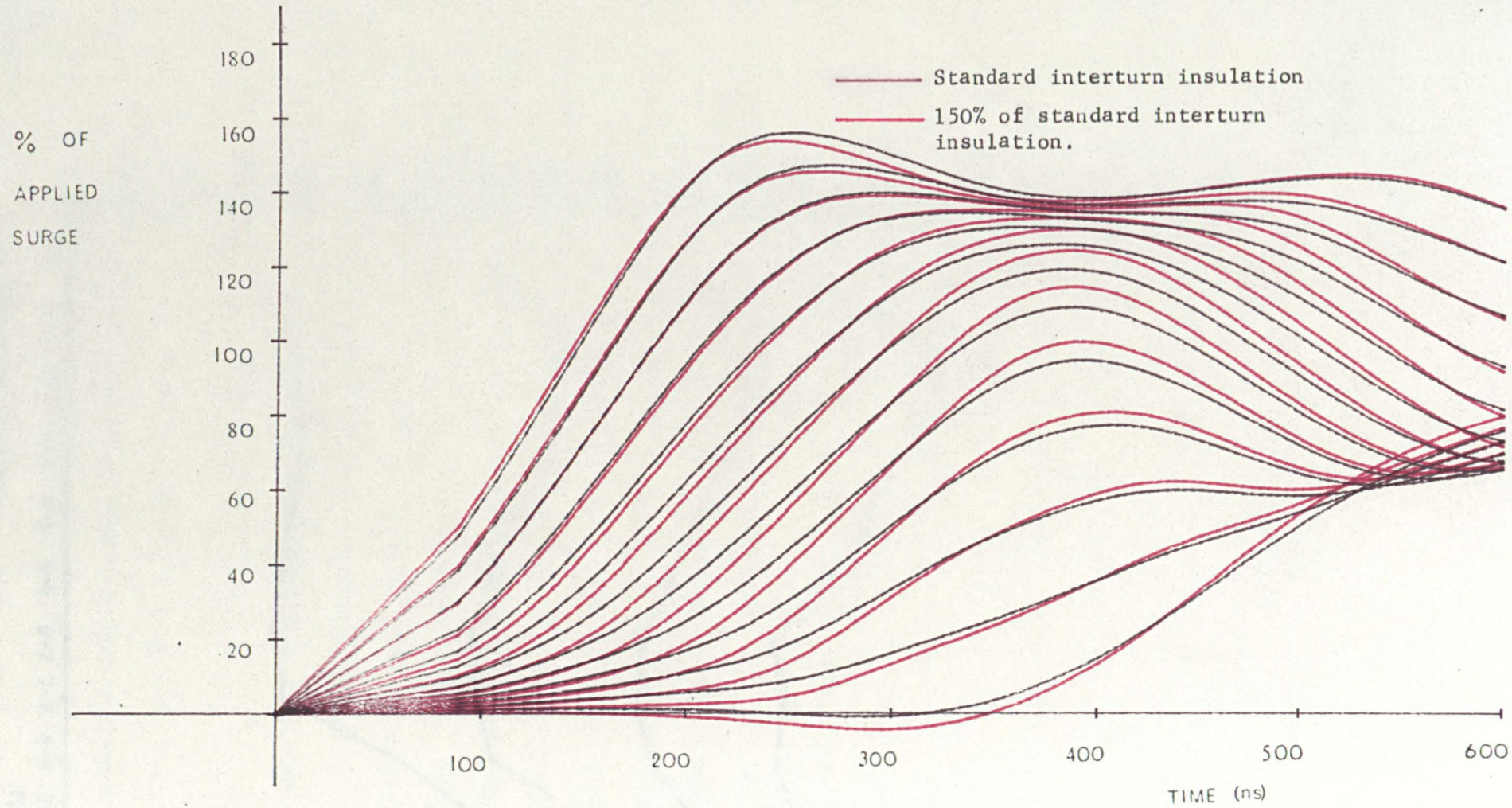

FIGURE 10.25 Turn to ground voltages on an 11kV, 12 turn line end coil with two interturn insulation levels - 200 ns rise time.

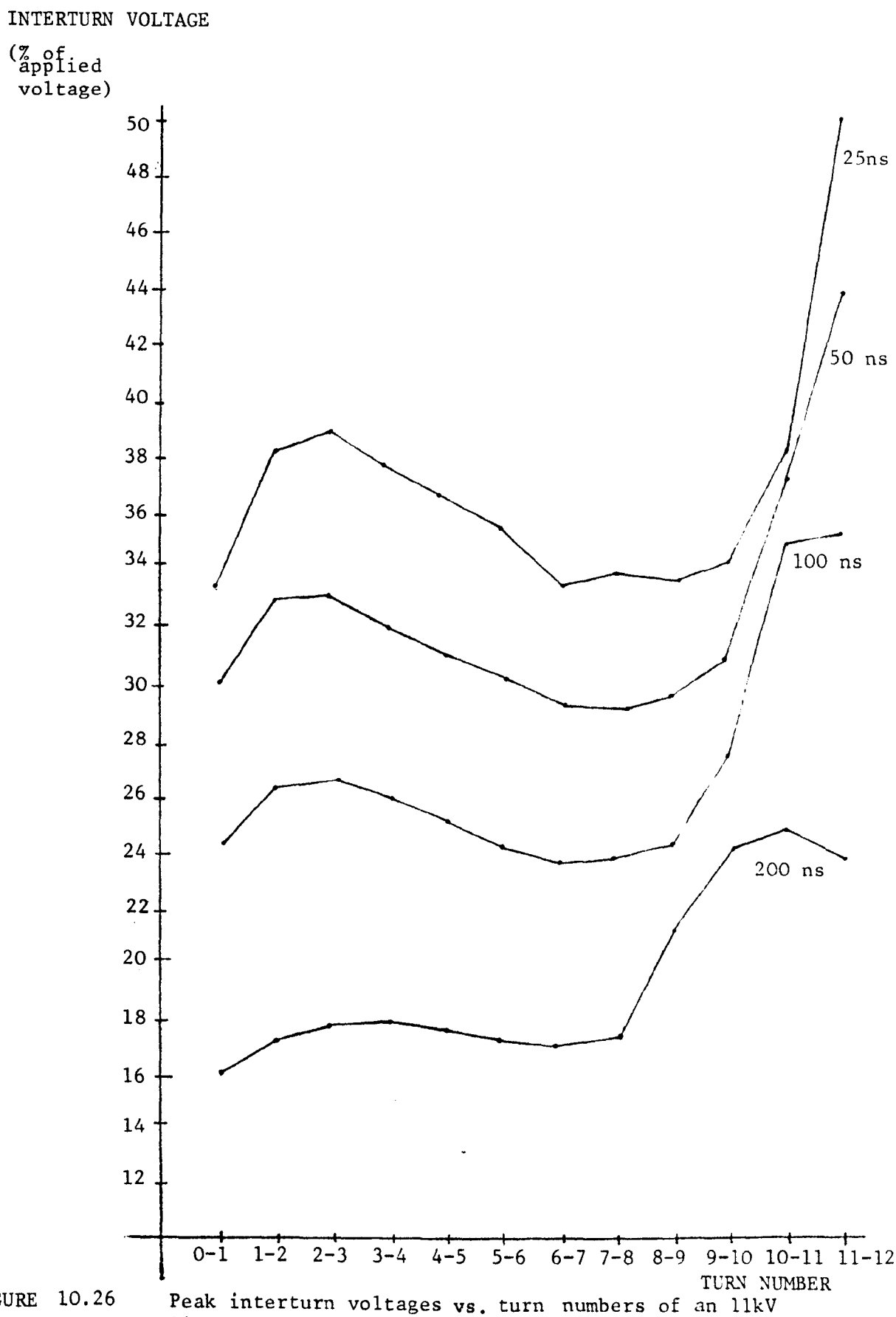

FIGURE 10.26 Peak interturn voltages vs. turn numbers of an 11kV line end coil with 150% of standard interturn insulation - various rise times

non-uniformity.

TABLE I

Insulation Level

Surge Rise Time (ns)	3.3 kV		11.0 kV		11.0 kV*		13.8 kV	
	NUF	σ_{n-1}	NUF	σ_{n-1}	NUF	σ_{n-1}	NUF	σ_{n-1}
25	1.265	3.282	1.332	3.697	1.356	4.635	1.363	4.983
50	1.288	3.359	1.328	3.487	1.355	4.221	1.357	4.404
100	1.293	3.299	1.295	3.334	1.319	4.061	1.326	4.179
200	1.263	2.795	1.256	2.692	1.286	3.166	1.294	4.237
400	1.176	2.033	1.173	2.090	-	-	1.185	2.355

* 50% extra interturn insulation.

Column 1 of Table I and figure 10.10 both indicate that the maximum peak interturn voltage in the 3.3 kV coil approaches a maximum value as the surge front time decreases. The cause of this is the high interturn coupling in the 3.3 kV coil, due to the relatively thin insulation, limiting the voltage difference between neighbouring turns. Thus any further decrease in rise time will only increase the average peak interturn voltage and so improve the non-uniformity factor. This trend is not seen in the 11.0 kV and 13.8 kV results since the interturn coupling is weaker and so the maximum possible interturn voltage is not reached for the range of surges used here. In the 3.3 kV case, the maximum non-uniformity factor was reached at about 100 ns.

Figures 10.22-10.25 show that the turn to ground voltages in the coil with the increased interturn insulation have a greater tendency to remain near zero until the surge has reached that particular turn than

do the turn to ground voltages on the standard coil. The part of the curve wnere the voltage rises due to the arrival of the surge is steeper than for the standard coil. This supports the hypothesis that increasing the turn insulation leads to the series transmission of the surge through the coil gaining in importance at the expense of the shunt transmission.

It snould be noted that while general trends in the variation of surge distribution with various parameters may be predicted, as above, a detailed analysis is necessary if accurate predictions are required.

10.2.3. Effect of Insulation Dimensions on Surge Impedance.

An effective surge impedance can be obtained for the coils over the range of rise times as before. It can be seen from figure 10.9 that there is a considerable variation of this impedance with the rise time and also that the impedance increases with the insulation level.

10.2.4. Conclusions.

This latter result combined with the increased interturn voltages, means that the insulation levels need to be increased disproportionately with the operating voltage level, i.e. a doubling in operating voltage must be accompanied by an increase in the thickness of the insulation by more than a factor of two to maintain a constant safety factor.

10.3. THE EFFECT OF NUMBER OF TURNS PER COIL ON VOLTAGE DISTRIBUTION.

The model was used to predict the voltage distributions on coils with various numbers of turns, having identical insulation, due to the range of surges. The maximum interturn voltages appearing in the line

end coil of a winding are plotted in figure 10.27 for 4, 6, 8, 10 and 12 turns per coil over the range of surge rise times. It can be seen that the interturn voltages are not sensitive to the number of turns per coil. There is, however, some variation, particularly for the very short rise times, but even here the 10 and 12 turns per coil values are equal, indicating that it is only in coils consisting of a few turns that any variation at all is seen. Only in the case of coils with as few as 4 turns per coil was there a significant increase in maximum interturn voltage when compared to the 10 and 12 turn coils.

The number of turns per coil also affects the effective surge impedance. It was found that in the case of short rise times coils with few turns cause a greater increase in voltage at the winding terminal than do the coils with many turns, i.e. the low turns per coil machine windings have a greater surge impedance, particularly at very low surge rise times. It can be seen from figure 10.28 that this trend is reversed for surges with greater rise times. It should be remembered that, while the surge impedance varies greatly with the turns, the larger surge impedances cause only a small increase in reflected voltage since the coil surge impedance is much larger than the cable surge impedance.

10.4. THE EFFECT OF COIL SHAPE ON DISTRIBUTION.

It has been shown in sections 10.1 and 10.2 how the voltage distribution in a coil of a winding varies with the dimensions of the insulation for various surge front times. In this section the variation of the voltage distribution with the shape of the coil will be examined.

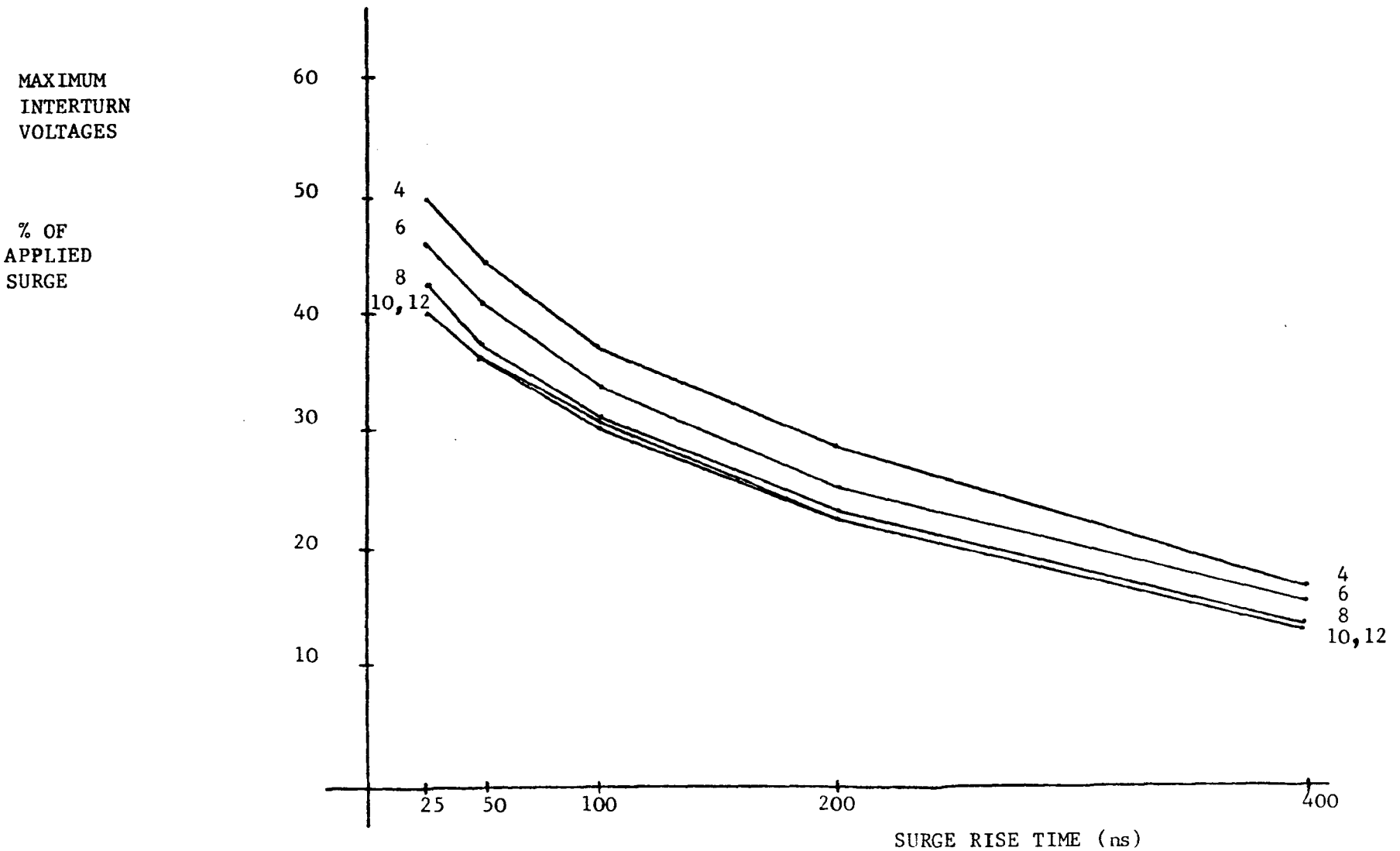

FIGURE 10.27 Maximum interturn voltage vs surge rise time for various turns per coil.

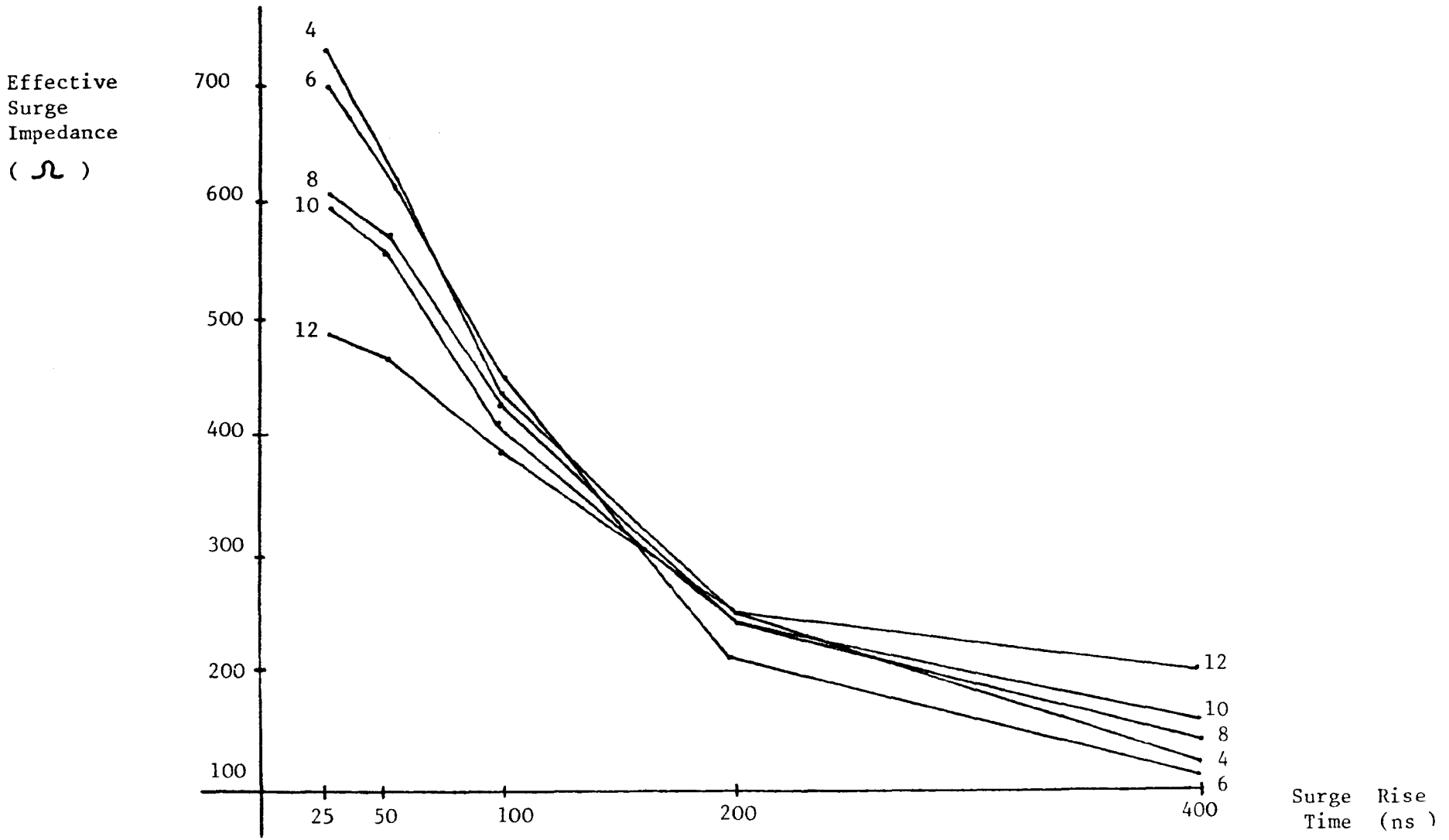

Figure 10.28 Effective surge impedance vs surge rise time for various turns per coil

The model of the coil makes no allowance for the complex shape of the end winding of the coil, and so for the purposes of this study the shape will be defined as the lengths of the slot portions and the end winding portions of the coil. It is reasonable to neglect any effects of the coil evolutes since they will be small and also since they will not vary from coil to coil. The effects of the coil shape were investigated on coils with 11 kV insulation and with surges which had front times ranging from 25 ns to 400 ns. Three shapes of coil were simulated on the computer model and the resulting voltage distributions were compared with the results obtained in section 10.2. The three variations in coil shape were:-

(i) the slot length increased by 50%,

(ii) the slot length and the end winding length increased by 20%,

(iii)the slot length and the end winding length reduced by 20%,

relative to the original 11 kV coil in previous chapters. Figure 10.29 shows the relative proportions of the coils.

Figure 10.30 shows the maximum voltage appearing between each successive pair of turns in the line end coil due to surges of 25, 50, 100 and 200 ns, showing how the distribution varies with the shape of the coils. It can be seen that, in general, the voltage distributions due to the faster wave fronts are less affected by the coil shape than are the voltage distributions due to the slower wavefronts. This is confirmed by figure 10.31 showing how the maximum interturn voltages in the line end coil of different shaped coils vary with surge rise time.

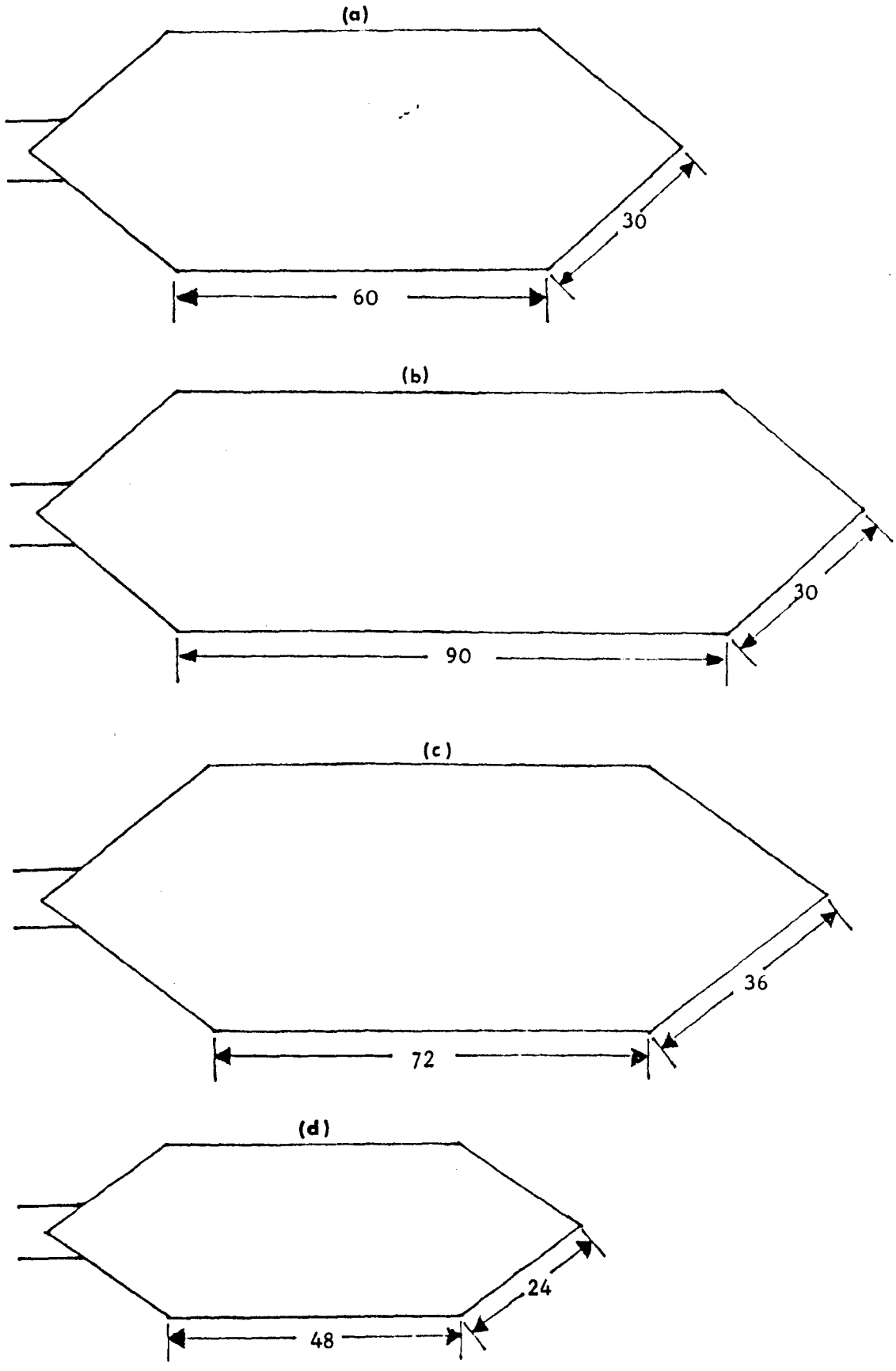

FIGURE 10.29 Proportions of coils used to investigate effect of coil shapes on voltage distribution
All dimensions in cm

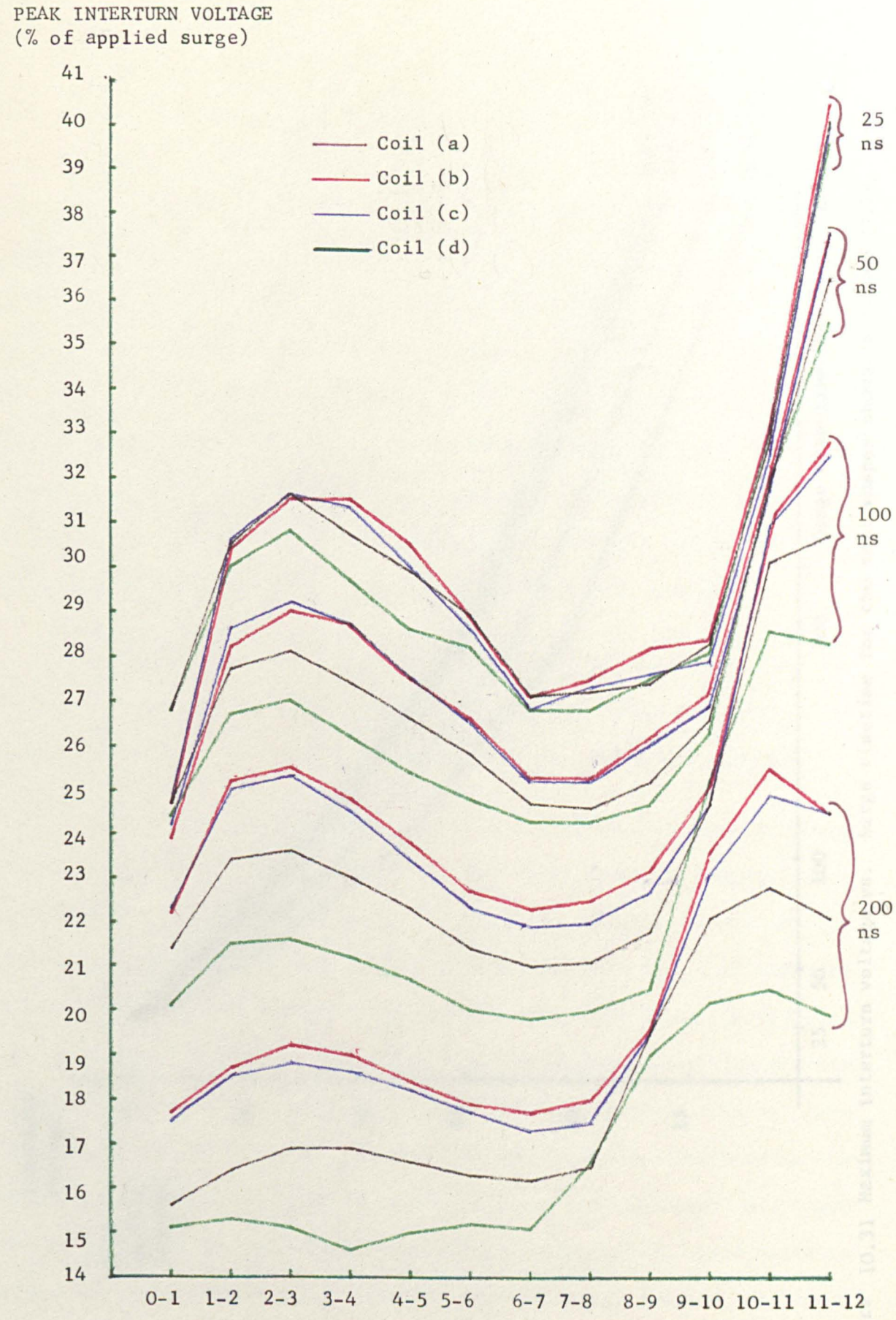

FIGURE 10.30 Interturn voltage distribution on line end, 11kV coils with shapes as shown in figure 10.29 - various rise times.

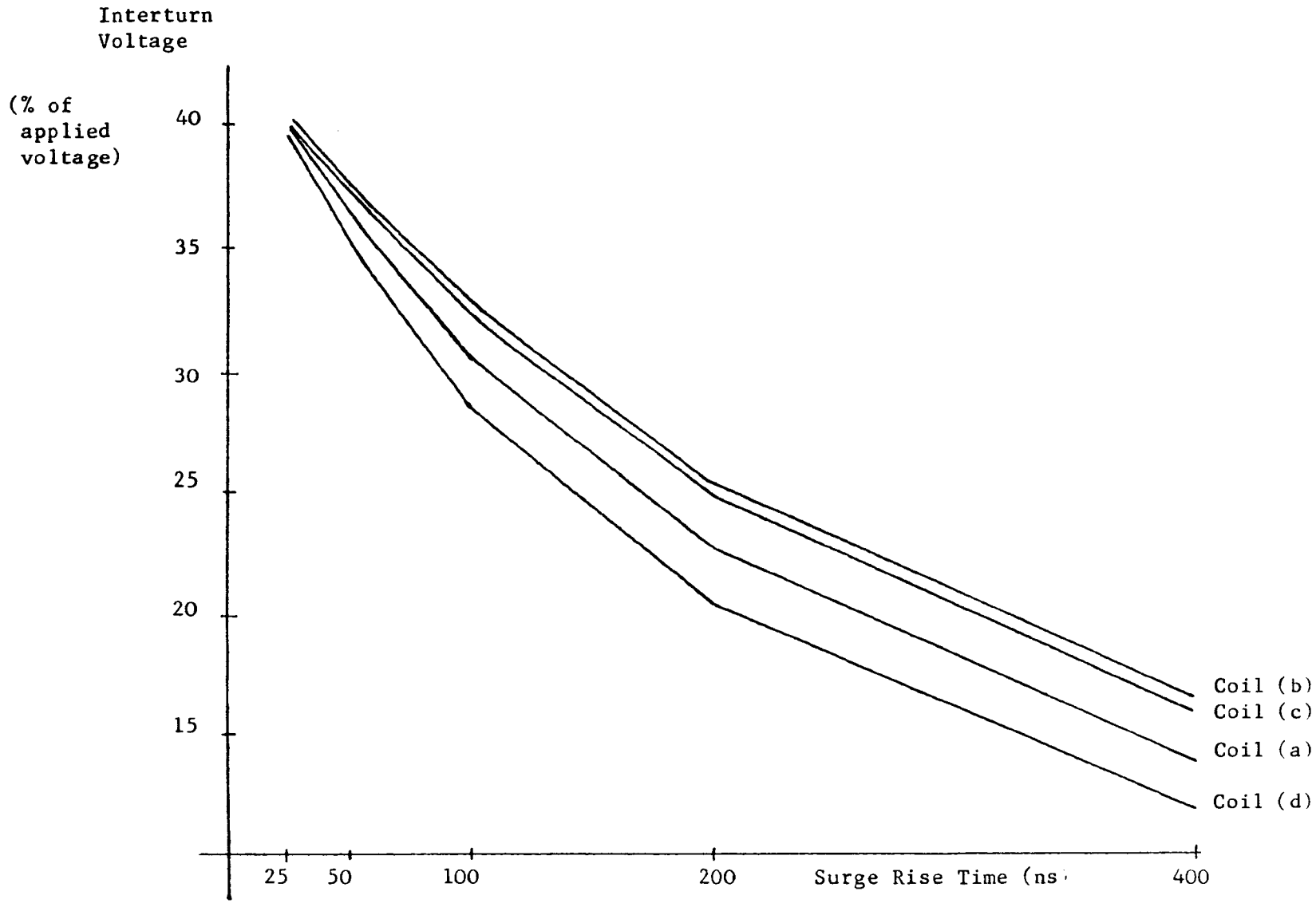

Figure 10.31 Maximum interturn voltage vs. Surge risetime for the coil shapes shown in figure 10.29

The explanation of figure 10.31, showing that for the very short rise times the maximum interturn voltages become independent of coil shape, is that for shorter wave fronts the maximum interturn voltage is limited more by the mutual coupling between turns than is the case for longer wavefronts. This is because as the front time of the surge approaches the turn travel time, the surge front is spread over one turn, or less, and so the interturn voltage is the result of the whole of the front time of the series portion of the surge appearing across the interturn insulation. Thus, as the wavefront of the applied surges becomes smaller the interturn voltages which are produced become more dependent on the cross sectional dimensions of the coil side and less dependent on the time taken to travel along each coil portion.

The results show that unless a machine winding is subject to very fast fronted surges (less than 30 ns) the coil shape does affect the magnitude of both the interturn voltages and the voltages to ground.

It can be seen from figure 10.31 that the difference between curves (b) and (c) is minimal, indicating that it is the total length of the coil and not the proportion of its constituent lengths which is the determining factor of the interturn distribution. (Coils (b) and (c) have the same overall length to within 4%). Increasing the overall size of the coil in steps of 20% ((d) to (a) to (c)) increases the maximum interturn voltage for rise times above approximately 30 ns. It is more likely, therefore, that high interturn stresses will be generated in the windings of high speed electric motors than in the windings of lower speed machines of equivalent rating and voltage level since coils in high speed motor windings have greater overall length because of their

large core length together with the large coil pitch (in mechanical degrees) which compensates for the smaller diameter of the slower machines.

The results described above indicate that the relationship between interturn voltages due to surges and coil length, or indeed core length, is complex. If a simple relationship, which accounts only for series surge propagation is used then the resulting variation of interturn voltage with coil, or core length will be erroneous. This simplification has been used in a recent publication (17) to give curves of interturn voltage versus core length for various surges. The present work demonstrates that these curves are incorrect.

The effective surge impedance of the winding is also affected by the change in shape of the coils. It can be seen from figure 10.32 that it is the ratio between the length of the slot portion and that of the end winding portion which has the major influence on surge impedance. An increase in the core length of the machine causes a decrease in surge impedance at low surge front times. The amount of variation in surge impedance should be kept in perspective since a large change in surge impedance can cause the overvoltage which is produced to change only slightly (see equation 10.1) e.g. a 400 Ω surge impedance at the end of a 75 Ω line will cause a reflection of 68.5% whereas a 500 Ω surge impedance causes a reflection of 73.9%. Thus in this case a 25% increase in the surge impedance will result in only a 3.2% increase in maximum voltage to ground. As stated previously, a knowledge of the surge impedance of a winding is no substitute for a full knowledge of the voltage distribution in the coils.

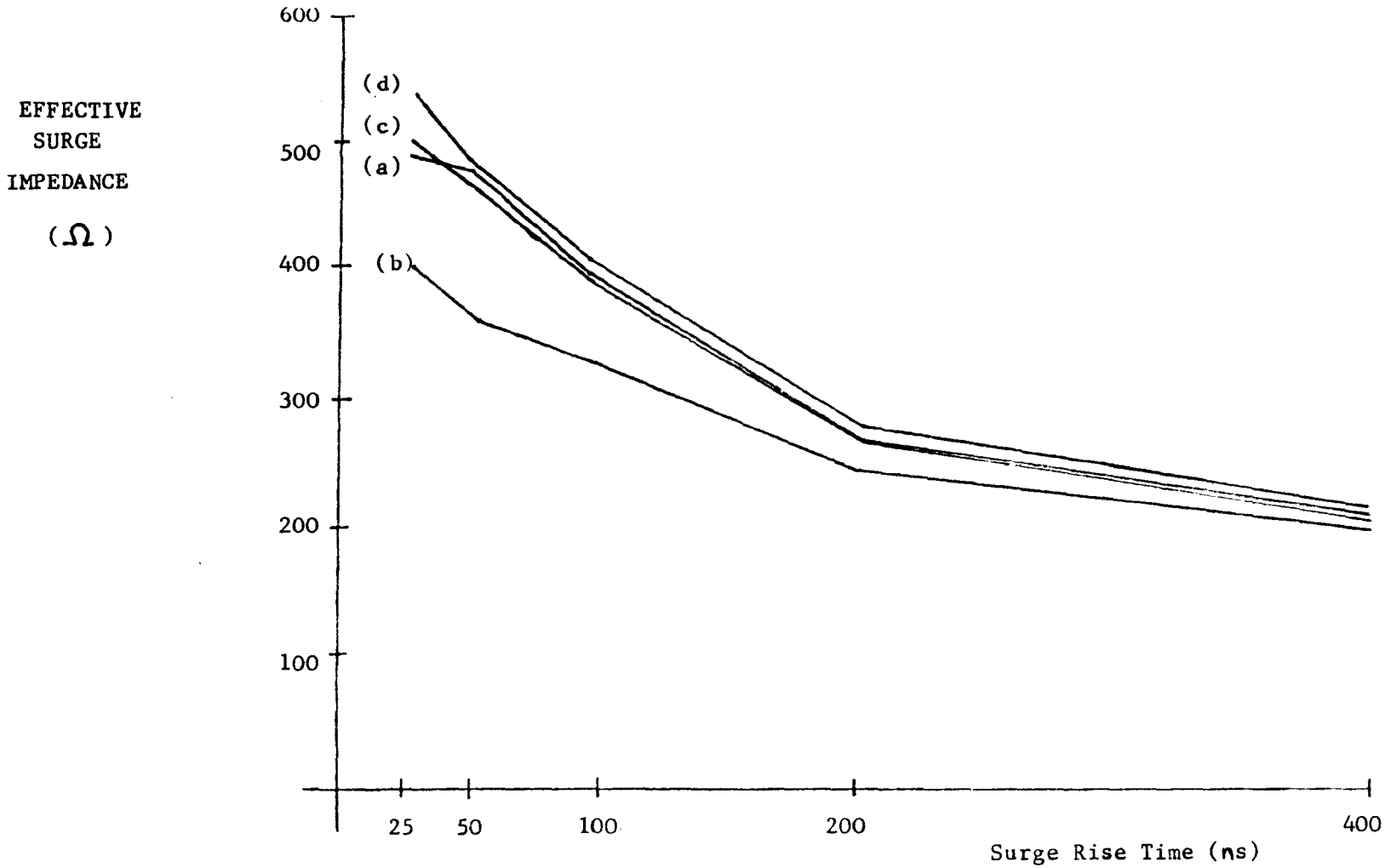

FIGURE 10.32 Effective surge impedance vs. Surge rise time for the coil shapes in figure 10.29

CHAPTER ELEVEN.

COMPARISON OF RESULTS WITH PREVAILING TEST STANDARDS.

It is worthwhile to compare the voltages which can occur between turns, as shown by the method of analysis described in this study, with the voltages which coils must withstand during the insulation tests. The most commonly used motor coil insulation test standard in the United Kingdom at present is the Electricity Supply Industry Standard 44-5, Issue 2, 1979 (18). This document details two types of test, (i) the Routine Quality Control Tests and (ii) the Type Tests.

The quality control tests, or proof tests, state that in the case of hairpin coils the interturn insulation should be tested by applying a voltage of V_n between each pair of turns at power frequency for a period of 1 seconds, where V_n is given by

$$V_n = 0.5(1 + V_L/3) \quad kV \text{ (r.m.s.)}$$

where V_L is the rated line voltage. Alternatively, where the turns are not available a high frequency impulse of peak voltage $\sqrt{2} \times V_n$ may be applied 5 times across the coil. There is an upper limit to the peak voltage applied to the coil given by

$$V_c = 0.5(4V_L + 5) \quad kV \text{ (peak)}$$

where V_c and V_L are in kV.

Thus for a 12 turn, 11 kV coil the coil voltage to be applied would be 24.5 kV peak. If the distribution is linear (there is no stipulation about the pulse shape and also, the voltage is applied across the coil

terminals) the interturn voltage would be 2.04 kV peak. These proof tests are carried out with the coils in their position in the motor core and so give an indication of the quality of the insulation after they have undergone the winding process.

A switching surge of 3 p.u. and a rise time of 25 ns would give rise, according to the new analysis, to an interturn voltage of 40.1% of that surge i.e. 10.8 kV, which is well in excess of the proof test level.

The E.S.I. 44-5 type tests state that a coil whose insulation system is the same as that used on the actual motor coils is to be used to test the type of insulation. The interturn insulation is tested by a voltage applied between adjacent turns of a coil which has been cut at an end winding arm. The interturn voltage to be applied is

$$V_n = (1 + V_L/3) \text{ kV (r.m.s.)}$$

which in the case of the 11 kV coil gives

$$V_n = 6.6 \text{ kV peak.}$$

Then the voltage is to be raised to 150% of this value i.e. 9.9 kV.

Clearly, neither of the two interturn test levels are as high as the the interturn voltage which is caused by a 3 p.u., 25 ns surge. In addition to this it should be noted that the type tests are not carried out on coils which have not been set in place in a winding i.e. they have not received any of the rough treatment which can occur during the winding process, and so may be in better condition than those in an actual motor. Also, surges which are more severe than the 3 p.u., 25 ns

surge could be applied to the motor terminals. The interturn voltage will increase pro-rata with the surge magnitude and also, as shown in section 10.1, as the rise time decreases. Even a 400 ns pulse of 3 p.u. magnitude will produce an interturn voltage of 4.6 kV which is much greater than the proof test level. Thus if a coil is damaged during the winding process, the proof test will not ensure than it can withstand even a 400 ns, 3 p.u. surge. It should be noted that a 3 p.u., 25 ns switching surge is equivalent to 5.25 p.u. appearing at the line end coil terminal.

The recent Oil Companies Materials Association specification (23) dealing with interturn insulation provides a much more stringent proof test than E.S.I. 44-5. It is stated that a 3 p.u. 200 ns rise time surge is to be used to test windings and in special cases a 5 p.u. surge with similar rise time is to be used. While this is an improvement on E.S.I. 44-5 it is no guarantee against surges with steeper fronts, even if the magnitude of these steep surges is below that which O.C.M.A. specifies for its surge. As yet no type tests have been issued by O.C.M.A.

The advantage of an accurate method of predicting coil and turn voltages is that a coil or winding can be rated for a certain surge magnitude and rise time and so may be designed to withstand the surge conditions which may exist in the system. However, the surge capability of a coil is only one of many considerations in the motor design. Therefore in practice the surge capability, if specified at all, will be involved in a trade off with other design criteria to ensure that the best motor for the particular application is obtained. If it is found that a machine cannot be designed to innerently meet the surge capability

specification, then protective devices can be applied. The decision whether or not to use protection should be based on an analysis of the type described here.

CHAPTER TWELVE.

DESCRIPTION OF PROGRAMMING METHODS.

12.1. INTRODUCTION.

From the preceding chapters, it is clear that in order to calculate the voltages in the coils over even a short time period of say 1000 ns, many matrix multiplications must be carried out. In addition to this, the theory is developed in chapters 3 & 7 for coils with small numbers of turns (2 or 3) whereas in practice most motor windings are designed with coils consisting of a larger number of turns. Thus, for say a 12 turn coil the slot/end winding junction will be modelled by a scatter matrix of 24 elements square and the terminal junction by a matrix 26 elements square. Therefore, since the model relies on a large number of calculations involving large matrices it was necessary to use a digital computer to execute the computations involved in predicting the coil voltages.

The computer programmes which were developed to model coils can be separated into the three well defined sections:-

(1) The formulation of the scatter matrices.

(2) The calculation of the impulse response of the coil or winding.

(3) The convolution of the impulse response with the input wave shape to give the actual response.

12.2. CHOICE OF COMPUTER AND LANGUAGE.

All the computer work involved in this study was carried out on a

Digital Equipment Corporation PDP 11/45 minicomputer. The operating system used on this computer was written in the `C' programming language (24), it was therefore decided, in order to make the most efficient use of c.p.u. time, to use `C' for all the coil modelling work. In addition `C' has the advantage of being more concise than other more commonly used languages e.g. Fortran.

There are many good matrix inversion programmes on existence, many of which could have been used in the calculation of the scatter matrix. However, the computer used in this study did not have such a programme available. It was decided that the the interactive nature of this computer was an advantage which outweighed the disadvantage of not having a ready made matrix inversion programme.

12.3. FORMULATION OF THE SCATTER MATRICES.

The programme which calculates the scatter matrices from the admittance matrices of the lines and the junction voltage and current connection matrices, initially constructs the matrices

$$\begin{bmatrix} -(C_v) \\ (C_i)(Y) \end{bmatrix} \quad \text{and} \quad \begin{bmatrix} (C_v) \\ (C_i)(Y) \end{bmatrix}$$

in the lossless case, or

$$\begin{bmatrix} -(C_v) - (C_v)(R)(Y) - (C_v)(G)(R) \\ (C_i)(Y) + (C_i)(G) \end{bmatrix}$$

and

$$\begin{bmatrix} (C_v) - (C_v)(R)(Y) + (C_v)(G)(R) \\ (C_i)(Y) - (C_i)(G) \end{bmatrix}$$

in the lossy case.

Following this the programme carries out the inversion procedure on the first of each of the above two sets of matrices and multiplies the result by the latter to give

$$(S) = \begin{bmatrix} -(C_v) \\ (C_i)(Y) \end{bmatrix}^{-1} \begin{bmatrix} (C_v) \\ (C_i)(Y) \end{bmatrix}$$

or

$$(S_L) = \begin{bmatrix} -(C_v) - (C_v)(R)(Y) - (C_v)(G)(R) \\ (C_i)(Y) + (C_i)(G) \end{bmatrix}^{-1} \begin{bmatrix} (C_v) - (C_v)(R)(Y) + (C_v)(G)(R) \\ (C_i)(Y) - (C_i)(G) \end{bmatrix}$$

The construction of the admittance matrices is straightforward and is done by simply assigning the appropriate values of each submatrix to that of the whole matrix.

The matrix inversion section of the programme uses the well known Gaussian elimination technique. The accuracy of the inversion programme was checked by multiplying the original matrix by its inverse. The nominally zero elements of the resulting identity matrix were found to have a magnitude of no more than 10^{-13}, thus showing the accuracy of the inversion to be excellent.

A problem which arises out of the use of this inversion method was that some of the elements in the leading diagonal of the original matrix

were zero, or nearly so. Thus it is not possible to divide the row by the magnitude of the leading diagonal element. This can be overcome by adding to that particular line another line from the matrix such that the leading diagonal element of the sum is non-zero. Due to the structure of the matrices in question, such a line can always be found. (In other words the matrix is always invertible.) This operation is necessary only on the matrices pertaining to the terminal junctions in the winding, since the leading diagonals of the slot/end-winding junction matrices have no zero, or near zero, elements.

The inverse of the first matrix is then multiplied with the second matrix as in equation 12.1 or 12.2 to give the resulting scatter matrix. The programme ESST, which carries out the above operations, is given in Appendix IV(a).

12.4. THE CALCULATION OF THE IMPULSE RESPONSE OF THE COIL OR WINDING.

This programme calculates the response of the coil to an input, which is an idealised impulse, entering the coil at its terminals at time t = 0. The response at any point on the coil to this input is, due to the lack of distortion in the multiconductor transmission lines of the model, simply a series of idealised impulses of varying magnitudes and with various time intervals between them.

The basic idea behind the programme was to calculate each scattering operation in chronological order and then put the resulting reflected impulses in to a store together with the number of the junction to which they next travelled and the time at which they impinged on it. The store was then searched for the next scattering operation to

take place. A flow diagram for this programme is shown in figure 12.1, overleaf.

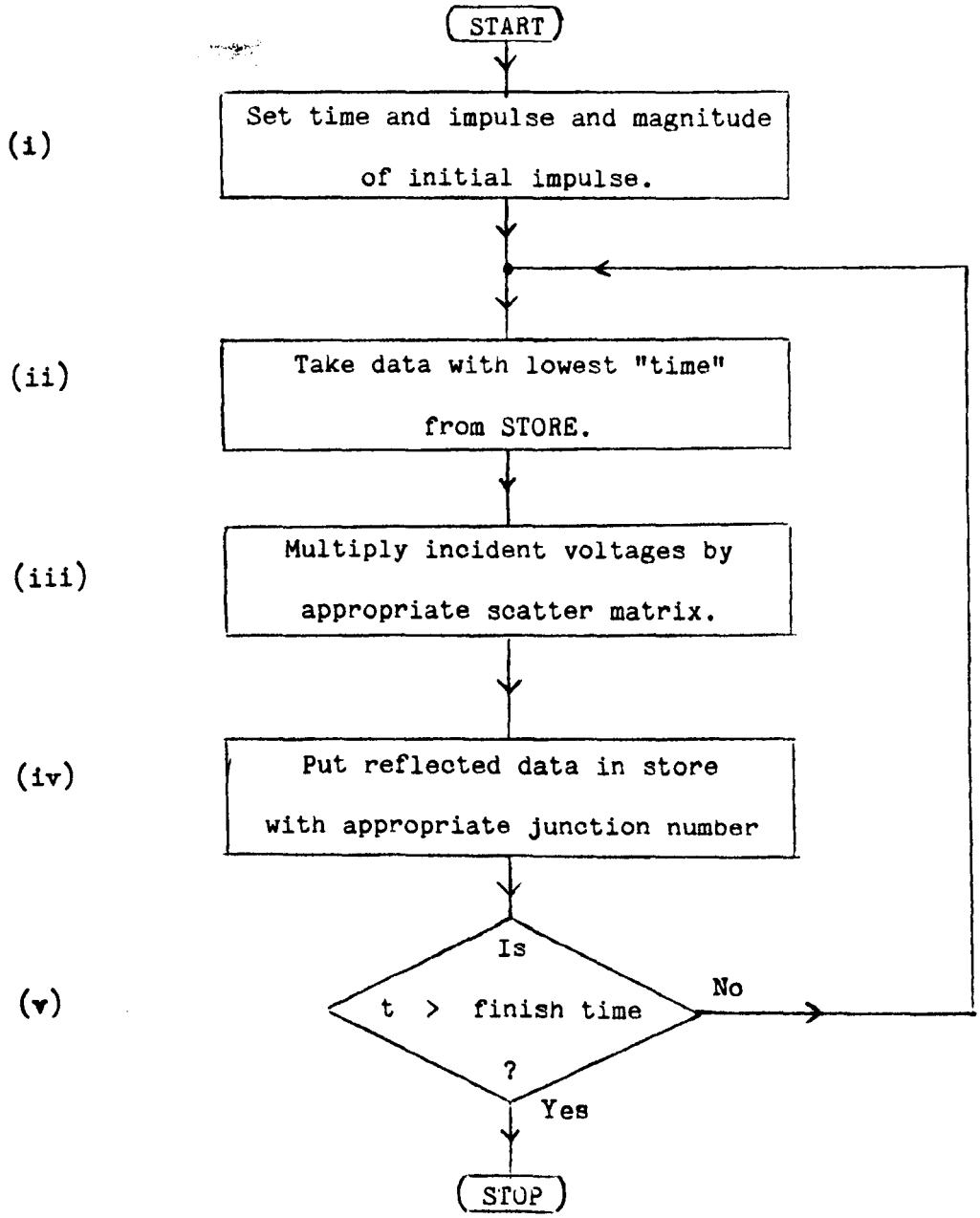

FIGURE 12.1 FLOWCHART OF IMPULSE RESPONSE PROGRAMME.

This simplified flowchart gives only the broad outline of the

programme. Sections (i), (iii) and (v) are self explanatory and can each be implemented in one line of `C'. Sections (ii) and (iv) however are complex and require some detailed explanation.

Section (ii) of the programme searches through all the entries in the store to find the one with the lowest time. The store is then searched again to find any other entries which have the same time and the same junction number. In other words all the sets of incident waves which impinge on a particular junction at or about the same time are treated as a single set of incident impulses irrespective of where in the system they originated.

The space reserved for each entry in the store is 2n + 2 places for the magnitude of the the impulses (2n + 2 is the size of the incident impulse array of the terminal junction) plus a place each for the junction number and the time of scattering.

There is an alternative to the method described above. When the entries are placed in the store they could be added to any other entry which had the same time and junction number. However this would necessitate searching through the store for every entry stored as opposed to every retrieval as before and is hence more time consuming. Even although the latter method has the advantage of using less temporary storage space, it was decided to use the former method as it is more time efficient. A flow diagram of this section of the programme is shown in figure 12.2, overleaf.

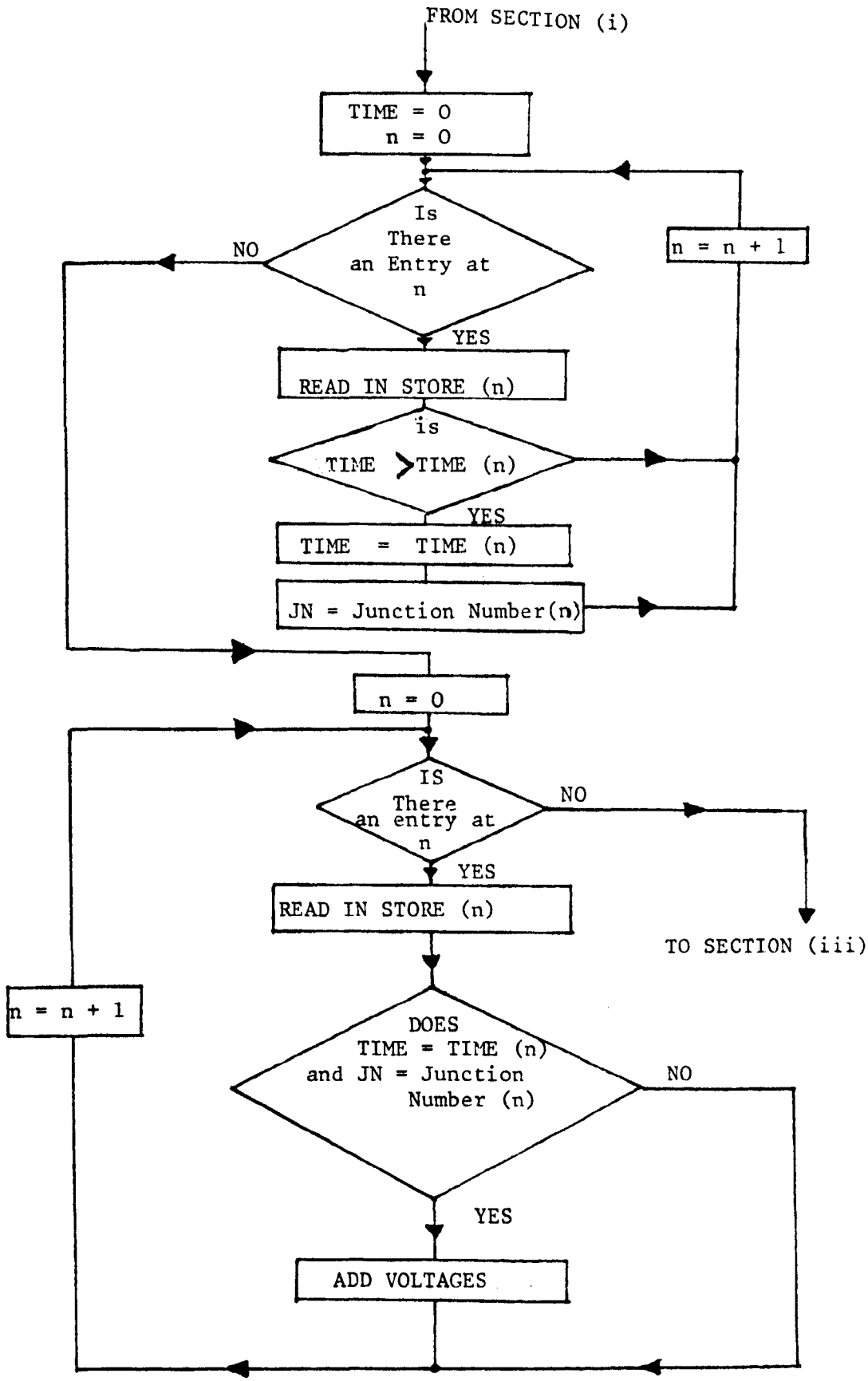

FIGURE 12.2 Flowchart of data extraction from STORE

Section (iv) of figure 12.1 puts the reflected voltages resulting from the scattering multiplication into the store together with the number of the junction to which they are travelling and the time at which they get there. In the case of the slot/end-winding junction each scattering operation will produce 2 entries in the store. A terminal junction scattering operation produces 3 or 4 entries in the store depending on whether or not the coil in question is at the end of the winding.

In the case of the single coil analysis it was found simpler to use a separate list of commands for each junction (0 - 4), than to use a general command list for all the junctions with complex conditional statements. In the case of the model for the whole winding a general command list could be used for junctions 1,6,11..., junctions 2,7,12... etc. and all the terminal junctions which were not at either the line end or the neutral end of the phase. The flowchart of this section of the programme, in the case of a four coil winding, is shown in figure 12.3, overleaf. The junction numbers and the travel times referred to in figure 12.3 are shown in the following diagram, figure 12.4. In order to negate the need for modelling the switchgear end of the cable by another junction, the reflection from junction 0 to the switchgear is accounted for by returning it to junction 0 after twice the cable travel time and multiplying it by the source reflection factor.

The impulse response programme (LOSSCAL), which calculates the lossy impulse reponse, is listed in Appendix IV(b).

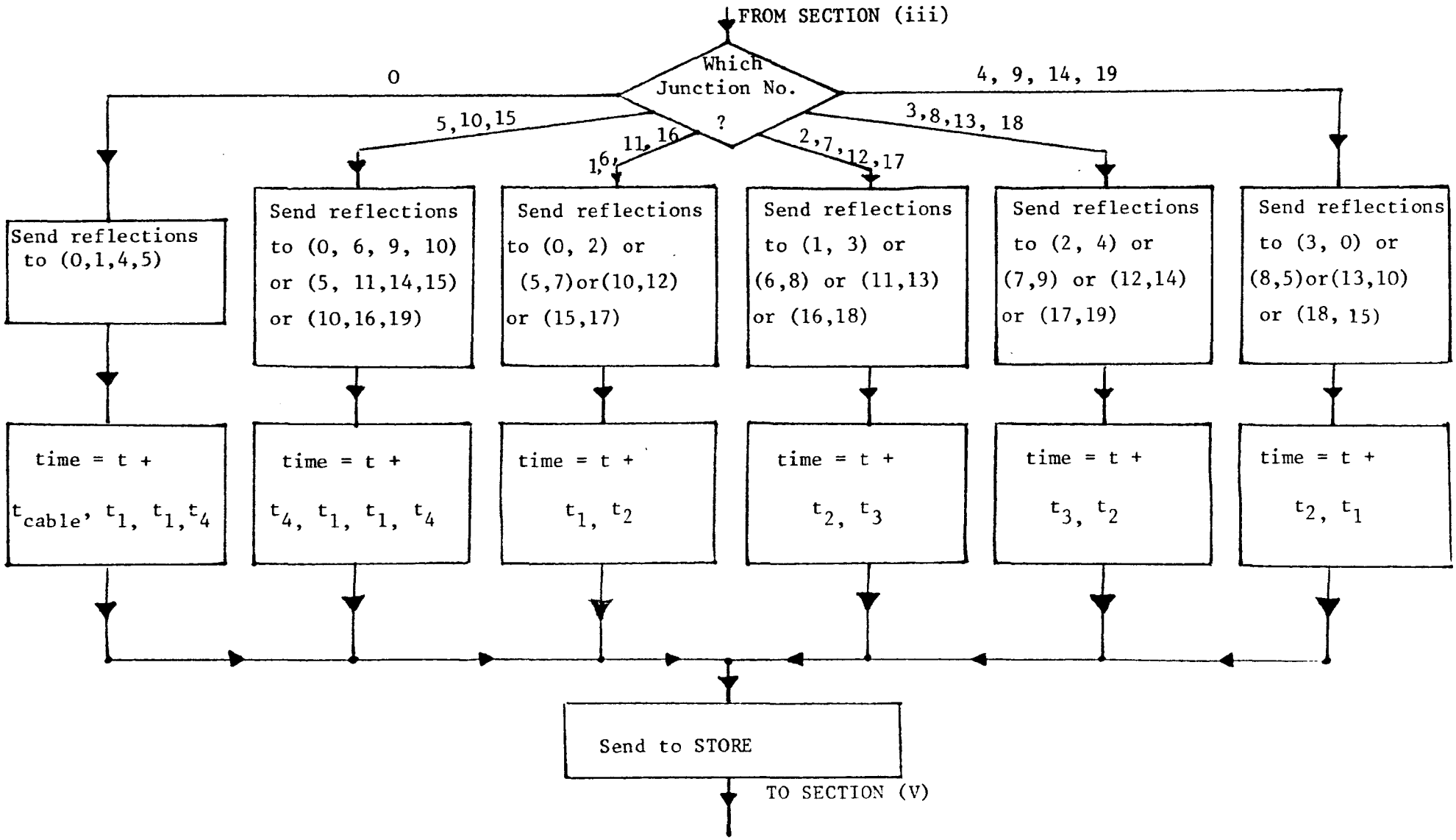

FIGURE 12.3 Allocation of Reflections to subsequent junctions

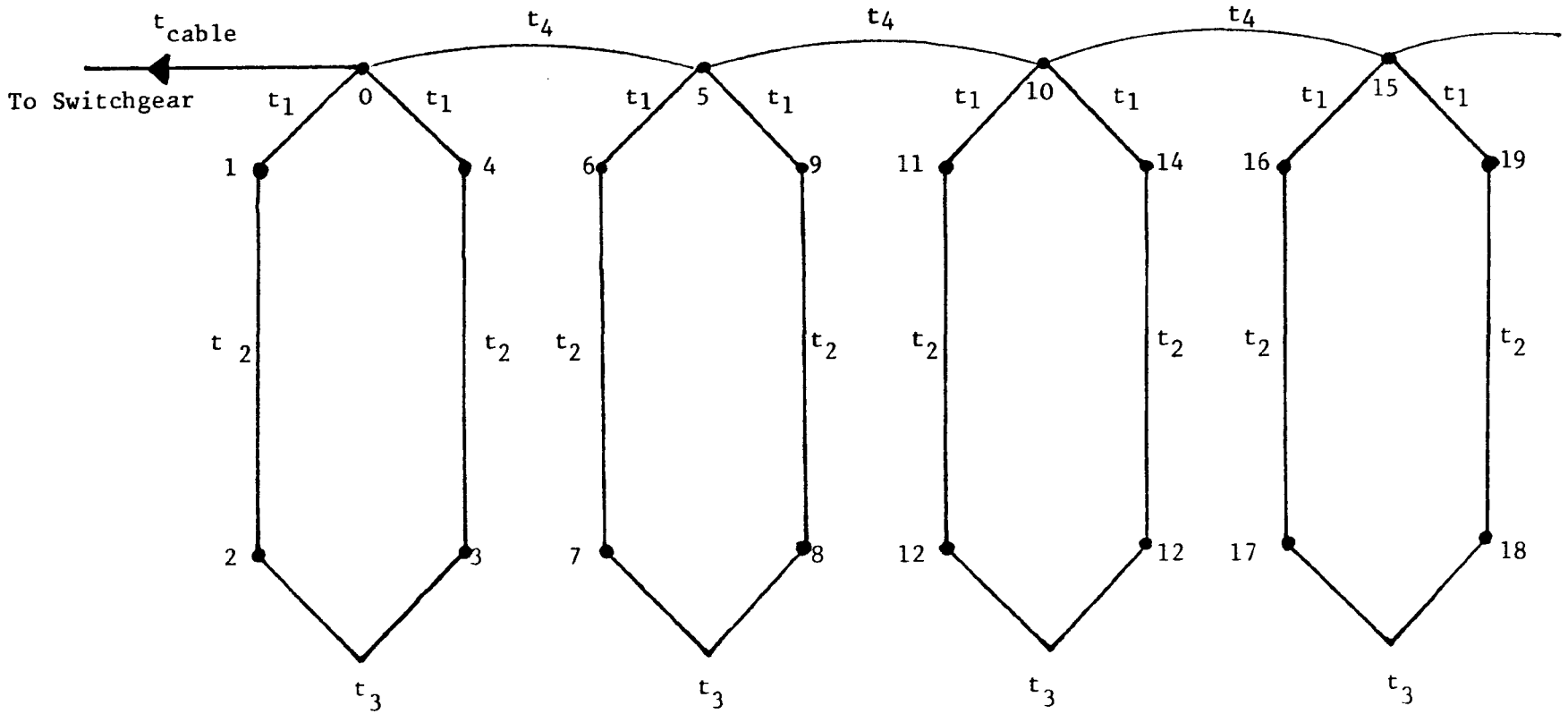

FIGURE 12.4 Junction numbers and travel times on a 4 coil winding

12.5. CONVOLUTION OF IMPULSE RESPONSE WITH ACTUAL SURGE WAVE SHAPES.

12.5.1. Selecting the Turn.

The programme described above calculates the impulse response of a coil or winding. The output is general in that it consists of the impulse response on all the turns at the specified point on the coil. The programme described in this section deals with the convolution of one turn voltage at a time. Therefore the first operation to be carried out is the retrieval from the general output file of the voltage impulses on the turn required. This was done using a programme named "getvolt". This programme is reproduced in Appendix IV(c).

12.5.2. Adding Simultaneous Impulses.

The output of the impulse responses consists of impulse magnitudes and the times at which they occur. Since it is the sum of both the incident and reflected waves at the junction gives the voltage caused by the scattering operation, then two impulses must be accounted for at each time at each junction. A programme called "adsims" (Appendix IV (d)), as the name suggests, adds together all simultaneous impulses, and so reduces the size of the data file to be handled.

12.5.3. Convolution.

The convolution itself is carried out in two stages. Firstly, each impulse in the impulse response is replaced by a series of impulses such that the addition of the series would give the shape of the actual applied surge. The magnitude of these series of impulses is in proportion to the magnitude of the impulse which they replace. The resulting

impulses are then sorted into chronological order and then the whole sequence is added to give the actual predicted response. For example, in the case of an actual input which is ramp shaped, each impulse is replaced by a series of equally spaced impulses of equal magnitude, i.e.

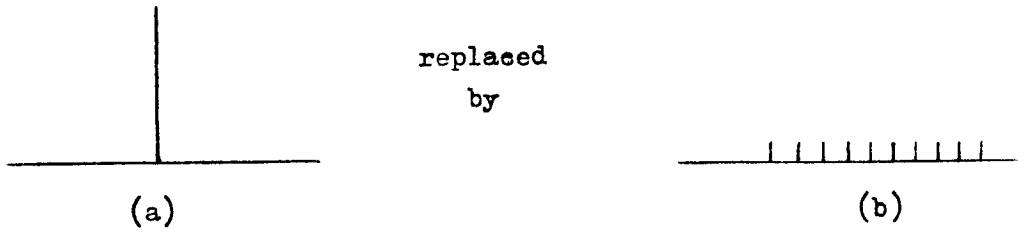

(a) (b)

Adding the impulses in (b) gives

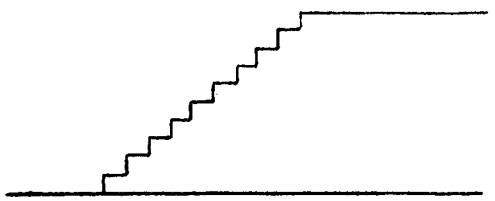

(c)

which approximates a ramp shaped surge.

The first stage of the convolution is carried out by programmes named "conv25", "conv50" etc. (the numbers represent the front times of the surges in question). These programmes replace each impulse of the impulse response by the appropriate impulse series. The output of this programme is then sent to a programme named "SORT" which sorts out the impulses into chronolgical order, since even with the steepest surges the front time is well in excess of the time interval between the impulses in the impulse response. The sorting programme takes, by far, more c.p.u. time than any other in this section. The programme simply repeatedly searches through the data to find the impulse with the lowest associated time and then outputs it. Thus the output data consists of the impulses in chronological order. It is possible, due to the nature of the data to be sorted, to modify this method to make it more

efficient by searching for the impulse with the lowest time value only in part of the data, thus saving c.p.u. time. The "convolute" and the "SORT" programmes are listed in Appendix IV(e) and (f).

12.5.4. Addition

Following a further addition of simultaneous impulses, the output impulses from the preceding programmes are repeatedly added to give the predicted waveform using "add", see Appendix IV(g).

12.5.5. Filtering.

It was found that the data on the file representing the predicted waveform contained much more information than was actually necessary, and that in most cases two thirds of it could be disregarded by retaining only every third point. This was done using a programme called "filter", which is listed in Appendix IV(n). The output from "filter" can be sent directly to the existing graph plotting procedures on the computer. Thus savings in both the c.p.u. time used by the plotting routines and the storage space used by the data files are achieved.

12.5.6. Interturn Voltages.

All the programmes used in the convolution procedure were used for each turn voltage required. Interturn voltages were calculated by a programme "diff1" which subtracted one set of data from another, and also found the maximum value of the difference.

12.5.7. Command Level Programming.

To enable the convolution to be carried out easily, a command level

programme was written which executed the programmes automatically. This was made possible by the nature of the computer operating system. A line in a command programme such as-

```
programme < input > output
```

will run "programme" using the file "input" as its input and the resulting data computed by "programme" is sent to a file named "output". Thus the command file used to execute the series of programmes described above was as shown below.

```
getvolt < impulse-response > f2
adsims < f2 > f3
rm f2
conv25 < f3 > f4
rm f3
SORT < f4 > f5
rm f4
adsims < f5 > f6
rm f5
add < f6 > f7
rm f6
filter < f7 > waveform
```

where "rm file" deletes "file".

Thus the file "waveform" contained all the points to be sent to the graph plotting routine.

A further command level programme was also written to enable the previous command programme to be run repetitively so that the voltages on all the turns of a coil could be predicted by writing only one command to the computer. This second command programme modified "command1" by altering "getvolt" to change the turn whose voltage was to be extracted from the general impulse response and also altered the final output file name so that each turn voltage was in a different file.

Then "command1" was run and the process repeated as many times as was necessary.

12.6. CONCLUSIONS.

The set of programmes described in this chapter were written solely to test the validity of the new theory presented in the thesis. While more efficient programmes may be feasible, the optimization of the programmes was not within the scope of the study. Thus the computer programmes given here, adequetely fulfil their purpose.

CHAPTER THIRTEEN.

CONCLUSIONS.

This study has shown that a need exists for a method of analysing surge propagation in stator coils in order that the voltages which the surges produce within the coils can be accurately predicted. The existing methods of analysis were reviewed. It was found that none of the existing analyses are capable of predicting, with acceptable accuracy, voltages within the coils. Further development of these analyses is not feasible since the winding models which they use are only tractable when assumptions, which invalidate them, are made. Consequently, a new method of analysis is necessary.

The new method of analysis was developed initially for a two turn lossless coil. It was shown that the iron of the stator acted as a flux barrier and that distortion of surges due to it could be neglected if the frequencies contained in the surge were very high. The coil was divided into five sections each of which was treated as a multiconductor transmission line. The junctions of these multiconductor transmission lines cause reflections within the coil. It was found that these reflections can be predicted using the scatter matrix technique developed by Agrawal et al (8). A computer programme utilising the new model was developed and used to predict voltages on the two turn coil. Experimental results for the two turn coil were obtained and, when compared to the computer predictions, they showed that the model is capable of predicting voltages in the coil to a greater degree of accuracy than has been attained previously.

Tne model was extended to cater for multi-turn coils and the validity was verified in the case of a twelve turn coil. Although the results from the multi-turn coil model were shown to be better than from any previous model, errors did exist in the predicted interturn voltages.

To improve the accuracy of the model, losses were included. The original scatter matrix theory, developed by Agrawal et al was limited to lossless multiconductor transmission line junctions, therefore lossy lines, as such, could not be used. However, a method was developed in which discrete lossy elements could be included in the scatter matrix. The assumption that losses, which are distributed throughout the coil, can be represented by discrete lossy elements was justified by consideration of the time constants involved in the computations. The voltages predicted by the lossy coil model are significantly more accurate than those from the lossless coil model. In particular, the predicted interturn voltages are accurate to within a few percent.

The model is capable, unlike previous models, of being used to predict voltages at any point on the coil.

The waveforms of the interturn voltages, both measured and predicted, showed that a travelling phenomenon exists in tne coil. A voltage peak is seen to propagate, turn by turn, down the coil, undergo a reflection at the neutral end of the coil and subsequently return to the beginning of the coil, there to undergo further reflection. Although this travelling wave phenomenon clearly exists, it cannot be used by itself as a method of voltage prediction, since it exists together with a mutual coupling phenomenon. These phenomena must be

analysed together (as they are in this study) if accurate predictions are required.

The coil model was used in the construction of a winding model. The results from this model showed that the first coil acted as a low pass filter to the surge and so no steep fronted surges can impinge on the remaining coils. This confirms results from previous experimental studies. Since only the voltages on the first coil in the winding are of interest, and these only for a short period of time after the surge has arrived at the coil, only a few coils are needed in the winding model. The actual number of coils needed depends on the number of turns per coil and the length of time for which the analysis is required. For the 12 turns per coil winding, two coils were sufficient to give the turn voltages for up to 800 ns.

Comparison of measured and computed turn voltages for the second coil in the winding showed that the model is not as accurate for the second and subsequent coils as it is for the line end coil. This is because the very high frequencies which are present in the initial surge do not exist in the voltages in the second coil, therefore the assumption that the core can be treated as a flux barrier is less valid than in the case of the first coil. Nevertheless the accuracy of the second coil voltage predictions is better than in any previous results.

The model was used to investigate how the rise time of the applied surge affected the voltage distribution in the line end coil. This investigation showed that the magnitude of the interturn voltages increases as the surge rise time is reduced. This was expected since large interturn voltages have been observed, in the past, only when the

winding was excited by fast fronted surges. The uniformity of the interturn voltage distribution also decreases as the surge rise time is reduced.

It was also seen that the effect of the losses on the predicted voltages increases as the rise time is reduced, even though frequency independent losses were used. The difference between the lossy and the lossless predictions of interturn voltage are only significant at surge rise times below 100 ns.

Voltage distributions in coils with a variety of insulation levels were predicted by the model. It was shown that the fraction of the applied surge which appears between turns during the transient disturbance is greater for the higher insulation levels. An increase in the thickness of the interturn insulation alone, significantly increases the interturn voltages which are generated. This is explained by the relative importance of the series and parallel modes of surge propagation through the coil. As the interturn insulation thickness is increased the series mode becomes more important in determining the voltage distribution.

The concept of a winding surge impedance was shown to be of limited worth since surge impedance values are dependent on surge shape as well as rise time. However, it is recognised that surge impedances will continue to be used in practice and the surge impedance values which were calculated for similarly shaped surges with differing rise times showed that decreasing rise time results in an increase in the surge impedance value of the winding. Increasing the insulation level was also found to increase the surge impedance.

It was demonstrated that the shape of the coil, i.e. the lengths of the slot and the end winding portions, have little effect on the interturn voltages for the very fast fronted surges. For surge front times above 50 ns, interturn voltages are greater in the larger coils. The relative lengths of the slot and end winding regions do not affect the interturn voltages.

Comparisons between the possible interturn voltages occurring on a machine and the insulation test levels, as given by the commonly used Electrical Supply Industry standards, show that the test levels are at present, inadequate. A more recent specification issued by O.C.M.A. (23) is based on a test surge which may be inadequate to ensure that the coil insulation is capable of withstanding surges in practice. Test levels which adequately ensure the ability of the coils to withstand fast fronted surges will make an analysis, of the type described here, essential in the design of coil insulation.

The possibility of improving the accuracy of the analysis beyond that attained in this study is hindered by the lack of accurate data pertaining to the coils. However, the shape and front time of any surge which may impinge on the machine winding in practice will not be accurately known, also the magnitude of the interturn voltages is sensitive to the surge shape, rise time and magnitude, therefore a degree of accuracy which greatly exceeds the degree of accuracy of the surge data is unnecessary.

The analysis presented here was carried out using parameters which are fairly simple to calculate. For the lossless model only capacitances need to be computed. For the lossy model reasonable assumptions were

shown to give values for the loss elements which lead to results of satisfactory accuracy. Thus the lossy multi-conductor transmission line model combines good accuracy with simple parameter determination and is therefore a great improvement on previous models. The new analysis has therefore significantly improved the understanding of surge distribution in coil. It is thought that it will be of importance in the design and testing of stator coil insulation systems.

----------oOo----------

REFERENCES.

[1] Cornick, K.J., Thompson, T.R.: "Steep-fronted switching voltage transients and their distribution in motor windings. Part 1: System measurements of steep-fronted switching voltage transients", Proceedings of the IEE, 1982, Vol. **129**, Part B. No. 2, pp.45-56.

[2] Murano, M., Fujii, T., Nishikawa, H., Nishikawi, S. and Okawa, M.: "Voltage escalation in interrupting inductive current by vacuum switches", IEEE Transactions on Power Apparatus and Systems, 1974, Vol. **PAS-93**, pp.264-271.

[3] Murano, M., Fujii, T., Nishikawa, H., Nisnikawi, S. and Okawa, M.: "Three phase simultaneous interruption in interrupting inductive current using vacuum switches", IEEE Transactions on Power Apparatus and Systems, 1974, Vol. **PAS-93**, pp.272-280.

[4] Knable, A. H.: "Short cuts in surge analysis", Allis-Chalmers Electrical Revue, First Quarter, 1957.

[5] Rudenderg, R.: "Performance of travelling waves in coils and windings", AIEE Transactions, 1940, **59**, pp.1031-1045.

[6] Jackson, D. W., "Surge Protection of Rotating Machines", Chapter 8 of the Tutorial Course on Surge Protection in Power Systems at the IEEE PES Winter Meeting, New York, N.Y., February 4-9, 1979.

[7] Lewis, T. J.: "The transient behaviour of ladder networks of the type representing macnine and transformer windings", Proceedings of the IEE, 1954, Vol. **101**, Part 2, pp.541-553.

[8] Heller, B. and Veverka, A.: "Surge phenomena in electrical machines", Iliffe, London, 1968.

[9] Lovass-Nagy, V. and Rozsa, P.: " Matrix analysis of transient voltage distributions in alternating ladder networks", Proceedings of the IEE, 1963, **110**, No. 9, pp.1663-1670.

[10] Clowes, R. J.: "Surges in high voltage A.C. motors: Resume of published information up to 1964", E.R.A. Report No. 5105, 1967.

[11] Parrot, P. G.: "Surge voltage distribution in the line end coils of high voltage motor windings", E.R.A. Report No. 5224, 1968.

[12] Kagonov, E.G.: "Wave phenomena in electrical machines", Novosibirsk Izdatelskij otdel sibirskogo otdelenija, AN S.S.S.P., 1964.

[13] Christiansen, K. L., and Pedersen, A., "An Experimental Study of Impulse Voltage Phenomena in a Large AC Motor", Proceedings of the Electrical Insulation Conference, 1968, pp.148-150, IEEE 68C6-EI-87.

[14] Johnston, H.R.: Parsons Peebles Research Division, Internal Report No. RL 79-11, 1979.

[15] Petrov, G.N. and Abramov, A.I.: "Overvoltage stresses in the turn insulation of electrical machinery windings during electromagnetic transients", Electrichestov, No. 7, March, 1954, pp.24-31.

[16] Adjaye, R.E. and Cornick, K.J.: "Distribution of switching surges in the line-end coils of cable connected motors", Proceedings of the IEE, Electric Power Applications, Vol. 2, No. 1, 1979, pp.11-

21.

[17] Cornick, K.J., Thompson, T.R.: "Steep-fronted switching voltage transients and their distribution in motor windings. Part 2: Distribution of steep-fronted switching voltage transients in motor windings.", Proceedings of the IEE, 1982, Vol. 129, Part B, No. 2, pp.56-63.

[18] Nailen, R.L.: "Transient surges and motor protection", Industrial and Commercial Power System Technical Conference, Seattle, WA., USA, 14-17 May 1979, (New York, USA: IEEE 1979), pp.86-91.

[19] Electricity Supply Industry Standard No. 44-5, Issue 2, 1978.

[20] Agrawal, A. K., Fowles, H.M., Scott, L.D. and Gurbaxani, S.H.: "Application of modal analysis to the transient response of multiconductor transmission lines with branches", IEEE Transactions on Electromagnetic Compatibility, Vol. EMC-21. No 3, August, 1979, pp.256-262.

[21] Weeks, W.T.: "Multiconductor transmission - line theory in the TEM approximation", IBM Journal of Research and Development, Vol. 16, No. 6, November 1972, pp.604-611.

[22] Lammeraner, J. and Stafl, G.: "Eddy currents", Iliffe, London, 1966.

[23] Oil Companies Materials Association, Specification No. ELEC 1., July, 1981.

[24] Ritchie, D.M.: "C Reference Manual." Bell Laboratories, 1974.

FURTHER REFERENCES.

[25] Andrä, W. and Sperling, P.G.: "Winding insulation stressing during the switching of electrical machines.", Siemans Review, XLIII, No. 8, 1976, pp.345-350.

[26] Belevitch,V.: "Theory of the proximity effect in multiwire cables. Part 1.", Philips Research Reports, **32**, 1977, pp.16-43.

[27] Belevitch, V.: "Theory of the proximity effect in multiwire cables. Part II.", Philips Research Reports, **32**, 1977, pp.96-117.

[28] Blower, R.W.: "Experiences with medium-voltage vacuum current breaker equipment in distribution systems.", Electronics and Power, Vol. **27**, No. 10, 1981, pp.728-731.

[29] Blower, R.W., Cornick, K.J. and Reece, M.P.: "Use of vacuum switchgear for the control of motors and transformers in industrial systems.", Proceedings of the IEE, Electric Power Applications, Vol. **2**, No. 3, 1979, pp.108-112.

[30] Grover, F. W.: "Inductance calculations, working formulas and tables", Dover, New York, 1962.

[31] McNaughton, H.S.: "Which system - resin-rich or VPI? A review of insulation systems for high voltage a.c. industrial machines.", GEC Journal for Industry, Vol. **5**, No. 1, 1981, pp.37-43.

[32] Slater, M.A.: "High voltage motor control", L.S.E. Engineering Bulletin, Vol. **13**, No. 2, 1975, pp.8-13.

[33] Smith, T.D.: "Machine winding design with respect to vacuum contacters", L.S.E. Engineering Bulletin, Vol. 13, No. 2, 1975, pp.14-18.

[34] White, E.L.: "The diagnosis of failure in power appuratus under impulse voltage acceptance tests", IEE Paper No. 3852, June, 1962.

[35] White, E.L.: "Investigation of switching surges in a high voltage motor installation", ERA Report No. 5055.

[36] Wright, M.T., McLeay, K.: "Voltage distribution in stator windings due to fast transient switching of induction motors". IEEE Conference Paper PCI-81-14, Petroleum and Chemical Industry Conference, Chicago, Illinios, U.S.A., 1981.

[37] Wright, M.T., Yang, S.J. and McLeay, K.: "The prediction of transient interturn voltages in stator windings", (To be presented at the IEE International Conference on Electrical Machines - Design and Applications, 13-15 July, 1982.)

[38] Wright, M.T., Yang, S.J. and McLeay, K.: "General theory of fast-fronted transient interturn voltage distribution in electrical machine windings", (Submitted to the Proceedings of the IEE, Part B, May, 1982.)

[39] Wright, M.T., Yang, S.J. and McLeay, K.: "The effects of coil and surge parameters on the transient interturn voltage distribution in stator windings", (Submitted to the Proceedings of the IEE, Part B, May, 1982.)

APPENDIX I

MULTICONDUCTOR TRANSMISSION LINE THEORY

The theory is developed here for the case of a two conductor line. Losses are omitted.

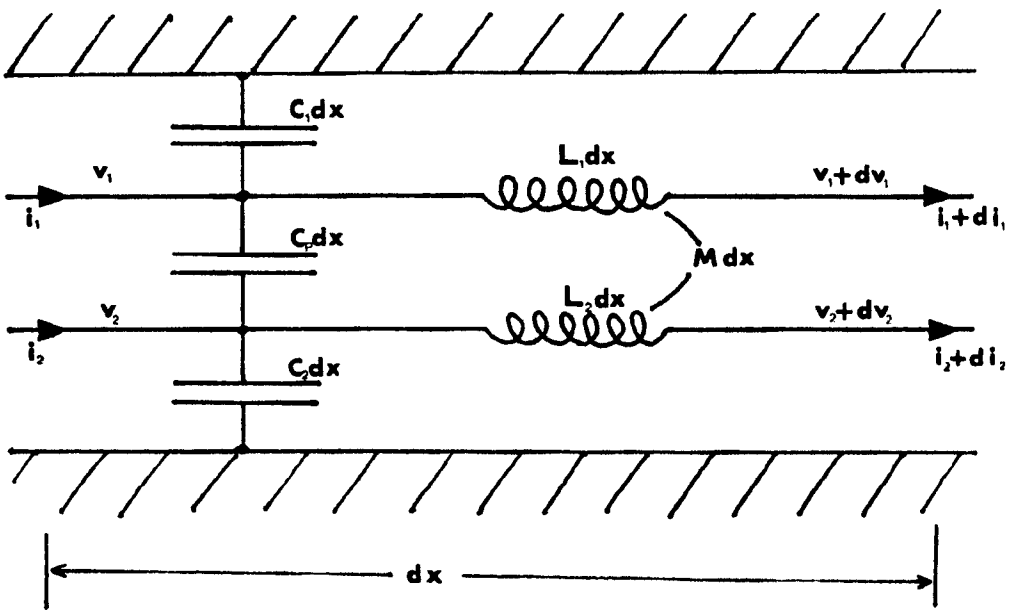

FIGURE (i) Elemental section of 2 conductor line.

From figure (i) above we have

$$\delta i_1 = -C_1 \delta x \frac{\partial v_1}{\partial t} - C_p \delta x \frac{\partial}{\partial t}(v_1 - v_2)$$

and

$$\delta i_2 = -C_2 \delta x \frac{\partial v_2}{\partial t} - C_p \delta x \frac{\partial}{\partial t}(v_2 - v_1)$$

$$\Rightarrow \frac{\partial i_1}{\partial x} = -(C_p + C_1) \frac{\partial v_1}{\partial t} + C_p \frac{\partial v_2}{\partial t}$$

and

$$\frac{\partial i_2}{\partial x} = C_p \frac{\partial v_1}{\partial t} - (C_p + C_2) \frac{\partial v_2}{\partial t}$$

giving/

/giving

$$\frac{\partial}{\partial x}\begin{bmatrix} i_1 \\ i_2 \end{bmatrix} = -\begin{bmatrix} C_1 + C_p & -C_p \\ -C_p & C_2 + C_p \end{bmatrix} \frac{\partial}{\partial t}\begin{bmatrix} v_1 \\ v_2 \end{bmatrix} \quad . \quad . \quad (1)$$

Also from figure (i)

$$\partial v_1 = -L_1 \partial x \frac{\partial i_1}{\partial t} - M \partial x \frac{\partial i_2}{\partial t}$$

and $$\partial v_2 = -M \partial x \frac{\partial i_1}{\partial t} - L_2 \partial x \frac{\partial i_2}{\partial t}$$

giving

$$\frac{\partial}{\partial x}\begin{bmatrix} v_1 \\ v_2 \end{bmatrix} = -\begin{bmatrix} L_1 & M \\ M & L_2 \end{bmatrix} \frac{\partial}{\partial t}\begin{bmatrix} i_1 \\ i_2 \end{bmatrix} \quad . \quad . \quad . \quad . \quad (2)$$

Differentiating (2) w.r.t. x gives

$$\frac{\partial^2}{\partial x^2}\begin{bmatrix} v_1 \\ v_2 \end{bmatrix} = -\begin{bmatrix} L_1 & M \\ M & L_2 \end{bmatrix} \frac{\partial^2}{\partial x \partial t}\begin{bmatrix} i_1 \\ i_2 \end{bmatrix} \quad . \quad . \quad . \quad . \quad (3)$$

Differentiating (1) w.r.t. t gives

$$\frac{\partial^2}{\partial x \partial t}\begin{bmatrix} i_1 \\ i_2 \end{bmatrix} = -\begin{bmatrix} C_p + C_1 & -C_p \\ -C_p & C_p + C_2 \end{bmatrix} \frac{\partial^2}{\partial t^2}\begin{bmatrix} v_1 \\ v_2 \end{bmatrix} \quad . \quad . \quad . \quad (4)$$

Combining (3) and (4) gives

$$\frac{\partial^2}{\partial x^2}\begin{bmatrix} v_1 \\ v_2 \end{bmatrix} = \begin{bmatrix} L_1 & M \\ M & L_2 \end{bmatrix} \begin{bmatrix} C_p + C_1 & -C_p \\ -C_p & C_p + C_2 \end{bmatrix} \frac{\partial^2}{\partial t^2}\begin{bmatrix} v_1 \\ v_2 \end{bmatrix}$$

or $$\frac{\partial^2}{\partial x^2}(V) = (L)(C)\frac{\partial^2}{\partial t^2}(V)$$

It can be shown [7] that for lossless lines in homogeneous media

$$(L)(C) = \frac{1}{u^2}(1)$$ where (1) is the unit matrix

Thus $$\frac{\partial^2}{\partial x^2}\begin{bmatrix} v_1 \\ v_2 \end{bmatrix} = \frac{1}{u^2}\begin{bmatrix} 1 & 0 \\ 0 & 1 \end{bmatrix} \frac{\partial^2}{\partial t^2}\begin{bmatrix} v_1 \\ v_2 \end{bmatrix}$$

$$\Rightarrow \frac{\partial^2}{\partial x^2} v_1 = \frac{1}{u^2} \frac{\partial^2}{\partial t^2} v_1 \text{ and } \frac{\partial^2}{\partial x^2} v_2 = \frac{1}{u^2} \frac{\partial^2}{\partial t^2} v_2$$

$$\Rightarrow v_1 = \hat{v}_1 \delta(x \pm ut) \text{ and } v_2 = \hat{v}_2 \delta(x \pm ut)$$ where $\delta(t)$ is the Dirac function

From (2) $$\frac{\partial}{\partial x}\begin{bmatrix} v_1 \\ v_2 \end{bmatrix} = \begin{bmatrix} v_1 \\ v_2 \end{bmatrix} = -\begin{bmatrix} L_1 & M \\ M & L_2 \end{bmatrix} \frac{\partial}{\partial t}\begin{bmatrix} i_1 \\ i_2 \end{bmatrix} \quad . \quad . \quad (5)$$

and also since $\begin{bmatrix} i_1 \\ i_2 \end{bmatrix} = \begin{bmatrix} \hat{i}_1 \\ \hat{i}_2 \end{bmatrix} \delta (x \pm ut)$

then $\frac{\partial}{\partial t} \begin{bmatrix} i_1 \\ i_2 \end{bmatrix} = \pm u \begin{bmatrix} i_1 \\ i_2 \end{bmatrix}$ . . . . . (6)

Combining (5) and (6)

$$\begin{bmatrix} v_1 \\ v_2 \end{bmatrix} = \pm u \begin{bmatrix} L_1 & M \\ M & L_2 \end{bmatrix} \begin{bmatrix} i_1 \\ i_2 \end{bmatrix}$$

Therefore $\begin{bmatrix} Z \end{bmatrix} = u \begin{bmatrix} L_1 & M \\ M & L_2 \end{bmatrix} = \quad u(L) = \frac{1}{u} (C)^{-1}$

giving $\quad (Y) = (Z)^{-1} = \frac{1}{u} (L)^{-1} = u(C)$

APPENDIX II(a)

Details of Two Turn Coil

Nominal Coil Insulation Level = 6·6kV.

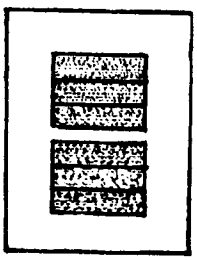

Main insulation 2·6 mm

Interturn insulation 0·32 mm

3 Uninsulated subconductors
7·1 x 3·75 mm.

Insulation Material

Resin rich glass fabric backed mica paper
Relative permittivity
$\varepsilon_r = 5$

Coil Dimensions

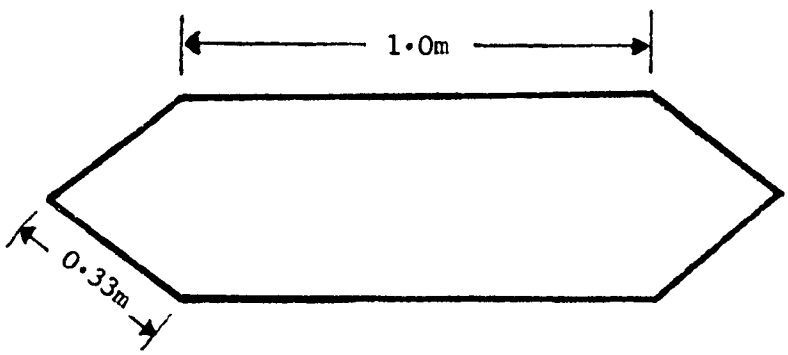

Admittance matrices

$$[Y_{slot}] = \begin{bmatrix} 0{\cdot}14550 & -0{\cdot}06103 \\ -0{\cdot}06103 & 0{\cdot}14550 \end{bmatrix}$$

$$[Y_{end}] = \begin{bmatrix} 0{\cdot}09103 & -0{\cdot}06103 \\ -0{\cdot}06103 & 0{\cdot}09103 \end{bmatrix}$$

NOTE: This coil was manufactured solely for the purposes of the study and does not represent the manufacturer's normal coil insulation dimensions.

APPENDIX II(b)

Details of Twelve Turn Coil

Nominal coil insulation level = 11·0kV

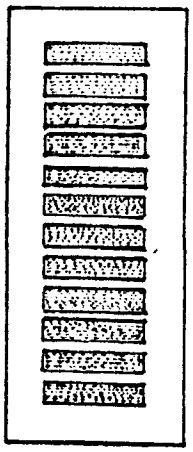

Main insulation 3·1 mm

Interturn insulation 0·6 mm

Conductor size 6·3 x 2·0 mm

Insulation material

Resin rich glass fabric backed mica paper
Relative permittivity
$\varepsilon_r = 5$

Coil dimensions

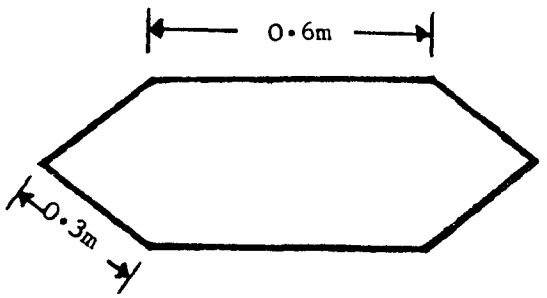

Admittance matrices/

Admittance matrices

$$[Y_{slot}] = \begin{bmatrix}
0.0821 & -0.0624 & & & & & & & & & \\
-0.0624 & 0.1324 & -0.0624 & & & & & & & & \\
 & -0.0624 & 0.1324 & -0.0624 & & & & & & & \\
 & & -0.0624 & 0.1324 & -0.0624 & & & & & & \\
 & & & -0.0624 & 0.1324 & -0.0624 & & & & & \\
 & & & & -0.0624 & 0.1324 & -0.0624 & & & & \\
 & & & & & -0.0624 & 0.1324 & -0.0624 & & & \\
 & & & & & & -0.0624 & 0.1324 & -0.0624 & & \\
 & & & & & & & -0.0624 & 0.1324 & -0.0624 & \\
 & & & & & & & & -0.0624 & 0.1324 & -0.0624 \\
 & & & & & & & & & -0.0624 & 0.0821
\end{bmatrix}$$

$$[Y_{end}] = \begin{bmatrix}
0.0654 & -0.0624 & & & & & & & & & \\
-0.0624 & 0.1257 & -0.0024 & & & & & & & & \\
 & -0.0624 & 0.1257 & -0.0624 & & & & & & & \\
 & & -0.0624 & 0.1257 & -0.0624 & & & & & & \\
 & & & -0.0624 & 0.1257 & -0.0624 & & & & & \\
 & & & & -0.0624 & 0.1257 & -0.0624 & & & & \\
 & & & & & -0.0624 & 0.1257 & -0.0624 & & & \\
 & & & & & & -0.0624 & 0.1257 & -0.0624 & & \\
 & & & & & & & -0.0624 & 0.1257 & -0.0624 & \\
 & & & & & & & & -0.0624 & 0.1257 & -0.0624 \\
 & & & & & & & & & -0.0624 & 0.0654
\end{bmatrix}$$

APPENDIX III

CROSS SECTIONAL DIMENSIONS AND ADMITTANCE DATA STUDY FOR VARIOUS INSULATION LEVELS.

Interturn . . .	0.06236
Turn to ground (slot)	
(a) . . .	0.01973
(b) . . .	0.00766
Turn to ground (end region)	
(a) . . .	0.003
(b) . . .	0.001

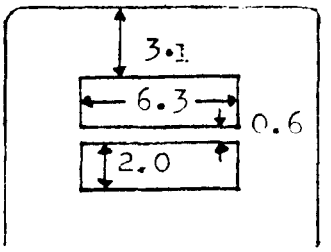

11.0kV

Interturn . . .	0.03747
Turn to ground (slot)	
(a) . . .	0.01631
(b) . . .	0.00634
Turn to ground (end region)	
(a) . . .	0.00240
(b) . . .	0.00080

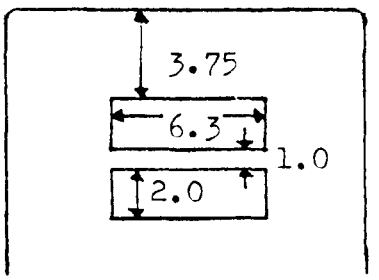

13.8kV

Interturn	0.07484
Turn to ground (slot)	
(a) . . .	0.04078
(b) . . .	0.01584
Turn to ground (end region)	
(a) . . .	0.00400
(b) . . .	0.00130

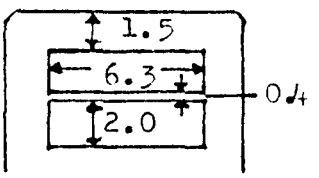

3.3kV

Interturn . .	0.04157
Turn to ground (slot)	
(a) . . .	0.01973
(b) . . .	0.00766
Turn to ground (end region)	
(a) . . .	0.003
(b) . . .	0.0010

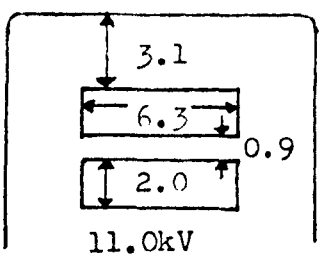

11.0kV
with 50% extra
interturn insulation

All dimensions in mm.

APPENDIX IV (a)

ESST

```
double Ys, Y[12][12], YY[26][26], mat1[26][26], cv[13][26], x, y, temp, a, b, c,
d, e, I, ci[13][26], Yf, T_no, mat[26][52], R[26][26], G[26][26], ADD[26][26], mat
2[26][26], ess;
main()
{
int i, j, k, m, q, p, h, n, turn;
scanf("%d\n", &turn);
n = (turn * 2) + 2;
scanf("%e\n", &YY[0][0]);
        for(i = 0; i < turn; i++){
                for(j = 0; j < turn; j++){
                        scanf("%e\t", &Y[i][j]);
                        }
                scanf("\n");
                }
scanf("%e\n", &Yf);
for( k = 0; k < 2; k++){
        for( i = 0; i < turn; i++){
                for(j = 0; j < turn; j++){
                        YY[i + 1 + (k * turn)][j + 1 + (k * turn)] = Y[i][j];
                        }
                }
        }
YY[(turn * 2) + 1][(turn * 2) + 1] = Yf;
ci[0][0] = cv[(n/2) - 1][n - 1] = ci[(n/2) - 1][n - 1] = 1;
cv[0][0] = -1;
for(i = 0; i < (n/2) - 1; i++){
        ci[i][i + 1] = ci[i + 1][i + (n/2)] = 1;
        cv[i][i + 1] = 1;
        cv[i + 1][i + (n/2)] = -1;
        }
for(i = 0; i < n; i++){
        cv[(n/2) - 1][i] = cv[(n/2) - 1][i] * -1.0;
        cv[0][i] = cv[0][i] * -1.0;
        }
for(i = 0; i < n - 1; i++){
        scanf("%e ", &R[i][i]);
        }
scanf("%e\n", &R[n - 1][n - 1]);
for(i = 0; i < n; i++){
        for(j = 0; j < n; j++){
                scanf("%e\t", &G[i][j]);
                }
        scanf("\n");
        }
for(i = 0; i < n; i++){
        for(j = 0; j < n; j++){
                if(j == i)ADD[i][j] = 1.0;
                for(k = 0; k < n; k++){
                        ADD[i][j] = (R[i][k] * YY[k][j]) + (G[i][k] * R[k][j]) +
ADD[i][j];
                        }
                }
        }
for(i = 0; i < n/2; i++){
        for(j = 0; j < n; j++){
                mat[i][j] = 0.0;
                for(k = 0; k < n; k++){
                        mat[i][j] = (cv[i][k] * ADD[k][j] * -1.0) + mat[i][j];
```

```
                        }
                }
        }
 for(i = 0; i < n/2; i++){
        for(j = 0; j < n; j++){
                for(k = 0; k < n; k++){
                        mat[(n/2) + i][j] = (ci[i][k] * (YY[k][j] + G[k][j])) + m
at[(n/2) + i][j];
                        mat1[(n/2) + i][j] = (ci[i][k] * (YY[k][j] - G[k][j])) +
mat1[(n/2) + i][j];
                        }
                }
        }
 for(i = 0; i < n; i++){
        mat[i][i + n] = 1.0;
        for(j = 0; j < n; j++){
                if(i == j)ADD[i][j] = 1.0;
                else{ADD[i][j] = 0.0;}
                for(k = 0; k < n; k++){
                        ADD[i][j] = (G[i][k] * R[k][j]) - (R[i][k] * YY[k][j]) +
ADD[i][j];
                        }
                }
        }
 for(i = 0; i < n/2; i++){
        for(j = 0; j < n; j++){
                for(k = 0; k < n; k++){
                        mat1[i][j] = (cv[i][k] * ADD[k][j]) + mat1[i][j];
                        }
                }
        }
  for(i = 0; i < n; i++){
        for(j = 0; j < n; j++){
                mat2[i][j] = mat[i][j];
                }
        }
 /*****************INVERT START***************/
 for(h = 0; h < n; h++)mat[h][h + n] = 1.0;
 for(h = 0; h < n; h++){
        for(i = 0; i < h; i++){
                x = mat[h][i];
                for(j = 0; j < 2 * n; j++){
                        mat[h][j] = mat[h][j] - (mat[i][j] * x);
                   }
                }
        a = 0.001; b = -0.001;
        if(mat[h][h] <= 0.01 && mat[h][h] >= -0.01){
                for(i = h + 1; i < n; i++){
                        if(mat[i][h] > 1e-03 || mat[i][h] < -1e-03){
                                for(j = 0; j < 2 * n; j++){
                                        mat[h][j] = mat[h][j] + mat[i][j];
                                        }
                                i = n + 1;
                                }
                        }
                        h--;
                }
        x = mat[h][h];
        for(i = 0; i < 2 * n; i++)mat[h][i] = mat[h][i]/x;
```

```
    if(h ) 0){
        for(i = h - 1; i )= 0; i--){
                x = mat[i][h];
                for(j = 0; j ( 2 * n; j++){
                        mat[i][j] = mat[i][j] - (mat[h][j] * x);
                    if(mat[i][j] ( 1e-10 && mat[i][j] ) -1e-10 && j ( n)mat[i][j]
= 0.0;
                        }
                }
          }
/*      if(h )= 24){
        for(i = 0; i ( h; i++){
                printf("H = %d\n", h);
                for(j = 0; j ( n * 2; j++){
                        printf("%e\t", mat[i][j]);
                        }
                printf("\n");
                }
        printf("-----------------\n");
        } */
        }
/*****************INVERT END***************/
for(i = 0; i ( n; i++){
        for(j = 0; j ( n; j++){
                I = 0.0;
                for(K = 0 ; K ( n; K++){
                        I = I + (mat2[i][K] * mat[K][j + n]);
                        }
                printf("%e\t", I);
                }
        printf("\n");
        }
printf("%d\n", turn);
for(i = 0; i ( n; i++){
        for(j = 0; j ( n; j++){
                ess = 0.0;
                for(K = 0; K ( n; K++){
                        temp = mat[i][K + n] * mat1[K][j];
                        ess = ess + temp;
                        }
                printf("%e\t", ess);
                }
        printf("\n");
        }
}
```

LOSSCAL

```
float ess[2][28][28], re[28], vee[30], time, T1, T2, T3, a, temp, templ, x, z, T4
, VEE, RE, R[26], so[80][28];
main()
{
int i, m, j, poi, pot, K, p, h, n, l, turn, X, sign;
scanf("%d\n", &X);  /*  X is the turn at which the voltage is required */
scanf("%d\n", &turn);
if(X == turn)X = X * 2;
m = (turn * 2) + 2;
for(K = 0; K < 1; K++){
        for(i = 0; i < m; i++){
                for(j = 0; j < m; j++){
                        scanf("%e\t", &ess[K][i][j]);
                        }
                scanf("\n");
                }
        }
for(i = 0; i < m-2; i++){
        for(j = 0; j < m-2; j++){
                scanf("%e\t", &ess[1][i][j]);
                }
        scanf("\n");
        }
for(i = 0; i < m; i++){
        scanf("%e ", &R[i]);
        }
scanf("\n");
p = 0;
so[0][0] = 100.0;
for(i = 1; i < m; i++)so[0][i] = 0.0;
so[0][m] = 0.00; so[0][m + 1] = 0.0;
p++;
while(p < 100){
  time = so[0][m]; h = 0;
  for(i = 1; i < p; i++){
        if(so[i][m] < time){
                time = so[i][m];
                h = i;
                }
        }
  for(i = 0; i < m + 2; i++){
        vee[i] = so[h][i];
        soth][i] = so[p - 1][i];
        so[p - 1][i] = 0.00;
        }
  p--;
 for(i = 0; i < p; i++){
        if(so[i][m] <= (1.0001 * vee[m]) && so[i][m] >= (0.9999 * vee[m]) && so[i
][m + 1] == vee[m + 1]){
                for(j = 0; j < m; j++){
                        vee[j] = vee[j] + so[i][j];
                        }
                for(j = 0; j < m + 2; j++){
                        so[i][j] = so[p - 1][j];
                        so[p - 1][j] = 0.00;
                        }
                p--;
                i = 0;
                }
```

```
        }
if(vee[m] < 1310){
        n = m;
        if(vee[m + 1] <= 1.0e-03 && vee[m + 1] >= -1.0e-03){
                l = 0;
                }
        else if(vee[m + 1] <= 5.1 && vee[m + 1] >= 4.9){
                 l = 0;
                }
        else if(vee[m + 1] < 10.1 && vee[m + 1] > 9.9){
                l = 0;
                }
        else if(vee[m + 1] < 15.1 && vee[m + 1] > 14.9){
                l = 0;
                }
        else{
                l = 1;
                n = m - 2;
                }
        for(i = 0; i < n; i++){
                re[i] = 0.00;
                for(j = 0; j < n; j++){
                        temp = vee[j] * ess[l][i][j];
                        re[i] = re[i] + temp;
                        }
                }
T1 = 2.8; T2 = 5.6;  T3 = 5.6; T4 = 2.8;
        a = vee[m + 1];
        if(a == 0.0 || a == 5.0 || a == 10.0 || a == 15.0){
            sign = 0;
            for(i = 0; i < m; i++){
                if(re[i] > 0.0005 || re[i] < -0.0005){
                        sign = 1;
                        i = m;
                        }
                }
            if(sign == 1){
                for(i = 0; i < (m - 2)/2; i++)sol[p][i] = re[i + 1];
                sol[p][m] = vee[m] + T1;
                sol[p][m + 1] = 1.0 + vee[m + 1];
                p++;
                for(i = 0; i < (m - 2)/2; i++)sol[p][i] = re[i + (m/2)];
                sol[p][m] = vee[m] + T1;
                sol[p][m + 1] = 4.0 + vee[m + 1];
                     if(vee[m + 1] < 4.5){
                        printf("%e\t", vee[m]);
                        VEE = ((R[0] * vee[1]) + (R[1] * vee[0]))/(R[1] + R[0]);
                        printf("%e\t", VEE);
                        for(i = 2; i < turn + 1; i++){
                                VEE = ((vee[i] * R[i + turn - 1]) + (vee[i + turn
- 1] * R[i]))/(R[i] + R[i + turn - 1]);
                                printf("%e\t", VEE);
                                }
                        VEE = ((R[m-2] * vee[m-1]) + (R[m-1] * vee[m-2]))/(R[m-1]
+ R[m-2]);
                        printf("%e\n", VEE);
                        printf("%e\t", vee[m]);
                        RE = ((R[0] * re[1]) + (R[1] * re[0]))/(R[1] + R[0]);
                        printf("%e\t", RE);
```

```
                        for(i = 2; i ( turn + 1; i++){
                                RE = ((re[i] * R[i + turn - 1]) + (re[i + turn -
1] * R[i]))/(R[i] + R[i + turn - 1]);
                                printf("%e\t", RE);
                                }
                        RE = ((R[m-2] * re[m-1]) + (R[m-1] * re[m-2]))/(R[m-1] +
R[m-2]);
                        printf("%e\n", RE);
                    }
                p++;
                if(vee[m + 1] (= 0.1 && vee[m + 1] )= -0.1){
                        sol[p][0] = re[0] * -0.5;
                        sol[p][m] = vee[m] + 95.2;
                        sol[p][m + 1] = 0.0;
                        p++;
                        sol[p][0] = re[m - 1];
                        sol[p][m] = vee[m] + T4;
                        sol[p][m + 1] = 5.0;
                        p++;
                        }
                else if(vee[m + 1] ) 14.9 && vee[m + 1] ( 15.1){
                        sol[p][m - 1] = re[0];
                        sol[p][m] = vee[m] + T4;
                        sol[p][m + 1] = vee[m + 1] - 5.0;
                        p++;
                        }
                else{
                        sol[p][m - 1] = re[0];
                        sol[p][m] = vee[m] + T4;
                        sol[p][m + 1] = vee[m + 1] - 5.0;
                        p++;
                        sol[p][0] = re[m - 1];
                        sol[p][m] = vee[m] + T4;
                        sol[p][m + 1] = vee[m + 1] + 5.0;
                        p++;
                        }
                }
            }
        else if(a (= 1.1 && a ) 0.9 || a (= 6.1 && a ) 5.9 || a (= 11.1  && a ) 1
10.9 || a ) 15.9 && a ( 16.1){
            sign = 0;
            for(i = 0; i ( m; i++){
                if(re[i] ) 0.0005 || re[i] ( -0.0005){
                        sign = 1;
                        i = m;
                        }
                }
            if( sign == 1){
                for(i = 0; i ( (m - 2)/2; i++)sol[p][i + 1] = re[i];
                sol[p][m] = vee[m] + T1;
                sol[p][m + 1] = vee[m + 1] - 1.0;
                p++;
                for(i = (m - 2)/2; i ( m - 2; i++)sol[p][i] = re[i];
                sol[p][m] = vee[m] + T2;
                sol[p][m + 1] = vee[m + 1] + 1.0;
                p++;
                }
            }
        else if(a (= 2.1 && a ) 1.9 || a (= 7.1 && a ) 6.9 || a (= 12.1  && a )
```

```
(0.9 || a > 16.9 && a < 17.1){
            sign = 0;
            for(i = 0; i < m; i++){
                 if(re[i] > 0.0005 || re[i] < -0.0005){
                          sign = 1;
                          i = m;
                          }
                 }
            if(sign == 1){
                 for(i = (m - 2)/2; i < m - 2; i++)sol[p][i] = re[i];
                 sol[p][m] = vee[m] + T2;
                 sol[p][m + 1] = vee[m + 1] - 1.0;
                 p++;
                 for(i = 0; i < (m - 2)/2; i++)sol[p][i] = re[i];
                 sol[p][m] = vee[m] + T3;
                 sol[p][m + 1] = vee[m + 1] + 1.0;
                 p++;
                 }
             }
        else if(a <= 3.1 && a > 2.9 || a <= 8.1 && a > 7.9 || a <= 13.1  && a > 12
   .9 || a > 17.9 && a < 18.1){
            sign = 0;
            for(i = 0; i < m; i++){
                 if(re[i] > 0.0005 || re[i] < -0.0005){
                          sign = 1;
                          i = m;
                          }
                 }
            if(sign == 1){
                 for(i = 0; i < (m - 2)/2; i++)sol[p][i] = re[i];
                 sol[p][m] = vee[m] + T3;
                 sol[p][m + 1] = vee[m + 1] - 1.0;
                 p++;
                 for(i = (m - 2)/2; i < m - 2; i++)sol[p][i] = re[i];
                 sol[p][m] = vee[m] + T2;
                 sol[p][m + 1] = vee[m + 1] + 1.0;
                 p++;
                 }
            }
        else if(a <= 4.1 && a > 3.9 || a <= 9.1 && a > 8.9 || a <= 14.1  && a > 13
   .9 || a > 18.9 && a < 19.1){
            sign = 0;
            for(i = 0; i < m; i++){
                 if(re[i] > 0.0005 || re[i] < -0.0005){
                          sign = 1;
                          i = m;
                          }
                 }
            if(sign == 1){
                 for(i = 0; i < (m - 2)/2; i++)sol[p][i + (m/2)] = re[i];
                 sol[p][m] = vee[m] + T1;
                 sol[p][m + 1] = vee[m + 1] - 4.0;
                 p++;
                 for(i = (m - 2)/2; i < m - 2; i++)sol[p][i] = re[i];
                 sol[p][m] = vee[m] + T2;
                 sol[p][m + 1] = vee[m + 1] - 1.0;
                 p++;
                 }
            }
```

```
        else{
                printf("JUNCTION NUMBER FAULT\t Junction Number = %e\n", veelm + 1
]);
                }
        if(p > 100){
/*              printf("P too big\n");    */
                vee[m] = 100000;
                }
/*      printf("P = %d\n", p);
        printf("Jn. No. = %e\n", veelm + 1]);      */
        }
     else{ p = 800;}
     }
printf("9999\n");
}
```

APPENDIX IV (c)

GETVOLT

```
main()
{
        int i, n, j;
        float a, b;
        j = 9;
        a = 1.0;
        scanf("%d\n", &n);
        while(a (= 9000){
        scanf("%e\t", &a);
                printf("%e ", a);
                for(i = 0; i ( n + 1; i++){
                        scanf("%e\t", &b);
                        if(i == j)printf("%e\n", b);
                        }
                scanf("\n");
                }
        printf("9999\n");
        }
```

```
main()
{
        int i;
        float a[2], b[2];
        scanf("%e %e\n", &a[0], &a[1]);
        for(i = 0; i ( 3000; i++){
                scanf("%e %e\n", &b[0], &b[1]);
                if(b[0] == 9999)i = 3000;
                else if(b[0] - a[0] (= 0.5  && a[0] - b[0] (= 2){
                        a[1] = a[1] + b[1];
                        }
                else{
                        printf("%e %e\n", a[0], a[1]);
                        a[0] = b[0];
                        a[1] = b[1];
                        }
                }
printf("9999\n");
        }
```

```
main()
{
int i, j, l, K;
float so[58][2], a[2];
for(K = 0; K ( 3000; K++){
scant("%e %e\n", &a[0], &a[1]);
if(a[0] == 9999)i = 3000;
else{
l = 0;
        for(j = 0; j ( 9; j++){
          so[j][0] = a[0] + (3.125 * j);
                }
          so[l][1] = a[1] * 0.00; l++;
          so[l][1] = a[1] * 0.05; l++;
          so[l][1] = a[1] * 0.15; l++;
          so[l][1] = a[1] * 0.15; l++;
          so[l][1] = a[1] * 0.15; l++;
          so[l][1] = a[1] * 0.15; l++;
          so[l][1] = a[1] * 0.15; l++;
          so[l][1] = a[1] * 0.15; l++;
          so[l][1] = a[1] * 0.05; l++;
        for(i = 0; i ( 9; i++){
                printf("%e %e\n", so[i][0], so[i][1]);
                }
        }
   }
printf("9999\n");
}
```

```
main()
{
        float ma[600][2];
        int i, P, j, l;
        for(i = 0; i < P; i++){
                scanf("%e %e\n", &ma[i][0], &ma[i][1]);
                }
        l = 0;
        while(ma[l][0] < 2000){
                l = 0;
                for(i = 0; i < 600; i++){
                        if(ma[i][0] < ma[l][0])l = i;
                        }
                printf("%e %e\n", ma[l][0], ma[l][1]);
                scanf("%e %e\n", &ma[l][0], &ma[l][1]);
                if(ma[l][0] > 2000){
                        l = 0;
                        for(j = 0; j < 600; j++){
                                for(i = 0; i < 600; i++){
                                        if(ma[i][0] < ma[l][0])l = i;
                                        }
                                printf("%e %e\n", ma[l][0], ma[l][1]);
                                ma[l][0] = 2999.0;
                                }
                        }
                }
        }
```

```
main()
{
int i;
float s[2], a;
a = 0.00;
for(i = 0; i ( 2000; i++){
        scanf("%e %e\n", &s[0], &s[1]);
        if(s[0] == 9999){
                i = 2000;
                }
   else{
        s[1] = s[1] + a;
        a = s[1];
        printf("%e %e\n",s[0], s[1]);
        }
   }
printf("9999\n");
} /* end */
```

APPENDIX IV (h)
FILTER

```
main()
{
int i;
double x, y, z, w, t, d, r, q;
for(i = 0; i < 700; i++){
        scanf("%e %e\n%e %e\n%e %e\n", &x, &y, &z, &w, &r, &q);
        if(x == 9999 || z == 9999 || r == 9999){
                i = 900;
                }
        else{printf("%e %e\n", x, y);}
        }
}
```

INTERTURN STATOR VOLTAGE DISTRIBUTION DUE TO FAST TRANSIENT SWITCHING OF INDUCTION MOTORS

Paper No. PCI-81-14

Michael T. Wright, Senior Member IEEE
Parsons Peebles Motors & Generators
Edinburgh, U.K.
and
Parsons Peebles Electric Products Inc.,
Cleveland, Ohio.

Keith McLeay
Parsons Peebles Motors & Generators
Edinburgh, U.K.

ABSTRACT

Steep fronted switching surges can cause severe stressing of the interturn insulation in induction motor windings. This may lead to failure. Experimental results show that severe non-linearity in the voltage distribution within the coil can occur. It is shown that an analytical method of quantifying interturn surge capability is required, if test methods and design procedures are to be used with confidence. Such a method is described and shown to conform well with measured results. The use of surge protection devices is briefly considered.

INTRODUCTION

The application of a high voltage transient to the stator winding of an induction machine causes interturn voltages which are in excess of those experienced during normal running conditions. If the interturn voltage is in excess of the interturn insulation withstand level, the insulation will break down.

The magnitude of interturn voltage is dependent on both the amplitude and rise time of the transient voltage applied to the machine terminals. For relatively slow transients (e.g. rise times of 1 μs or more) the interturn voltage may be considered to be uniformly distributed between the turns of any stator coil. For fast transients (e.g. rise times of 200 ns or less) a non-uniform distribution occurs and the interturn voltage is much higher. It is therefore possible for a stator winding to fail in the interturn mode, when subjected to a fast transient, having a lower voltage amplitude than that for a slower transient.

The occurrence of high voltage fast transients has been demonstrated by field tests on vacuum interrupter systems, where transient line voltages in excess of 6 pu rated voltage, with rise times of approximately 200 ns, have been recorded. Laboratory experiments have shown that rise times of 100 ns or less can occur.

The foregoing illustrates the importance of assessing the ability of a stator winding to withstand a prescribed surge wave. Ideally this should be done using proven design software at the machine design stage. To date this has not been possible: no reliable analytical models have been available.

This paper reports the results of a programme of experimental and theoretical work aimed at determining stator interturn voltage distribution due to fast transients.

EXPERIMENTAL INTERTURN VOLTAGE DISTRIBUTIONS

The experimental investigation was carried out in order to examine interturn voltage distribution in a coil subject to transient voltages of various rise times. Rise times of 1000 ns, 100 ns and 10 ns (1 ns = 10^{-9} seconds) were applied to a typical 12 turn induction motor coil. Voltages were measured on each of the twelve turns. The experiments were carried out in air with equipotential sheaths fitted over the slot portions to represent the iron core. Test results from coils fitted in an iron core showed no significant difference to those obtained from sheathed coils, which gives confidence in the method adopted.

Examination of the wave leaving the coil and comparison with the rise time of the wave entering the coil (see Figs. 1, 2 & 3) shows clearly that the coil acts as a low pass filter. Therefore the probability of any critical interturn voltages occurring in any coil can be seen to decrease as the wave progresses through the winding. Although each coil can be treated as a low pass filter, and each turn has series inductance and shunt capacitance, individual turns cannot be considered as independent low pass filters, since this would be equivalent to treating the coil as a ladder network. This can be seen to be invalid because each turn is inductively coupled with all other turns.

Figures 1, 2 and 3 clearly show that, for fast transient voltages, the interturn voltage distribution is not linear and that, consequently, a large proportion of the applied voltage can appear between turns. Thus large fast transient voltages (such as those due to multiple re-ignition and voltage escalation in vacuum switchgear) may create interturn voltages which are greater than those allowed for in users insulation standards and may lead to interturn insulation breakdown. In the case of the 1000 ns transient the interturn voltages are not large enough to critically stress the interturn insulation system: we shall, therefore, devote our attention to cases where transient surges have rise times below 1000 ns.

0090-3507/81/0000-0145$00.75

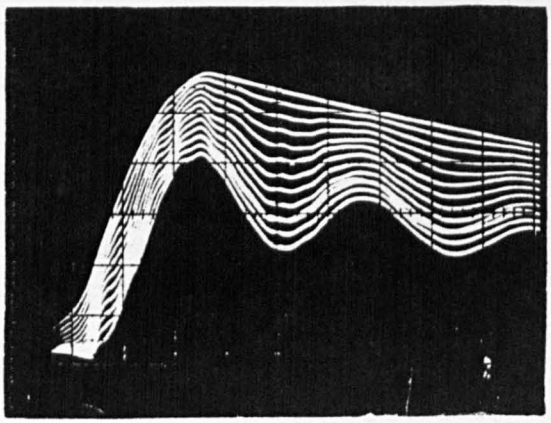

FIGURE 1 VOLTAGE DISTRIBUTION DUE TO A 1000 ns PULSE

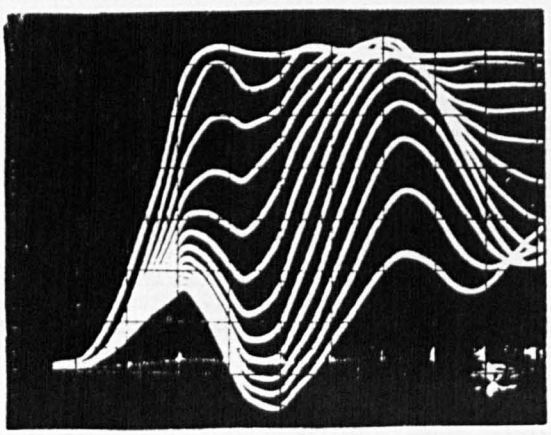

FIGURE 2 VOLTAGE DISTRIBUTION DUE TO A 100 ns PULSE

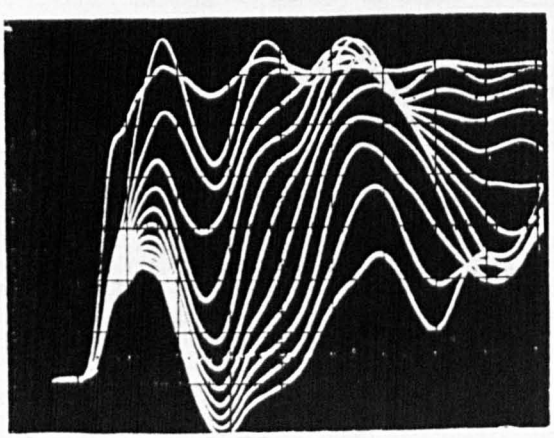

FIGURE 3 VOLTAGE DISTRIBUTION DUE TO A 10 ns PULSE

Current informed opinion in Europe and the USA seems to be that interturn test voltage rise times should be stipulated in the region of 200 ns and that peak test coil voltages should be of the order of four to five times rms line volts. Whilst this would be a significant advance on present test procedures, the results of our experiments show that the proposed 200 ns rise times may be too long to simulate conditions which may occur in practice.

However, in order to assess, at the system or machine design stage, the effect of a given surge rise time and voltage combination, a greater knowledge of surge propagation in stator coils is required. Without this information, any proposals for effective interturn test procedures must be considered as somewhat speculative; hence the need for a general analytical method of quantifying surge distribution.

COMPUTER MODEL : VERIFICATION AND RESULTS

The results for one particular experimental configuration may not be generally representative of other experimental arrangements or of any specific practical situation. Consequently, no firm conclusions can be drawn from these tests, as they stand, other than that a problem exists. What is needed is a general method of predicting stator interturn voltages which can be applied to any configuration of switchgear, cables and machines and which is valid for any realisable winding. This would increase our understanding of the problem, and provide a powerful analytical tool for the avoidance of interturn insulation failure.

The conventional transmission line model, which visualises the surge arriving on the first turn, travelling along each turn in succession until finally leaving the coil, has been proven invalid by the tests. It can be seen from Figures 2 and 3, that upon application of the surge, a voltage appears on each turn simultaneously, albeit with a differing magnitude, thus producing high interturn stresses. As a consequence of this, it may be deduced that magnetic and electric coupling between turns plays an important part in the propagation of surges through a coil.

A new theoretical approach using multiconductor transmission line theory has been found to be successful in predicting transient response within motor coils. This method is an improvement on previous methods in that it predicts wave propagation within the turns of the coil as opposed to predicting terminal conditions of the whole winding or a single coil. It thus allows prediction of the interturn voltage between any two turns, at any point on those turns.

The following three main assumptions are used in the construction of the model.

1. The spectral content of the surge wave is of sufficiently high frequency to render the iron core a flux barrier.

2. These high frequencies render all parameters frequency independent.

3. The losses can be discounted, or at least can be lumped at discrete intervals in order to make them tractable.

These assumptions are considered to be valid and can be experimentally verified.

A section of our model is shown in Figure 4 (two turns are shown, although the principle applies to any number).

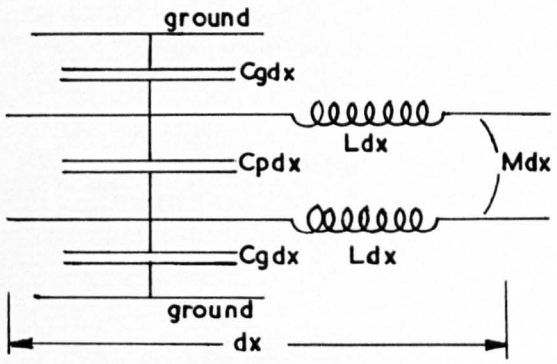

MODEL OF A TWO TURN SECTION OF A COIL

FIGURE 4

The response of the coil is constructed by calculating the effects of a surge as it is propagated and reflected inside the coil. The surge propagates along the coil as in a multiconductor transmission line and with multiple reflections at any discontinuities (e.g. at the iron/air interface and at the coil terminals). The propagation of the surge along each section of line can be calculated using the equations of multiconductor transmission line theory, and the reflections can be calculated using the scatter matrix technique developed by Agrawal et al.[1] The method employed is essentially a lattice diagram technique which is used to compute the impulse response of the coil. Time-convolution with the input surge is then applied to obtain the actual time response of the system.

Figure 5 is a simplified schematic of the experimental arrangement used to test the theory.

The voltage appearing on each turn of the coil was recorded for a switching surge of 30 ns rise time.

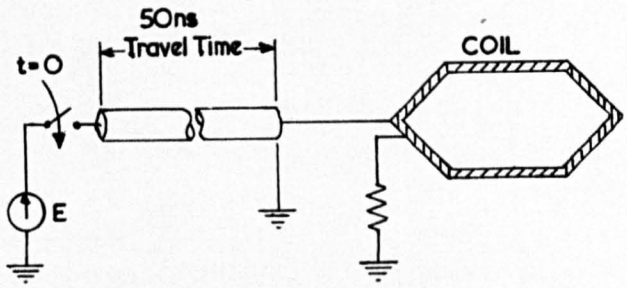

TEST CIRCUIT FOR A SINGLE COIL

FIGURE 5

Correlation of the experimental results with those obtained from the computer model is shown in Figure 6. (In Figures 6, 7 and 8 voltage magnitudes are presented as a percentage of the voltage at the switch). The correlation can be seen to be excellent, thus giving confidence in model predictions. The single coil model used to produce the calculated waves in Figure 6 can be used as a building block in the modelling of a complete winding by simple repetition and appropriate interconnection of each coil element.

Since the iron core behaves as a flux barrier during fast transients, adjacent coils may be considered to have no mutual coupling, but are linked only by their physical electrical connections. This series nature of the wave propagation suggests that remote conditions (i.e. at the neutral end of the phase) do not influence the initial voltage distribution within the line end coils. This postulate is supported by the results of Figure 7, which shows the voltage distribution in the first of four series connected coils and is almost identical to that calculated and measured for a single coil shown in Figure 6.

The effect on line end coil voltage distribution, of introducing more coils into the model, diminishes as the number of additional coils is increased. There is, therefore, a limiting number of discrete coil models, above which the line end coil voltage distribution is unmodified by further extensions to the model. In practice this means that it is possible to simulate complete machine windings without including every single coil in the model.

The computer model can clearly be used to investigate the influence of winding parameters and surge rise times on maximum interturn voltage. An important result of such an investigation is shown in Figure 8. Figure 8 shows maximum interturn voltage as a function of rise time forvarious turns per coil of an 11kV insulation system and indicates that this voltage is not sensitive to the number of turns employed. Similar results are obtained for 3.3, 4.16, 6.6 and 13.8kV coils. Consequently, it is the authors' view that the interturn insulation withstand level, adopted for a particular winding, should be decided with the rate of rise of a potential switching surge as a fundamental parameter. No existing standards take note of this, as far as is known.

Due to impedance mismatch at the machine terminals, the maximum voltage to ground on the winding will be higher than the voltage generated at the switching device. The magnitude of the increase in voltage to ground appearing at the machine end of the cable can be used to calculate an effective surge impedance for the machine winding. (This impedance is not a true surge impedance since the voltage on the winding is determined by the overall effect of a large number of wave reflections inside each coil). Figure 9 shows how this effective surge impedance varies with the rise time of the switching surge for a range of turns per coil for the 11kV insulation system analysed in Figure 8. In spite of the assumption that the distributed coil parameters are frequency independent, the effective surge impedance of thewinding can be seen to be highly dependent on the spectral content of the surge. An interesting aspect of our results is that surge impedance at low rise times varies proportionally as the insulation level (e.g. surge impedance of an "identical" coil insulated for 3.3kV is about half that of a 6.6kV coil).

The practical advantage of a good theoretical understanding of surge propagation in motor coils is that the knowledge can be applied at the design stage,

FIGURE 6.

TRANSIENT VOLTAGE DISTRIBUTION IN A TWELVE TURN COIL. (EVERY THIRD TURN SHOWN FOR CLARITY.)

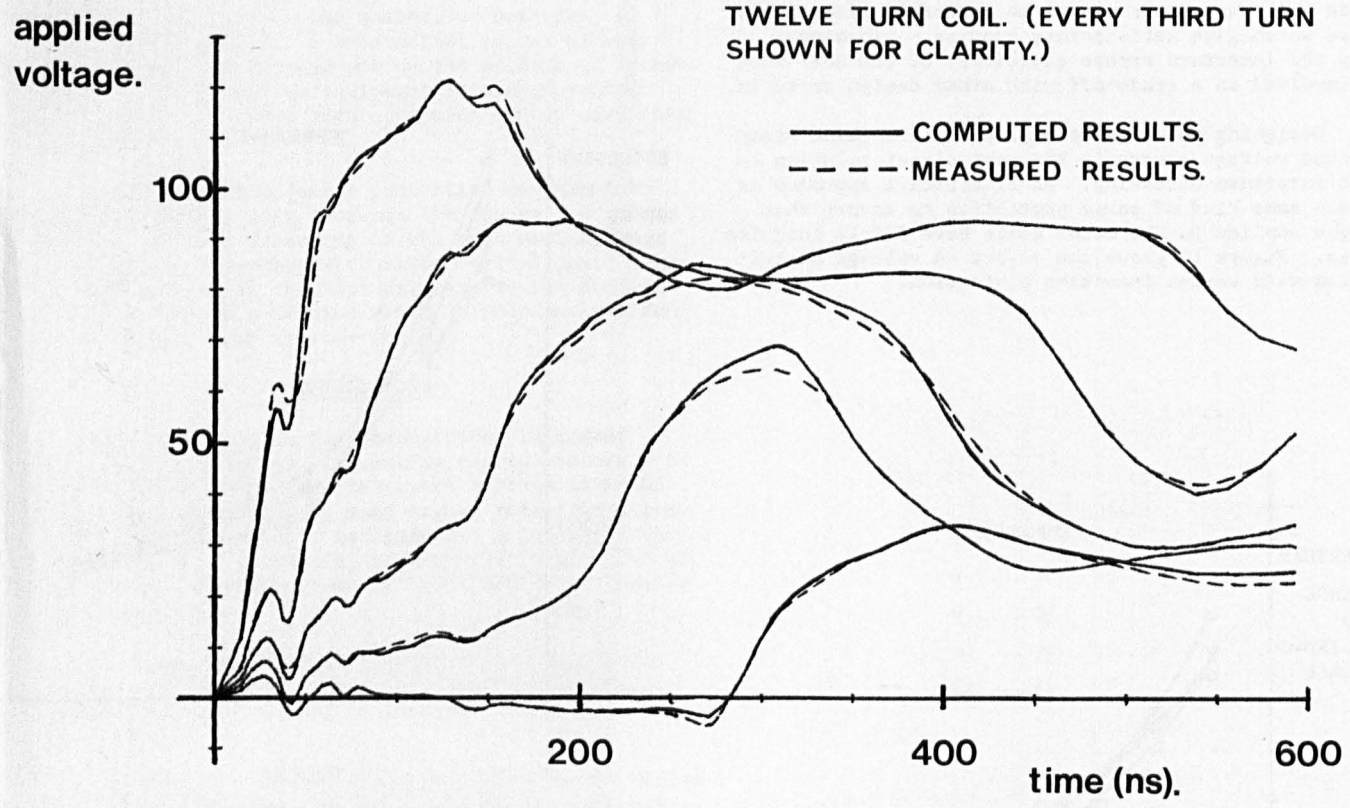

FIGURE 7.

COMPUTED VOLTAGE DISTRIBUTION ON THE FIRST OF FOUR TWELVE TURN COILS. (EVERY THIRD TURN SHOWN.)

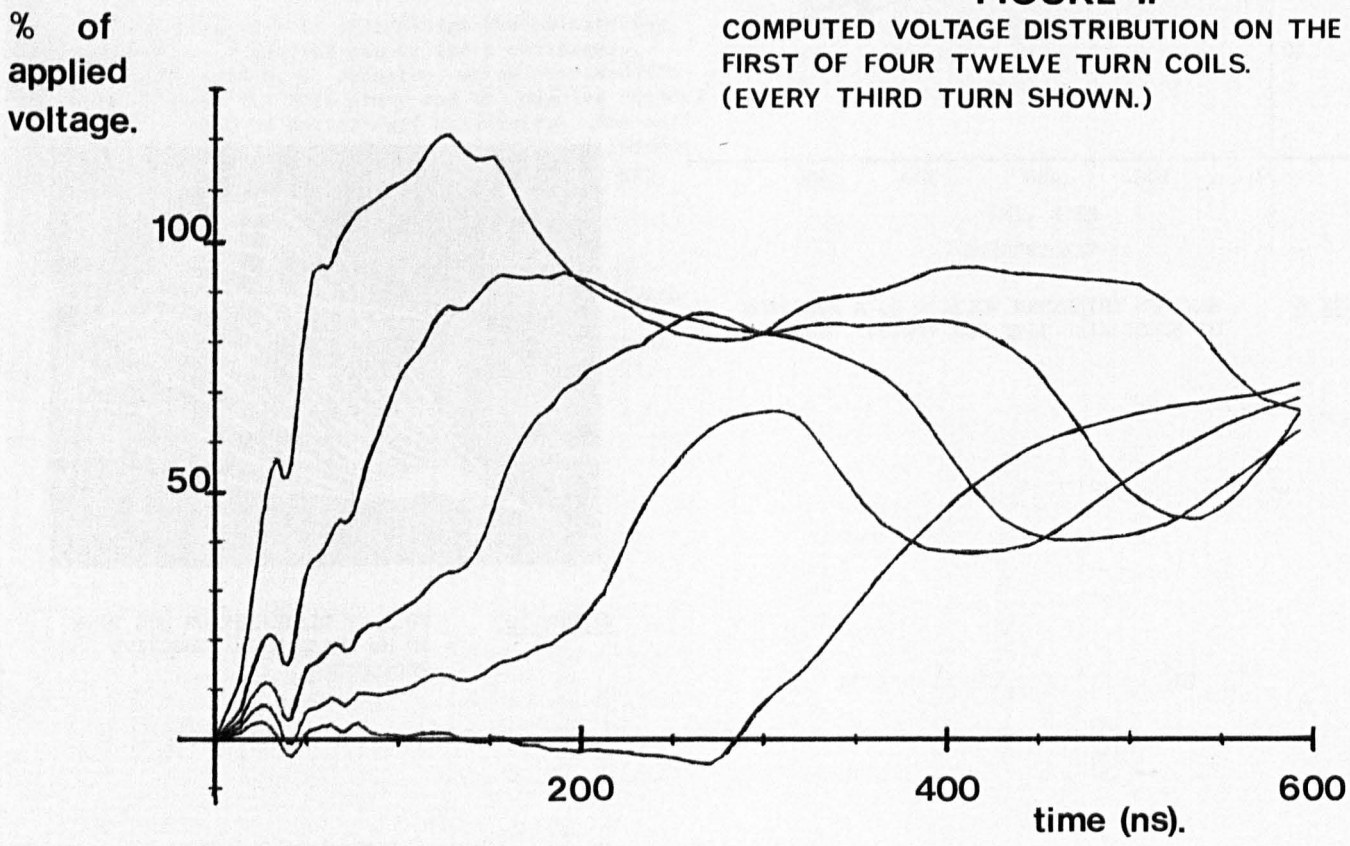

to assess whether specific coils can withstand steep fronted surges. There will clearly be a limit to the severity of surge that a given coil can withstand since coil parameters cannot be radically altered from those which give satisfactory running performance. Thus the interturn stress capability of the coil must be involved in a trade-off with other design criteria.

Designing the coil to explicitly withstand steep fronted voltage surges is the most direct solution to high interturn stressing. An alternative approach is to use some kind of surge protection to ensure that surges applied to the motor coils have fairly long rise times. Figure 10 shows the effect on voltage distribution with series inductive protection.

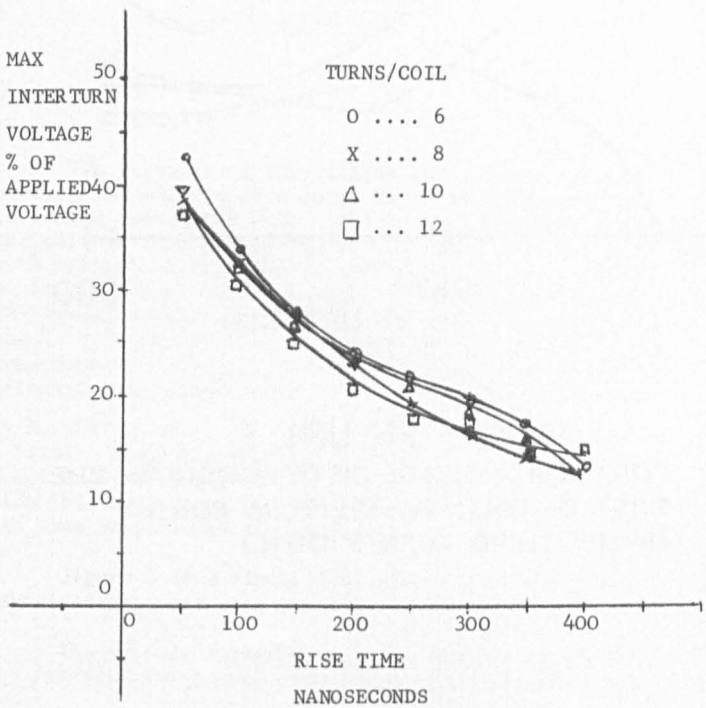

FIGURE 8 MAXIMUM INTERTURN VOLTAGE AS A FUNCTION OF SURGE RISE TIME FOR VARIOUS TURNS/COIL

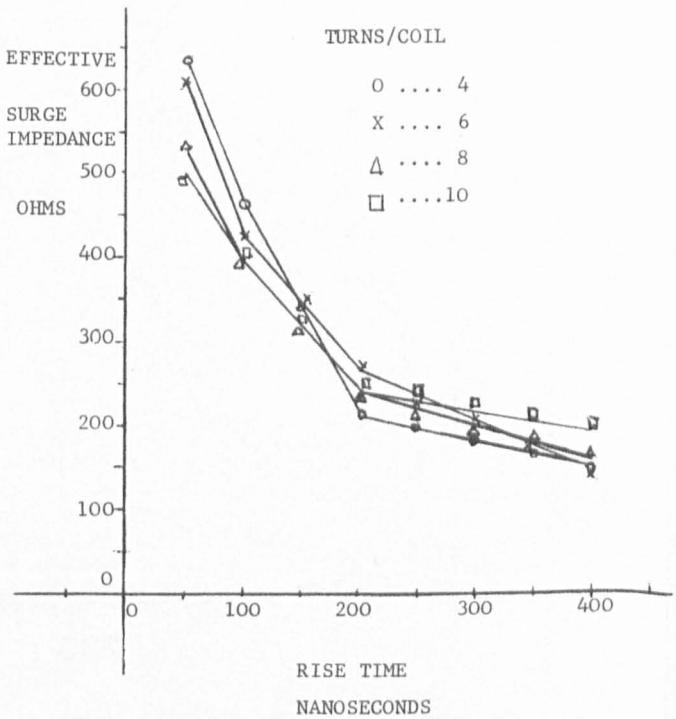

FIGURE 9 EFFECTIVE SURGE IMPEDANCE AS A FUNCTION OF RISE TIME AND TURNS

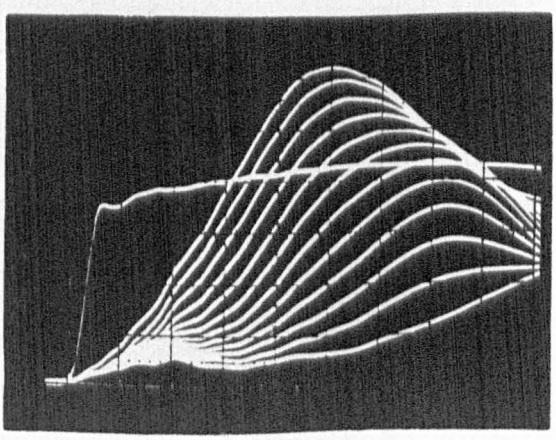

FIGURE 10 VOLTAGE DISTRIBUTION DUE TO A 10 ns PULSE WITH INDUCTIVE PROTECTION

Surge protection may prove to be difficult to apply in many circumstances, since the protection apparatus will modify the system parameters and could well lead to an increase in the number, or severity, of switching transients. A substantial amount of work still needs to be carried out on the effects of introducing surge protection equipment into high voltage motor circuits, before such equipment can be used with confidence.

The inclusion of surge protection devices into a motor circuit may also increase the losses, or reduce the power factor, depending on the type used. These disadvantages, together with extra capital cost, suggest that in general the best solution to the problem will be to design a machine which is inherently capable of tolerating steep fronted surges.

CONCLUSIONS

This contribution has demonstrated that fast transient switching of alternating current motors produces severely non-linear interturn voltage distributions which may result in much higher interturn stress levels than is generally recognised. A general theoretical method of predicting such stress levels has been outlined and has been shown to agree well with experimental results.

The theoretical method should be of fundamental value in assessing the surge withstand capability of machine windings and will be published in full in the near future.

It is hoped that the preliminary results presented in this paper will provide some stimulus for a realistic appraisal of current interturn test procedures.

ACKNOWLEDGEMENTS

The authors wish to acknowledge the painstaking experimental work carried out by their colleagues, W. A. Sharpley and H. R. Johnston, which provided the initial stimulus for this study and the ongoing support of Dr. S. J. Yang of Heriot-Watt University. The assistance of the U.K. Science Research Council in funding Mr. McLeay for this work is gratefully acknowledged.

REFERENCE

[1] AGRAWAL, A.K., FOWLES, H.M., SCOTT, L.D. and GURBAXANI, S.H.: 'Application of modal analysis to the transient response of multiconductor transmission lines with branches', IEEE Transactions on Electromagnetic Compatability, Vol. EMC-21, No. 3, August 1979, pp. 256 - 262.

Reprinted from IEEE 1981 PCI Conference Record
PRINTED IN U.S.A. - PRINTCRAFT, INC., CONNEAUT, OHIO 44030

THE PREDICTION OF TRANSIENT INTERTURN VOLTAGES IN STATOR WINDINGS

M. T. Wright, S. J. Yang,* and K. McLeay

Parsons Peebles Motors and Generators, U.K. *Heriot-Watt University, U.K.

INTRODUCTION

The distribution of voltage in induction motor stator coils, due to the application of steep fronted switching surges, has aroused much interest in recent years amongst motor manufacturers and users alike. This interest has been prompted by the increased occurrence of winding failure in the interturn mode. The increased use of modern low loss cables has meant that surges are transmitted almost unaltered to the motor. In addition the undoubted advantages of vacuum switchgear have led to their increased popularity in motor control systems. The ability of this type of switchgear to produce repetitive steep fronted transient voltages, however, has in some cases, led to stator coils being subject to more severe surge conditions.

It is well known that steep fronted surges can cause high interturn stressing. Unless stator coils are designed to withstand these surges interturn failures, possibly leading to turn to ground failure, may occur.

The continuing increase in the output coefficients of modern motors has led to a tendency to minimise the size of stator coils. Thus the insulation design of modern coils leaves less margin for error, although the better quality of modern insulation material has offset this to a considerable extent.

This contribution shows that an accurate method of predicting transient voltage distribution in the coils is necessary.

Following a brief resumé of pertinent work on the topic, it is found that further development of previous analyses would be ineffective and that a completely new analysis is required. The development of such an analysis is outlined here and its validity is experimentally confirmed.

Due to the lack of understanding of surge propagation in stator coils in the past, the insulation testing of coils has been carried out at voltages which were set at levels which may be exceeded in practice. Current test standards are compared with voltage distributions as predicted by the new theory, for various surge shapes and insulation levels.

PREVIOUS INVESTIGATIONS

In the past, voltage distribution has been analysed by an oversimplified model for the winding, i.e. by modelling the winding either as a simple transmission line or as a ladder network. Neither of these methods gives accurate predictions of turn voltages. Further development of existing analyses was not feasible, therefore a new approach to the problem was required.

DESCRIPTION OF THE NEW THEORY

Assumptions and Approximations

A rigorous analysis of electromagnetic fields in and around a stator winding during a transient disturbance is certainly not practicable. Therefore certain approximations and assumptions must be made to enable the analysis to develope.

It has been shown that, at high frequencies, core iron acts as a shield to electromagnetic flux.[3] It can therefore be assumed that over the stator core length, the flux is confined to within the slot. This assumption, together with the assumption that intercoil coupling in the endwinding region is negligible, means that coils can be treated independently since they influence each other only through their series connections.

At the high frequencies associated with the surges of interest here (i.e. surges with front times below 1 us,: frequencies above 1MHz) the surge current in the conductors will be severely skin effect limited. Consequently the internal inductances of the coil can be neglected.

In estimating the copper losses in the coil conductors, both skin and proximity effects must be taken into account. To estimate the skin effect it is assumed that all the current flows in an outer layer the depth of which is found from one dimensional theory, i.e. skin depth, d, is given by

$$d = \sqrt{\frac{2\rho_c}{\mu\omega}}$$

The proximity effect is estimated by multiplying the losses, accounting for skin effect, by a proximity factor, kp, such that

$$R = k_p R_{a.c.}$$

It can be shown that for the dimensions of stator coil conductors and the range of frequencies in question, k_p is a constant.[2]

Although, in reality, losses are distributed evenly along the coil conductors, it was found to be sufficiently accurate to account for their effect by modelling them as discrete resistances at five points on the coil.

Modelling the Coil

The coil is visualised as comprising five distinct sections as in Figure 1. The five sections are connected to each other at five junctions. Four of these junctions are at the point where a slot section meets an endwinding section. The fifth junction is the terminal junction where the coil terminals join at the coil evolute.

The cross sectional dimensions of all coil sections, at the frequencies involved in analysis, preclude all modes of wave propagation except TEM. Each coil section can therefore be treated as a multi-conductor transmission line. Consequently the five junctions are seen as multiconductor transmission line junctions. The propagation of waves along multiconductor transmission lines is well understood for both lossless and lossy lines. However only lossless multiconductor transmission line junctions have been analysed in the literature.[3]

The relationship between the incident voltage waves on each line and the reflections which are caused to propagate from the lossless junctions is given by Agrawal et al [3] as,

$$(V)^{re} = (S)(V)^{in} \qquad (1)$$

where $(V)^{re}$ and $(V)^{in}$ are the column vectors of the voltages on the conductors.

(S) can be shown to be related to the transmission line admittances and the junction topology by

$$(S) = \begin{bmatrix} -(Cv) \\ (C_i)\ (Y) \end{bmatrix}^{-1} X \begin{bmatrix} (Cv) \\ (C_i)\quad (Y) \end{bmatrix} \qquad (2)$$

where (C_v) and (C_i) are the voltage connection matrix and current connection matrix respectively and are determined entirely by the interconnections of the conductors at the junction.

Equations (1) and (2) are valid only for lossless junctions. However a further development of the theory which includes discrete loss elements at the junction has now been achieved. Both copper and dielectric losses can be included in this method.

Including the losses in the analysis gives,

$$(V)^{re} = (S_L)(V)^{in}$$

where (S_L) is the lossy scatter matrix for the junction and is found to be:

$$(S_L) = \begin{bmatrix} -(C_v)-(C_v)(R)(Y)-(C_v)(G)(R) \\ (C_i)(Y) + (C_i)(G) \end{bmatrix}^{-1} X$$

$$\begin{bmatrix} (C_v)-(C_v)(R)(Y) + (C_v)(G)(R) \\ (C_i)(Y) - (C_i)(G) \end{bmatrix}$$

where (R) and (G) represent the copper and dielectric losses respectively.

In this way, wave reflections at each junction can be calculated taking account of losses.

Computer programmes were developed to model the coil as sections of lossless multiconductor transmission lines interconnected by lossy junctions. This computer model can be used as a building block to model a complete phase winding. The predictions from the computer model are compared with experimental results below.

CAPTION AREA

TERMINATION OF COLUMN 1

EXPERIMENTAL CONFIRMATION OF THE THEORY

Only low voltage tests were practicable because of the necessity to remove some insulation to gain access to the turns.

The results of the tests revealed that the theoretical turn to ground voltages on the line end coil, due to the application of a surge of irregular shape, followed very closely the measured turn to ground voltages.

A more stringent test of the theory is the prediction of interturn voltages. High accuracy is more difficult to obtain for these voltages since they are calculated as the difference between two large turn to ground voltages. Figure 2 shows that the theory is extremely accurate in calculating both the shape and magnitude of the interturn voltages. The theory can therefore be used to investigate the effects of various system parameters on the voltage distribution in the coils and the results of this investigation can be compared to the prevailing standards for coil insulation.

Figure 2 also shows that surge propagation in stator coils is the result of two distinct phenomena. The progression of the voltage peaks shows series surge propagation. The fact that interturn voltages appear at the end of the coil well before the peaks arrive demonstrates that there is also parallel propagation due to interturn coupling.

Since the theory has been shown to be accurate, it can be used to predict voltage distribution due to various surges and on coils with various insulation levels.

EFFECTS OF SURGE RISE TIME ON INTERTURN VOLTAGES

To investigate the variations in voltage distribution due to various surge front times, the theoretical model was used to predict voltages due to surges with front times varying from 25ns - 400ns. Front times below 25ns are unlikely to occur in practice and front times greater than 400ns will not cause severe interturn stressing.

The peak voltage appearing between each pair of turns of the terminal junction of a 13.8kV, 12 turn line end coil is plotted against the turn number in Figure 3 for each surge. These curves clearly indicate that the maximum peak voltage appearing across the turn insulation always occurs towards the neutral end of the line end coil. In the case of surges with rise times below 100ns (0.1μs) the maximum interturn voltage occurs between the final two turns in the coil. This is due to reflection, of the series transmitted portion of the surge at the end of the coil. The result that the maximum interturn voltage (or a voltage of almost equal magnitude) occurs across several interturn spacings at the neutral end of the coil, for the case of the slower rise times, indicates that the surge front and its reflection are spread over a number of the neutral end turns.

It is emphasised that the voltage distribution is due only in part to the series propagation of the surge and that a quantitative analysis cannot be based on the series propagation mode alone.

TERMINATION OF COLUMN 2

The peak interturn voltages in Figure 4 show clearly that maximum interturn voltage increases with decreasing surge front time. Thus the 5 p.u. 200ns test surge of the OCMA[5] standard, for example, will not ensure that interturn insulation can withstand a 5 p.u. surge of smaller front time. In fact, a surge of well below 5 p.u. can cause greater interturn stressing than the test surge, if the front time is short enough.

The ESI standard[4] when applied to a 13.8kV coil gives an interturn test voltage of 2.8kV r.m.s. or 3.96kV peak. To find the voltage which the OCMA test surge causes on this coil, Figure 3 can be used. The maximum interturn voltage for the 200ns surge is 25% of the applied surge. The applied surge is that which is produced at the surge generator. (The surge which actually appears at the winding terminal is greater than this due to a frequency dependent impedance mismatch effect.) In this case, the surge at the winding terminal was 157% of the original surge.

Therefore the 3 p.u. OCMA surge produces an interturn voltage of

$$13.8\text{kV} \times \sqrt{\frac{2}{3}} \times 3 \times \frac{25\%}{157\%} = 5.38\text{kV}$$

The 5 p.u. OCMA surge gives 8.97kV.

Thus it can be seen that the OCMA surge test stresses the interturn insulation much more severely than does the ESI test.

EFFECT OF INSULATION DIMENSIONS ON INTERTURN VOLTAGES

Three insulation levels were used to investigate the effect of the insulation dimensions. These were 3.3kV, 11.0kV and 13.8kV. In addition a fourth set of dimensions was used to show the effect of the interturn insulation dimensions alone. For this purpose the 11.0kV level was used but with 50% extra interturn insulation. The permittivity was kept constant throughout.

It was anticipated that the coils with thicker insulation would produce the higher p.u. interturn voltages, since the reduced interturn coupling would cause the series propagation mode to become more effective than the parallel mode. Figure 4 shows this to be the case. In particular, the curves relating to 11kV coils, with differing interturn insulations, show that the interturn voltage increases by 24.4% due solely to a 50% increase in interturn insulation thickness.

Variation in interturn insulation clearly causes variation in interturn stressing, therefore allowance should be made for the anticipated voltage distribution during the design process. In interturn insulation type tests, the test voltage is applied directly across a typical sample of interturn insulation, so no allowance is made for voltage distribution. Thus a coil which has a severely non-linear surge distribution can pass the type test and yet may not be adequately tested by the proof test surge.

CAPTION AREA

TERMINATION OF COLUMN

EFFECT OF OTHER PARAMETERS ON INTERTURN VOLTAGE

Other coil parameters can be altered in the model in order to discover the manner in which they affect voltage distribution. It was found that fast fronted surges produce maximum interturn voltages which are substantially independent of the number of turns in the coil.[6] This result and the effect of coil shape on voltage distribution will be reported in detail in a future publication.

SURGE IMPEDANCE

Figure 5 shows the voltages to ground on each turn at the terminal junction of a 12 turn line end coil. The rise time of the surge as it left the switch was 50ns (0.05μs). The increase in voltage at the terminal of the coil is considerable. This increase in voltage is commonly thought of as being due to a mismatch of cable and winding surge impedances. In reality the effect is the net result of many internal reflections in the coil. However an effective surge impedance can be calculated using the impedance mismatch concept. The variation of surge impedance with surge front time is shown for 3.3kV, 11.0kV and 13.8kV coil in Figure 6.

Also included in Figure 6 is the surge impedance of an 11kV coil when subjected to the surge of irregular shape shown in Figure 7. This indicates that the shape of the surge, if different from the classical short rise time and long tail, modifies effective surge impedance. Consequently surge impedance alone is not a reliable indicator of overvoltage magnitudes as it is heavily dependent on frequency.

RECOMMENDATIONS AND CONCLUSIONS

It has been suggested in this contribution that the number and severity of surges which motor windings must endure has increased in recent years. Present methods of analysis of surge propagation through stator coils are inadequate and cannot be developed further.

A new general theory based on multiconductor transmission line theory and scatter matrices was briefly described. The further development of scatter matrices to include losses was also given, and a computer programme incorporating multiconductor transmission line theory and lossy scatter matrices was shown to give predictions of interturn voltages which reproduced the measured voltages with a high degree of accuracy.

The increase in interturn voltage with decreasing front time was expected and confirms the results of previous investigations. The non-linearity of the distribution also increases with decreasing rise time.

The larger percentage interturn voltage appearing on the higher voltage coils is clearly due to the decreased interturn coupling caused by the increased insulation thickness. Consequently interturn insulation thickness must be increased by a factor greater than that by which the voltage level is increased if the same safety margin is to be maintained.

While the OCMA test levels are a significant improvement on ESI 44-5, they may not be adequate where surges of very fast rise time exist. Type testing of interturn insulation takes no account of voltage distribution.

The surge impedance of windings has been shown to be dependent on both surge shape and rise time and is therefore of limited value as a machine parameter The surge impedances, calculated for surges with a smooth rise and long tail, show an increase in surge impedance magnitude with decreasing rise time.

The investigation into the effects of coil and surge parameters on voltage distribution has indicated various trends. However, the major benefit of the new method of analysis lies in its use as a design tool, which can be used to co-ordinate coil insulation to provide adequate factors of safety without overdesign.

ACKNOWLEDGEMENTS

The assistance of the Science and Engineering Research Council in funding Mr. McLeay for this work is gratefully acknowledged.

REFERENCES

1. Heller, B. and Veverka, A., 1966, "Surge phenomena in electrical machines", Iliffe, London.

2. Lammeraner, J. and Stafl, M., 1966, "Eddy currents", Iliffe, London.

3. Agrawal, A. K., Fowles, H. M., Scott, L. D. and Gurbaxani, S. H., August 1979, "Application of modal analysis to the transient response of multiconductor transmission lines with branches", IEEE Transactions on Electromagnetic Compatibility, Vol. EMC-21 No. 3, p.p. 256-262.

4. Electricity Supply Industry Standard 44-5, September 1978, Issue 2.

5. Oil Companies Materials Association, July 1981, Specification No. ELEC.1.

6. Wright, M. T. and McLeay, K., 1981, "Interturn voltage distribution due to fast transient switching of induction motors", IEEE Conference Paper PCI-81-14, Petroleum and Chemical Industry Conference.

CAPTION AREA

ILLUSTRATION

CAPTION AREA

ILLUSTRATION

CAPTION AREA

TERMINATION OF COLUMN 1

CAPTION AREA

TERMINATION OF COLUMN 2

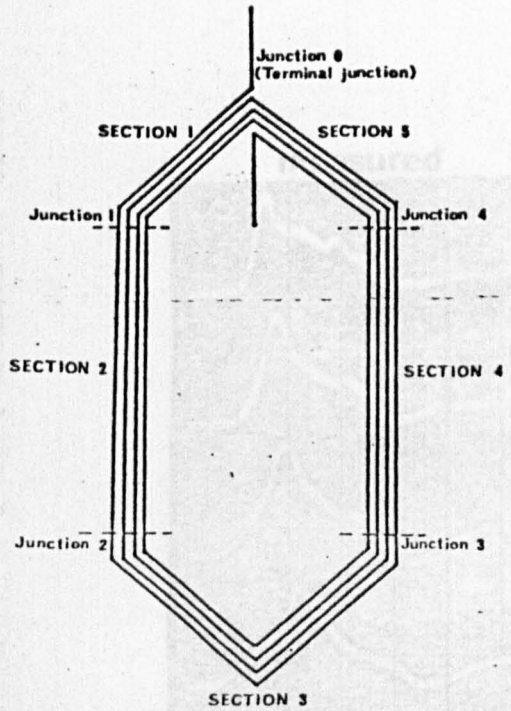

Figure 1 Sectionalised 4 turn coil

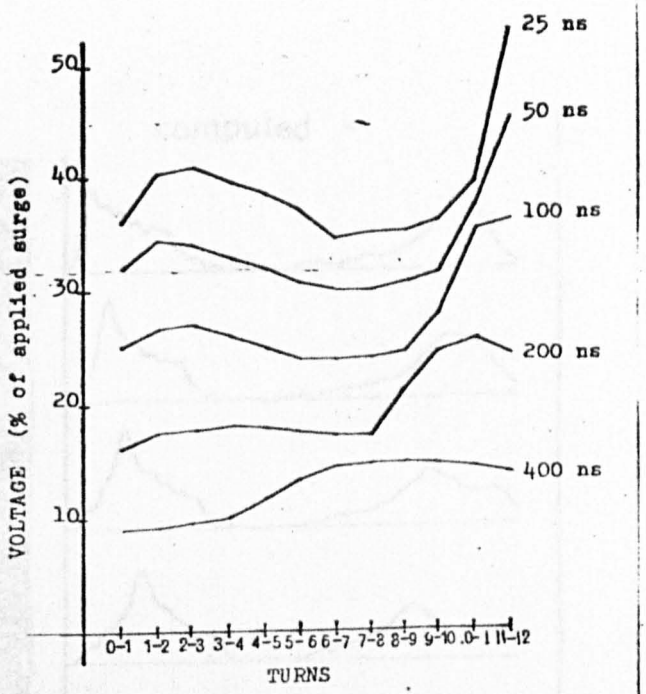

Figure 3 Interturn voltage distribution on a 13.8kV, 12 turn coil due to the various rise times

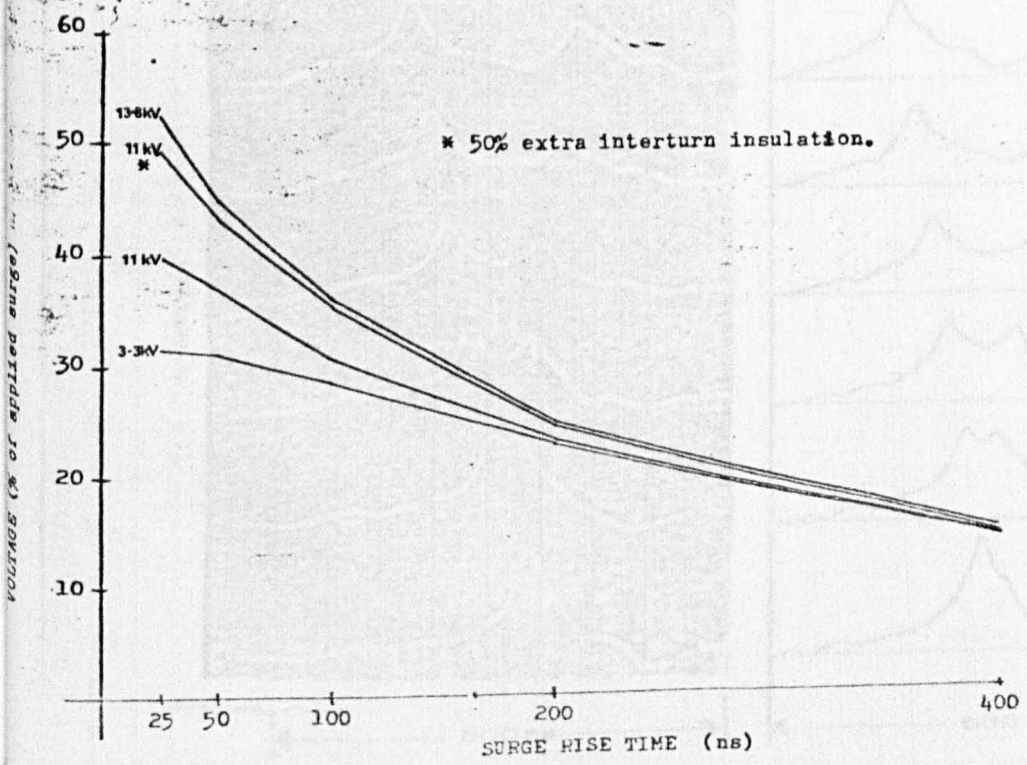

Figure 4 Maximum interturn voltage vs. Surge rise time for various insulation levels.

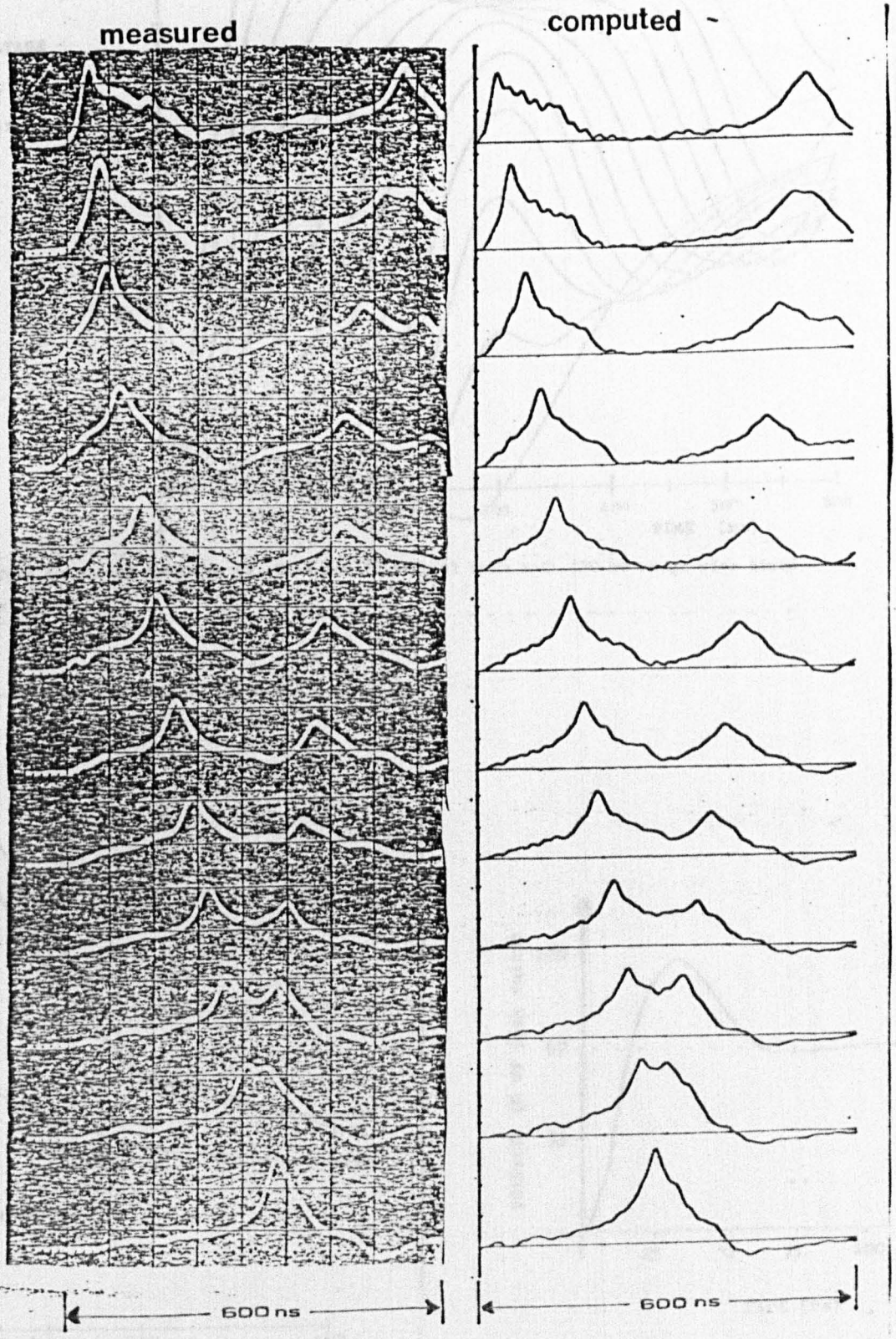

Figure 2 Measured and computed interturn voltages on a 12 turn coil

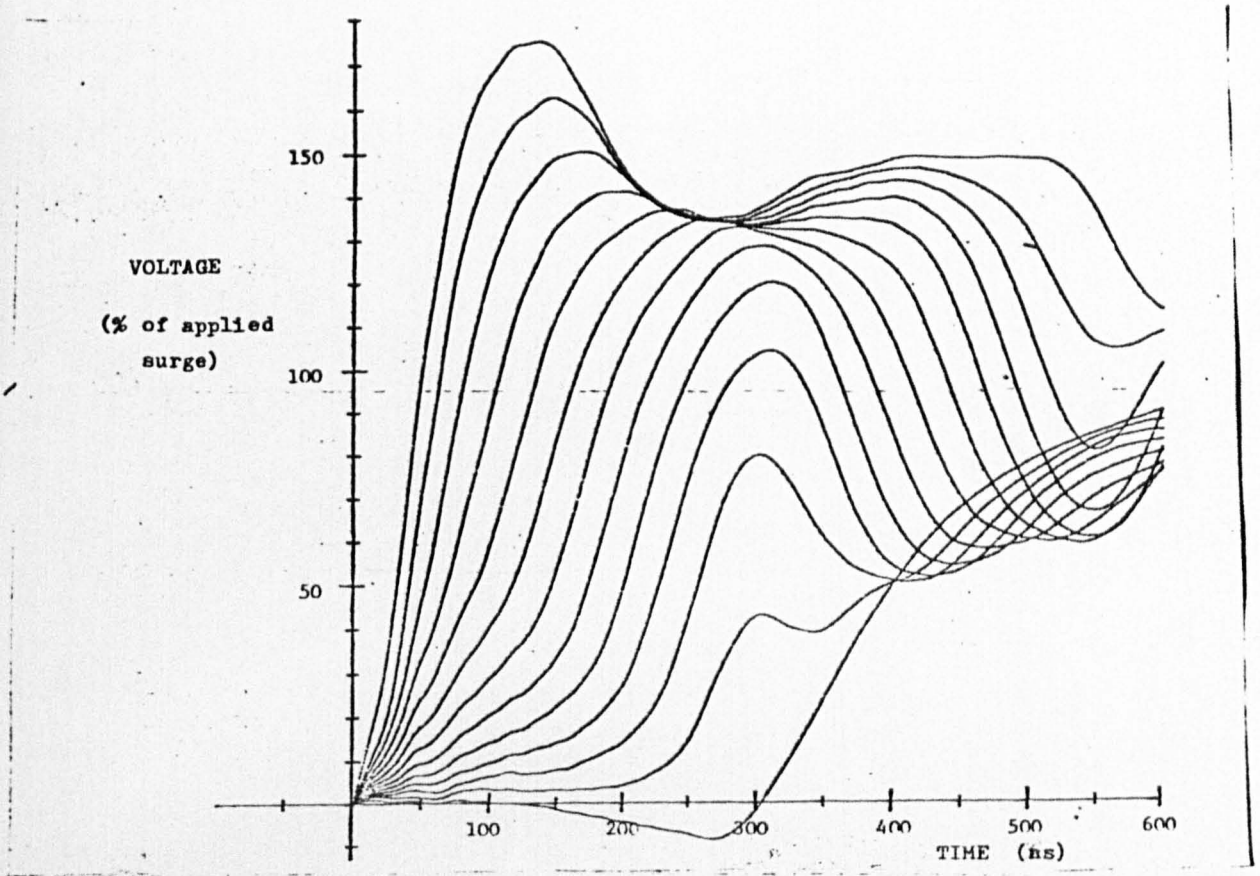

Figure 5 Turn to ground voltages vs. Time for 13.8kV, 12 turn coil (50 ns surge rise time)

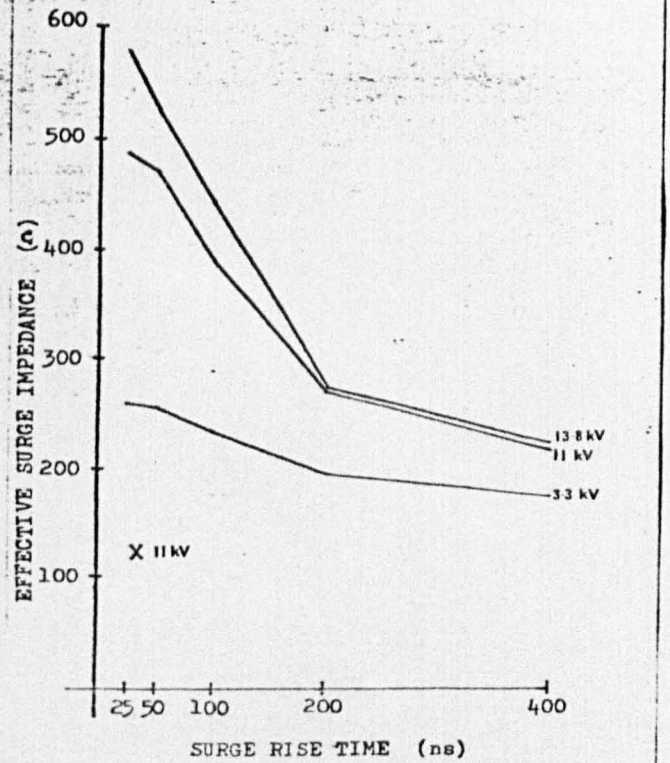

Figure 6 Effective surge impedance vs. surge rise time (various insulation levels)

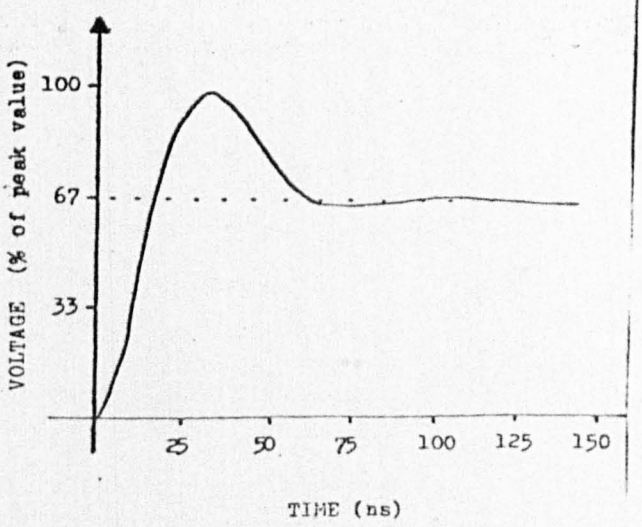

Figure 7 Irregular surge wave form